Case No. 78701

In the Supreme Court of Nevada

MOTOR COACH INDUSTRIES, INC.,

Appellant,

vs.

KEON KHIABANI; ARIA KHIABANI, MINORS, by and through their Guardian MARIE-CLAUDE RIGAUD; SIAMAK BARIN, as Executor of the Estate of KAYVAN KHIABANI, M.D.; the Estate of KAYVAN KHIABANI; SIAMAK BARIN, as Executor of the Estate of KATAYOUN BARIN, DDS; and the Estate of KATAYOUN BARIN, DDS,

Respondents.

Electronically Filed
Dec 04 2019 05:32 p.m.
Elizabeth A. Brown
Clerk of Supreme Court

APPEAL
from the Eighth Judicial District Court, Clark County
The Honorable ADRIANA ESCOBAR, District Judge
District Court Case No. A-17-755977-C

APPELLANT'S APPENDIX
VOLUME 10
PAGES 2251–2500

D. LEE ROBERTS (SBN 8877)
HOWARD J. RUSSELL (SBN 8879)
WEINBERG, WHEELER,
HUDGINS, GUNN & DIAL, LLC
6385 S. Rainbow Blvd., Ste. 400
Las Vegas, Nevada 89118
(702) 938-3838

DANIEL F. POLSENBERG (SBN 2376)
JOEL D. HENRIOD (SBN 8492)
JUSTIN J. HENDERSON (SBN 13,349)
ABRAHAM G. SMITH (SBN 13,250)
LEWIS ROCA
ROTHGERBER CHRISTIE LLP
3993 Howard Hughes Pkwy, Ste. 600
Las Vegas, Nevada 89169
(702) 949-8200

DARRELL L. BARGER (*pro hac vice)*
MICHAEL G. TERRY (*pro hac vice*)
HARTLINE BARGER LLP
800 N. Shoreline Blvd.
Suite 2000, N. Tower
Corpus Christi, Texas 78401

JOHN C. DACUS (*pro hac vice)*
BRIAN RAWSON (*pro hac vice)*
HARTLINE BARGER LLP
8750 N. Central Expy., Ste. 1600
Dallas, Texas 75231

Attorneys for Appellant

CHRONOLOGICAL TABLE OF CONTENTS TO APPENDIX

14	Reporter's Transcription of Motion for Preferential Trial Setting	07/20/17	1	172–213
15	Notice of Entry of Order (CMO)	08/18/17	1	214–222
16	Notice of Entry of Order	08/23/17	1	223–227
17	Stipulated Protective Order	08/24/17	1	228–236
18	Reporter's Transcription of Motion of Status Check and Motion for Reconsideration with Joinder	09/21/17	1 2	237–250 251–312
19	Defendant SevenPlus Bicycles, Inc. d/b/a Pro Cyclery's Motion for Determination of Good Faith Settlement	09/22/17	2	313–323
20	Defendant's Notice of Filing Notice of Removal	10/17/17	2 3	324–500 501–586
21	Civil Order to Statistically Close Case	10/24/17	3	587–588
22	Motion for Summary Judgment on Foreseeability of Bus Interaction with Pedestrians or Bicyclists (Including Sudden Bicycle Movement)	10/27/17	3	589–597
23	Transcript of Proceedings	11/02/17	3	598–618
24	Second Amended Complaint and Demand for Jury Trial	11/17/17	3	619–637
25	Order Regarding "Plaintiffs' Motion to Amend Complaint to Substitute Parties" and "Countermotion to Set a Reasonable Trial Date Upon Changed Circumstance that Nullifies the Reason for Preferential Trial Setting"	11/17/17	3	638–641
26	Motion for Summary Judgment on Punitive Damages	12/01/17	3	642–664
27	Volume 1: Appendix of Exhibits to Motion for Summary Judgment on Punitive Damages	12/01/17	3 4	665–750 751–989
28	Volume 2: Appendix of Exhibits to Motion for Summary Judgment on Punitive Damages	12/01/17	4 5	990–1000 1001–1225

29	Volume 3: Appendix of Exhibits to Motion for Summary Judgment on Punitive Damages	12/01/17	5 6	1226–1250 1251–1490
30	Motor Coach Industries, Inc.'s Motion for Summary Judgment on All Claims Alleging a Product Defect	12/04/17	6 7	1491–1500 1501–1571
31	Defendant's Motion in Limine No. 7 to Exclude Any Claims That the Subject Motor Coach was Defective Based on Alleged Dangerous "Air Blasts"	12/07/17	7	1572–1583
32	Appendix of Exhibits to Defendant's Motion in Limine No. 7 to Exclude Any Claims That the Subject Motor Coach was Defective Based on Alleged Dangerous "Air Blasts"	12/07/17	7 8	1584–1750 1751–1801
33	Defendants' Motion in Limine No. 13 to Exclude Plaintiffs' Expert Witness Robert Cunitz, Ph.d., or in the Alternative, to Limit His Testimony	12/07/17	8	1802–1816
34	Appendix of Exhibits to Defendants' Motion in Limine No. 13 to Exclude Plaintiffs' Expert Witness Robert Cunitz, Ph.D., or in the Alternative, to Limit His Testimony	12/07/17	8 9	1817–2000 2001–2100
35	Motion for Determination of Good Faith Settlement Transcript	12/07/17	9	2101–2105
36	Defendants' Motion in Limine No. 17 to Exclude Claim of Lost Income, Including the August 28 Expert Report of Larry Stokes	12/08/17	9	2106–2128
37	Plaintiffs' Joint Opposition to MCI Motion for Summary Judgment on All Claims Alleging a Product Defect and to MCI Motion for Summary Judgment on Punitive Damages	12/21/17	9	2129–2175
38	Appendix of Exhibits to Plaintiffs' Joint Opposition to MCI Motion for Summary Judgment on All Claims	12/21/17	9 10 11	2176–2250 2251–2500 2501–2523

	Alleging a Product Defect and to MCI Motion for Summary Judgment on Punitive Damages			
39	Opposition to "Motion for Summary Judgment on Foreseeability of Bus Interaction with Pedestrians of Bicyclists (Including Sudden Bicycle Movement)"	12/27/17	11	2524–2580
40	Notice of Entry of Findings of Fact Conclusions of Law and Order on Motion for Determination of Good Faith Settlement	01/08/18	11	2581–2590
41	Plaintiffs' Joint Opposition to Defendant's Motion in Limine No. 3 to Preclude Plaintiffs from Making Reference to a "Bullet Train" and to Defendant's Motion in Limine No. 7 to Exclude Any Claims That the Motor Coach was Defective Based on Alleged Dangerous "Air Blasts"	01/08/18	11	2591–2611
42	Plaintiffs' Opposition to Defendant's Motion in Limine No. 13 to Exclude Plaintiffs' Expert Witness Robert Cunitz, Ph.D. or in the Alternative to Limit His Testimony	01/08/18	11	2612–2629
43	Plaintiffs' Opposition to Defendant's Motion in Limine No. 17 to Exclude Claim of Lost Income, Including the August 28 Expert Report of Larry Stokes	01/08/18	11	2630–2637
44	Reply to Opposition to Motion for Summary Judgment on Foreseeability of Bus Interaction with Pedestrians or Bicyclists (Including Sudden Bicycle Movement)"	01/16/18	11	2638–2653
45	Plaintiffs' Addendum to Reply to Opposition to Motion for Summary Judgment on Forseeability of Bus	01/17/18	11	2654–2663

	Interaction with Pedestrians or Bicyclists (Including Sudden Bicycle Movement)”			
46	Reply to Plaintiffs’ Opposition to Motion for Summary Judgment on Punitive Damages	01/17/18	11	2664–2704
47	Motor Coach Industries, Inc.’s Reply in Support of Its Motion for Summary Judgment on All Claims Alleging a Product Defect	01/17/18	11	2705–2719
48	Defendant Bell Sports, Inc.’s Motion for Determination of Good Faith Settlement on Order Shortening Time	01/17/18	11	2720–2734
49	Plaintiffs’ Joinder to Defendant Bell Sports, Inc.’s Motion for Determination of Good Faith Settlement on Order Shortening Time	01/18/18	11	2735–2737
50	Plaintiffs’ Motion for Determination of Good Faith Settlement with Defendants Michelangelo Leasing Inc. d/b/a Ryan’s Express and Edward Hubbard Only on Order Shortening Time	01/18/18	11	2738–2747
51	Calendar Call Transcript	01/18/18	11 12	2748–2750 2751–2752
52	Motor Coach Industries, Inc.’s Pre-Trial Disclosure Pursuant to NRCP 16.1(a)(3)	01/19/18	12	2753–2777
53	Defendant’s Reply in Support of Motion in Limine No. 7 to Exclude Any Claims that the Subject Motor Coach was Defective Based on Alleged Dangerous “Air Blasts”	01/22/18	12	2778–2787
54	Defendants’ Reply in Support of Motion in Limine No. 13 to Exclude Plaintiffs’ Expert Witness Robert Cunitz, Ph.D., or in the Alternative to Limit His Testimony	01/22/18	12	2788–2793

69	Reporter's Transcription of Proceedings	02/16/18	19	4501–4727
70	Motor Coach Industries, Inc.'s Response to "Bench Brief on Contributory Negligence"	02/16/18	19	4728–4747
71	Defendant's Trial Brief in Support of Level Playing Field	02/20/18	19 20	4748–4750 4751–4808
72	Reporter's Transcription of Proceedings	02/20/18	20 21	4809–5000 5001–5039
73	Reporter's Transcription of Proceedings	02/21/18	21	5040–5159
74	Reporter's Transcription of Proceedings	02/22/18	21 22	5160–5250 5251–5314
75	Findings of Fact, Conclusions of Law, and Order	02/22/18	22	5315–5320
76	Bench Brief in Support of Preinstructing the Jury that Contributory Negligence in Not a Defense in a Product Liability Action	02/22/18	22	5321–5327
77	Reporter's Transcription of Proceedings	02/23/18	22 23	5328–5500 5501–5580
78	Reporter's Transcription of Proceedings	02/26/18	23 24	5581–5750 5751–5834
79	Reporter's Transcription of Proceedings	02/27/18	24 25	5835–6000 6001–6006
80	Reporter's Transcription of Proceedings	02/28/18	25	6007–6194
81	Reporter's Transcription of Proceedings	03/01/18	25 26	6195–6250 6251–6448
82	Reporter's Transcription of Proceedings	03/02/18	26 27	6449–6500 6501–6623
83	Reporter's Transcription of Proceedings	03/05/18	27 28	6624–6750 6751–6878
84	Addendum to Stipulated Protective Order	03/05/18	28	6879–6882
85	Jury Trial Transcript	03/06/18	28 29	6883–7000 7001–7044

103	Reporter's Transcription of Proceedings	03/22/18	40 41	9881–10000 10001–10195
104	Reporter's Transcription of Proceedings	03/23/18	41	10196–10206
105	Proposed Jury Instructions Not Given	03/23/18	41	10207–10235
106	Amended Jury List	03/23/18	41	10236
107	Special Jury Verdict	03/23/18	41	10237–10241
108	Jury Instructions	03/23/18	41 42	10242–10250 10251–10297
109	Proposed Jury Verdict Form Not Used at Trial	03/26/18	42	10298–10302
110	Jury Instructions Reviewed with the Court on March 21, 2018	03/30/18	42	10303–10364
111	Notice of Entry of Judgment	04/18/18	42	10365–10371
112	Special Master Order Staying Post-Trial Discovery Including May 2, 2018 Deposition of the Custodian of Records of the Board of Regents NSHE	04/24/18	42	10372–10374
113	Plaintiffs' Verified Memorandum of Costs and Disbursements Pursuant to NRS 18.005, 18.020, and 18.110	04/24/18	42	10375–10381
114	Appendix of Exhibits in Support of Plaintiffs' Verified Memorandum of Costs (Volume 1 of 2)	04/24/18	42 43 44 45 46	10382–10500 10501–10750 10751–11000 11001–11250 11251–11360
115	Appendix of Exhibits in Support of Plaintiffs' Verified Memorandum of Costs (Volume 2 of 2)	04/24/18	46 47	11361–11500 11501–11735
116	Amended Declaration of Peter S. Christiansen, Esq. in Support of Plaintiffs' 4/24/18 Verified Memorandum of Costs and Disbursements Pursuant to NRS 18.005, 18.020, and 18.110	04/25/18	47	11736–11742
117	Motion to Retax Costs	04/30/18	47 48	11743–11750 11751–11760

131	Motor Coach Industries, Inc.'s Response to "Plaintiffs' Supplemental Opposition to MCI's Motion to Alter or Amend Judgment to Offset Settlement Proceeds Paid to Other Defendants"	09/24/18	50	12322–12332
132	Transcript	09/25/18	50	12333–12360
133	Notice of Entry of Stipulation and Order Dismissing Plaintiffs' Claims Against Defendant SevenPlus Bicycles, Inc. Only	10/17/18	50	12361–12365
134	Notice of Entry of Stipulation and Order Dismissing Plaintiffs' Claims Against Bell Sports, Inc. Only	10/17/18	50	12366–12370
135	Order Granting Motion to Dismiss Wrongful Death Claim	01/31/19	50	12371–12372
136	Notice of Entry of Combined Order (1) Denying Motion for Judgment as a Matter of Law and (2) Denying Motion for Limited New Trial	02/01/19	50	12373–12384
137	Notice of Entry of Findings of Fact, Conclusions of Law and Order on Motion for Good Faith Settlement	02/01/19	50	12385–12395
138	Notice of Entry of "Findings of Fact and Conclusions of Law on Defendant's Motion to Retax"	04/24/19	50	12396–12411
139	Notice of Appeal	04/24/19	50	12412–12461
140	Case Appeal Statement	04/24/19	50	12462–12479
141	Notice of Entry of Court's Order Denying Defendant's Motion to Alter or Amend Judgment to Offset Settlement Proceeds Paid by Other Defendants Filed Under Seal on March 26, 2019	05/03/19	50	12480–12489

Filed Under Seal

ALPHABETICAL TABLE OF CONTENTS TO APPENDIX

9	Defendant Sevenplus Bicycles, Inc. d/b/a Pro Cyclery's Demand for Jury Trial	06/30/17	1	137–139
19	Defendant SevenPlus Bicycles, Inc. d/b/a Pro Cyclery's Motion for Determination of Good Faith Settlement	09/22/17	2	313–323
31	Defendant's Motion in Limine No. 7 to Exclude Any Claims That the Subject Motor Coach was Defective Based on Alleged Dangerous "Air Blasts"	12/07/17	7	1572–1583
20	Defendant's Notice of Filing Notice of Removal	10/17/17	2 3	324–500 501–586
55	Defendant's Reply in Support of Motion in Limine No. 17 to Exclude Claim of Lost Income, Including the August 28 Expert Report of Larry Stokes	01/22/18	12	2794–2814
53	Defendant's Reply in Support of Motion in Limine No. 7 to Exclude Any Claims that the Subject Motor Coach was Defective Based on Alleged Dangerous "Air Blasts"	01/22/18	12	2778–2787
71	Defendant's Trial Brief in Support of Level Playing Field	02/20/18	19 20	4748–4750 4751–4808
5	Defendants Michelangelo Leasing Inc. dba Ryan's Express and Edward Hubbard's Answer to Plaintiffs' Amended Complaint	06/28/17	1	81–97
56	Defendants Michelangelo Leasing Inc. dba Ryan's Express and Edward Hubbard's Joinder to Plaintiffs' Motion for Determination of Good Faith Settlement with Michelangelo Leasing Inc. dba Ryan's Express and Edward Hubbard	01/22/18	12	2815–2817
33	Defendants' Motion in Limine No. 13 to Exclude Plaintiffs' Expert Witness	12/07/17	8	1802–1816

	Robert Cunitz, Ph.d., or in the Alternative, to Limit His Testimony			
36	Defendants' Motion in Limine No. 17 to Exclude Claim of Lost Income, Including the August 28 Expert Report of Larry Stokes	12/08/17	9	2106–2128
54	Defendants' Reply in Support of Motion in Limine No. 13 to Exclude Plaintiffs' Expert Witness Robert Cunitz, Ph.D., or in the Alternative to Limit His Testimony	01/22/18	12	2788–2793
6	Demand for Jury Trial	06/28/17	1	98–100
147	Exhibits G–L and O to: Appendix of Exhibits to: Motor Coach Industries, Inc.'s Motion for a Limited New Trial (FILED UNDER SEAL)	05/08/18	51 52	12705–12739 12740–12754
142	Findings of Fact and Conclusions of Law and Order on Motion for Determination of Good Faith Settlement (FILED UNDER SEAL)	03/14/18	51	12490–12494
75	Findings of Fact, Conclusions of Law, and Order	02/22/18	22	5315–5320
108	Jury Instructions	03/23/18	41 42	10242–10250 10251–10297
110	Jury Instructions Reviewed with the Court on March 21, 2018	03/30/18	42	10303–10364
64	Jury Trial Transcript	02/12/18	15 16	3537–3750 3751–3817
85	Jury Trial Transcript	03/06/18	28 29	6883–7000 7001–7044
87	Jury Trial Transcript	03/08/18	30	7266–7423
92	Jury Trial Transcript	03/13/18	33	8026–8170
93	Jury Trial Transcript	03/14/18	33 34	8171–8250 8251–8427
94	Jury Trial Transcript	03/15/18	34 35	8428–8500 8501–8636
95	Jury Trial Transcript	03/16/18	35	8637–8750

			36	8751–8822
98	Jury Trial Transcript	03/19/18	36 37	8842–9000 9001–9075
35	Motion for Determination of Good Faith Settlement Transcript	12/07/17	9	2101–2105
22	Motion for Summary Judgment on Foreseeability of Bus Interaction with Pedestrians or Bicyclists (Including Sudden Bicycle Movement)	10/27/17	3	589–597
26	Motion for Summary Judgment on Punitive Damages	12/01/17	3	642–664
117	Motion to Retax Costs	04/30/18	47 48	11743–11750 11751–11760
58	Motions in Limine Transcript	01/29/18	12 13	2998–3000 3001–3212
61	Motor Coach Industries, Inc.'s Answer to Second Amended Complaint	02/06/18	14	3474–3491
90	Motor Coach Industries, Inc.'s Brief in Support of Oral Motion for Judgment as a Matter of Law (NRCP 50(a))	03/12/18	32 33	7994–8000 8001–8017
146	Motor Coach Industries, Inc.'s Motion for a Limited New Trial (FILED UNDER SEAL)	05/07/18	51	12673–12704
30	Motor Coach Industries, Inc.'s Motion for Summary Judgment on All Claims Alleging a Product Defect	12/04/17	6 7	1491–1500 1501–1571
145	Motor Coach Industries, Inc.'s Motion to Alter or Amend Judgment to Offset Settlement Proceed Paid by Other Defendants (FILED UNDER SEAL)	05/07/18	51	12647–12672
96	Motor Coach Industries, Inc.'s Opposition to Plaintiff's Trial Brief Regarding Admissibility of Taxation Issues and Gross Versus Net Loss Income	03/18/18	36	8823–8838
52	Motor Coach Industries, Inc.'s Pre-Trial Disclosure Pursuant to NRCP 16.1(a)(3)	01/19/18	12	2753–2777

120	Motor Coach Industries, Inc.'s Renewed Motion for Judgment as a Matter of Law Regarding Failure to Warn Claim	05/07/18	48 49	11963–12000 12001–12012
47	Motor Coach Industries, Inc.'s Reply in Support of Its Motion for Summary Judgment on All Claims Alleging a Product Defect	01/17/18	11	2705–2719
149	Motor Coach Industries, Inc.'s Reply in Support of Motion to Alter or Amend Judgment to Offset Settlement Proceeds Paid by Other Defendants (FILED UNDER SEAL)	07/02/18	52	12865–12916
129	Motor Coach Industries, Inc.'s Reply in Support of Renewed Motion for Judgment as a Matter of Law Regarding Failure to Warn Claim	06/29/18	50	12282–12309
70	Motor Coach Industries, Inc.'s Response to "Bench Brief on Contributory Negligence"	02/16/18	19	4728–4747
131	Motor Coach Industries, Inc.'s Response to "Plaintiffs' Supplemental Opposition to MCI's Motion to Alter or Amend Judgment to Offset Settlement Proceeds Paid to Other Defendants"	09/24/18	50	12322–12332
124	Notice of Appeal	05/18/18	49	12086–12097
139	Notice of Appeal	04/24/19	50	12412–12461
138	Notice of Entry of "Findings of Fact and Conclusions of Law on Defendant's Motion to Retax"	04/24/19	50	12396–12411
136	Notice of Entry of Combined Order (1) Denying Motion for Judgment as a Matter of Law and (2) Denying Motion for Limited New Trial	02/01/19	50	12373–12384
141	Notice of Entry of Court's Order Denying Defendant's Motion to Alter or Amend Judgment to Offset Settlement Proceeds Paid by Other	05/03/19	50	12480–12489

	Defendants Filed Under Seal on March 26, 2019			
40	Notice of Entry of Findings of Fact Conclusions of Law and Order on Motion for Determination of Good Faith Settlement	01/08/18	11	2581–2590
137	Notice of Entry of Findings of Fact, Conclusions of Law and Order on Motion for Good Faith Settlement	02/01/19	50	12385–12395
111	Notice of Entry of Judgment	04/18/18	42	10365–10371
12	Notice of Entry of Order	07/11/17	1	158–165
16	Notice of Entry of Order	08/23/17	1	223–227
63	Notice of Entry of Order	02/09/18	15	3511–3536
97	Notice of Entry of Order	03/19/18	36	8839–8841
15	Notice of Entry of Order (CMO)	08/18/17	1	214–222
4	Notice of Entry of Order Denying Without Prejudice Plaintiffs' Ex Parte Motion for Order Requiring Bus Company and Bus Driver to Preserve an Immediately Turn Over Relevant Electronic Monitoring Information from Bus and Driver Cell Phone	06/22/17	1	77–80
13	Notice of Entry of Order Granting Plaintiffs' Motion for Preferential Trial Setting	07/20/17	1	166–171
133	Notice of Entry of Stipulation and Order Dismissing Plaintiffs' Claims Against Defendant SevenPlus Bicycles, Inc. Only	10/17/18	50	12361–12365
134	Notice of Entry of Stipulation and Order Dismissing Plaintiffs' Claims Against Bell Sports, Inc. Only	10/17/18	50	12366–12370
143	Objection to Special Master Order Staying Post-Trial Discovery Including May 2, 2018 Deposition of the Custodian of Records of the Board of Regents NSHE and, Alternatively, Motion for Limited Post-Trial	05/03/18	51	12495–12602

	Discovery on Order Shortening Time (FILED UNDER SEAL)			
39	Opposition to "Motion for Summary Judgment on Foreseeability of Bus Interaction with Pedestrians of Bicyclists (Including Sudden Bicycle Movement)"	12/27/17	11	2524–2580
123	Opposition to Defendant's Motion to Retax Costs	05/14/18	49	12039–12085
118	Opposition to Motion for Limited Post-Trial Discovery	05/03/18	48	11761–11769
151	Order (FILED UNDER SEAL)	03/26/19	52	12931–12937
135	Order Granting Motion to Dismiss Wrongful Death Claim	01/31/19	50	12371–12372
25	Order Regarding "Plaintiffs' Motion to Amend Complaint to Substitute Parties" and "Countermotion to Set a Reasonable Trial Date Upon Changed Circumstance that Nullifies the Reason for Preferential Trial Setting"	11/17/17	3	638–641
45	Plaintiffs' Addendum to Reply to Opposition to Motion for Summary Judgment on Forseeability of Bus Interaction with Pedestrians or Bicyclists (Including Sudden Bicycle Movement)"	01/17/18	11	2654–2663
49	Plaintiffs' Joinder to Defendant Bell Sports, Inc.'s Motion for Determination of Good Faith Settlement on Order Shortening Time	01/18/18	11	2735–2737
41	Plaintiffs' Joint Opposition to Defendant's Motion in Limine No. 3 to Preclude Plaintiffs from Making Reference to a "Bullet Train" and to Defendant's Motion in Limine No. 7 to Exclude Any Claims That the Motor Coach was Defective Based on Alleged Dangerous "Air Blasts"	01/08/18	11	2591–2611

37	Plaintiffs' Joint Opposition to MCI Motion for Summary Judgment on All Claims Alleging a Product Defect and to MCI Motion for Summary Judgment on Punitive Damages	12/21/17	9	2129–2175
50	Plaintiffs' Motion for Determination of Good Faith Settlement with Defendants Michelangelo Leasing Inc. d/b/a Ryan's Express and Edward Hubbard Only on Order Shortening Time	01/18/18	11	2738–2747
42	Plaintiffs' Opposition to Defendant's Motion in Limine No. 13 to Exclude Plaintiffs' Expert Witness Robert Cunitz, Ph.D. or in the Alternative to Limit His Testimony	01/08/18	11	2612–2629
43	Plaintiffs' Opposition to Defendant's Motion in Limine No. 17 to Exclude Claim of Lost Income, Including the August 28 Expert Report of Larry Stokes	01/08/18	11	2630–2637
126	Plaintiffs' Opposition to MCI's Motion to Alter or Amend Judgment to Offset Settlement Proceeds Paid by Other Defendants	06/06/18	49	12104–12112
130	Plaintiffs' Supplemental Opposition to MCI's Motion to Alter or Amend Judgment to Offset Settlement Proceeds Paid by Other Defendants	09/18/18	50	12310–12321
150	Plaintiffs' Supplemental Opposition to MCI's Motion to Alter or Amend Judgment to Offset Settlement Proceeds Paid by Other Defendants (FILED UNDER SEAL)	09/18/18	52	12917–12930
122	Plaintiffs' Supplemental Verified Memorandum of Costs and Disbursements Pursuant to NRS 18.005, 18.020, and 18.110	05/09/18	49	12019–12038

91	Plaintiffs' Trial Brief Regarding Admissibility of Taxation Issues and Gross Versus Net Loss Income	03/12/18	33	8018–8025
113	Plaintiffs' Verified Memorandum of Costs and Disbursements Pursuant to NRS 18.005, 18.020, and 18.110	04/24/18	42	10375–10381
105	Proposed Jury Instructions Not Given	03/23/18	41	10207–10235
109	Proposed Jury Verdict Form Not Used at Trial	03/26/18	42	10298–10302
57	Recorder's Transcript of Hearing on Defendant's Motion for Summary Judgment on All Claims Alleging a Product Defect	01/23/18	12	2818–2997
148	Reply in Support of Motion for a Limited New Trial (FILED UNDER SEAL)	07/02/18	52	12755–12864
128	Reply on Motion to Retax Costs	06/29/18	50	12269–12281
44	Reply to Opposition to Motion for Summary Judgment on Foreseeability of Bus Interaction with Pedestrians or Bicyclists (Including Sudden Bicycle Movement)"	01/16/18	11	2638–2653
46	Reply to Plaintiffs' Opposition to Motion for Summary Judgment on Punitive Damages	01/17/18	11	2664–2704
3	Reporter's Transcript of Motion for Temporary Restraining Order	06/15/17	1	34–76
144	Reporter's Transcript of Proceedings (FILED UNDER SEAL)	05/04/18	51	12603–12646
14	Reporter's Transcription of Motion for Preferential Trial Setting	07/20/17	1	172–213
18	Reporter's Transcription of Motion of Status Check and Motion for Reconsideration with Joinder	09/21/17	1 2	237–250 251–312
65	Reporter's Transcription of Proceedings	02/13/18	16 17	3818–4000 4001–4037
66	Reporter's Transcription of Proceedings	02/14/18	17 18	4038–4250 4251–4308

68	Reporter's Transcription of Proceedings	02/15/18	18	4315–4500
69	Reporter's Transcription of Proceedings	02/16/18	19	4501–4727
72	Reporter's Transcription of Proceedings	02/20/18	20 21	4809–5000 5001–5039
73	Reporter's Transcription of Proceedings	02/21/18	21	5040–5159
74	Reporter's Transcription of Proceedings	02/22/18	21 22	5160–5250 5251–5314
77	Reporter's Transcription of Proceedings	02/23/18	22 23	5328–5500 5501–5580
78	Reporter's Transcription of Proceedings	02/26/18	23 24	5581–5750 5751–5834
79	Reporter's Transcription of Proceedings	02/27/18	24 25	5835–6000 6001–6006
80	Reporter's Transcription of Proceedings	02/28/18	25	6007–6194
81	Reporter's Transcription of Proceedings	03/01/18	25 26	6195–6250 6251–6448
82	Reporter's Transcription of Proceedings	03/02/18	26 27	6449–6500 6501–6623
83	Reporter's Transcription of Proceedings	03/05/18	27 28	6624–6750 6751–6878
86	Reporter's Transcription of Proceedings	03/07/18	29 30	7045–7250 7251–7265
88	Reporter's Transcription of Proceedings	03/09/18	30 31	7424–7500 7501–7728
89	Reporter's Transcription of Proceedings	03/12/18	31 32	7729–7750 7751–7993
99	Reporter's Transcription of Proceedings	03/20/18	37 38	9076–9250 9251–9297
100	Reporter's Transcription of Proceedings	03/21/18	38 39	9298–9500 9501–9716
101	Reporter's Transcription of Proceedings	03/21/18	39 40	9717–9750 9751–9799

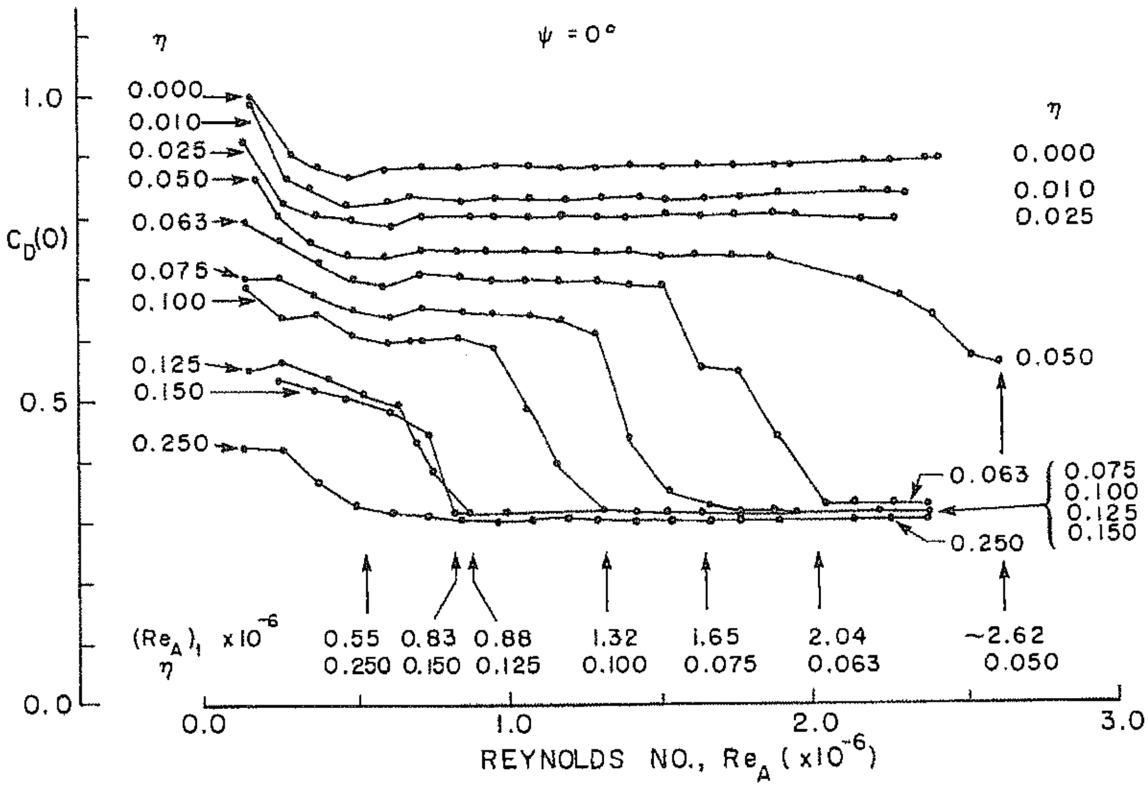

FIG. 11: VARIATION OF DRAG COEFFICIENT AT ψ = 0° WITH REYNOLDS NUMBER (EDGE RADIUS AS PARAMETER)

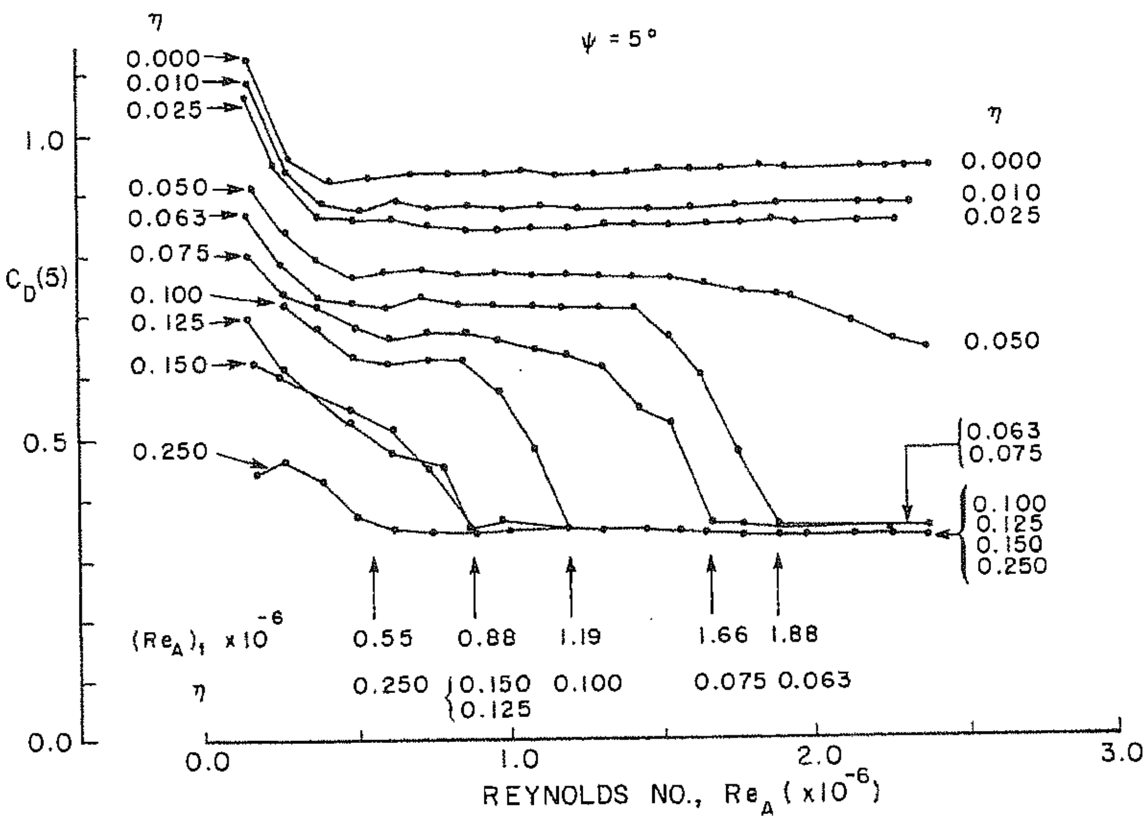

FIG. 12: VARIATION OF DRAG COEFFICIENT AT ψ = 5° WITH REYNOLDS NUMBER (EDGE RADIUS AS PARAMETER)

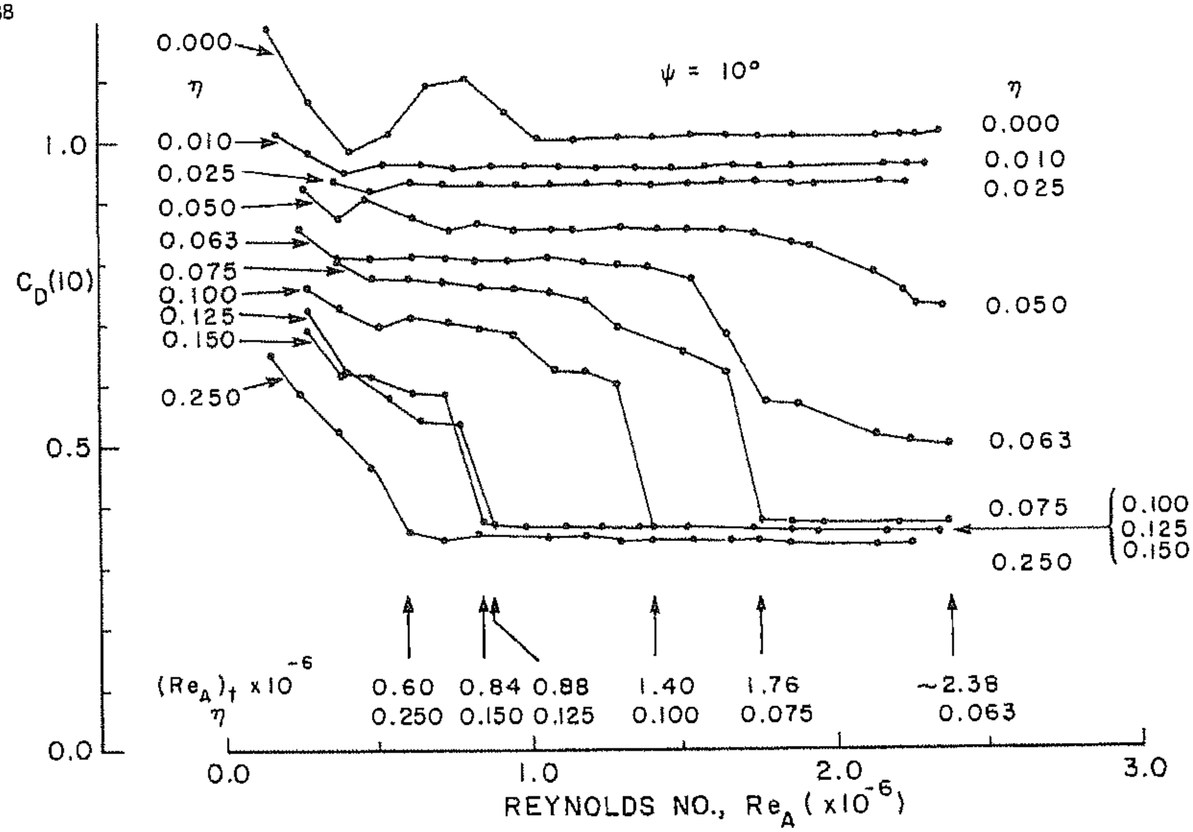

FIG. 13: VARIATION OF DRAG COEFFICIENT AT ψ = 10° WITH REYNOLDS NUMBER (EDGE RADIUS AS PARAMETER)

002252

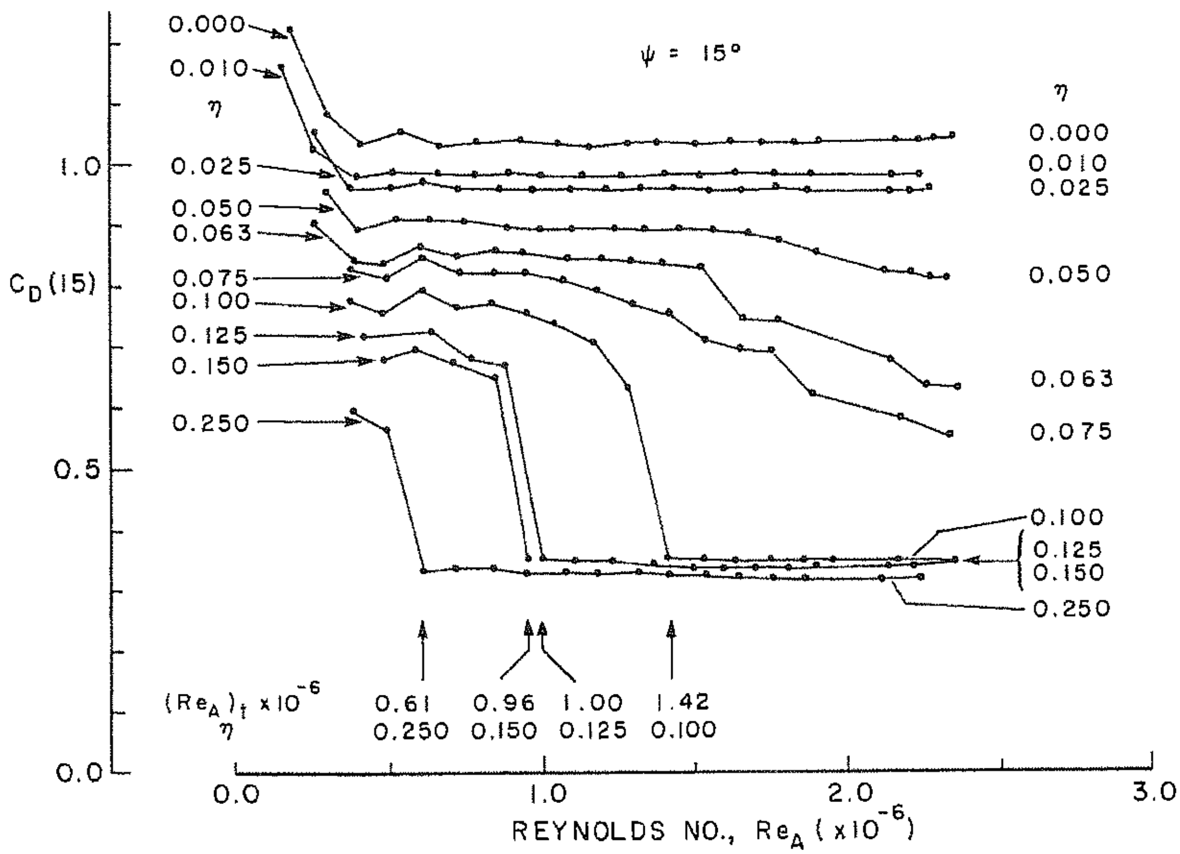

FIG. 14: VARIATION OF DRAG COEFFICIENT AT ψ = 15° WITH REYNOLDS NUMBER (EDGE RADIUS AS PARAMETER)

002252

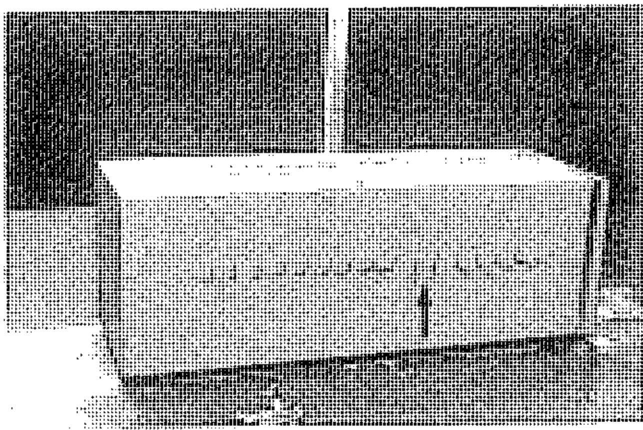

$Re_A = 1.82 \times 10^6$, $C_D = 0.734$, $x_r/L = 0.356$

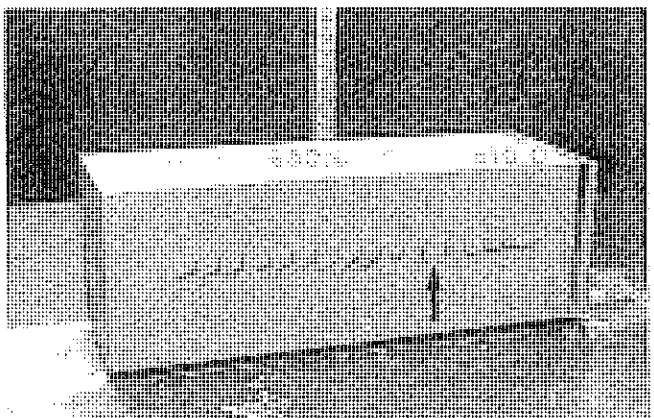

$Re_A = 2.08 \times 10^6$, $C_D = 0.701$, $x_r/L = 0.311$

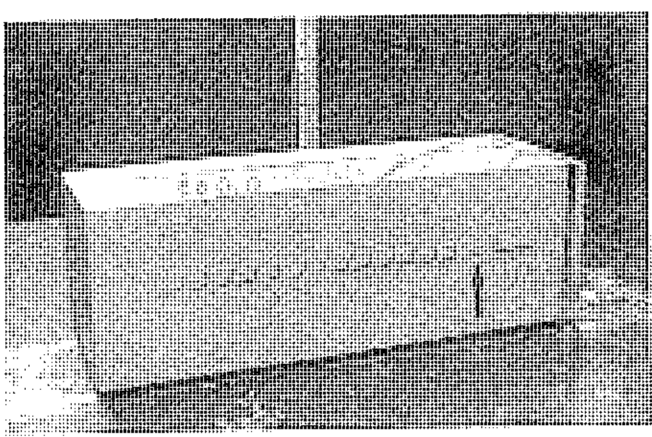

$Re_A = 2.30 \times 10^6$, $C_D = 0.663$, $x_r/L = 0.200$

FIG. 15: SURFACE FLOW AT $\psi = 0°$ WITH $\eta = 0.05$
(REATTACHMENT POINTS INDICATED BY ARROWS)

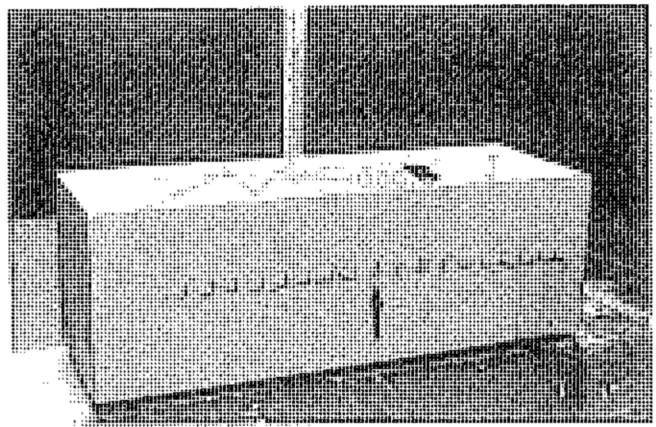

$Re_A = 1.29 \times 10^6$, $C_D = 0.695$; Flow separated on top and side

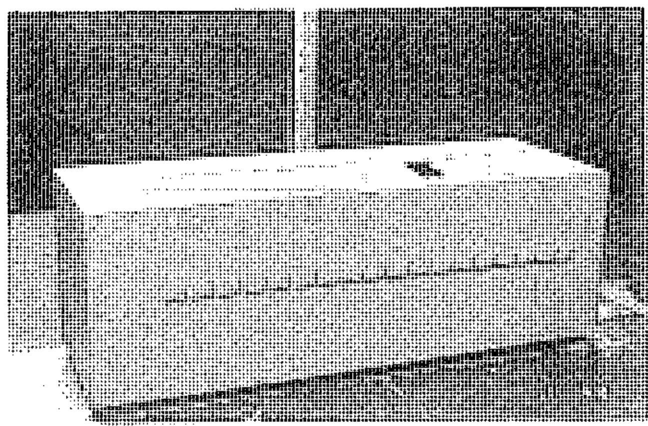

$Re_A = 1.67 \times 10^6$, $C_D = 0.550$; Flow separated on top, attached on side

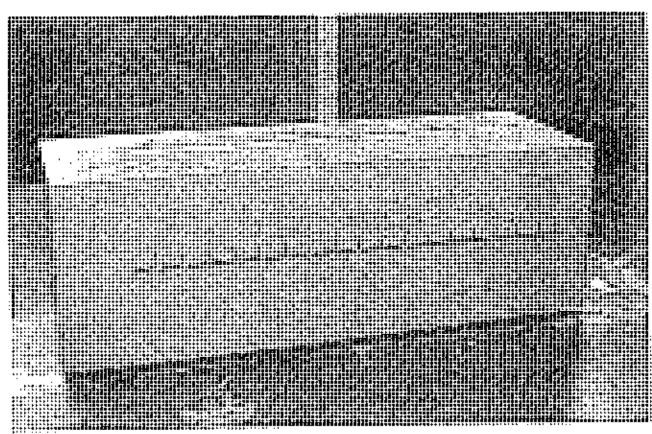

$Re_A = 2.04 \times 10^6$, $C_D = 0.324$; Flow attached on top and side

FIG. 16: SURFACE FLOW AT $\psi = 0°$ WITH $\eta = 0.063$
(REATTACHMENT POINTS INDICATED BY ARROWS)

002253

different asymptotic flow separation and flow reattachment points. Measurements on square and rectangular two-dimensional prisms [8] have also shown nearly identical drag coefficients for combinations of radius and Reynolds number that produce fully-attached leading-edge flow.

An alternate way of looking at the data is provided by cross-plotting the measurements in Figures 11 through 14 as functions of edge radius with the Reynolds number as a parameter. This type of measurement is most commonly found in the literature [1,2,3]. An example of such a cross-plot is shown in Figure 17, taken from Figure 12 for $\psi = 5°$, at six different Reynolds numbers. These curves define the optimum edge radius for a given Reynolds number, where the optimum is taken to be the smallest radius that provides fully-attached flow at that Reynolds number. It is immediately apparent that a test designed to define this optimum will give different answers at different test Reynolds numbers, except at very high values, as shown. This situation is unacceptable to the designer and is a serious problem faced, and often unrecognized, in many small-scale, low-Reynolds number tests.

Later in the paper it will be shown how these data can be collapsed, allowing an accurate extrapolation of model scale data to full scale and providing a clear indication of the optimum front-edge rounding needed to efficiently reduce the drag of box-shaped vehicles.

The graphs of Figures 11 to 14 were based on runs with test speed increasing, and when the measurements were then made with test speed decreasing different behaviour was found. Figure 18 shows this situation. The shaded regions are regions of flow hysteresis where two values of drag coefficient can occur depending on whether speed is increasing or decreasing, as indicated by the arrows on the curves. Once the flow has become attached it stays attached to a lower Reynolds number before separating once again. The hysteresis was usually small at high and low Reynolds numbers but was large at transitional values, especially for $0.05<\eta<0.10$.

An indication of the Reynolds number behaviour of the other aerodynamic coefficients is presented in Figure 19. The data are at a yaw angle of 5° and are typical of the data at other angles. Side force, rolling moment, and lift to a lesser extent, all seem relatively independent of both Reynolds number and edge radius, while pitching moment and yawing moment are sensitive to both radius and Reynolds number.

The pitching moment reflects the drag coefficient changes since, with the origin of co-ordinates at ground level, it is primarily due to the drag vector acting roughly in the middle of the body. The yawing moment changes reflect the forward shift in the centre of pressure of the side force as the sidewall separation bubble is reduced or disappears at large values of radius or Reynolds number.

YAW BEHAVIOUR - The influence of yaw angle on Reynolds number behaviour can be seen in Figure 20, which clearly shows the increase in transcritical Reynolds number as yaw angle increases, for an edge radius of $\eta = 0.075$. It is evident that attached flow on the body sides occurs up to 10° yaw angle but not at 15° angle with this edge radius.

Another perspective of the model's yaw behaviour, with edge radius as a parameter at fixed Reynolds number, can be found in Figure 21 and Figure 22. Figure 21 shows the drag coefficients for all edge radii at $Re_A = 2.2\times10^6$. These measurements are symmetrical about 0° yaw angle, for small and large radii, but are asymmetrical for values of radius that are in the transitional Reynolds number region for $Re_A = 2.2\times10^6$. Here, the asymmetry is due to a yaw hysteresis where double-valued drag coefficients can occur at mid-range yaw angles, depending on whether yaw angle is increasing or decreasing. A few measurements of this yaw hysteresis were made and one example is presented as the shaded region in Figure 21 for $\eta = 0.063$. It is the author's experience that the large hysteresis seen here is common for very simple or aerodynamically clean shapes but that it is usually much reduced by typical vehicle details like break lines, seams and protuberances, or by the incident wakes from other vehicle components such as the cab or exhaust wakes flowing over the truck body or the trailer front face.

The yaw behaviour of the other forces and moments is shown in Figure 22 at four selected radii. Again, the relative insensitivity of side force and rolling moment with edge radius are apparent, although some change does occur as indicated by changes in the side force and rolling moment coefficient slopes presented in the figure. These slopes, $C_{S,\psi}$ and $C_{RM,\psi}$, respectively, were obtained from linear regression through the seven data points between ±3° yaw angle. The reductions in lift and pitching moment are probably a result of reduced roof suctions and lower drag, respectively, as edge radius is increased. The change in yawing moment is also striking as the yawing moment slope near 0° yaw angle is negative for square edges and for small radii (note data for a fifth radius of $\eta = 0.025$ has been added to this graph only). This slope becomes positive for radii equal to or greater than $\eta = 0.050$, and increases with increasing radius - a result of the forward shift of the centre of pressure of side force. The negative yawing moment slopes are a result of the centre of pressure lying aft of the body centre.

FLOW TRIPPING - A brief study into the use of strips of grit or other particles to reduce the critical and transcritical Reynolds numbers was made using three of the radii employed in the main part of the test. A strip was formed by painting on a band of glue and sprinkling on the particles. The strip was placed near the top and side edges on the front face only, as seen in Figure 5.

The effects of grit size, strip width and strip location were examined. Figure 23 shows the influence of the most effective trip used - 0.9 mm spherical glass beads. The transcritical Reynolds number for $\eta = 0.063$ has been reduced by a factor of nearly two, from $(Re_A)_t = 2.05\times10^6$ to $(Re_A)_t = 1.08\times10^6$.

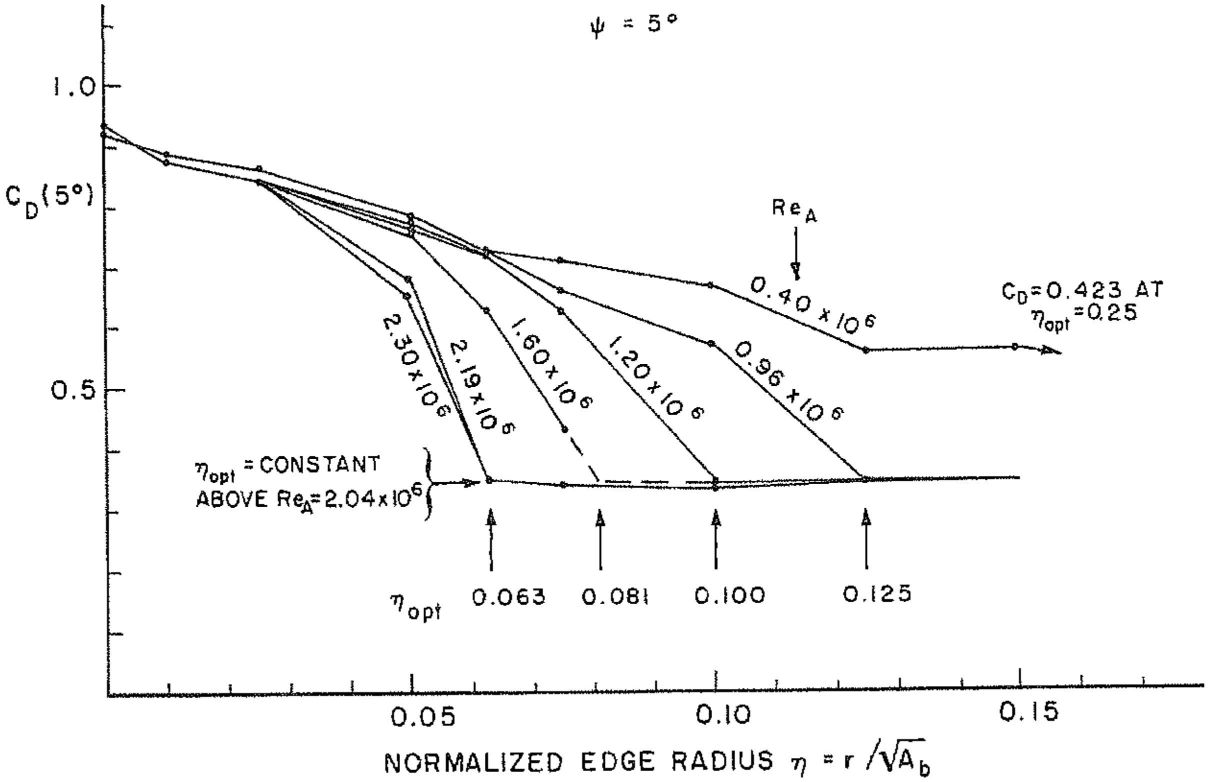

FIG. 17: VARIATION OF OPTIMUM FRONT-EDGE RADIUS WITH REYNOLDS NUMBER

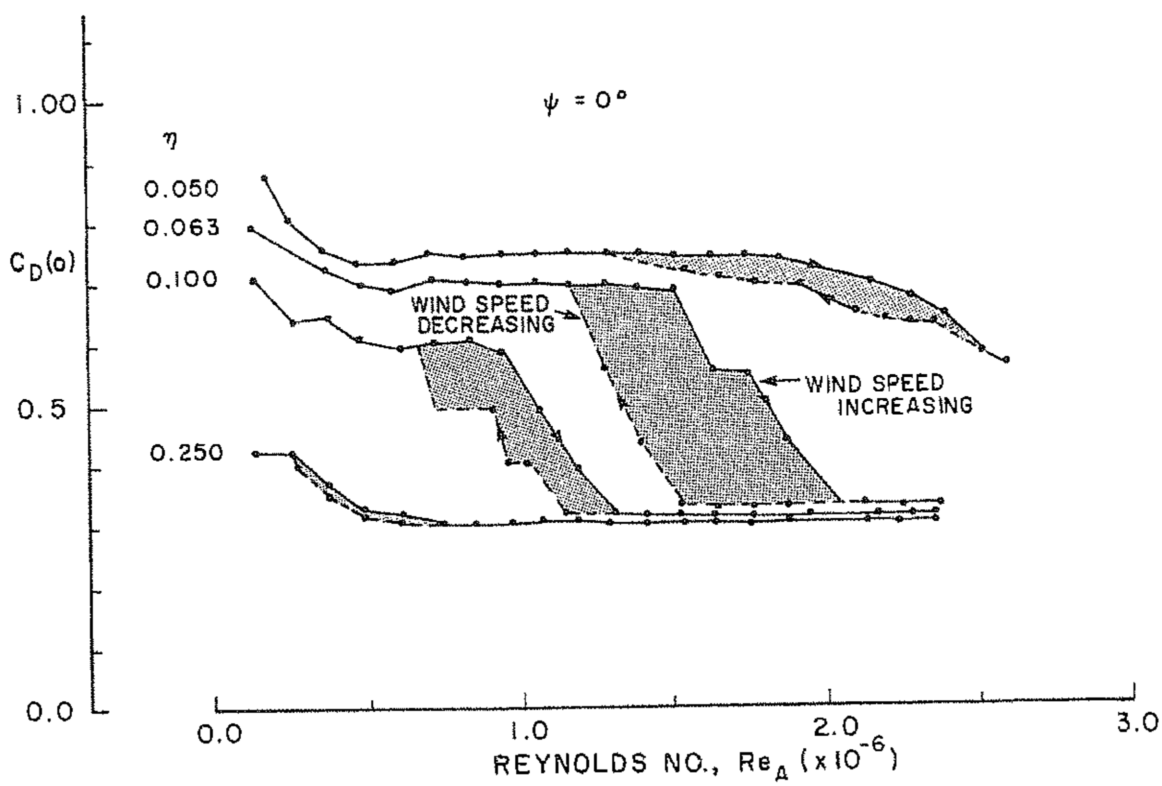

FIG. 18: EXAMPLE OF REYNOLDS-NUMBER-DEPENDENT FLOW HYSTERESIS

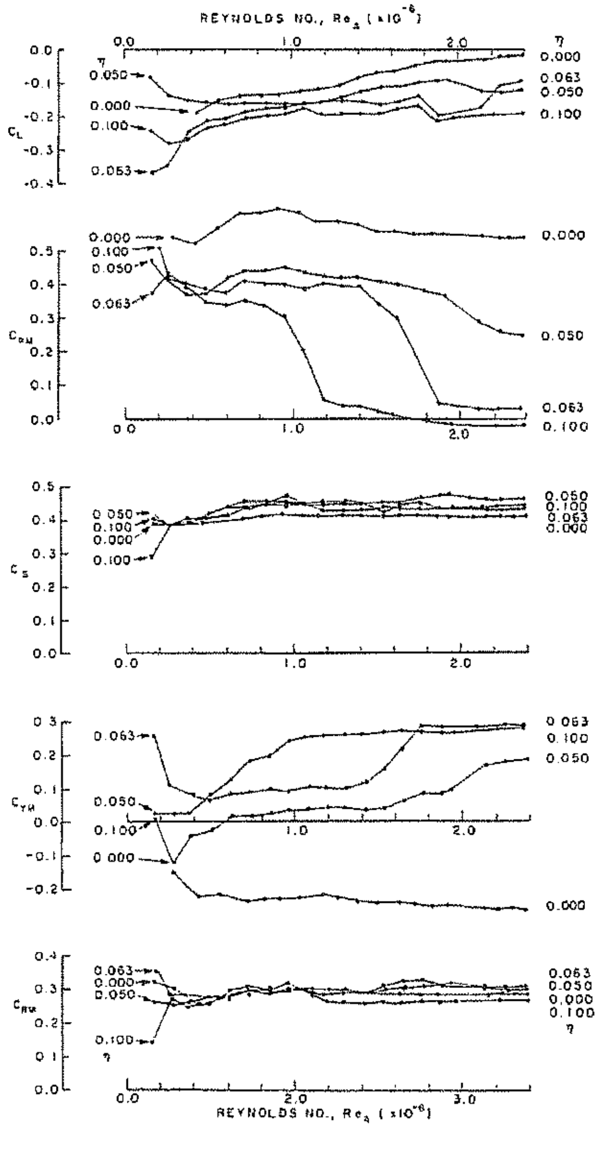

FIG. 19: EFFECT OF REYNOLDS NUMBER AND EDGE RADIUS ON LIFT, PITCHING MOMENT, SIDE FORCE, YAWING MOMENT AND ROLLING MOMENT AT $\psi = 5°$

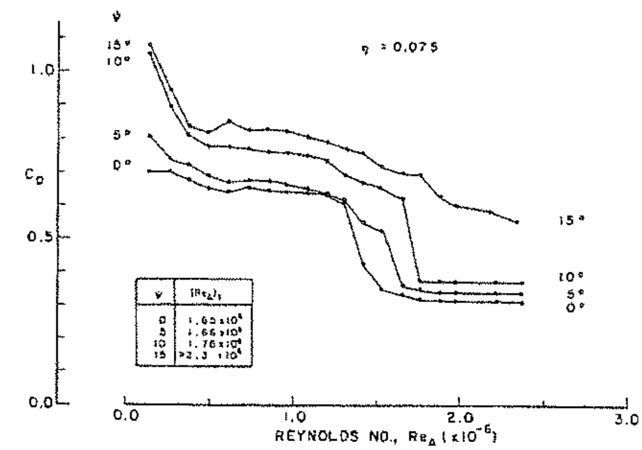

FIG. 20: VARIATION OF TRANSCRITICAL REYNOLDS NUMBER WITH YAW ANGLE FOR η = 0.075

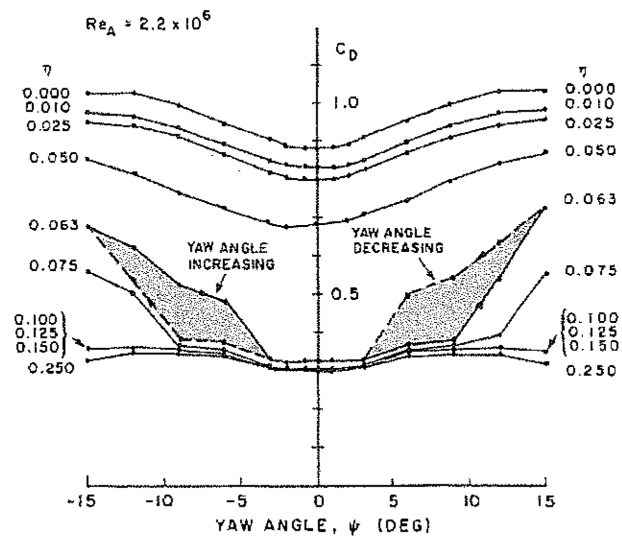

FIG. 21: VARIATION OF DRAG COEFFICIENT WITH YAW ANGLE SHOWING YAW-DEPENDENT FLOW HYSTERESIS

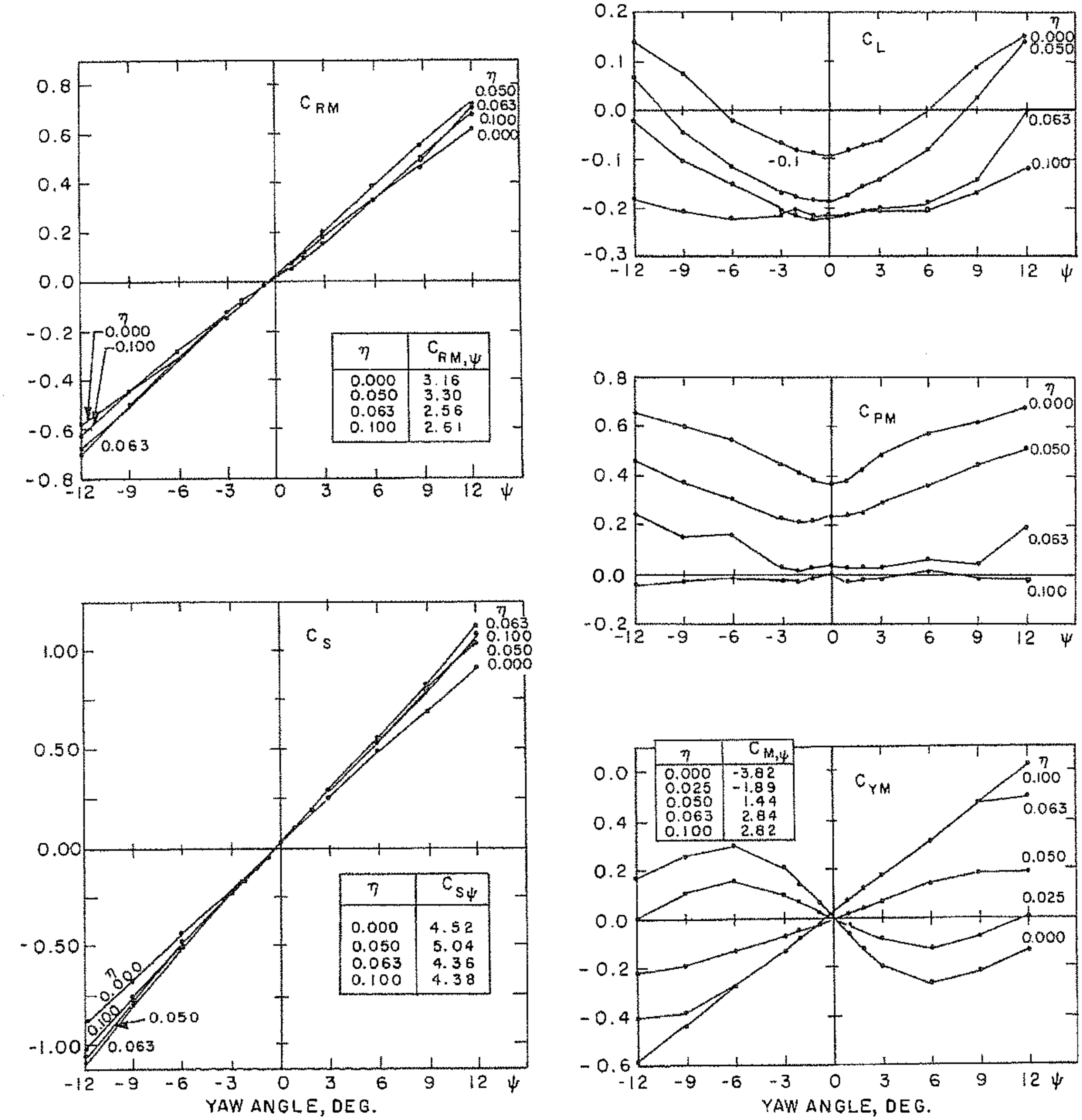

FIG. 22: VARIATION OF LIFT, PITCHING MOMENT, SIDE FORCE, YAWING MOMENT AND ROLLING MOMENT WITH YAW ANGLE

The size of the trip particles and the strip location on the front face were important to the overall behaviour, as shown in Figure 24. The strip was located on the front face the same distance in from the side and top edges, as shown in the inset sketch. A trip strip was not used for the bottom, square edge. The width of the trip strip, over the range from 3 mm to 12 mm, was found to be of secondary importance.

Different particle sizes and locations were found to result in different reductions in transcritical Reynolds number and, unfortunately, in different asymptotic drag values at high Reynolds number. Not enough tests were performed to generalize with certainty, but indications were that a particle strip-width of one-quarter the edge radius, located at a distance equal to the radius of the edge ($y/r = 1$) toward the centre of the front face, and with a particle size that gave the lowest drag would be close to the best choice.

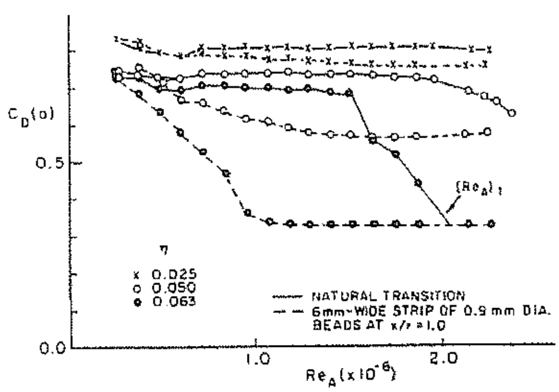

FIG. 23: EFFECT OF PARTICLE STRIPS ON REYNOLDS NUMBER DEPENDENT BEHAVIOUR OF DRAG COEFFICIENT AT $\psi = 0°$

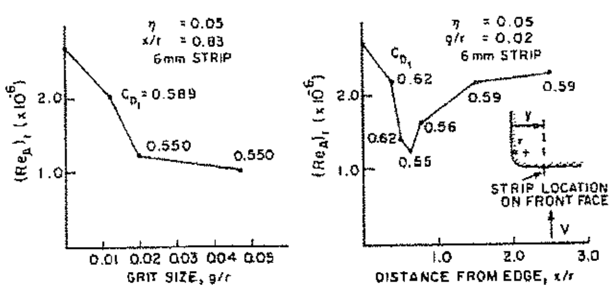

FIG. 24: EFFECTS OF PARTICLE SIZE AND STRIP LOCATION ON TRANSCRITICAL REYNOLDS NUMBER AND DRAG COEFFICIENT AT $\psi = 0°$

TRANSCRITICAL REYNOLDS NUMBER COLLAPSE

An interesting result was obtained when the transcritical Reynolds numbers, $(Re_A)_t$, of Figure 11 to Figure 14 are plotted against non-dimensional radius, η, using a log-log scale. The locus of these data points was a straight line that completely defined the transcritical Reynolds number behaviour, as shown in the right-hand curve of Figure 25. The transcritical Reynolds number can be related to edge radius by:

$$\eta = r/\sqrt{A} = k(Re_A)_t^a \qquad (2)$$

Linear regression results in

$$k = 1.30 \times 10^5$$

and

$$a = -1$$

giving

$$\eta = 1.30 \times 10^5/(Re_A)_t \qquad (3)$$

From this it is apparent that the transcritical Reynolds number is a constant, if based on edge-radius, where:

$$(Re_r)_t = rV_t/\nu = (Re_A)_t(r/\sqrt{A}) = 1.30 \times 10^5 \qquad (4)$$

The collapse of the measured data on this functional form is shown in the left-hand curve of Figure 25. The measured values of transcritical Reynolds number are seen to increase only a small amount with yaw angle over the range tested, up to 15°, and this effect is ignored in the fit above.

A preliminary version of this collapse was presented previously by Cooper [9] using sparse data from the literature. The current study arose from the possibilities suggested by that analysis. Polhamus [8] had also suggested that the critical Reynolds number for two-dimensional rectangular prisms with rounded edges was approximately constant when edge radius was selected as the reference length for the Reynolds number calculation.

OPTIMUM EDGE RADIUS

The major application of the data presented in Figures 11 to 14 is to the determination of the optimum edge radius required for minimum drag. As before, the optimum is the value of radius that reduces the drag to the lowest level through fully-attached, leading-edge flow. The optima are found from typical cross-plots like Figure 17, for $\psi = 5°$. It is evident from this figure that the optimum radius reduces with increasing Reynolds number, up to a value of $Re_A = 2.04 \times 10^6$, but that the optimum radius has a constant minimum value of $\eta_{opt} = 0.063$ above this Reynolds number. Fully-attached, front-end flow does not occur at smaller radii, no matter how high the Reynolds number. The tendency of the drag coefficient to

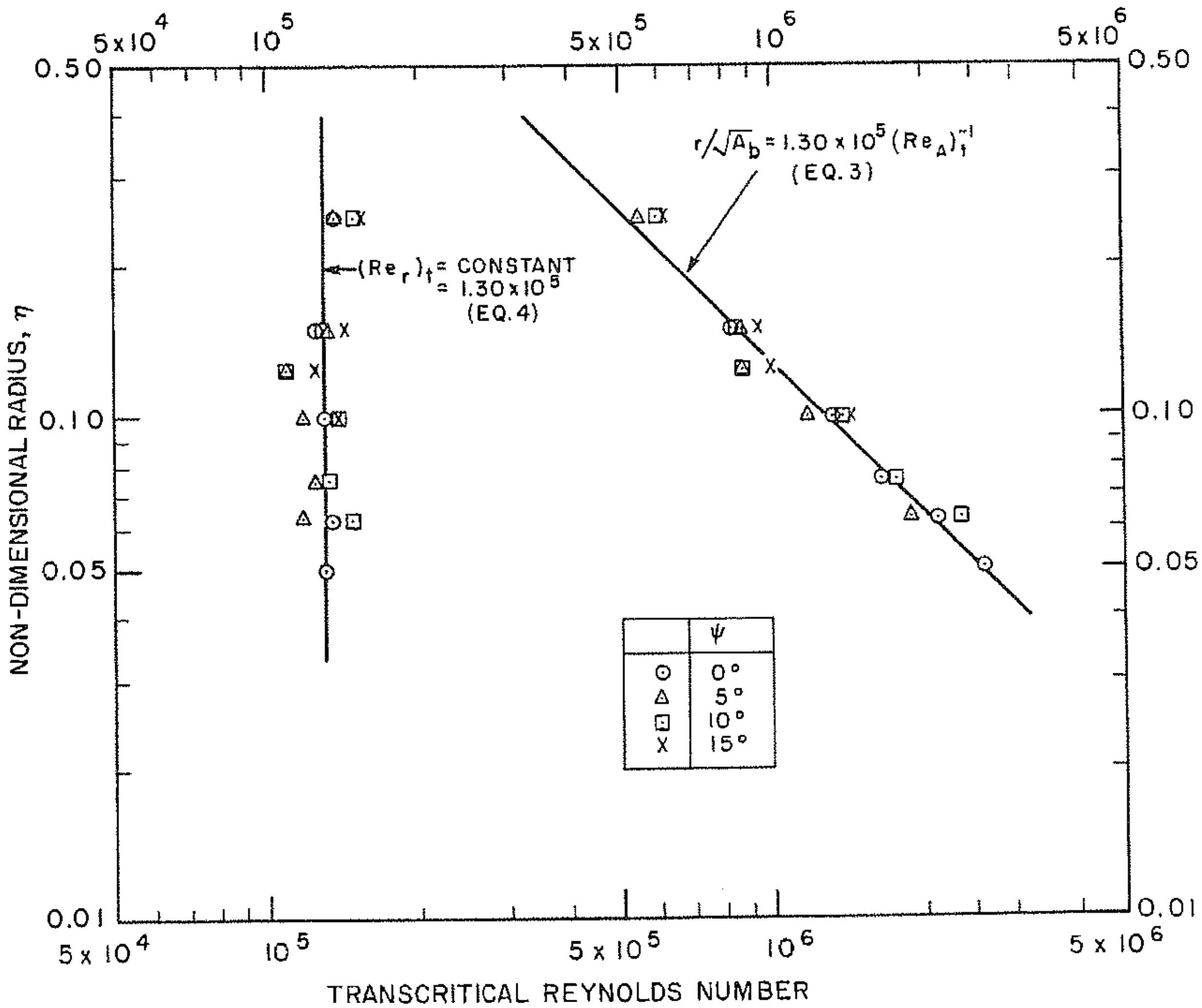

FIG. 25: COLLAPSE OF FRONT-EDGE RADIUS DATA ONTO A UNIVERSAL CURVE

plateau at a higher value for $\eta < 0.050$, compared to the much lower drag plateau for $\eta > 0.063$, as can be seen in Figure 12, indicates that this is the case.

Almost identical behaviour is found at 0° yaw angle, and similar behaviour occurs at 10° and 15° yaw angle. The only difference in the latter two cases is that the Reynolds number break points at which the minimum values of η_{opt} occur become successively lower and the value of constant radius successively larger, as yaw angle increases. All four yaw angles follow the same relationship with Reynolds number, at low Reynolds number, until the minimum allowable value for a given yaw angle is reached, at which point η_{opt} becomes constant. Thus, a single curve with a series of yaw-angle-dependent branches is formed, as shown by the data points in Figure 26. At Reynolds numbers below the break points the values of optimum radii follow the same curve as in Figure 25. An examination of Figures 11 to 14 show that this must be the case.

The solid lines drawn through the points in Figure 26 are proposed as the optimum-edge-radius design boundaries required to minimize aerodynamic drag for box-like vehicles. They depend on Reynolds number and maximum yaw angle only.

The upper bound, at low Reynolds numbers, is set at $\eta_{opt} = 0.500$ since, for radii larger than body height or width, the rounded edges would not be parallel to the roof or sides. The lower limits depend on yaw angle and are set by the minimum radii for fully-attached flow at high Reynolds number. The maximum yaw angle limits are specified in the inset graph of Figure 26 and were determined from the data of Figures 11, 12, 13, 14 and 21.

A yaw range greater than 15° is probably not necessary for two reasons. Firstly, as will be shown, higher yaw angles are uncommon at typical road speeds. Secondly, attached flow is unlikely to occur at higher yaw angles, especially on geometrically more complex, less smooth shapes typical of real vehicles.

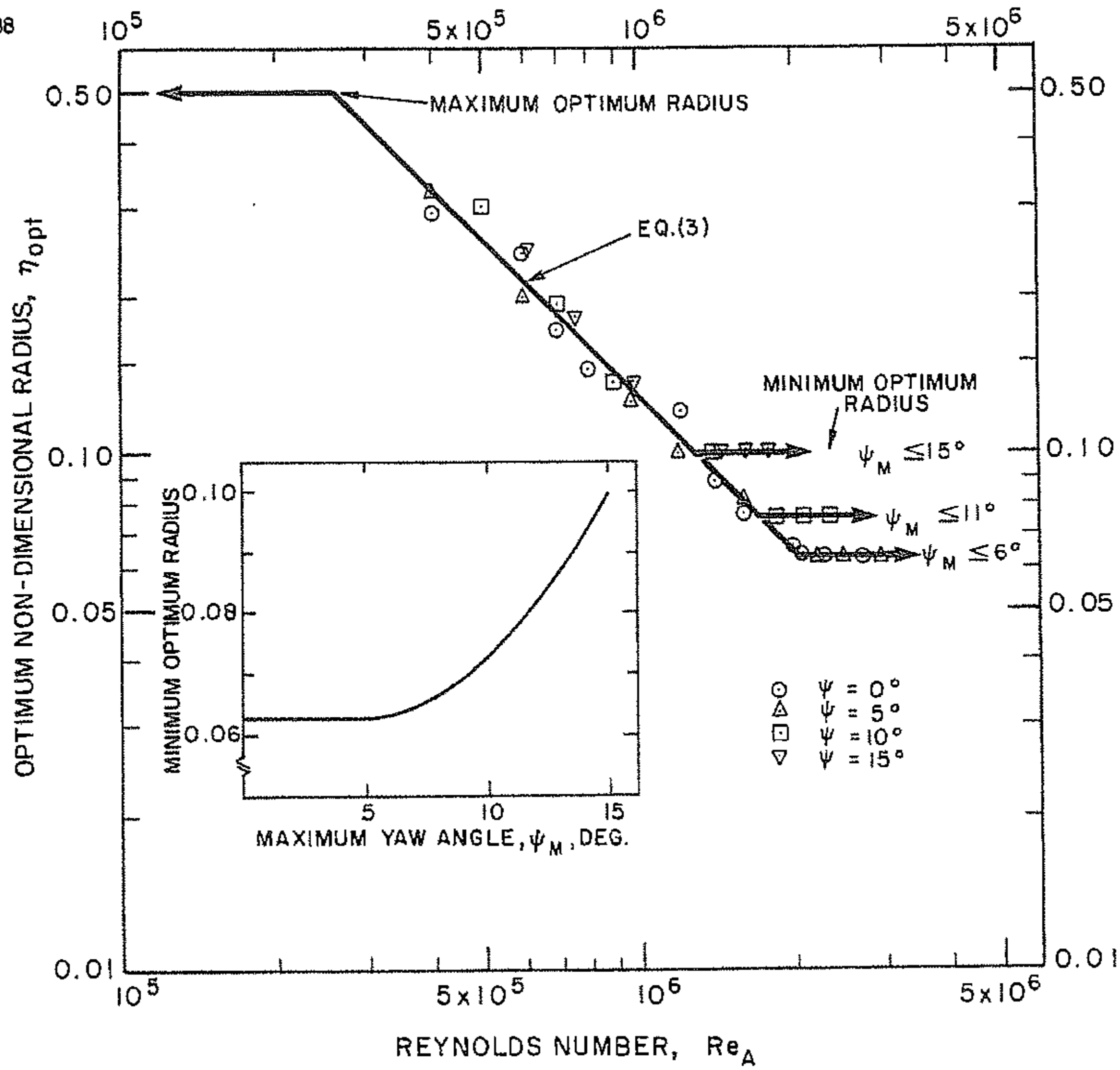

FIG. 26: OPTIMUM FRONT-EDGE RADIUS DESIGN BOUNDARIES

The lower bounds are subject to interpretation, of course, because the limiting behaviour must occur somewhere between the boundary values found in the tests. For example, at $\psi = 5°$, the minimum radius will be between $\eta_{opt} = 0.050$ and $\eta_{opt} = 0.063$, the next higher value tested. In each case the higher value was chosen as being conservative.

The straight line joining the constant upper and lower bounds is identical to that found in Figure 25 and given by eq. (3).

CORRELATION WITH OTHER DATA - The question still remains as to how well the measurements on a simple rectangular body apply to trucks, buses or rail vehicles, at either model or full scale. An answer is provided, in part, in Figure 27 where the optimum radii derived from other sources and on other vehicle types [1,3,8,10,12,13,14] are plotted and compared to the boundaries of Figure 26. Most of the data are at 0° yaw angle, although the truck measurements are based on wind-averaged drag coefficient, which include yaw angles up to 7°. The open symbols, in particular, are from measurements on detailed models of real vehicles and, in one instance [3], on full scale vans. In general, the optimum edge-radius-Reynolds-number boundaries of Figure 26 appear to correlate well with most other available measurements. It would be expected that surface discontinuities, roughness, and upstream disturbances could reduce the optimum radii compared to the smooth body used in the current tests, as is generally seen.

An additional correlation is provided in the data of Figure 28, which also demonstrates the differences in drag reduction possible between the simple, rectangular body and more complex vehicle shapes. The comparison contains front-edge-rounding data for the current rectangular body, for two tractor-trailers [10] and two straight trucks [14] at 1:10 scale, and for a full-scale Ford straight truck [15] in the 9m × 9 m wind tunnel of the National Research Council of Canada. The graph shows some interesting trends. As mentioned previously, the drag-reducing potential of edge rounding is much greater for a

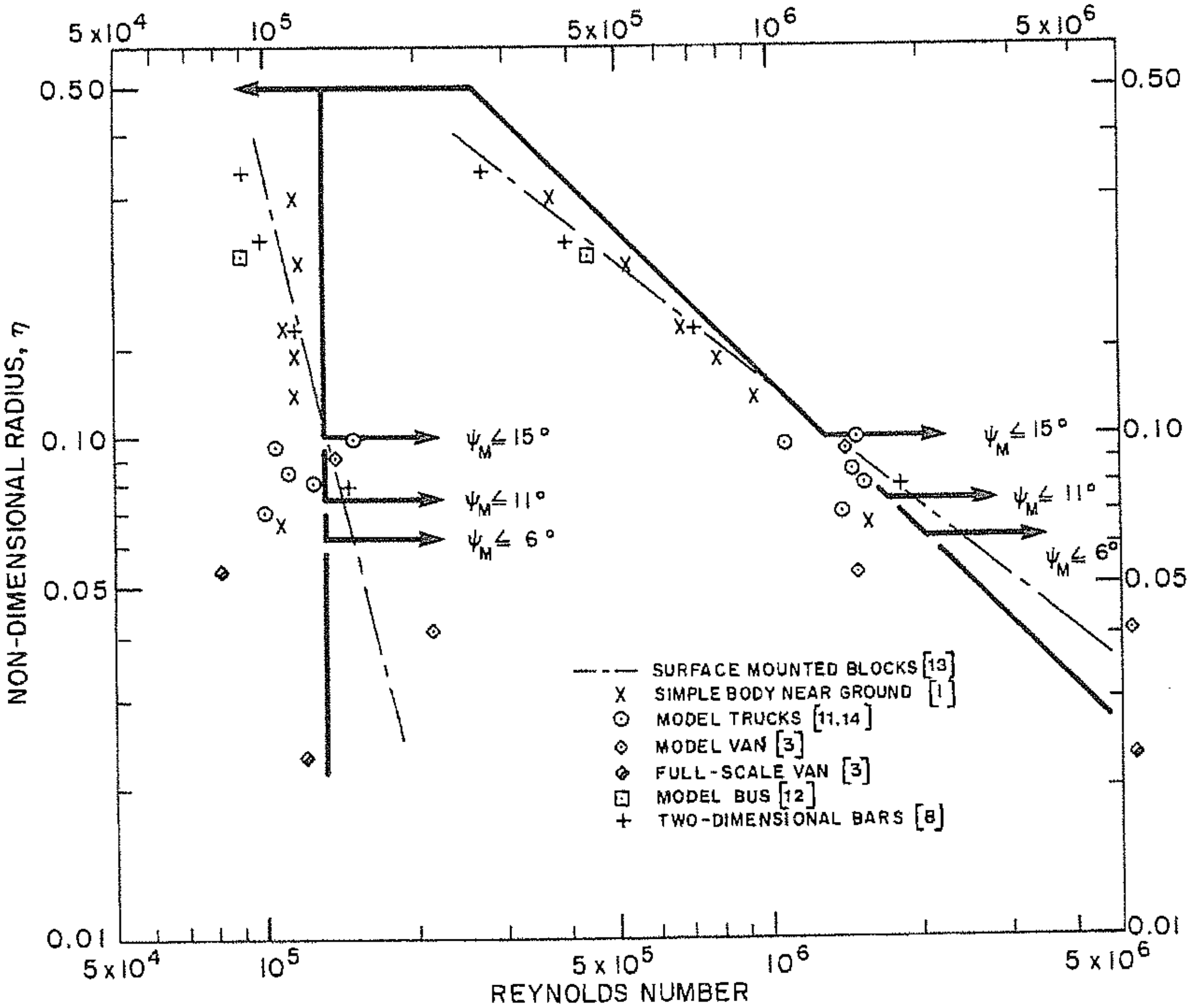

FIG. 27: COMPARISON OF FRONT-EDGE RADIUS DESIGN BOUNDARIES WITH OTHER MEASUREMENTS

simple body like a bus or van than it is for more complex vehicles like truck bodies or trailers. In the former case, the edge rounding must cause a significant change in the pressure distribution over the whole front face when the radius reaches the optimum value. Fully-attached edge flow occurs and the consequent large drag drop to nearly constant values at greater radii is found. In the latter case, the cab wake flow shelters a majority of the truck body or trailer and so the pressure changes are more localized near the front edges, and the drag reduction is less. At lower values of edge radius the rectangular body and the road vehicles tend to behave similarly.

The optimum radii for all the configurations shown have nearly the same value as that for the rectangular body, as indicated, and it is this correlation - the break point in the drag curves being at the same radius - that is of most significance.

Using smoke, Ford's engineers observed that even at $\eta = 0.104$ some flow separation remained on the roof of the body; a finding that differs with the rectangular body results and that could be due to the short body length used by Ford, only 1.5 times the body width. Nevertheless, the current test results would predict a required edge radius that would be close to the value giving lowest drag on the full-scale truck. Finally, the fractional drag reductions for the model and full-scale straight trucks are nearly identical - an encouraging finding for the wind-tunnel aerodynamicist.

REQUIRED MODEL REYNOLDS NUMBERS

The data from the first test can also be used to help guide the selection of the model Reynolds number required to give wind tunnel data that will correlate with full-scale. The SAE Standard Practice, J1252 [7], recommends $Re_A=0.7\times10^6$. Test results from Cooper et al [16] made in support of this Practice found that 1.0×10^6 or even higher was a better choice and found that small Reynolds number effects could still be seen at $Re_A=1.6\times10^6$. Examination of Figures 11 to 14 and Figure 17 suggest that the required Reynolds number should be increased to about 2.0×10^6, roughly in line with the findings of [16].

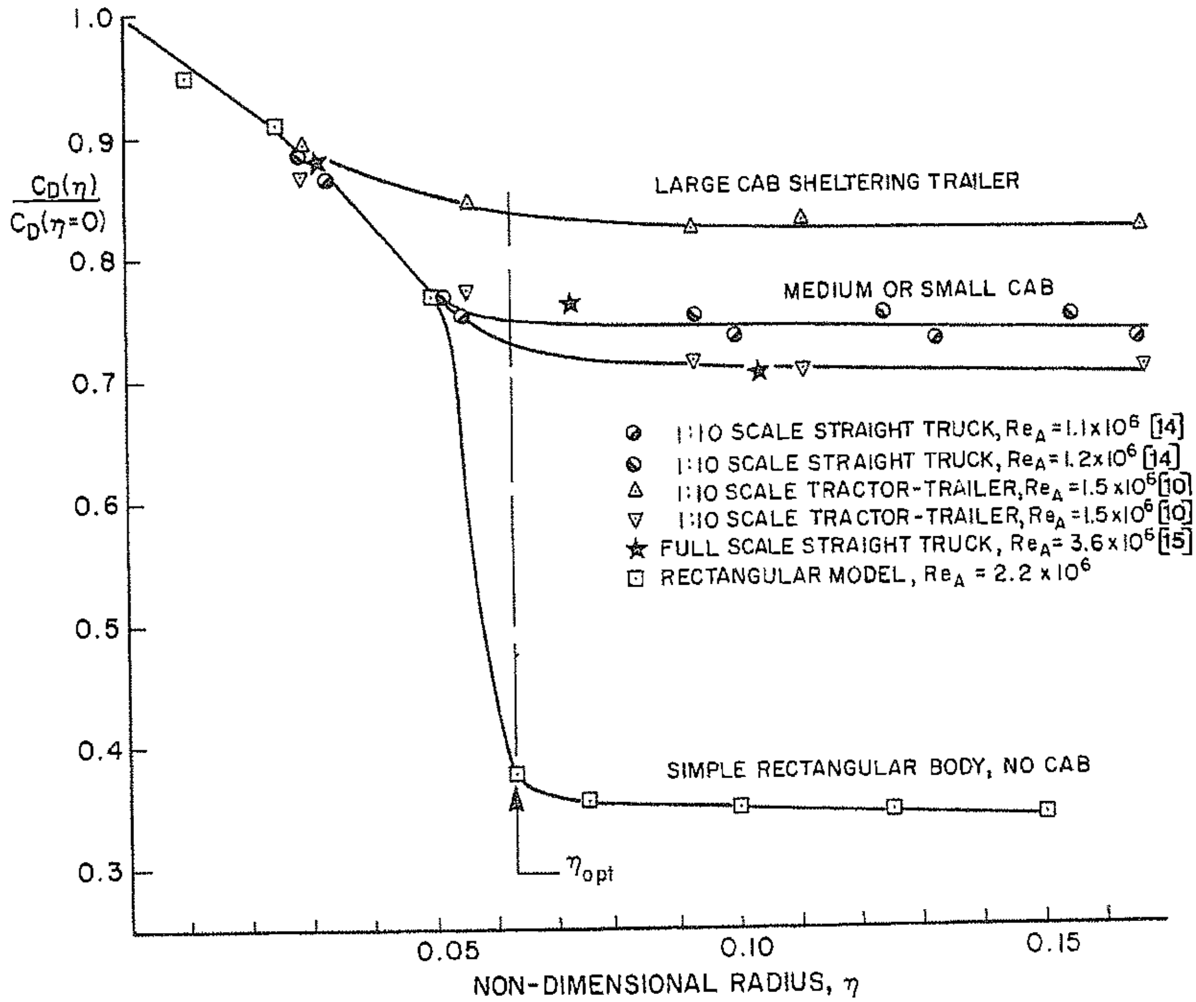

FIG. 28: COMPARISON OF FRACTIONAL DRAG REDUCTION AND OPTIMUM EDGE RADIUS FOR MODEL AND FULL SCALE TRUCKS WITH DATA FOR A RECTANGULAR BODY

APPLICATION OF EDGE-RADIUS BOUNDARIES

The application of the boundaries in Figure 26 is straightforward, although various assumptions are implicit in the use of the data. These assumptions are:

i) The design boundaries developed for a rectangular body and shown in Figure 26 can be applied to more complex, box-like vehicles. This is supported by the measurements presented in Figure 27.

ii) The effect of body height-to-width ratio is small for the differences between the model value used in this program, h/w = 1.0, and the values common to real commercial vehicles where h/w > 1.0, usually.

iii) The square-root of body frontal area, $\sqrt{A_b}$, is an adequate reference length with which to non-dimensionalize edge radius. Obviously, for high or wide bodies this will fail and width or height, respectively, would be a better choice.

Accepting these points, it is only necessary to determine the operating Reynolds number and the maximum yaw angle of concern.

The selection of operating Reynolds number can be based on a vehicle speed for which aerodynamic influences become important and one obvious choice, then, is the speed at which aerodynamic and rolling resistances are equal. This speed will be below the vehicle's cruising speed and so would be conservative. Assuming a crude model for the rolling resistance of 0.01 N resistance for each Newton of weight, the design speed would be:

$$V_o = \{[0.02/(\rho\bar{C}_D)](W/A)\}^{\frac{1}{2}} \text{ m/s} \quad (5)$$

Strictly speaking, since $\bar{C}_D$ is a function of V_o, an iterative solution is required to solve correctly for V_o, but a first approximation using $\bar{C}_D$ at 90 km/h is sufficient for design purposes.

Finally, some rationale must be established for choosing the maximum yaw angle for which attached flow is required. As seen in Figure 26, the price for good aerodynamic performance at large yaw angles is increased edge radius. The maximum probable yaw angle is a function of vehicle speed and local wind statistics. It would be impractical to include information from specific locales, so annual hourly mean wind statistics typical of the North American average and the method of Cooper [10] will be used to assess the probability of exceeding a given yaw angle (the cumulative probability of yaw angle) for various road speeds from 50 km/h to 130 km/h.

The probabilities are given in Figure 29 and it is apparent that the yaw angle associated with a given probability level increases with decreasing road speed. For example, 6° has a 0.1 chance of being exceeded at 130 km/h road speed, but at 50 km/h 16° is exceeded with the same probability. That is, the more rapidly a vehicle travels, the lower the incident yaw angles produced by natural winds. Assuming that a resonable probability level for design is 0.10, then the maximum yaw angle range of concern can be obtained as a function of road speed, as indicated in the graph.

As an example, one can choose two design cases, one for a straight truck and the other for a tractor-trailer, using the vehicle configurations employed in the tests reported in the following section of this paper. The vehicle's

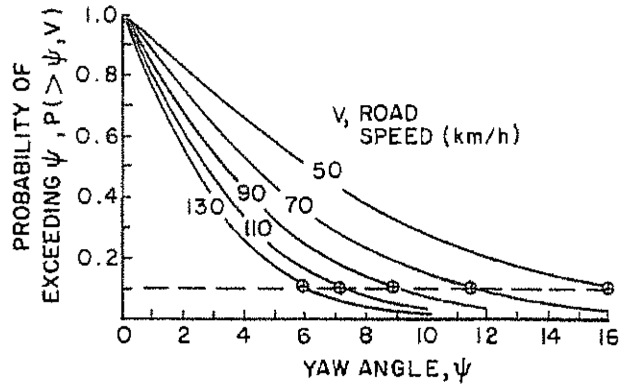

FIG. 29: PROBABILITY OF A VEHICLE EXCEEDING A GIVEN YAW ANGLE AT VARIOUS ROAD SPEEDS

properties and design operating speeds (from eq. (5)) are given in Table 6.

The values of radius obtained for these configurations, at the operating Reynolds number obtained using eq. (5), are less than the minimum allowable value of η_{opt}. Thus the inset graph of Figure 26 must be used to select the radii - 250 mm for the straight truck body and 200 mm for the trailer. The 200 mm value is close to the value of 250 mm commonly found on trailers.

002263

TABLE 6

DATA FOR DESIGN EXAMPLES

	Straight Truck Body	Tractor-Trailer
Vehicle area, A	8.39 m^2	9.85 m^2
Body area, A_b	6.25 m^2	7.06 m^2
$\sqrt{A_b}$	2.50 m	2.66 m
W	88200 N	264600 N
$\tilde{C}_D$	0.775	0.968
V_o	54 km/h	70 km/h
Initial radius [Eqn. (4)], r	126 mm	97 mm
$r/\sqrt{A_b}$	0.050	0.036
Design yaw angle	15°	11.4°
Final radius	$r/\sqrt{A_b}$ = 0.100	$r/\sqrt{A_b}$ = 0.075
(Inset graph from Fig. 26)	r = 250 mm	r = 200 mm

LEVELS OF FRONT-EDGE DRAG REDUCTION

The levels of drag reduction indicated by Figures 11 to 14 are generally not realizeable on most trucks, although they should be available for the less complex shapes used for buses, vans and rail vehicles. The differences in drag levels between those for the trucks and those for the rectangular body shown in Figure 28 must be due to interference effects between the cabs and the truck bodies or trailers. The surface pressures on the straight truck body behind and above the cab will be determined, in large part, by the cab flow-field and will reduce the area over which edge-related pressure changes can act. Some similar behaviour must occur with the tractor-trailer. Thus, one would expect that the lowest drags would be found for the least cab interference, and this is the case in Figure 28. The least drag reduction occurs with a large cab sheltering the trailer, the straight trucks are in the middle, and a small cab with very exposed, large trailer has the greatest drag reducing potential. Comparing these three curves with that for the rectangular body clearly indicates that the future for low drag commercial vehicles requires improved integration of cab and body.

Additional indications of available levels of drag reduction are provided by the two trucks employed in the final section of this paper. They were tested with rounded forebodies as well as with the standard versions, and a reduction in wind-averaged drag coefficient of 0.160 was measured for the straight truck while a reduction of 0.069 was measured for the tractor-trailer. By comparison, a cab-mounted deflector provided a wind-averaged drag coefficient reduction of 0.078 for the straight truck and 0.079 for the tractor-trailer.

DISCUSSION OF EFFECTS OF REAR-EDGE SHAPING

BASE DRAG LEVELS - As a prelude to the discussion of base drag reduction, a brief commentary on the magnitude and nature of base drag is in order. Generally speaking, base drag results from the pressure reduction over the rear face of a vehicle due to the entrainment of fluid from the base region by the shear layers separating from the rear edges. It has been suggested [2] that vehicles with reduced drag resulting from a good fore-body shape may have increased base drag because of the higher entrainment due to the thinner separating shear layers, although this simple concept may be upset by changes in underbody flows when a body is in ground proximity.

Typical measurements of base drag against yaw angle by Marks et al [5] and Cooper [11] are shown in Figure 30. Marks' measurements were obtained from integrated base pressures on truck models while those of Cooper were from direct force measurements on the base of a bus. The base drag coefficients are similar, even though the total bus drag levels are only one-half of those of the trucks. This is not surprising when one considers that both have parallel-sided rear ends, cut-off perpendicular to the vehicle's lengths. The bus drag levels were referred to true frontal area while those of the trucks were referred to height times width. The coefficient errors introduced by the different reference areas should be small since height times width is usually only a few percent larger than true frontal area for a truck.

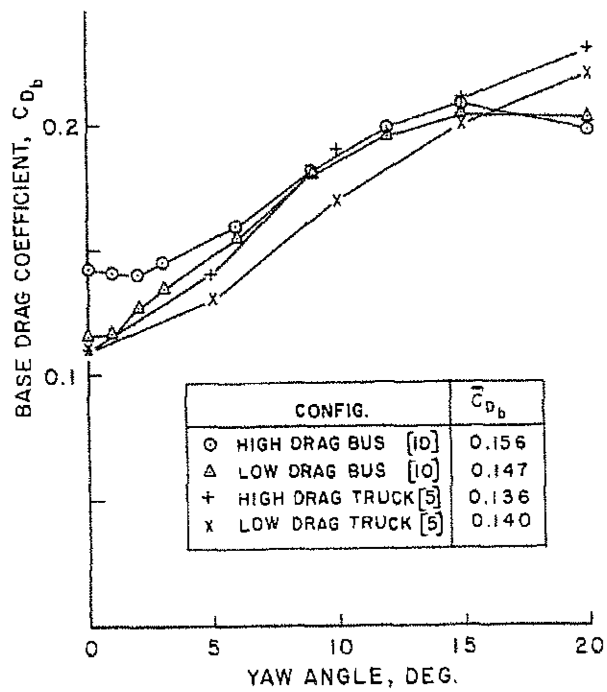

FIG. 30: BASE DRAG COEFFICIENTS OF TYPICAL TRUCKS AND BUSES

YAW BEHAVIOUR - The primary measurements were made over a range of yaw angles, rather than Reynolds numbers, at a fixed test speed of 73 m/sec. The resulting Reynolds numbers were 1.5×10^6 for the Ford truck and 1.6×10^6 for the Astro 95 tractor-trailer. Typical yaw results can be seen for the Ford truck with standard body front-end and bevelled or curved rear panels (sides and top only, Figure 9) in Figure 31 and Figure 32, respectively. The upper graph in each figure shows the drag coefficient while the lower graph shows the change, or increment, in drag coefficient defined as:

$$\Delta C_D = C_{D_{base}} - C_{D_{modified}} \quad (6)$$

Solid lines are used to highlight the data for the standard configurations and for the panel angles giving the lowest drag. Both the bevel and the radius produce similar results - an increasing drag reduction with increasing panel angle, to a maximum at the optimum angle, followed by a decrease in drag reduction beyond this angle. The drag reduction was fairly constant with yaw angle, showing a tendency to increase with yaw angle at the better (lower drag) panel angles. Qualitatively, similar results were found for the tractor-trailer configurations, but the levels of drag reduction were always about 70 percent of those found for the straight truck. These smaller drag reductions could be a result of the thicker boundary layers on the longer trailers and, perhaps, could be due to differences in the trailer's underbody flow.

The wind-averaged drag coefficients and drag coefficient increments are included in the keys to the figures and provide a better appreciation of the average drag changes. They provide a more convenient summary of the data than detailed plots like Figures 31 and 32 and permit a clear, accurate assessment of the yaw measurements.

The wind-averaged drag increment, $\Delta\bar{C}_D$, of all eight vehicle configurations (two trucks, two front faces, two types of rear-edge modification) investigated are shown against panel angle in Figure 33. The optimum panel angle is readily identified in each instance as are the significant differences in off-optimum performance of the curved and bevelled panels. It is also apparent that performance reduces less rapidly for the bevels at angles below optimum than above. The opposite is true with the radii. The bevelled panels produced the larger base drag reductions, at the optimum angles. The drag reductions for either truck and either type of rear panel were greater when the rounded front faces were fitted to the truck body or trailer. The lower drag reductions previously noted for the tractor-trailers can be seen. Also, it is evident that zero angle, parallel extensions of the body roof and side walls lead to a drag increase for both trucks.

The optimum panel angle was always 10° or 15°, depending on configuration and panel length. The measurements discussed, so far, were at a panel length of 457 mm, full-scale, giving $\bar{\ell}$ = 0.183 for the straight truck and $\bar{\ell}$ = 0.172 for the trailer. For convenience, the lengths of the rear panels will be discussed in terms of their equivalent full-scale values, which were the same for both trucks. However, the graphs and any applications of the data will be based on the non-dimensional panel length, $\bar{\ell}$.

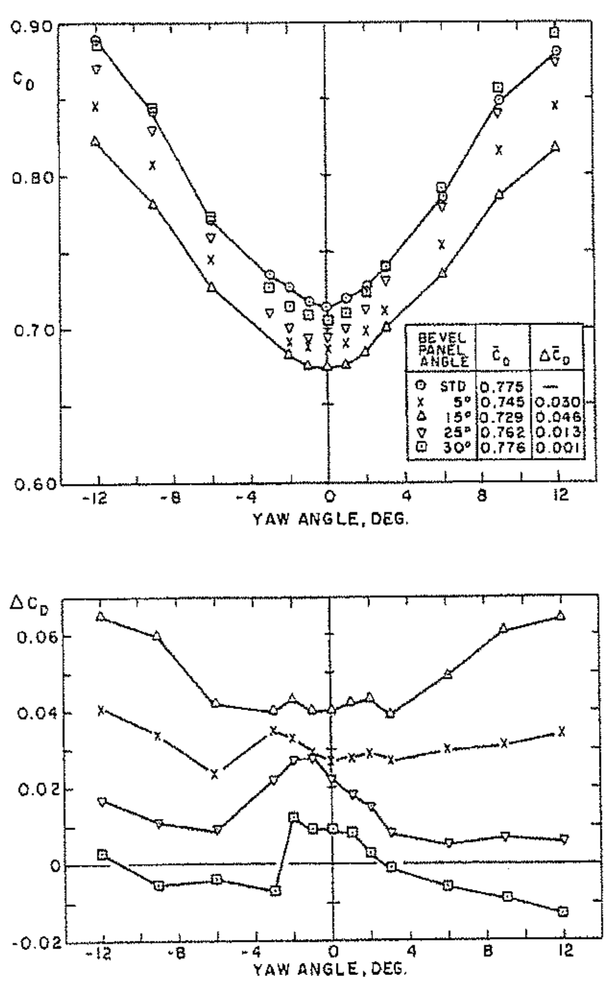

FIG. 31: EFFECT OF REAR BEVEL FITTED TO SIDES AND TOP OF FORD LN700 STRAIGHT TRUCK BODY. STANDARD FRONT FACE ON BODY, $\bar{\ell}$ = 0.183

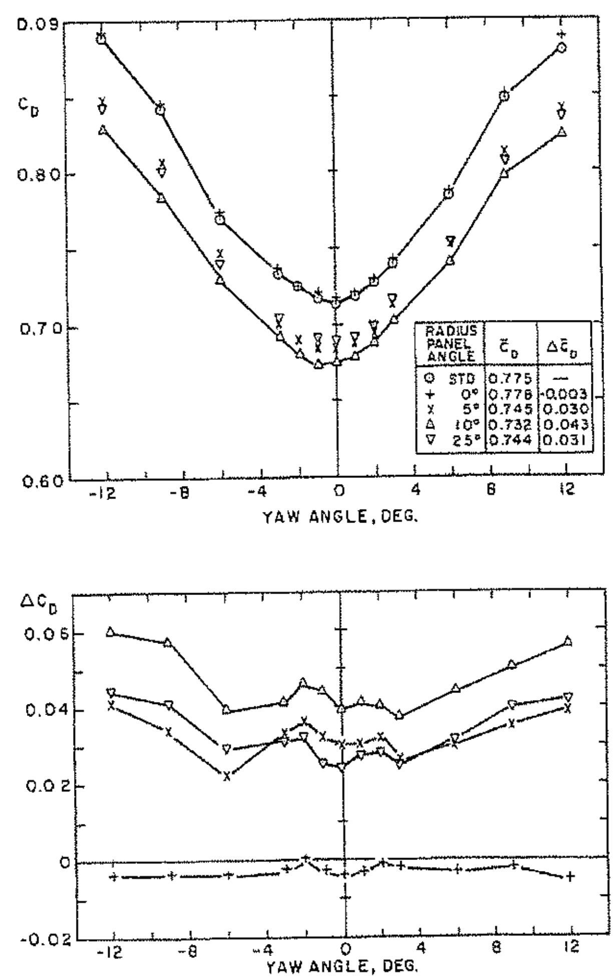

FIG. 32: EFFECT OF REAR RADIUS FITTED TO SIDES AND TOP OF FORD LN700 STRAIGHT TRUCK BODY. STANDARD FRONT FACE ON BODY, $\bar{\ell}$ = 0.183

Assuming that the base drags of the test trucks were identical to the average of the trucks used as examples in Figure 30, then the bevelled rear panels reduce the base drag, with standard front faces, by 35 percent for the straight truck and by 25 percent for the tractor-trailer. These percentages are referenced to the average wind-averaged base drag coefficient for both trucks in Figure 30, $\Delta\bar{C}_{D_b} = 0.138$.

The effect of rear panel length is presented in Figure 34. Each measurement was made at the optimum angle, as determined from a set of measurements like those of Figure 33. The optimum panel angle was 15°, unless a given data point is labelled otherwise. Initially, the drag reduction is seen to increase with panel length, whether bevel or radius, and then it levels off. While no optimum length can be found, it is evident that a non-dimensional panel length of 0.18 (full scale panel length of 457 mm) need not be exceeded. Further, even a small panel length of only one-third this value, 152 mm, still provides one-half the drag reduction of the longer panel. The straight truck and the tractor-trailer show the same functional behaviour with panel length. The latter, as noted previously, had the smaller drag increments.

A series of tests were performed with the open, lower side of the cavity closed by a straight panel parallel to the ground. The tests were done for all bevelled and curved panel lengths but at the optimum angle only. Figure 35 shows that this closure further increases the drag reduction. A bevelled panel length of 457 mm now provides a 42 percent base drag reduction for the truck and a 28 percent reduction for the tractor-trailer, with standard front faces. The results are only presented for the rear bevels, but the same fractional gain was also available with the radius.

A final comparison of the optimum behaviour of both types of rear-edge modifications, as a function of panel length, is made in Figure 36. On average, the bevel provides slightly greater drag reduction except at short lengths. Considering possible experimental error, the two have nearly identical performance.

A comparison of the importance of shaping individual rear edges was made using a bevelled-panel length of 457 mm at 15°. These results are presented in Table 7, which also includes a measurement with the base cavity filled to determine whether the shaping or the shaping-plus-cavity were most important. An attempt was

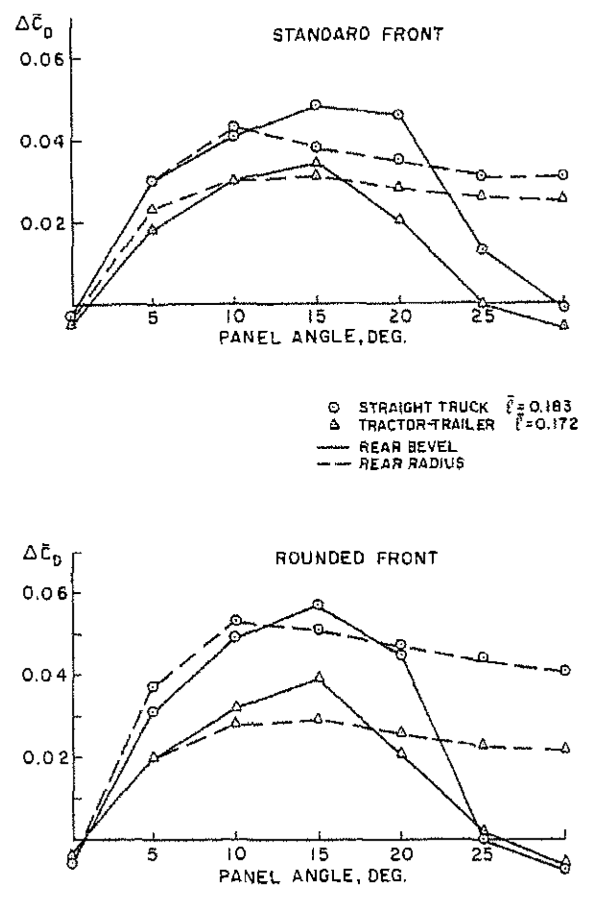

FIG. 33: EFFECT OF REAR PANEL ANGLE ON BASE DRAG REDUCTION

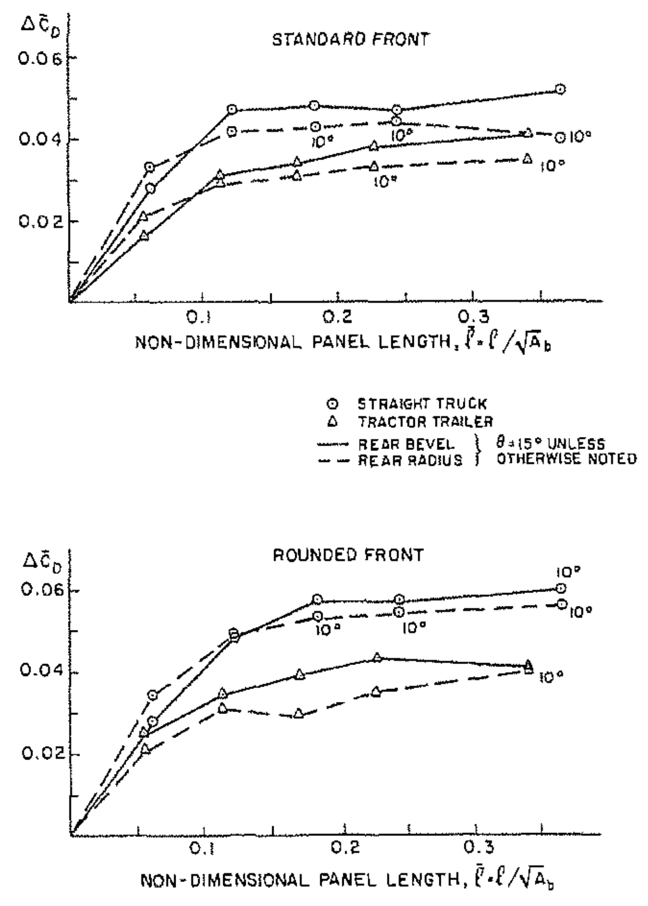

FIG. 34: EFFECT OF REAR PANEL LENGTH ON BASE DRAG REDUCTION (SIDES AND TOP ONLY, OPTIMUM ANGLE)

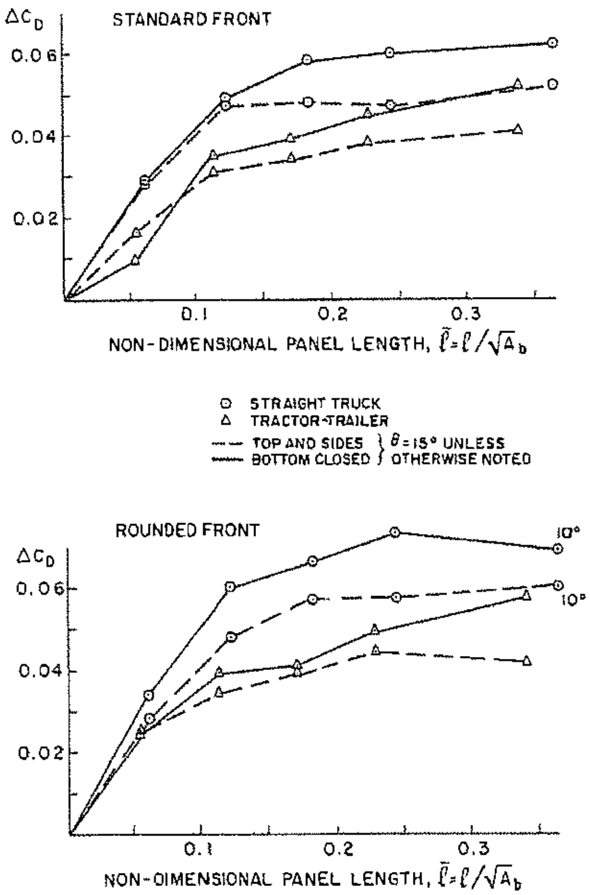

FIG. 35: EFFECT OF CLOSING THE LOWER SIDE OF THE BASE CAVITY FORMED BY BEVELLED REAR PANELS (OPTIMUM ANGLE)

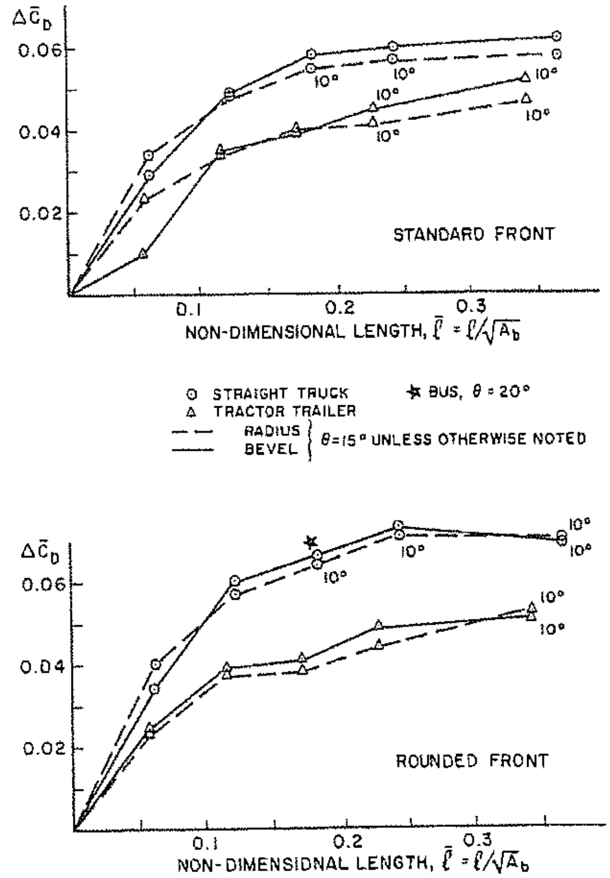

FIG. 36: COMPARISON OF REAR BEVEL AND REAR RADIUS WITH BOTTOM CLOSED (OPTIMUM PANEL ANGLE)

TABLE 7

EFFECT OF VARIATIONS TO 30 mm, 15° BEVELLED PANEL GEOMETRY FOR FORD TRUCK WITH ROUNDED FRONT FACE

Configuration	$\tilde{C}_D$	$\Delta\tilde{C}_D$	Fraction of Reduction Produced by Simultaneously Modifying the Top, Sides, Bottom
Standard	0.615	—	—
Top bevel only	0.612	0.023	5
Side bevels only	0.592	0.023	39
Top and side bevels	0.568	0.047	80
Top and side bevels, bottom closed	0.556	0.059	100
Top and side bevels, cavity filled	0.561	0.054	92
5% slots	0.573	0.042	71
10% slots	0.574	0.041	70

made to determine whether bevelled panels perforated with slots (see Figure 10) would be superior to solid panels. Two different slot porosities (percent area removed) were tried - one with 5 percent porosity and the other with twice this value.

Bevelled panels attached to the top alone or the sides alone produced a drag reduction far less than that found for top and sides together, with the side panels being the better of the two possiblities. The sum of the drag reductions for each modification performed individually was only about one-half that when they were used in combination. Filling the cavity produced only a very small decrease in drag reduction, so the major effect appears to be due to the new shape introduced by the panel rather than due to the shape plus base cavity. The use of perforated panels, at the levels of porosity employed, produced a smaller drag reduction than with solid panels.

The streamlined tail (Figure 10) produced drag reductions that were no larger than those resulting from the much smaller rear panels. The drag reduction for the straight truck was $\Delta\bar{C}_D = 0.071$ with just the first two elements of the tail installed and only increased to 0.074 with all six elements.

A few Reynolds number runs were performed with several of the optimum configurations, up to a maximum of about $Re_A = 2 \times 10^6$. No influence of Reynolds number up to this value was found, except for leading-edge radius effects with the rounded front faces.

A comparison of some of the major methods of truck drag reduction is made in the graphs of Figure 37. The corresponding wind-averaged drag coefficients are summarized in Table 8. While the rear-edge modifications do not give the largest drag reductions, they provide a useful improvement and should be simple to implement.

The side force and yawing moment coefficients for the same four configurations of truck and tractor-trailer are shown in Figure 38 and Figure 39, respectively. Only these aerodynamic components are shown because of their influence on cross-wind response. Rolling moment, in all cases, reflects the changes exhibited by side force.

Side force is reduced with the rear panels and, surprisingly, yawing moment becomes more postive indicating a forward shift of the centre of pressure of side force. The center of pressure location at small yaw angles can be obtained from:

$$x_o/\sqrt{A_b} = C_{YM,\psi}/C_{S,\psi} \qquad (7)$$

where the aerodynamic coefficient slopes, $C_{YM,\psi}$ and $C_{S,\psi}$, are given in the inset tables of Figures 38 and 39. The yaw angle range over which the linear least squares fit was applied to obtain the slopes is given in parentheses in these figures. The centre of pressure shift was found

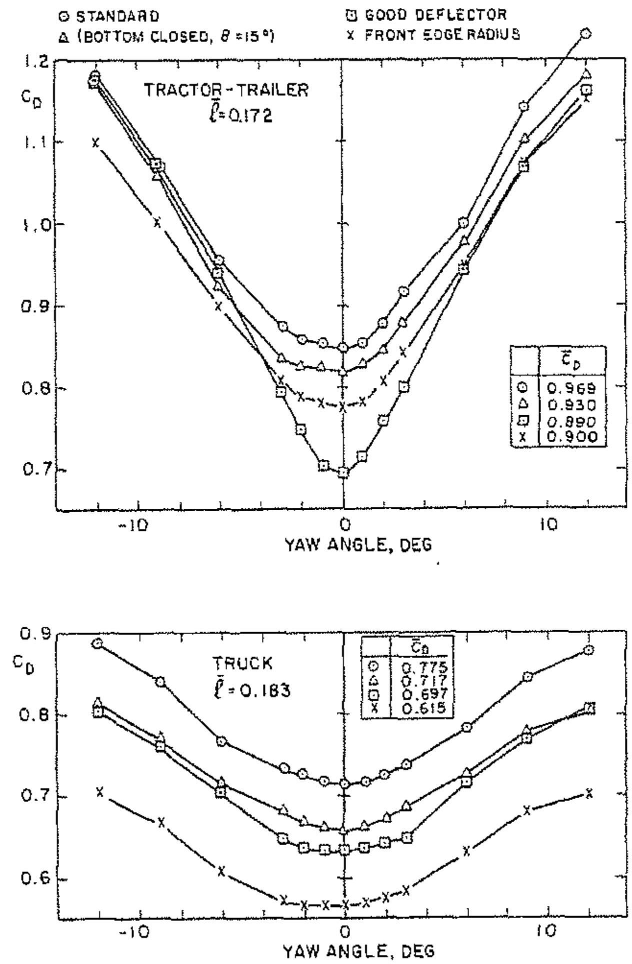

FIG. 37: COMPARISON OF METHODS OF DRAG REDUCTION ON BOTH TRUCKS

TABLE 8

COMPARISON OF DRAG-REDUCTION TECHNIQUES

Configuration	GMC Tractor $\bar{C}_D$	GMC Tractor $\Delta\bar{C}_D$	Ford Truck $\bar{C}_D$	Ford Truck $\Delta\bar{C}_D$
Standard	0.969	–	0.775	–
Rear bevels (457 mm, 15°)	0.930	0.039	0.717	0.058
Front face radius	0.900	0.069	0.615	0.160
Deflector	0.890	0.079	0.697	0.078

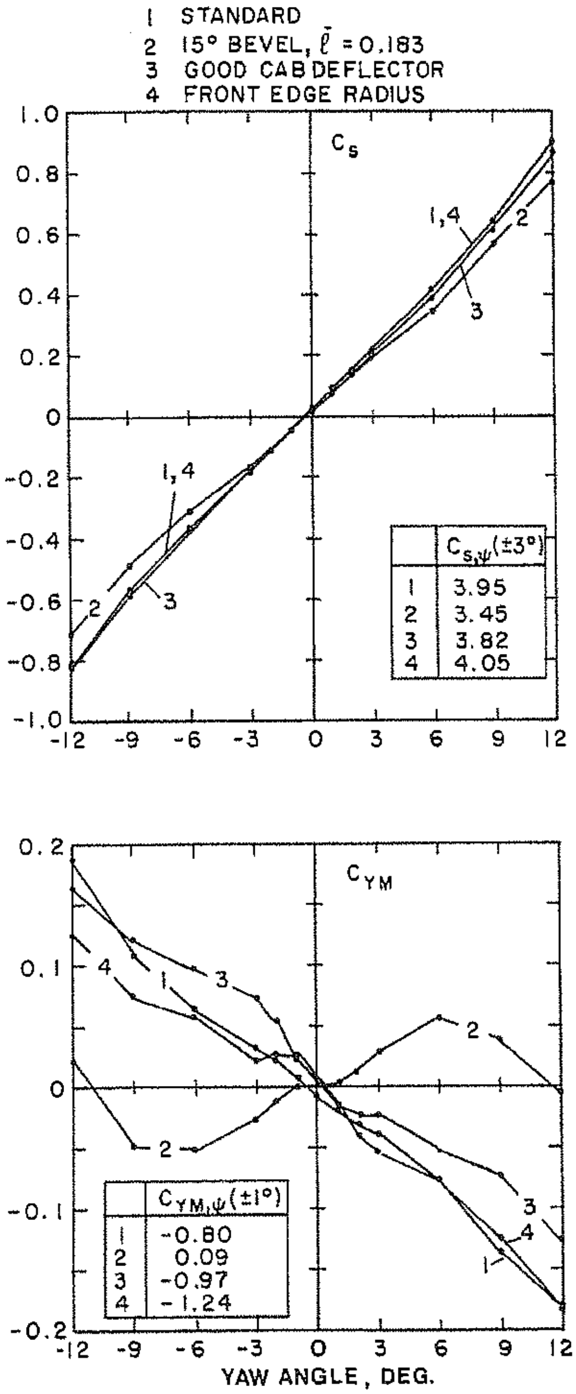

FIG. 38: COMPARISON OF SIDE FORCE AND YAWING MOMENT COEFFICIENTS WITH METHOD OF DRAG REDUCTION (STRAIGHT TRUCK)

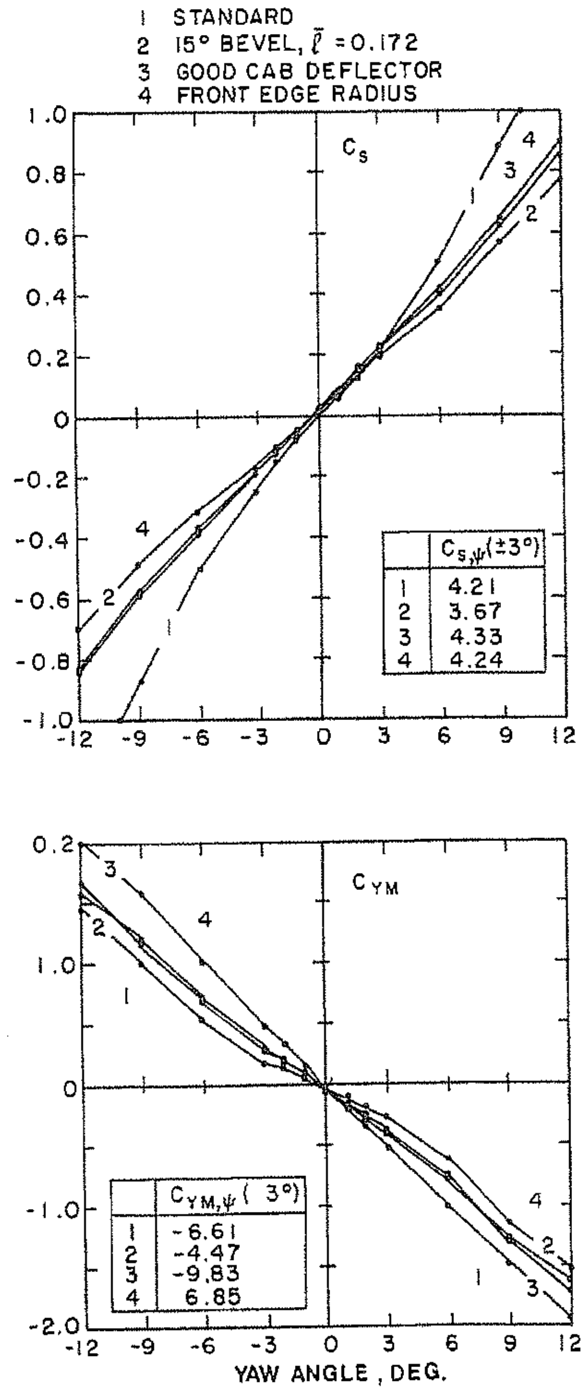

FIG. 39: COMPARISON OF SIDE FORCE AND YAWING MOMENT WITH METHOD OF DRAG REDUCTION (TRACTOR-TRAILER)

to be 573 mm forward for the truck and 936 mm forward for the tractor-trailer. The forward shift on the straight truck is statically destabilizing in cross winds, although this effect is minimized by the side force reduction. No similar comment can be made regarding the changes to the tractor-trailer as separate force and moment measurements on both cab and trailer would have been necessary.

Bevels on the rear side and roof edges were used on the low-drag bus referred to in Figure 30. A wind-averaged base drag coefficient reduction of 0.070, or 48 percent, was measured for the bus with a 500 mm long ($\bar{\ell}$ = 0.177), 20° bevel. This agrees reasonably well with the rounded-front, straight-truck data of Figure 36 and suggests that the straight-truck data might be sufficiently general to apply to other vehicles.

CORRELATION WITH FULL-SCALE - At the same time that Ford performed the front-edge rounding studies they also tested one radius on the rear top and side edges, with the same radius fitted to the front edges. The radius used was 254 mm, giving η = 0.108 for the front edges. The rear radius was a quarter-round set into the rear side and top edges, giving $\bar{\ell}$ = 0.147 and θ = 45°. The drag reduction provided by the rounded rear edges was:

$$\Delta C_D(\psi=0°) = 0.043$$

This compares reasonably well with the value found in the current tests for $\bar{\ell}$ = 0.122 and θ = 30° (the largest angle tested) of:

$$\Delta C_D(\psi=0°) = 0.040$$

The differences in panel angle should not invalidate this comparison because the drag increments are nearly constant with curved rear panels for panel angles greater than 20°. These data, then, indicate that the levels of drag reduction found in the model-scale tests should be expected at full-scale.

CONCLUDING REMARKS

Methods for the aerodynamic design of the front and rear edges of box-like vehicles, such as truck bodies, vans, buses or rail vehicles, have been presented. The techniques discussed are based on wind tunnel tests and employ simple rounding of the front edges and bevelling or rounding of the rear edges. Comparisons of the model-scale measurements with limited full-scale measurements on a straight truck in a large wind tunnel show an encouraging level of agreement. These methods are capable of lowering the aerodynamic drag as much or more than many other techniques and result in little loss of vehicle volume.

FRONT EDGE DESIGN - A design method has been developed to determine the edge radius required to minimize aerodynamic drag according to vehicle size, operating Reynolds number and maximum expected yaw angle. A universal collapse of the edge-radius-Reynolds-number behaviour in Figure 26 can be used for this purpose. The size and operating speeds of contemporary road vehicles will usually place the edge radius at a value below the threshold optimum non-dimensional value of η = 0.063 and so the inset graph in Figure 26 will most commonly be used. Correlation of detailed-model and full-scale observations of front-edge-rounding behaviour suggest that Figure 26 may be conservative in that it predicts the need for somewhat larger edge radii than appear necessary. This could be caused by flow-tripping effects due to the impingement of flow from other components ahead of the main body. With this in mind, a non-dimensional edge radius of η = 0.063 may be adequate for all purposes. Two examples were presented that showed wind-averaged drag coefficient reductions of about 0.08 for a tractor-trailer and 0.16 for a straight truck.

The data were developed on a simplified body at one height-to-width ratio and at one height-to-length ratio, and so should be employed with caution until more supporting data become available, possibly through testing a full scale straight truck in the 9 m × 9 m wind tunnel of the National Research Council of Canada. However, the information presented offers the most complete investigation of front-edge rounding on surface vehicles published to date.

Studies of simple rounding are only the beginning of the development of leading edge shaping. It is possible that other shapes, elliptical edges for example, can produce similar savings with even less intrusion into the body, and this suggests a worthwhile future study. In addition the investigation of boundary layer energizers, like the vortex generators often used on aircraft wings and tails, might permit attached flow at radii smaller than the optima reported in this paper.

The front-edge rounding data also suggest that the minimum test Reynolds number needed is of the order of $Re_A = 2.0 \times 10^6$, considerably higher than the current SAE Recommended Practice requires.

The uses of computational methods would be a powerful adjunct to additional experimentation. In this vein, the measurements presented in this paper should provide a useful test case for some of the computational codes now being developed.

REAR-EDGE DESIGN - The reduction of base drag through the simple expedient of rounding or bevelling the rear of a straight truck body or trailer was demonstrated. It was found that the bevelling was slightly superior in performance to the radius, as shown in Figure 36. The bevel could be produced equally well by a chamfer on the sides and the top of the body or by angled extension panels on the sides and roof, with a matching horizontal panel at the bottom to close the cavity so formed. These panels could either be fixed, or could be arranged to fold with the doors. It was discovered that the best panel angle was 10° to 15° from parallel to the roof or sides of the vehicle, depending on vehicle configuration, panel type, and panel length. Panel lengths greater than 0.18 times the square-root of the base area offered little additional drag reduction. Panels only one-third this length, 0.06 times the square-root of the base area still produced about one-half the drag reduction of the longer panels. The longer panels produced a wind-averaged drag-coefficient reduction of 0.058 for a straight truck and 0.039 for a tractor-trailer. The long panel would be about 450 mm in length on a typical straight truck and, at an angle of 15°, would only intrude into the body sides and roof by 116 mm. The short panel of 150 mm would only intrude 39 mm. The curved panels would intrude less in each case.

This concept has already been applied successfully on a truck body and a bus. Its simplicity and effectiveness recommend it even at shallower than optimum angles and at reduced length, where body intrusion is negligible.

NOTATION

A	total frontal area at zero degrees yaw angle; reference area used to non-dimensionalize aerodynamic forces and moments; m^2
A_b	cargo carrying body reference area; used to non-dimensionalize front-edge radii and rear panel lengths; values at front and rear of body assumed equal; same as total frontal area for rectangular body; m^2
C_D	body-axis drag coefficient; D/q_cA
C_{D_b}	base drag coefficient; drag coefficient resulting from base pressures
C_{D_u}	measured wind-axis drag coefficient uncorrected for blockage
$\bar{C}_D$	wind-averaged drag coefficient; a function of road speed and assumed wind conditions that attempts to account for the occurrence of varying yaw angles and wind speeds on the road.
ΔC_D	increment in drag coefficient; the drag coefficient difference between a baseline (standard or rounded front) and a modified configuration; positive for drag reduction; $C_{D_{base}} - C_{D_{modified}}$
$\Delta\bar{C}_D$	increment in wind-averaged drag coefficient; $\bar{C}_{D_{base}} - \bar{C}_{D_{modified}}$
C_L	body-axis lift coefficient; L/q_cA
C_{PM}	body-axis pitching moment coefficient; PM/q_cAw
C_{RM}	body-axis rolling moment coefficient; RM/q_cAw
C_S	body axis side force coefficient; C_S/q_cA
C_{YM}	body-axis yawing moment coefficient; YM/q_cAw
$C_{S,\psi}$	side force coefficient curve slope; $dC_S/d\psi$; deg^{-1}
$C_{RM,\psi}$	rolling moment coefficient curve slope; $dC_{YM}/d\psi$; deg^{-1}
$C_{YM,\psi}$	yawing moment coefficient curve slope; $dC_{YM}/d\psi$, deg^{-1}
D	aerodynamic drag force; N (Figure 4)
d	body diameter; mm
g	diameter of roughness or grit particle; mm
h	overall height of vehicle above ground; mm
L	overall length of vehicle; mm lift force; N
ℓ	rear-edge panel length; mm (Figure 9)
$\bar{\ell}$	non-dimensional rear panel length; $\ell/\sqrt{A_b}$
$P(>\psi,V)$	the probability of exceeding a given yaw angle, ψ, at a road speed of V km/h
PM	aerodynamic pitching moment; Nm
q	measured test section dynamic pressure; $\frac{1}{2}\rho V^2$
q_c	test-section dynamic pressure corrected for blockage (eq. (1))
r	front-edge radius; mm (Figure 3)
Re_A	Reynolds number referenced to $\sqrt{A_b}$; $V\sqrt{A_b}/\nu$
$(Re_A)_t$	transcritical value of Reynolds number referenced to $\sqrt{A_b}$
Re_d	Reynolds number referenced to diameter; Vd/ν
Re_r	Reynolds number referenced to radius; Vr/ν
$(Re_r)_t$	transcritical Reynolds number referenced to radius
RM	aerodynamic rolling moment; Nm
S	aerodynamic side force; N
V	wind speed; m/s
V_o	design road speed for leading-edge radius estimation; m/s (eq. (5))
W	weight of vehicle; N

002271

w vehicle maximum width; mm (m when used to define aerodynamic coefficients)

x_1 distance of leading-edge of model downstream of groundboard leading-edge; mm (Figure 1)

x_{cg} distance of moment reference centre for body-axis co-ordinates downstream of vehicle leading-edge; mm (Table 2)

x_o location of centre of pressure of side force relative to co-ordinate origin, positive forward; m

x_r distance from leading-edge to flow reattachment point; mm

y distance on front face of roughness strip centre-line from body edge; mm (Figure 24)

YM aerodynamic yawing moment; Nm

θ angle of rear panel (chord for circular arc); deg (Figure 9)

ν kinematic viscosity of air; 1.458×10^{-5} m^2s^{-1} at STP

η non-dimensional leading-edge radius; $r/\sqrt{A_b}$

η_{opt} optimum or best value of η; provides lowest drag at least radius

ψ yaw angle; deg (Figure 4)

ψ_M maximum value of yaw angle for which attached flow is required; deg

ACKNOWLEDGEMENTS

The author would like to thank Mr. Roy Higginson of the Morgan Trailer Mfg. Co. for permission to publish a selection of the test data used to design their new van bodies. He would also like to thank Mr. Jack Williams of the Ford Motor Company for permission to quote the full-scale straight truck measurements. The availability of both these sets of data has added valuable support to the measurements presented in this paper.

REFERENCES

1. G.W. Carr, "The Aerodynamics of Basic Shapes for Road Vehicles", Motor Industries Research Association Report No. 1968/2, Nov. 1967.

2. S.F. Hoerner, "Fluid-Dynamic Drag", published by the author, New Jersey, 1965.

3. W-H. Hucho, E.L. Janssen and H.J. Emmelmann, "The Optimization of Body Details - A Method for Reducing the Aerodynamic Drag of Road Vehicles", SAE 760185, Detroit, Feb. 1976.

4. K.R. Cooper, "The Wind Tunnel Testing of Heavy Trucks to Reduce Fuel Consumption", SAE 821285, Truck and Bus Meeting and Exposition, Indianapolis, Nov. 1982.

5. C.H. Marks, F.T. Buckley Jr., W.H. Walston Jr., "A Study of The Base Drag of Tractor-Trailer Trucks", Journal of Fluids Engineering, Dec. 1978, Vol. 100.

6. E.C. Maskell, "A Theory of the Blockage Effect on Bluff Bodies and Stalled Wings in a Closed Wind Tunnel", ARC R&M 3400, Nov. 1963.

7. "SAE Test Procedure for Trucks and Buses - SAE J1252 Jul 81", Society of Automotive Engineers Recommended Practice.

8. E.C. Polhamus, "Effect of Flow Incidence and Reynolds Number on Low-Speed Aerodynamic Characteristics of Several Noncircular Cylinders with Application to Directional Stability and Spinning", NACA TN 4176, Jan. 1958.

9. K.R. Cooper, "The Wind Tunnel Simulation of Surface Vehicles", Journal of Wind Engineering and Industrial Aerodynamics, 17 (1984), 167-198.

10. K.R. Cooper, "A Wind Tunnel Investigation Into the Fuel Savings Available from the Aerodynamic Drag Reduction of Trucks", DME/NAE Quarterly Bulletin, The National Research Council of Canada, 1976 (3).

11. K.R. Cooper, "unpublished measurements", The National Research Council of Canada.

12. A.T. McDonald, G.M. Palmer, "Aerodynamic Drag Reduction of Intercity Buses", SAE 801404.

13. ESDU, Wind Engineering. Vol. 26. "Fluid Forces and Moments on Rectangular Blocks", Engineering Sciences Data Unit, London, England, Item 71016, 1971.

14. K.R. Cooper, "A Wind Tunnel Investigation of the Fuel Saving Potential of Aerodynamic Drag Reducing Modifications to Morgan Trailer Truck Bodies", LTR-LA-238, National Research Council of Canada, Ottawa.

15. J.W. Williams, Private communication from the Ford Motor Company, Dearborn, Mi.

16. K.R. Cooper, W.T. Mason, Jr., W.H. Bettes, "Correlation Experience with the SAE Wind Tunnel Test Procedure for Trucks and Buses", SAE 820375, International Congress and Exhibition, Detroit, Feb., 1982.

002273

002273

P02410

002274

002274

P02411

002275

This paper is subject to revision. Statements and opinions advanced in papers or discussion are the author's and are his responsibility, not SAE's; however, the paper has been edited by SAE for uniform styling and format. Discussion will be printed with the paper if it is published in SAE Transactions. For permission to publish this paper in full or in part, contact the SAE Publications Division.

Persons wishing to submit papers to be considered for presentation or publication through SAE should send the manuscript or a 300 word abstract of a proposed manuscript to: Secretary, Engineering Activity Board, SAE.

Printed in U.S.A.

002276

002276

EXHIBIT 6

002276

MOTOR COACH INDUSTRIES
ENGINEERING TEST REPORT

TEST NO.: 93-0026 **DATE:** AUGUST, 1993

DESCRIPTION:
A WIND TUNNEL INVESTIGATION OF THE AERODYNAMIC CHARACTERISTICS OF BUSES

REPORT BY: INSTITUTE FOR AEROSPACE RESEARCH

SECTION NO.: –

PART/ASSY NO.: –

COACH UNIT NO.: –

REF: –
–
–
–

COMMENTS: –
–
–

002277

002277

APPENDIX 1: RUN LOG

RUN	TYPE	FRONT	REAR	TRIP	HATCH	RAIL	MIRROR	MISC	$\bar{C}_D(90)$	PHOTO
13	YAW	SMOOTH CJ3	STANDARD CJ3	NO	NONE	NONE	NONE	NONE	0.376	P1
14	Re									
16	YAW				STD	STD			0.377	P2
18	Re	STANDARD CJ3								P3
19	YAW								0.584	
21	Re	MERCEDES								P4
22	YAW								0.620	
25	Re	PROPOSAL 1								P5
26	YAW								0.363	
28	Re	PROPOSAL 2								P6
29	YAW								0.436	
31	Re	PREVOST								P7
32	YAW								0.404	
34	Re	SETRA								P8
35	YAW								0.625	
37	YAW	STANDARD CJ3					CJ3 FWD		0.596	P9
39	Re	PROPOSAL 2		YES			NONE			P10
40	YAW								0.365	
42	YAW						CJ3 FWD		0.394	P11
44	YAW						CJ3 AFT		0.405	P12

right Appendix

MCI - 039854

002278
002278
002278

RUN	TYPE	FRONT	REAR	TRIP	HATCH	RAIL	MIRROR	MISC	$C_D(90)$	PHOTO
46	YAW	PROPOSAL 2	STANDARD CJ3	YES	STD	STD	SETRA		0.434	P13
48	YAW						PREVOST		0.422	P14
50	Re		BEVELLED				NONE			P15
51	YAW								0.299	
53	YAW						CJ3 FWD		0.339	P11
55	YAW						CJ3, RIGHT FWD, LEFT AFT		0.349	P16
57	YAW							SKIRTS	0.330	P17
58	YAW							AIR DAM	0.393	P18
59	YAW							TIRE FAIRING	0.353	P19
60	YAW							VORTEX GEN.	0.354	P20
61	YAW					MOD		NONE	0.351	P21
63	YAW	PREVOST	STANDARD CJ3	YES	STD	STD	PREVOST		0.447	P22
65	YAW	PREVOST					NONE		0.418	P23
66	Re									
68	Re	PROPOSAL 1								P24
69	YAW								0.367	
71	Re	SMOOTH CJ3								P25
72	YAW	0.380								

MCI - 039855

002279
002279
002279

INSTITUTE FOR AEROSPACE RESEARCH

INSTITUT DE RECHERCHE AÉROSPATIALE

Pages 93 Total

Fig.
Diag.

REPORT
RAPPORT

APPLIED AERODYNAMICS LABORATORY

LABORATOIRE D'AÉRODYNAMIQUE APPLIQUÉE

Date August 1993

Lab. Order
Comm. Lab. 5602

File
Dossier

For
Pour Motor Coach Industries

Reference
Référence MCI P.O.#M151843

002280

002280

LTR-AA- 9

A WIND TUNNEL INVESTIGATION OF THE AERODYNAMIC CHARACTERISTICS OF BUSES FOR MOTOR COACH INDUSTRIES

Submitted by
Présenté par Dr. L. Elias
Laboratory Head/Chef de laboratoire

Author
Auteur K.R. Cooper

Approved
Approuvé Dr. G.F. Marsters
Director General/Le directeur général

Copy No
Copie Nr.

TABLE OF CONTENTS

002281

ABSTRACT

A wind tunnel test was performed to evaluate the aerodynamic drag of seven front-end shapes and 2 rear-end shapes for an intercity bus for Motor Coach Industries . The front-end shapes represented the current production bus - the CJ3, three competing buses, and three new designs. The rear-end shapes represented the current production bus and a new design. The wind tunnel measurements demonstrated that the best combination, consisting of the new rear plus the Proposal 1 front, produced a reduction in wind-averaged drag coefficient of 41.5% compared to the standard CJ3 configuration. This drag reduction is equivalent to a fuel saving of 8.75 litres for each 100 km travelled at a steady speed of 90 km/h and 14.63 litres for each 100 km travelled at 120 km/h. The new configuration had a lower drag coefficient than the three competitors.

RESUMÉ

Un essai en soufflerie a été réalisé pour évaluer la traînée aéreodynamique de sept formes d'avant et de deux formes d'arrière d'autocar pour Motor Coach Industries. Les formes de l'avant étaient celles d'un modèle de série (le CJ3), de trois modèles concurrents et de trois nouveaux modèles. Les formes de l'arrières étaient celles du modèle de série et d'un nouveau modèle. Les mesures ont permis de constater que la meilleure combinaison, soit le nouveau modèle d'arrière avec le projet d'avant n° 1, produisait une réduction de 41,5% du coefficient de traînée pondéré en fonction du vent par rapport à la configuration CJ3. Cette réduction représente une économie de carburant de 8,75 litres pour 100 kilomètres parcourus à une vitesse stabilisée de 90 km/h et de 14,63 litres pour 100 kilomètres parcourus à une vitesse stabilisée de 120 km/h. Le coefficient de traînée de la nouvelle configuration était plus faible que celui des trois modeles concurrents.

002282

002282

1.0 INTRODUCTION

Aerodynamic forces and moments have an important influence on the operation of a high-speed, intercity bus. Aerodynamic drag absorbs a significant proportion of the engine power required at speed, thus affecting fuel consumption and passing acceleration. The aerodynamic side force, rolling moment, and yawing moment are important to handling because they provide a disturbance that deflects a bus from its path in the presence of side winds or passing vehicles.

A wind tunnel investigation was performed in the 2m x 3m wind tunnel of the Applied Aerodynamics Laboratory of the National Research Council to evaluate the influence of these parameters for a new bus designed by Motor Coach Industries, Winnipeg, Manitoba. The wind tunnel program was conducted with a 1:10 scale model of the bus and the purposes of the wind tunnel tests were:

1) to investigate alternative front-end and rear-end designs to determine which provided the lowest aerodynamic drag,
2) to determine the effect of mirrors and other detail modifications on the best front and rear combination from (1),
3) to compare the aerodynamic performance of the best combination with several competitive buses,
4) to estimate the fuel savings provided by the new design, relative to the current production bus and to the competition.

002283

002283

2.0 WIND TUNNEL SIMULATION

The wind tunnel simulation provides an approximation of the environment encountered by a bus moving along a road [1][1]. In the wind tunnel, Figure 1, air is blown over a model mounted above a fixed groundboard that is specially-designed to simulate the effects of the road surface over which the real bus moves. The accuracy of the wind tunnel measurements will be functions of several parameters, the most important of which are the test Reynolds number, the level of model detail, and the effectiveness of the ground simulation. The level of model detail and the fixed ground plane will produce small errors in the absolute values of the measured aerodynamic forces. For example, the smooth model surfaces and fixed groundboard will cause the model drag measurements to be lower than for the full-scale bus. However, the differences in aerodynamic forces between any two configurations will not be influenced by these factors. Thus, the wind tunnel will be an accurate predictor of the changes between configurations and, therefore, provides a powerful tool for the aerodynamic optimization of a new bus design. The measured aerodynamic changes can be used to provide accurate estimates of the performance changes produced by any shape modification.

Many small details like side window framing, break lines in the body surface, wheel rotation, and heat exchanger airflows were not included in the model because past experience has shown that their effects were small and did not affect the aerodynamic differences measured

[1] Numbers in square parentheses indicate references to be found following the main body of the text.

002283

between major configurations. Previous wind tunnel tests have demonstrated that the measured aerodynamic changes correlate well with road measurements for commercial road vehicles [2]. In summary, the wind tunnel's main strength comes from its ability to predict the differences or increments between the various test configurations. Thus, even though a model might have simplified surface detailing, accurate drag differences between configurations will be obtained, and the wind tunnel will permit the reliable selection of the best aerodynamic configuration. In fact, the wind tunnel can provide much more accurate measurements of small aerodynamic changes than is possible from road tests.

The data measured in the wind tunnel need to be extrapolated to full scale. This requires a method of converting the measured forces and moments from model scale to full scale - done through the concept of the aerodynamic coefficient - and a mechanism for incorporating a realistic interpretation of the wind environment in which a road vehicle operates - provided by the wind-averaged drag coefficient. These items, as well as the effects of Reynolds number, will be discussed in the following sections.

2.1 Reynolds Number Effects

The Reynolds number is the aerodynamic similarity parameter, defined as

$$Re = 1.9 \times 10^4 V_r w \qquad (1)$$

002284

where V_r = resultant airspeed due to combined wind and vehicle motion, equal to the wind tunnel test speed, km/h.

w = characteristic length, chosen as the maximum legal width, 2.59 m full scale, 0.259 m. model scale.

002284

Ideally, the Reynolds number should have the same value in the wind tunnel test as for the bus on the road to guarantee that the two flow fields are identical. This is not possible with a 1:10-scale model because the required test speed is approaching a speed where supersonic effects become significant. Fortunately, it turns out that the Reynolds number must only be high enough to guarantee that the boundary layers on the front face of the model becomes turbulent before reaching the front edges, requiring a Reynolds number of only 1.0×10^6 to 2.0×10^6 [3], compared to the full-scale value of 5.0×10^6 at 100 km/h. The present tests were run near the maximum speed of the wind tunnel, providing a test Reynolds number of 1.4×10^6, 28% of full scale at 100 km/h. This is sufficiently high for the majority of the tests, although flow tripping may be required for some of the smaller edge radii [3] to ensure full-scale behaviour.

2.2 Extrapolation to Full Scale - The Aerodynamic Coefficient

The measurements of aerodynamic force and moment made on the bus can be converted to a dimensionless form that are independent of model size and test speed, and are only a function of model shape and Reynolds number. This is done by dividing the measured forces and moments by reference forces and moments that are related to the test airspeed and to the model size. Taking drag as an example, if the drag force is divided by a reference force formed as a product of the test airstream pressure, the reference dynamic pressure, and a model reference area, commonly chosen to be the frontal area at zero yaw angle, then the drag coefficient is defined as

$$C_D = \left[\frac{D}{qA}\right] = \left[\frac{D}{3.858 \times 10^{-2}\, \rho V_r^2 A}\right] \qquad (2)$$

where D = aerodynamic drag force, N.
$(3.858 \times 10^{-2}\, \rho V_r^2)$ = dynamic pressure, Pascals
ρ = air density, 1.226 kg/m^3 at S.T.P.
A = reference frontal area, 8.358 m^2 full scale, 0.08358 m^2 model scale

Equation (2) has units of N./N., and so possess no dimensions. The full-scale drag value can be calculated from the same relationship, at any full-scale airspeed, by substitution of that airspeed, the full-scale frontal area, and the measured, model-scale drag coefficient into the inverted equation.

The moments are non-dimensionalized in a similar fashion, except that a reference moment is required in these cases. This moment is based on the reference force defined above, times an arbitrary moment arm that is commonly chosen to be the vehicle wheelbase, which is taken here as the distance between the front axle and the drive axle. Using yawing moment as an example, the yawing moment coefficient is defined as

$$C_N = \left[\frac{N}{qAb}\right] = \left[\frac{N}{3.858 \times 10^{-2}\, \rho V_r^2 Ab}\right] \qquad (3)$$

where N = aerodynamic yawing moment, N-m.
b = reference length, chosen as wheelbase, 7.225 m. full scale, 0.7225 m. model scale.

The other two force coefficients - lift and side force - and the other two moment coefficients - pitch and roll - are defined in exactly the same way.

2.3 Effects of the Natural Wind

The Earth's surface winds blow with random magnitude and direction relative to the direction of motion of a bus, causing random, time-varying changes in the resultant velocity vector at the bus. The main effect of the wind, from the perspective of the wind tunnel flow simulation, is to produce a non-zero yaw angle at the bus. This angle can be simulated in the wind tunnel by rotating the model about a vertical axis, relative to the direction of the approaching airstream. The resultant velocity vector produced by a combination of wind and bus motion is shown in the vector diagram of Figure 2, and its direction and magnitude can be calculated from

002285

$$\psi = \tan^{-1}\left\{\frac{\left[(V_w/V_b)\sin\phi\right]}{\left[1 + (V_w/V_b)\cos\phi\right]}\right\} \quad \text{deg.} \tag{4}$$

and

$$V_r = V_b\left\{1 + (V_w/V_b)^2 + 2(V_w/V_b)\cos\phi\right\}^{1/2} \quad \text{km/h.} \tag{5}$$

where
ψ = wind-induced yaw angle, deg.
ϕ = wind direction relative to the direction of bus motion, deg.
V_W = wind speed, km/h.
V_b = bus road speed, km/h.
V_r = resultant airspeed, km/h.

An example of the effect of the natural wind on the yaw angles encountered by a vehicle operating at constant speed is presented in Figure 3. This graph shows the probability of exceeding a given yaw angle at a road speed of 90 km/h and it can be seen that the yaw angle induced by the wind is at or below 9° for 90% of the time. A higher road speed reduces the angle range while a lower road speed increases it.

The random variation of the resultant velocity vector means that no single yaw angle represents the average drag of a bus on the road and that the resultant airspeed is almost never equal to the road speed. The typical drag level on the road consists of a weighted average over the yaw curve, where the weighting must reflect the probabilistic effects of the wind. The concept of the "*wind-averaged*" drag coefficient, $\overline{C}_D(V_b)$, has been developed to quantify these wind effects, as defined in the SAE Recommended Practice for the Wind Tunnel Testing of Trucks and Buses [4], and as discussed in [5]. The wind-averaged drag coefficient is defined as

$$\overline{C}_D(V_b) = \frac{1}{2\pi}\int_0^{2\pi} C_D(\psi)\left[V_r/V_b\right]^2 \, d\phi = \frac{1}{2\pi}\int_0^{2\pi} C_D(\psi)\left[1 + (11/V_b)^2 + 2\cdot(11/V_b)\cdot\cos\phi\right] d\phi \tag{6}$$

The wind-averaged drag coefficient is obtained by averaging the drag coefficient curve over the range of yaw angles produced by the national annual average mean hourly wind at bus mid-height of 11 km/h, assumed to blow equally probably from all directions, weighted by the ratio of the resultant speed to the road speed, $(V_r/V_b)^2$, to convert to the road speed of the bus as the reference speed. The use of this single wind speed and the equally-probable directional assumption are well supported by meterological data averaged at 32 sites across Canada. In this fashion, each drag-coefficient-versus-yaw-angle curve is reduced to a single, weighted, average, drag coefficient for every road speed, V_b, greatly facilitating data comparisons and providing a more meaningful number for the estimation of global fuel usage. The wind-averaged drag coefficient also simplifies the computation of bus fuel consumption or speed performance since the road speed is now the reference speed, rather than the varying, resultant airspeed, whose effects are now included in the drag coefficient. The wind-averaged drag coefficient represents the average performance of many buses operated over the entire country for a long period of time. The average drag coefficients for specific regions and specific seasons would differ from this value.

002286
002286

As the road speed varies, the yaw angles produced by the mean wind will change. At low bus speeds, V_r will be increasingly larger than V_b (equation 2) and the maximum yaw angle (equation 1) will increase also. Both of these trends will increase $\overline{C}_D(V_b)$ as V_b decreases. The change in $\overline{C}_D(V_b)$ with road speed can be conveniently related to the value at 90 km/h, a common maximum legal speed, by

$$\overline{C}_D(V_b) = \overline{C}_D(90)\,[90/V_b]^{0.22} \qquad (7)$$

This equation is a fit of the wind-averaged drag coefficient between 70 km/h and 120 km/h and slightly under-predicts the wind-averaged drag coefficient below 70 km/h. The wind-averaged drag coefficient is now based on the road speed, V_b, and the wind-averaged aerodynamic drag is given by

$$\overline{D}(V_b) = 3.858\times10^{-2}\rho V_b^2\left(\overline{C}_D(V_b)\cdot A\right) \qquad (8)$$

The variation of the wind-averaged drag and of wind-averaged drag coefficient with changing bus road speed are emphasized by explicitly indicating their functional dependence on V_b.

002287

3.0 EFFECTS OF AERODYNAMICS ON PERFORMANCE

002287

Aerodynamic forces and moments can affect several aspects of the performance of a bus. Aerodynamic drag is a major component of the total resistance which must be overcome by the engine. Thus, it will have an effect on fuel consumption and on high-speed acceleration. As previously mentioned, the aerodynamic side force and yawing moment produced by the action of the natural wind or adjacent vehicles, and to a lesser extent the associated aerodynamic rolling moment, can deflect the bus from its intended path. The aerodynamic lift and pitching moment cause a change to the vertical reaction forces at the wheels, typically reducing the load on the front wheels and increasing the load on the rear wheels. These latter effects are so small for a bus, compared to passenger and cargo weight changes, that their effects can be ignored. The other items will be discussed in the following sections.

3.1 Fuel Consumption

The fuel consumed by the engine is directly proportional to the total tractive effort required to propel the bus at a given speed. The total resistance that the engine must overcome at a constant speed is composed of the following major elements:

- rolling resistance due to tires and wheel bearings,
- drive line losses in transmitting engine power from the flywheel to the drive wheels,
- grade resistance due to climbing or descending hills,
- cornering resistance due to increased tire rolling resistance in corners,

- parasitic losses due to pumps and fans,
- aerodynamic drag due to an interaction between the moving bus and the windy atmosphere.

At speeds above 90 km/h, the aerodynamic drag becomes the largest component of propulsive power. For example, at a constant speed of 90 km/h on a flat, straight road, it is estimated by equation (15) that 40% of the fuel is consumed by aerodynamic drag, 30% by rolling resistance and 30% by accessories for the standard MCI CJ3 bus (Fig. 5). At 120 km/h, the aerodynamic component of fuel usage increases to 52% of the fuel consumed. Even if the terrain is curved and hilly, the aerodynamic drag will consume the same amount of fuel as on a flat road at the same average speed although, because of the additional fuel required for corners and hill climbing, the percentage of the total will be reduced. The aerodynamic drag on a bus is primarily due to retarding pressure forces - positive on the front end and negative on the rear end. Smaller additional contributions are made by skin friction and parasitic losses due to exposed running gear, miscellaneous protruding frames, and underbody roughness.

The power at the drive wheels required to propel the bus at a road speed of V_b km/h can be written as

$$P(V_b) = \left[\frac{D_t(V_b)\ V_b}{3600}\right] \quad \text{kw.} \qquad (9)$$

and the corresponding engine power is

$$P_e(V_b) = \left[\frac{D_t(V_b)\ V_b}{3600\ \eta}\right] + P_o \quad \text{kw.} \qquad (10)$$

where η = transmission efficiency factor, assumed to be 0.85 for a single drive axle

P_a = power used by the accessories, kw.

$D_t(V_b)$ = total resistance to motion, aerodynamic drag plus rolling resistance, N.

= $[\bar{D}(V_b) + R]$

The rolling resistance, R, can be represented by

$$R = (a_1 + a_2 V_b) M \quad \text{N.} \qquad (11)$$

where V_b = road speed, km/h.

M = bus mass, kg.

a_i = rolling resistance coefficients

Typical values for the two rolling resistance constants for radial truck or bus tires are

$$a_1 = 5.3\text{x}10^{-2} \ \text{N/kg.} \quad \text{and} \quad a_2 = 4.0\text{x}10^{-4} \ \text{N-hr/kg-km.} \qquad (12)$$

002288

002288

The accessory power requirements are difficult to determine. Part of the accessory load will be variable, even at constant rpm, due to fluctuating demands for electrical power and air conditioning. Other components of this load, such as power to the cooling fan, will be rpm dependent. A single linear dependence of accessory power requirements versus road speed was assumed as an approximation to the accessory power demand. While the assumed power function will probably under-predict the accessory power requirements at low speeds, in the intermediate gears, it should provide a reasonable full-load estimate at higher speeds in top gear, where aerodynamic effects are dominant. The following function was assumed for the accessory power requirements as a function of engine power level and road speed

$$P_a = P_o\left[7.70\times10^{-3} + 1.50\times10^{-3}\,V_b\right] \quad \text{kw.} \qquad (13)$$

where P_o = engine power rating, kw.

Substitution of equations (2), (7), (11), and (13) in equation (10) gives the total engine power as

$$\overline{P}_e(V_b) = \left[\frac{\left(5.30\times10^{-2} + 4.00\times10^{-4}V_b\right)MV_b}{3600\ \eta}\right] + \left[\frac{3.858\times10^{-2}\rho V_b^3\left(\overline{C}_D(V_b)\cdot A\right)}{3600\ \eta}\right]$$

$$+ \left[P_o\cdot\left(7.70\times10^{-3} + 1.50\times10^{-3}V_b\right)\right] \qquad (14)$$

Note that the wind-averaged drag coefficient is used in the aerodynamic drag equation in place of the regular drag coefficient, so necessitating the use of the road speed, V_b, in the calculation, instead of the resultant airspeed. The three major terms in equation (14) are plotted in Figure 4 for the standard CJ3 configuration. The wind-averaged drag coefficient used was the speed-dependent wind-averaged drag coefficient, equation (8). The drag coefficient at 90 km/h was 0.732, the frontal area was 8.36 m^2, the assumed bus mass was 16500 kg, the engine power was 300 kw, and the transmission efficiency was 0.85. The fuel consumed at a given power level is obtained by using the specific fuel consumption of the engine. A useful average value, characteristic of turbo-charged diesel engines, is SFC = 0.275 ℓ/kw-h (0.045 Imp. gal/hp-h or 0.38 lb/hp-h). The fuel consumed per 100 kilometres is given by

$$\mu = \left[\frac{100\cdot SFC\cdot P_e}{V_b}\right] = 27.5\left[\frac{P_e}{V_b}\right] \quad \ell/100\text{-km.} \qquad (15)$$

Combining equations (14) and (15), the wind-averaged bus fuel consumption, $\overline{\mu}(V_b)$, can be expressed in terms of vehicle size, mass, road speed, and wind-averaged drag coefficient by

002289

002289

$$\bar{\mu}(V_b) = \left[\frac{\left(1.46 + 1.10\times10^{-2}V_b\right)M}{3600\ \eta}\right] + \left[\frac{1.061\rho V_b^2\left(\bar{C}_D(V_b)\cdot A\right)}{3600\ \eta}\right]$$

$$+ \left[P_o \cdot \left(\frac{2.12\times10^{-1}}{V_b} + 4.13\times10^{-2}\right)\right] \quad \ell/100\text{-km}. \qquad (16)$$

Inverting the fuel usage calculated from equation (16) and dividing by 100 will give the fuel consumption in km/ℓ . Equation (16) shows that the fuel consumed by aerodynamic drag varies directly with the frontal area, the drag coefficient and with the square of speed. The latter variation is the reason for the importance of aerodynamic effects at higher speeds. The primary aerodynamic parameter is the product of drag coefficient and frontal area, $\bar{C}_D(V_b)\cdot A$, often termed the drag-area. The fuel consumed by rolling friction is only a weak function of speed, being approximately proportional to $V_b^{1/4}$. The three terms of equation (16) are plotted in Figure 5 and the relative importance of the fuel consumed to overcome aerodynamic drag at high speed is evident. The change in fuel consumption due to a change in aerodynamic drag is given by

$$\Delta\mu(V_b) = 2.947\times10^{-4}\rho V_b^2\left(\Delta\bar{C}_D(V_b)\cdot A\right)/\eta \quad \ell/100\text{-km}. \qquad (17)$$

002290

where $\Delta\bar{C}_D = \bar{C}_D(\text{reference}) - \bar{C}_D(\text{modified})$ is the difference in wind-averaged drag coefficient between the original and the modified configurations. This equation will be used frequently to compute fuel savings in the discussions that follow.

3.2 Cross-wind Handling

The deflection of the bus from it's path under the influence of side winds cannot be computed simply from aerodynamic force and moment measurements alone, but must be obtained from a dynamic analysis of the bus and its driver. However, it is possible to make a few general statements about the static directional stability of the bus as a guide to assessing the qualitative effects of changes in the lateral aerodynamic forces and moments. The lateral aerodynamic quantities that affect cross-wind handling are comprised of the side force, the yawing moment, and the rolling moment, and are defined in the sketch of Figure 6.

The side force and the yawing moment have the strongest effect on the lateral deviation of the bus from its path when acted on by a side wind, with the yawing moment being the most important parameter. The rolling moment is a second-order parameter through the influence of roll angle on roll-induced steering - a function of the suspension design.

The side force and the yawing moment both act to deflect the bus away from the direction of the incident wind and are, as a consequence, statically destabilizing (weathercock unstable). If the driver takes no corrective action, the bus would leave the road. The side force and the yawing moment are coupled, since the side force, acting at some point along the length of the bus termed the yaw centre of pressure, can be considered to have produced the yawing moment.

002290

Similarly, the side force and the rolling moment are coupled, except that the roll centre of pressure is measured vertically from the co-ordinate reference centre at ground level.

The side force variation with yaw angle is nearly the same for most bus configurations while the yawing moment varies more with bus shape. Effectively, the yaw centre of pressure moves forward or rearward along the length of the bus as the front and rear shapes are changed. A bluff body, like a square-edged rectangular block, has a yaw centre of pressure at the mid-length point of the body. A streamlined shape, like an aerofoil, has the yaw centre of pressure at a point one-quarter of the aerofoil length aft of the leading edge. A bus, being well streamlined at the front end, may have its centre of pressure even farther forward. As a bus becomes more streamlined and develops lower aerodynamic drag, so its centre of pressure moves forward, and the bus becomes less weathercock stable. Simply put, it blows around more in the wind. Again, without a complete dynamic analysis, it is impossible to quantify the degradation in cross-wind handling. However, there is an anecdotal measure of this effect available.

It was reported by MCI engineering staff that a few drivers have commented that the MCI CJ3 bus is better handling in a cross wind than the Prevost H3-40. It appears that only some drivers have noticed this handling difference, and they say that it is not large. Thus the aerodynamic differences between these configurations, both of which were tested in this program, define the boundary of a just-perceptible threshold in yawing moment change or, equivalently, yaw centre of pressure movement. The centre of pressure location for a small range of yaw angles near zero yaw can be obtained from the ratio of the slope of the yawing moment coefficient curve divided by the slope of the side force coefficient curve. Analytically, this is expressed as

002291 002291

$$\left(x_{cp}/b\right) = \left[\frac{dC_N/d\psi}{dC_S/d\psi}\right] \tag{18}$$

where x_{cp} = location of the centre of pressure ahead of the chosen moment centre at the mid-wheelbase point, m.

b = reference length, 7.225 m.full scale, 0.7225 m. model scale

$dC_N/d\psi$ = slope of the yawing moment coefficient versus yaw angle curve for the yaw range between ±3°, $deg.^{-1}$

$dC_S/d\psi$ = slope of the side force coefficient versus yaw angle curve for the yaw range between ±3°, $deg.^{-1}$

The locations of the yaw centres of pressure for the two configurations just mentioned, measured forward from the mid-wheelbase point, were found to be

CONFIGURATION	(x_{cp})
MCI (#37)	2.06 m.
Prevost (#63)	2.29 m.

Thus a forward, destabilizing movement of the centre of pressure of about 0.23 m. is just detectable by some drivers and several times this change might be acceptable.

4.0 TEST PROGRAM

The primary purpose of the wind tunnel test program was to select the front and rear end shapes from the new proposals that gave the lowest aerodynamic drag, while a secondary purpose was the comparison of the best of the new proposals with the current MCI bus and with buses from competing manufacturers. At the same time, the remaining aerodynamic forces and moments were measured so that their effects on stability and cross-wind handling could be assessed. Both smoke and a surface oil film were used to visualize the flow over and on the surface of the best combination. The test program is summarized in the Run Log of Appendix 1.

4.1 Model Installation

A 1:10 scale model of the bus chassis was mounted on the standard NRC vehicle ground plane, Figure 1. The model accurately duplicated the external geometry of the bus. The seven front-end shapes, one of the two rear-end shapes, and the body side and roof panels were numerically milled from mahogany. The second rear end was manufactured using stereo-lithography. The body components were attached to chassis and running gear manufactured from aluminum. The model included such details as fenders, wheels and wheel wells, drip rails, escape hatches, and mirrors. No internal flows, air intakes, underbody roughness, engine bay openings, or window frames were reproduced. The former were excluded because of the difficulty of representing cooling flows adequately at model scale and because their effects would be the same for each configuration, and the latter because the frames were so shallow as to be unimportant and the other openings were too complex and, once again, would cause no relative difference between configurations. The external surfaces of the model were smooth and leak-free, representing flush windows, doors, and seals. The front and rear faces of the bus could be readily removed to permit the testing of alternate components.

002292

002292

The bus was connected to the six-component, mechanical balance of the wind tunnel by pins extending from the standard model-mounting plate, through the groundboard cover plate, into the front and rear tire contact patches. This provided an aerodynamic-interference-free mounting. The six balance outputs were averaged digitally over a 10 second period at repetition rates of 20 samples per second per channel to form stable averages with an overall measuring accuracy of ±0.5%.

4.2 Model Configurations

The two prototype front-end shapes had been designed to provide good aerodynamics through a combination of windshield slope, face curvature, and edge rounding, within the bounds of aesthetic, engineering, and operational requirements. The other five front ends included the current MCI CJ3 production bus and three competitors designs. One alternate rear-end shape to the standard was tested, based on the optimal-design information presented in [3]. The effect of additional components such as drip rails, escape hatches, and mirror shape and location were also investigated. The bus model was designed to permit the rapid evaluation of alternate front-end and rear-end designs through the use of removable components. The model chassis, the seven front ends, and the two rear ends that were tested are shown in the drawings of Figure 7 and the photographs of Figure 1. A complete set of photographs of all of the model configurations tested is presented in Appendix 2.

The front-end shapes consisted of the following:

1) **Standard CJ3**	The standard CJ3 front including all window moulding details.
2) **Smooth CJ3**	A modified CJ3 front with larger edge radii and flush glass.
3) **Proposal 1**	A new design with flush glass.
4) **Proposal 2**	A new design with flush glass.
5) **Prevost H3-40**	Competitor.
6) **Mercedes 0404**	Competitor.
7) **Setra S315**	Competitor.

The rear-end shapes consisted of the following:

1) **Standard CJ3**	Top and sides parallel to the top and sides of the main bus with 204 mm rear-edge radii.
2) **Bevelled Rear**	Roof and sides of the body bevelled at an angle of 15° to the main panels over the last 1m of the body with rear-edge radii of 51 mm.

4.3 Definition of the Measurement Coordinate System

Six components of aerodynamic force and moment were measured simultaneously. The measurements in this report are presented in a body-fixed co-ordinate system that is defined in Figure 6. These measured forces and moments were reduced to coefficient form as defined in the Notation, Section 8.0, and as discussed in Section 2.2.

4.4 Test Procedure

Each configuration was tested over a range of eight yaw angles from -3° to +12° in the following sequence: -3.0°, -1.5°, 0.0°, 1.5°, 3.0°, 6.0°, 9.0°, 12.0°. The yaw angles were set by rotating the model in the wind tunnel sequentially through the required set of angles, under computer control, and pausing at each angle sufficiently long to acquire the necessary measurements. The yaw tests were performed at a wind speed of 302 km/h (84 m/sec). At this speed, the model Reynolds numbers were 0.34 and 0.26 of those of the full-scale bus at 90 km/h and 115 km/h, respectively. Additional tests were also made over a range of Reynolds numbers at 0° yaw angle to investigate the Reynolds number sensitivity of the drag. Some tests were also run with strips of grit upstream of the rounded front edges to ensure that the boundary layers on the front face had gone through transition before the flow reached the edges.

5.0 RESULTS

The following presentations, discussions and interpretations of results focus primarily on aerodynamic drag, although the location of the yaw centre of pressure for important configurations will be presented to allow an assessment of cross-wind handling changes. A total of 37 runs were performed during the wind tunnel test. A detailed summary of these runs is given in Appendix 1. In addition, this Appendix summarizes the wind-averaged drag coefficients at a road speed of 90 km/h. Appendix 3 contains a complete tabulation of the wind tunnel data and Appendix 4 presents plots of all the aerodynamic coefficients.

6.0 DISCUSSION AND INTERPRETATION OF RESULTS

This Section presents the major findings of the investigation and summarizes these in terms of the measured changes in wind-averaged drag coefficients, in terms of the expected changes in fuel consumption that would result, and in terms of the changes in cross-wind sensitivity that accompany the drag changes. The changes in fuel consumption were computed only at 90 km/h and 120 km/h.

The best combination of front and rear components was selected from the three new front-end and two rear-end designs. This combination was compared in detail to the standard MCI 102 CJ3 bus and to the three competitors from the point of view of fuel usage.

002294

002294

6.1 Reynolds Number Effects

After the first set of measurements were made with the seven front ends, an examination of the data showed an apparent anomaly in the yaw data for the Proposal 2 front end at yaw angles greater than +3°, where the drag was observed to increase more rapidly than would be expected. This was judged to be a result of leading-edge flow separation due to insufficiently high Reynolds number for this configuration. No other configuration showed this effect. It was decided to trip the flow on this and the three other smooth, front-end configurations - Proposal 1, Smooth CJ3, and Prevost H3-40 - to make sure that such effects were eliminated. Fine, #40-grit particles were sprinkled sparsely on 0.5-cm wide strips of glue painted on each front face, just upstream of the front edges, to encourage early boundary layer transition. A typical application is shown in photograph P??. A comparison of the variation of drag coefficient with Reynolds number at 0° yaw angle of the four, smooth-edged configurations is presented in Figure 8, with and without the trip strips.

Generally, the absence of a trip results in high drag coefficients at low Reynolds numbers, followed by a rapid drop in drag coefficient above some threshold Reynolds number that varies from model to model. This drop results from the natural transition of the boundary layer on the front face of each model from laminar to turbulent, so reducing the occurrence of flow separation from the front edges. The presence of the grit strips ensures that the flow is turbulent, causing the drag drop at much lower Reynolds numbers. The end result is a flow field on the model that is more typical of the full scale bus at its higher operating Reynolds number.

The effect of the flow trips on the yaw behaviour of these four configurations at the test Reynolds number of 1.4×10^6 is summarized in Figure 9. The measurements with and without grit on the Smooth CJ3 front and the Proposal 1 front are identical. The presence of the trip lowers the drag on the Prevost front slightly at yaw angles ≤6° and smooths the drag curve at higher yaw angles. The flow trip had the greatest effect on the Proposal 2 front configuration substantially lowered its drag coefficients for yaw angles above 3°.

The remainder of the measurements on these four configurations were made with the trips present because they were felt to better represent full scale.

6.2 Front-End Shape Effects

The first set of measurements were made to select the best new front-end shape from the new proposals. All the front ends were tested without mirrors and with the standard CJ3 rear end. Figure 10 summarizes the drag results for the new front-end shapes. It shows that all three of the new shapes are nearly identical to each other and are better than the current MCI CJ3 front. The Proposal 2 shape was chosen by the attending MCI engineers as the best shape because of its good aerodynamic performance, its ease of manufacture compared to Proposal 1, and because of its styling. Figure 11 compares the standard MCI front end and the Proposal 2 shape with shapes used by the competition. Both the Setra and the Mercedes front ends have higher drag than the standard MCI shape and much higher drag than the Prevost or the MCI Proposal 2 shapes. The MCI Proposal 2 shape has slightly lower drag than the Prevost shape for $\psi \leq 3°$ and increasingly lower drag at higher yaw angles. Table 6.1 summarizes the wind-averaged drag coefficients, the fuel consumption changes, and centre-of-pressure locations for these seven geometries. Figure 12 compares the side force and the yawing moment coefficients. The higher-drag front ends usually have the lower yawing moments and, consequently, smaller magnitudes for the yaw centre of pressure locations, as also seen in Table 6.1.

002295

TABLE 6.1: FRONT-END SHAPE EFFECTS WITH CJ3 REAR

	90 km/h			120 km/h			
CONFIGURATION	$\overline{C}_D$	$\Delta\overline{C}_D$	$\Delta\overline{\mu}^*$	$\overline{C}_D$	$\Delta\overline{C}_D$	$\Delta\overline{\mu}^*$	x_{cp}#
STD CJ3, #19	0.584			0.558			1.95
SMOOTH CJ3, #72	0.380	0.204	5.87	0.370	0.188	9.62	2.29
PROPOSAL 1, #69	0.367	0.217	6.25	0.360	0.198	10.13	2.40
PROPOSAL 2, #40	0.365	0.219	6.30	0.357	0.201	10.29	2.25
PREVOST, #65	0.418	0.166	4.78	0.386	0.172	8.8	2.06
SETRA, #35	0.625	-0.041	-1.18	0.601	-0.043	-2.20	1.98
MERCEDES, #22	0.620	-0.036	-1.04	0.598	-0.040	-2.05	1.62

* change in fuel consumption, ℓ/100-km., positive represents a fuel saving.

\# distance in m. forward of the mid-wheelbase point.

6.3 Rear-End Shape Effects

The alternate rear end utilized the optimum rear body bevel angle of 15° and bevel length of 1.0 m full scale, as specified in [3]. This geometry has the potential to reduce the base drag by 40% to 60%, based on the data presented in [3], with the level of reduction being dependant on the shape of the forward part of the bus. This rear shape is compared to the standard, CJ3 rear shape, both with and without the standard, CJ3 mirrors in Figure 13. The effects of mirrors will be discussed in more detail in the following Section. The new rear shape reduces the drag and moves x_{cp} forward in both cases. The wind-averaged drag coefficients, fuel consumption changes, and centre-of-pressure locations are presented in Table 6.2.

TABLE 6.2: EFFECT OF BEVELLED REAR WITH PROPOSAL 2 FRONT

CONFIGURATION	90 km/h			120 km/h			
	$\overline{C}_D$	$\Delta\overline{C}_D$	$\Delta\overline{\mu}^*$	$\overline{C}_D$	$\Delta\overline{C}_D$	$\Delta\overline{\mu}^*$	x_{cp} #
CJ3 REAR, NO MIR, #40	0.365			0.357			2.25
BEV REAR, NO MIR, #51	0.299	0.066	1.90	0.295	0.062	3.17	2.78
CJ3 REAR, CJ3 MIR, #42	0.394			0.385			2.28
BEV REAR, CJ3 MIR, #53	0.339	0.055	1.58	0.331	0.054	2.76	2.80

* change in fuel consumption, ℓ/100-km., positive represents a fuel saving.

\# distance in m. forward of the mid-wheelbase point.

6.4 Mirrors

The effects of mirror shape and position were investigated for the Proposal 2 front with the CJ3 rear. Three sets of mirrors were fabricated - the current MCI design, the Prevost design, and the Setra design. The Setra and Prevost mirrors were mounted in one position only, photographs P13 and P14, while the MCI mirrors were mounted with three alternate positions. These positions were forward, aft, and asymmetrical, as shown in photographs P11, P12, and P16. The asymmetrical configuration is more representative of real operation, where the left-hand mirror was set more aft than the right-hand mirror, which was set in the forward position. The effect of mirror position and type can be seen in Figure 14. The addition of any mirror is seen to increase the drag, with the Setra mirrors causing the largest increase. The standard MCI mirrors produced higher drag in the aft position than in the forward position. This may be explained by the fact that the planes of the mirrors in the forward positions were nearly parallel to the flow around the front, side edges, whereas they were more nearly perpendicular to the flow in the aft position. The drag coefficients for the asymmetrical positions were between the values for the other two positions. The Prevost mirrors provided slightly lower drag than the MCI mirrors for $\psi \leq 3°$ but much higher drag above this angle. Apparently, the Prevost mirrors caused flow separation over at least part of the downwind side of the bus. The results of the mirror variations are summarized in Table 6.3.

TABLE 6.3: MIRROR EFFECTS WITH PROPOSAL 2 FRONT AND CJ3 REAR

CONFIGURATION	90 km/h $\overline{C}_D$	90 km/h $\Delta\overline{C}_D$	90 km/h $\Delta\overline{\mu}$*	120 km/h $\overline{C}_D$	120 km/h $\Delta\overline{C}_D$	120 km/h $\Delta\overline{\mu}$*
NO MIRRORS, #40	0.365			0.357		
MCI MIRRORS FWD, #42	0.394	-0.029	-0.83	0.385	-0.028	-2.20
MCI MIRRORS AFT, #44	0.405	-0.040	-1.15	0.398	-0.041	-3.07
MCI ASSYM. MIRRORS✢	0.415	-0.050	-1.44	0.403	-0.046	-2.35
SETRA MIRRORS, #46	0.434	-0.069	-1.99	0.425	-0.068	-4.35
PREVOST MIRRORS, #48	0.422	-0.057	-1.64	0.397	-0.040	-1.84

* change in fuel consumption, ℓ/100-km., positive represents a fuel saving.

✢ estimated as #40+(#55-#51).

6.5 Miscellaneous Modifications

A series of small modifications were made to investigate the following:

- wheel skirts closing the sides of the wheel wells, P17; Run # 57
- a front air dam below and behind the bumper, P18; Run # 58
- tire fairings to shield the tires from the oncoming flow, P19; Run # 59
- rear side vortex generators, P20; Run # 60
- a modified drip rail, P21; Run # 61

Most of these modifications had only small effects on the drag. Of them, only the wheel skirts produced a drag reduction while the remainder produced no change or a drag increase. The results of these tests are summarized in Table 6.4.

TABLE 6.4: MISCELLANEOUS SMALL MODIFICATIONS TO THE PROPOSAL 2 FRONT WITH BEVELLED REAR AND ASYMMETRICAL MIRRORS

CONFIGURATION	90 km/h $\overline{C}_D$	90 km/h $\Delta\overline{C}_D$	90 km/h $\Delta\overline{\mu}$*	120 km/h $\overline{C}_D$	120 km/h $\Delta\overline{C}_D$	120 km/h $\Delta\overline{\mu}$*
STANDARD, #55	0.349			0.341		
WHEEL FAIRINGS, #57	0.330	0.019	0.55	0.324	0.017	0.31
AIR DAM, #58	0.393	-0.044	-1.27	0.380	-0.038	-1.94
TIRE FAIRINGS, #59	0.353	-0.004	-0.23	0.349	-0.008	-0.41
VORTEX GENERATORS, #60	0.354	-0.005	-0.14	0.346	-0.005	-0.31

* change in fuel consumption, ℓ/100-km., positive represents a fuel saving.

002297
002297

6.6 The Best Combination

A comparison can now be made between the best new configuration, the Proposal 2 front with the bevelled rear, the current production MCI CJ3 bus, the Prevost H3-40 bus, the Mercedes 0404 bus, and the Setra S315 bus. These configurations were composed of the following elements:

New MCI	-	Proposal 2 front, bevelled rear, asymmetrical mirrors
MCI CJ3	-	CJ3 front, CJ3 rear, asymmetrical mirrors (estimate)
Prevost H3-40	-	Prevost front, CJ3 rear, Prevost mirrors
Mercedes 0404	-	Mercedes front, CJ3 rear, Prevost mirrors (estimate)
Setra S315	-	Setra front, CJ3 rear, Setra mirrors (estimate)

Estimates were used for the drag of most of the mirror geometries because not all of the front-end configurations were tested with the required mirrors or mirror locations. In each case where an estimate was made, the additional drag increment due to the mirror change, based on the mirror measurements made with the Proposal 2 front, were added to account for these mirrors on the other bus shapes. Table 6.5 summarizes the differences in drag and fuel consumption between these configurations, using the Proposal 2 configuration as the reference. The drag increments added to account for the incorrect mirror geometries are summarized in the table. Thus, the wind-averaged drag coefficients quoted are those for the run indicated, plus the additional mirror drag increment, $\Delta\overline{C}_{D_{mir}}$.

TABLE 6.5: COMPARISON OF FULLY-EQUIPPED BUSES

CONFIGURATION	90 km/h				120 km/h				
	$\Delta\overline{C}_{D_{mir}}$	$\overline{C}_D$✤	$\Delta\overline{C}_D$	$\Delta\overline{\mu}$*	$\Delta\overline{C}_{D_{mir}}$	$\overline{C}_D$	$\Delta\overline{C}_D$✤	$\Delta\overline{\mu}$*	x_{cp}#
NEW MCI, #55		0.349				0.341			2.81
MCI CJ3, #37	0.010	0.606	-0.257	-7.40	0.010	0.581	-0.240	-12.28	2.06
PREVOST, #63		0.447	-0.098	-2.82		0.415	-0.074	-3.79	2.29
MERCEDES, #22	0.029	0.649	-0.300	-8.64	0.029	0.627	-0.286	-14.63	1.62
SETRA, #35	0.069	0.694	-0.345	-9.93	0.068	0.669	-0.328	-16.78	1.98

✤ equal to the wind-averaged drag coefficient for the run number stated plus the mirror drag increment $\Delta\overline{C}_{D_{mir}}$.

* change in fuel consumption, ℓ/100-km., positive represents a fuel saving.

\# distance in m. forward of the mid-wheelbase point.

The drag coefficient curves for these configurations are compared in Figure 15 and the side force and yawing moment coefficient curves are presented in Figure 16. Once again, estimated mirror drag coefficients have been added to the configurations noted above. The key for Figure 15 summarizes the measurements that were combined to produce the curves plotted.

Figure 17 compares the fuel consumption of the new design with those of the other four main configurations, as functions of road speed, for identical masses of 16,500 kg, identical drive-line losses of 15%, and identical frontal areas of 8.36 m^2. The new bus is seen to provide a large reduction in fuel consumption compared to the standard MCI CJ3 bus and the two European buses, and a substantial advantage over the Prevost bus. The current MCI CJ3 is inferior to the Prevost H3-40. The improvement of the new configuration over the MCI CJ3 results from both front and rear shape improvements while the advantage over the Prevost bus comes primarily from the rear-end shape. The new MCI configuration would have a yaw centre of pressure location that is 0.52 m ahead of that for the Prevost bus.

6.7 Flow Visualization

The flow over the best combination was observed, or visualized, using two techniques. First, smoke was used to obtain a gross overview of the external flow field and, second, a fine pigment suspended in an oil mixture was painted on the surface of the bus to show the details of the surface flow. Both flow visualization techniques were performed at zero yaw angle only.

The smoke flow photographs of Figure 18 show a few important details of the flow. Figures 18a, 18b, and 18c clearly indicate that the gross flow follows the contour of the bus, both up over the front top edges and down over the rear bevel. Figure 18d shows the wake of a mirror extending along the side of the bus.

The surface-oil-flow photographs of Figure 19 contain more detail than do the smoke flow photographs. Figure 19a shows the stagnation point on the front face of the bus. The flow streamline that strikes the bus at this point comes to a complete stop, providing the point of highest positive pressure on the front face. The remaining streamlines turn and diverge from this point. While the smoke showed that the flow around the front edges was attached, the oil flow shows that there is a very small separation region, or bubble, at the downstream edges of the top and side corners. Here, the flow separates and immediately re-attaches, producing a small separated cavity parallel to these corners, as indicated by the accumulations of oil. The small separation causes little or no drag increase although it indicates that the edge radius should be increased for a greater margin from separation - an observation that is consistent with the Reynolds number sensitivity observed for this configuration.

The influence of the mirror can be seen over the full length of the side of the bus in Figures 19b and 19c. The two lines above and below the mirror on the bus body indicate separation lines feeding a pair of vortices induced by the mirror. These vortices contribute to the drag increase caused by the mirrors and could be a source of aerodynamic noise. The mirror on the driver's side, in the aft position, showed an almost identical flow pattern.

Figure 19d shows the rear-end flow. The flow is attached on the bevelled top and side panels and is separated over the bluff base. It appears that a horizontal, trapped vortex sits on the upper third of the base, in the region that is covered with the oil mixture. It is fed by the flow over the roof and along the upper sides of the body. The strength of this vortex flow may tend to keep this region scoured clear of dirt. The remaining, lower, separated flow region is fed by the underbody flow and by the side flows coming over and out of the rear wheel wells. It should be the dirtier region because it is fed by the most dirt-laden flow from the wheels and because the larger, more diffuse vortex contains lower-speed flows.

7.0 CONCLUSIONS

A wind tunnel test was performed to select the best aerodynamic configuration for a new bus - Proposal 2 with a bevelled rear end - from a set of proposed designs, and to compare this configuration to the current production MCI CJ3 and to three competitors - the Prevost H3-40, the Mercedes 0404, and the Setra S315. The new design had lower aerodynamic drag than the other buses, resulting in lower predicted power consumptions and lower fuel consumptions. The reduced fuel consumption has an obvious and strong impact on the direct operating cost of the bus while the lower required power level should result in reduced noise, increased drive line reliability, better passing acceleration, and greater drive tire life. An indication of the superior performance of the new bus is given in the following table.

PERFORMANCE COMPARISON AT 120 km/h

BUS	$\overline{C}_D$	TOTAL POWER, kw	FUEL CONSUMPTION ℓ/100-km.
New MCI	0.349	197.8	45.3
MCI CJ3	0.606	252.8	57.9
Prevost H3-40	0.447	214.8	49.2
Mercedes 0404	0.649	260.9	59.8
Setra S315	0.694	271.4	62.2

002300

This design is a good compromise between low drag, as shown by these tests, and ease of manufacture, according to the attending MCI engineers. It would be possible to design a lower-drag front end for this new configuration, one that might have a wind-averaged drag coefficient below 0.30, but it may require a significant change to the driving position and mirrors, as well as being a more difficult and expensive geometry to manufacture.

8.0 NOTATION

- a_i rolling resistance coefficients, equation (12)
- b reference width for moment coefficients, wheelbase, 7.225 m. full scale, 0.7225 m. model scale
- C_D drag coefficient, $D/(1/2\rho V^2 A)$
- $\overline{C}_D(V_b)$ wind averaged drag coefficient based on *bus road speed*, $\overline{C}_D(V_b) = \overline{D}/(1/2\rho V_b^2 A)$
- C_L drag coefficient, $L/(1/2\rho V^2 A)$
- C_M drag coefficient, $M/(1/2\rho V^2 Ab)$
- C_N drag coefficient, $N/(1/2\rho V^2 Ab)$
- C_R drag coefficient, $R/(1/2\rho V^2 Ab)$
- C_S drag coefficient, $S/(1/2\rho V^2 A)$
- D aerodynamic drag force, N.

$\overline{D}(V_b)$	wind-averaged drag, includes the effects of the 11 km/h annual hourly mean wind speed blowing with equal probability from all directions, N.
D_t	total resistance to the forward motion of a bus due to aerodynamic drag, rolling resistance of tires, and wheel bearing losses, N.
$dC_N/d\psi$	slope of the yawing moment coefficient versus yaw angle curve, $deg.^{-1}$
$dC_S/d\psi$	slope of the side force coefficient versus yaw angle curve, $deg.^{-1}$
M	bus mass, kg.
$P(V_b)$	power required at the rear wheels for propulsion of the bus at speed V_b, kw.
P_a	accessory power consumption, kw.
P_e	engine power, P_a/η , kw.
$\overline{P}_e(b)$	wind-averaged engine power, kw.
P_o	engine power rating, kw.
R	rolling resistance of tires and wheel bearings, N.
V_b	bus road speed, km/h.
V_r	resultant air speed due to wind and bus motion, equivalent to wind tunnel test speed, equation (5), km/h.
V_w	speed of the natural wind, km/h.
w	reference length for Reynolds number, maximum legal vehicle width, 2.56 m.
x_{cp}	centre of pressure of the side force vector relative to the mid-wheelbase origin of coordinates, equation (18), m.
ρ	air density, 1.226 kg/m^3 at S.T.P.
ψ	yaw angle, the angle between the direction of the resultant wind and the direction of bus motion, equation (4), deg.
ϕ	direction of the natural wind relative to the direction of bus motion
η	transmission efficiency
μ	bus fuel consumption, ℓ/100-km.
$\overline{\mu}(V_b)$	wind-averaged bus fuel consumption, equation (16), ℓ/100-km.

002301 002301

9.0 REFERENCES

1. Cooper, K. R., The Wind Tunnel Simulation of Surface Vehicles.
2. Cooper, K. R., The Effect of Aerodynamics on the Performance and Fuel Consumption of Trucks and Buses.
3. Cooper, K. R., The Effect of Front-Edge Rounding and Rear-Edge Shaping on the Aerodynamics of Bluff Vehicles in Ground Effect.
4. The Wind Tunnel Testing of Buses and Trucks.
5. Cooper, K. R., The Wind Tunnel Testing of Eight Commercially-Available Aerodynamic Drag Reducing Devices.

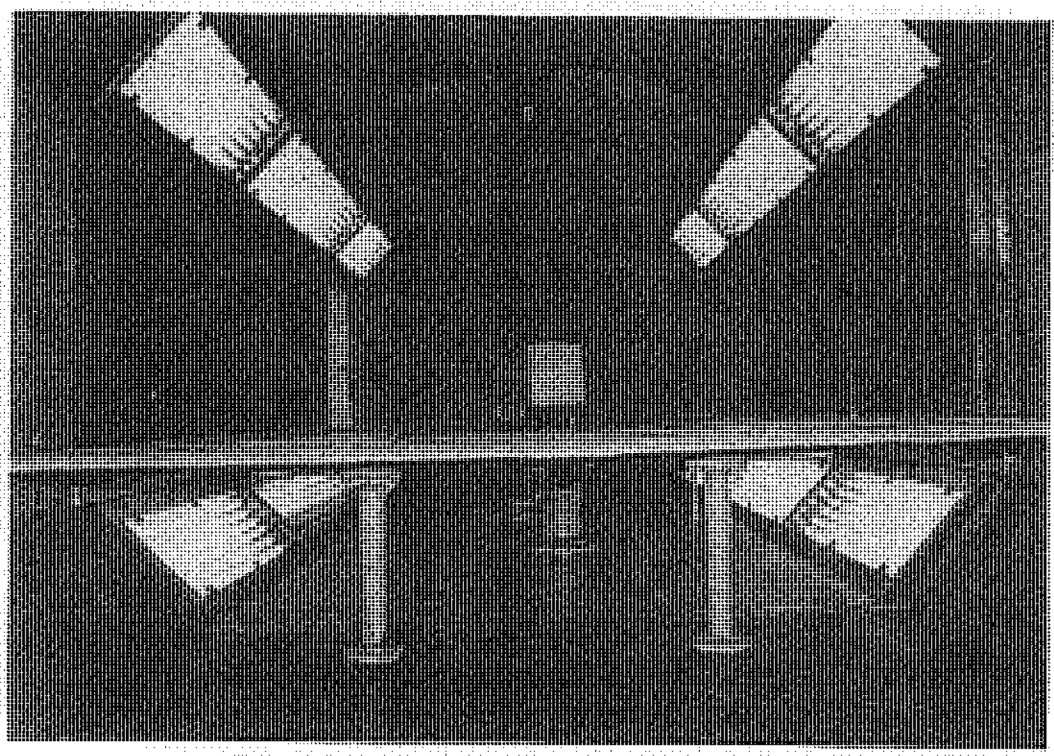

FIG. 1a: SMOOTH CJ3 MODEL ON GROUNDBOARD LOOKING DOWNSTREAM

002302

002302

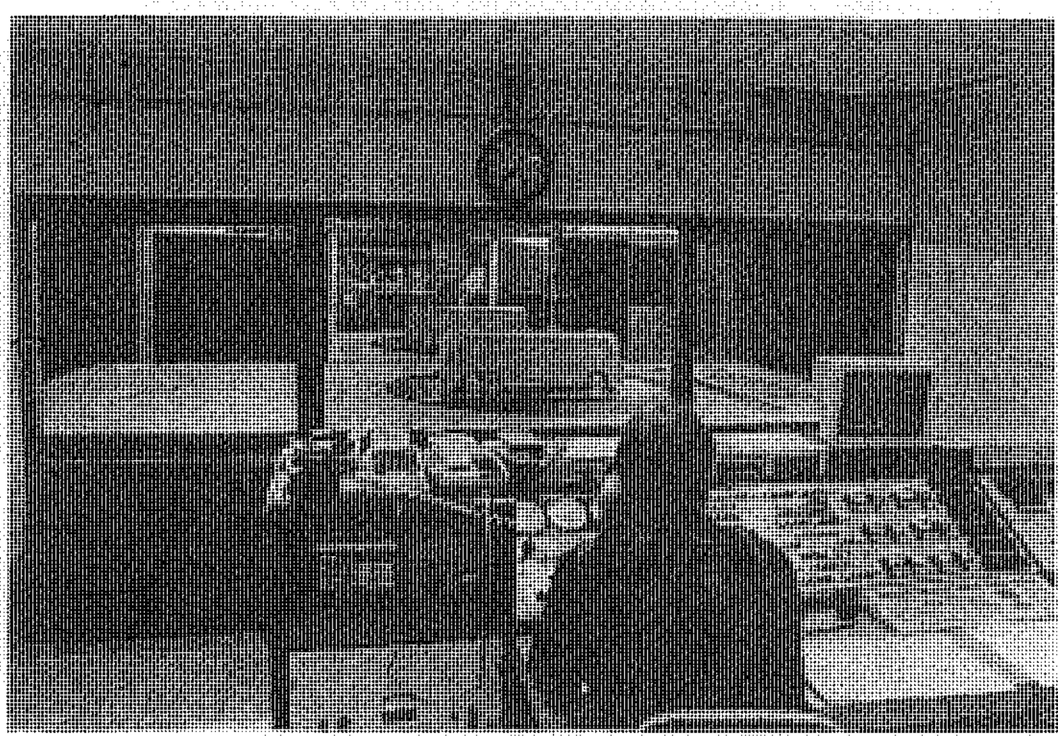

FIG. 1b: TEST SECTION AND CONTROL ROOM VIEWED FROM BEHIND OPERATOR

002302

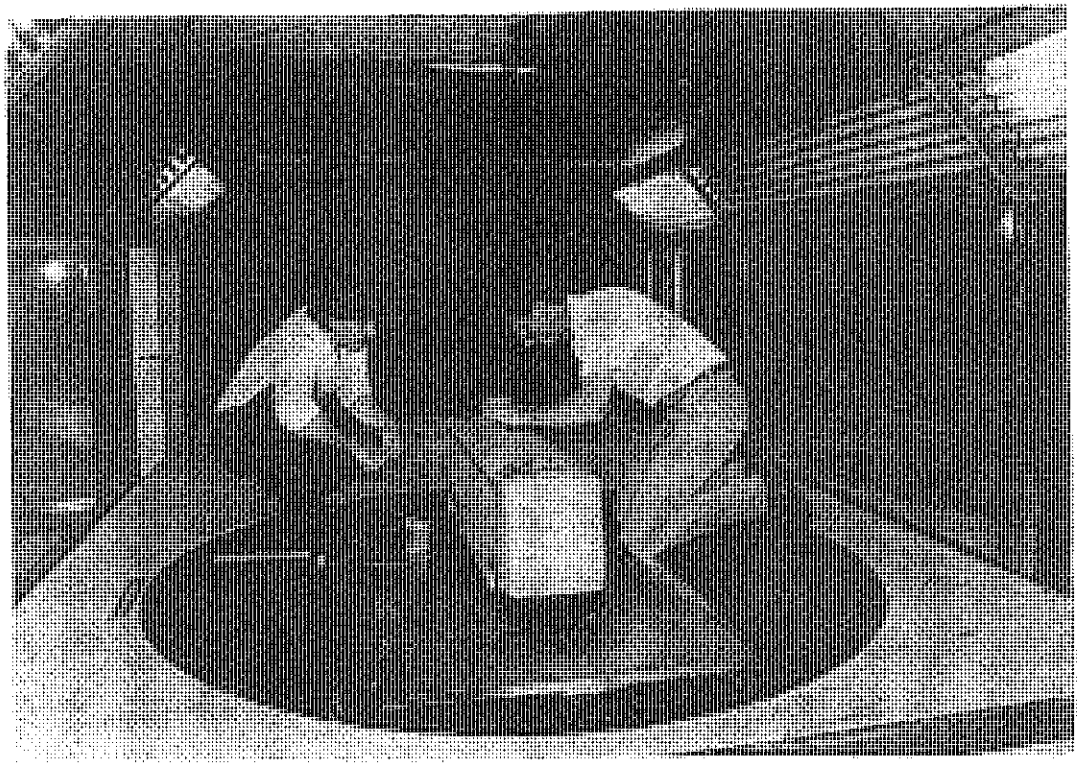

FIG. 1c: FITTING HATCHES, SMOOTH CJ3

002303

002303

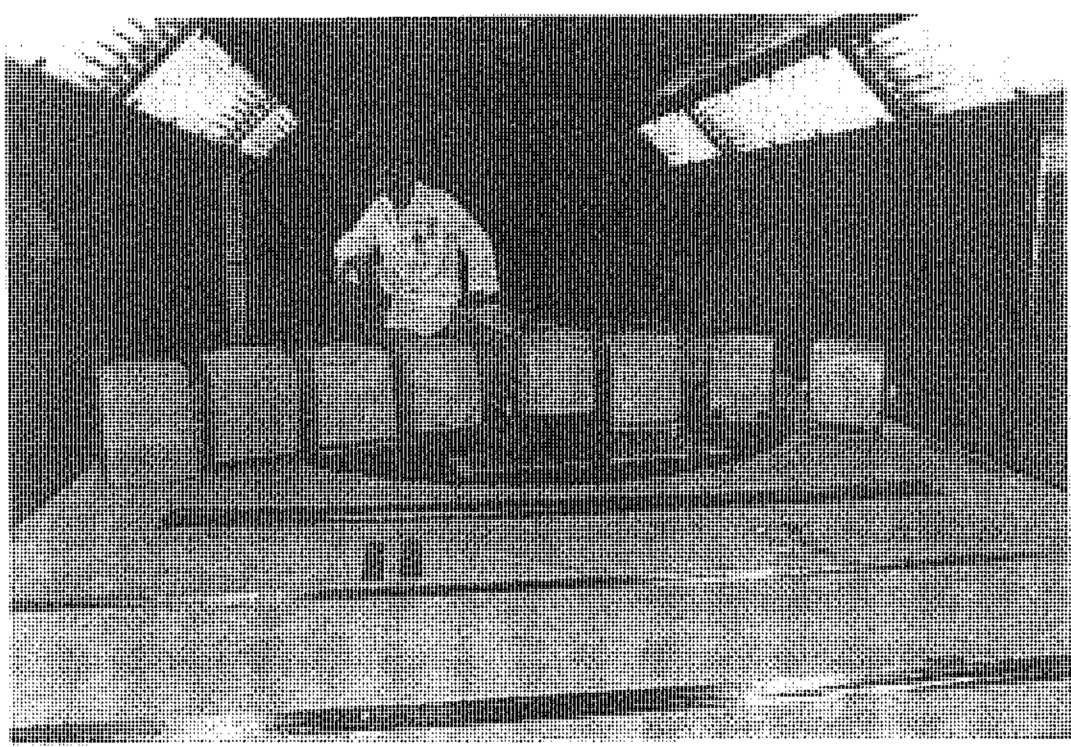

FIG. 1d: MODEL WITH ALTERNATE FRONT AND REAR COMPONENTS

(from left to right - Standard CJ3, Setra S315, Prevost H3-40, Mercedes 0404, Smooth CJ3, Proposal 1, Bevelled Rear, Proposal 2 - note suction slot just upstream of the turntable)

002303

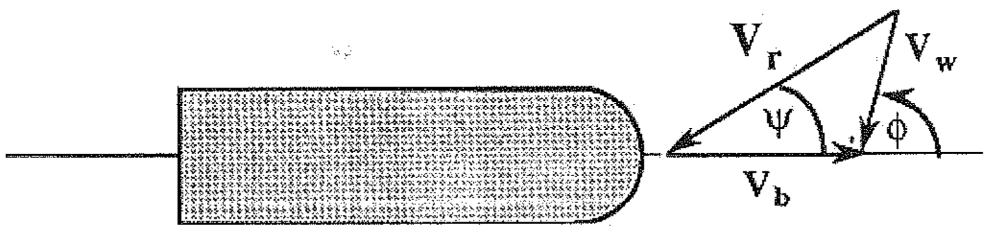

FIG. 2: RESULTANT VELOCITY VECTOR DIAGRAM

002304

002304

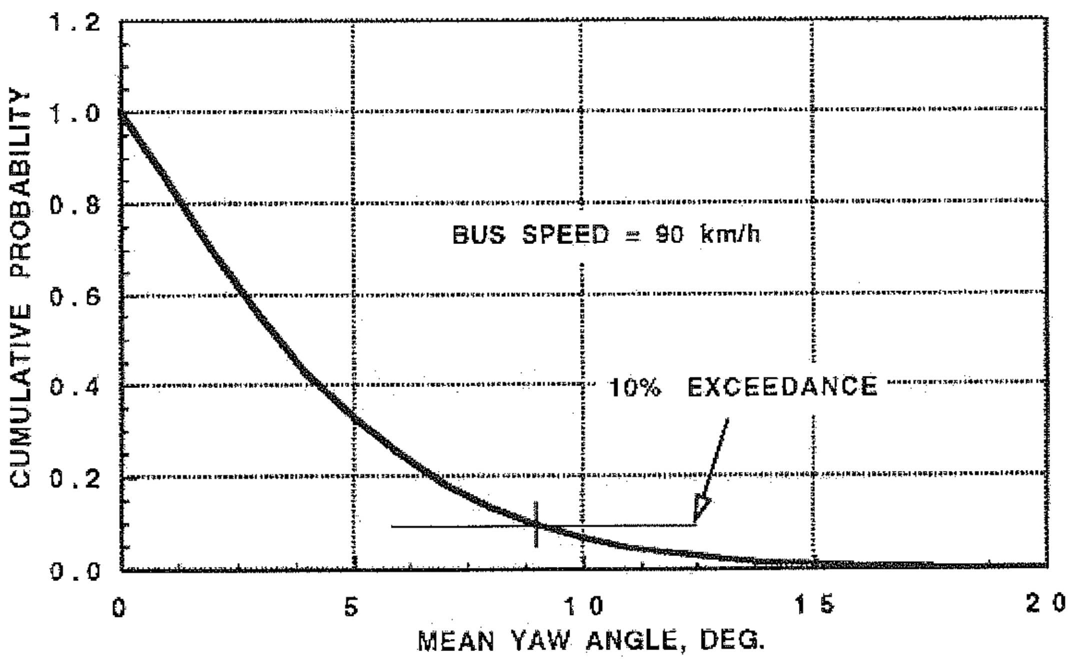

FIG. 3: PROBABILITY OF EXCEEDING A GIVEN YAW ANGLE AT A BUS SPEED OF 90 km/h

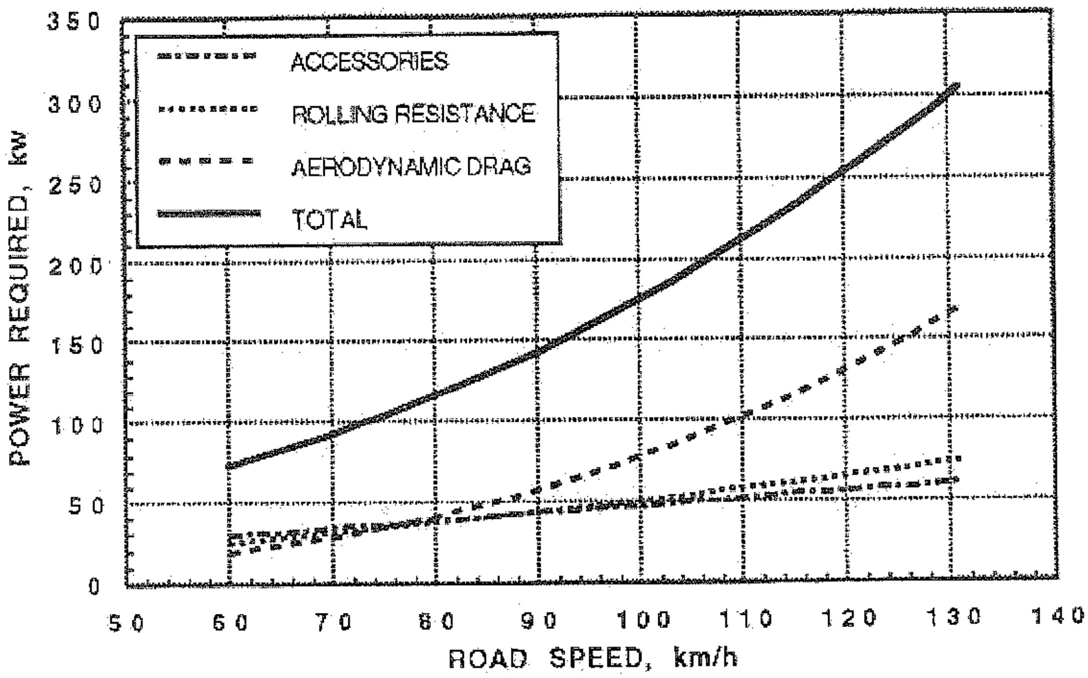

FIG. 4: POWER COMPONENTS FOR THE STANDARD CJ3

002305

002305

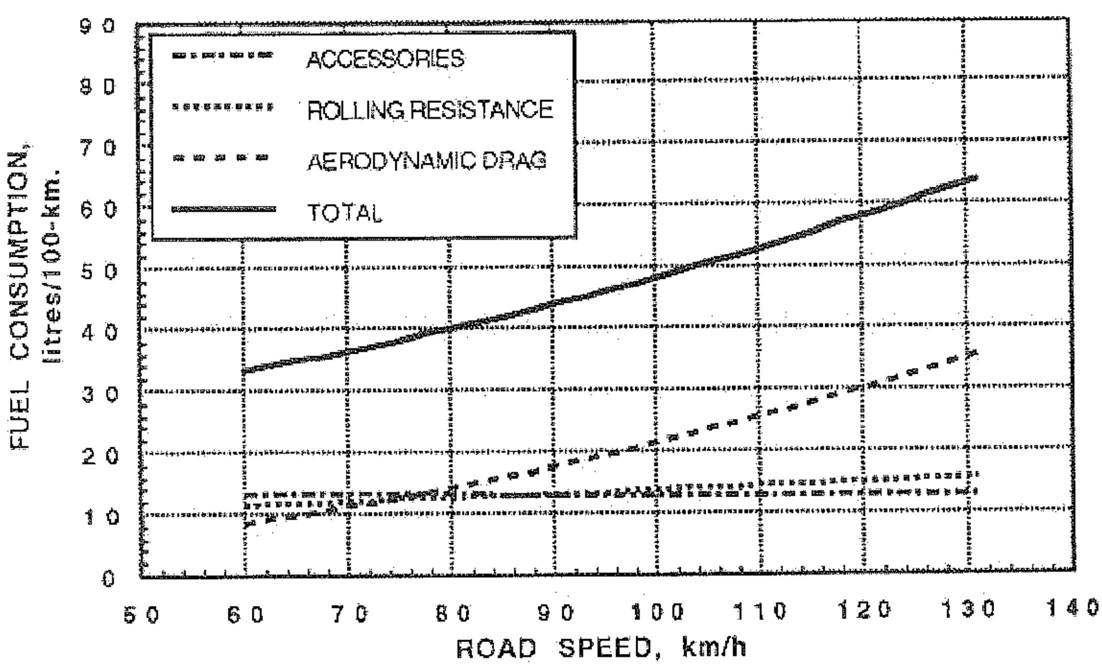

FIG. 5: COMPONENTS OF FUEL CONSUMPTION FOR THE STANDARD CJ3

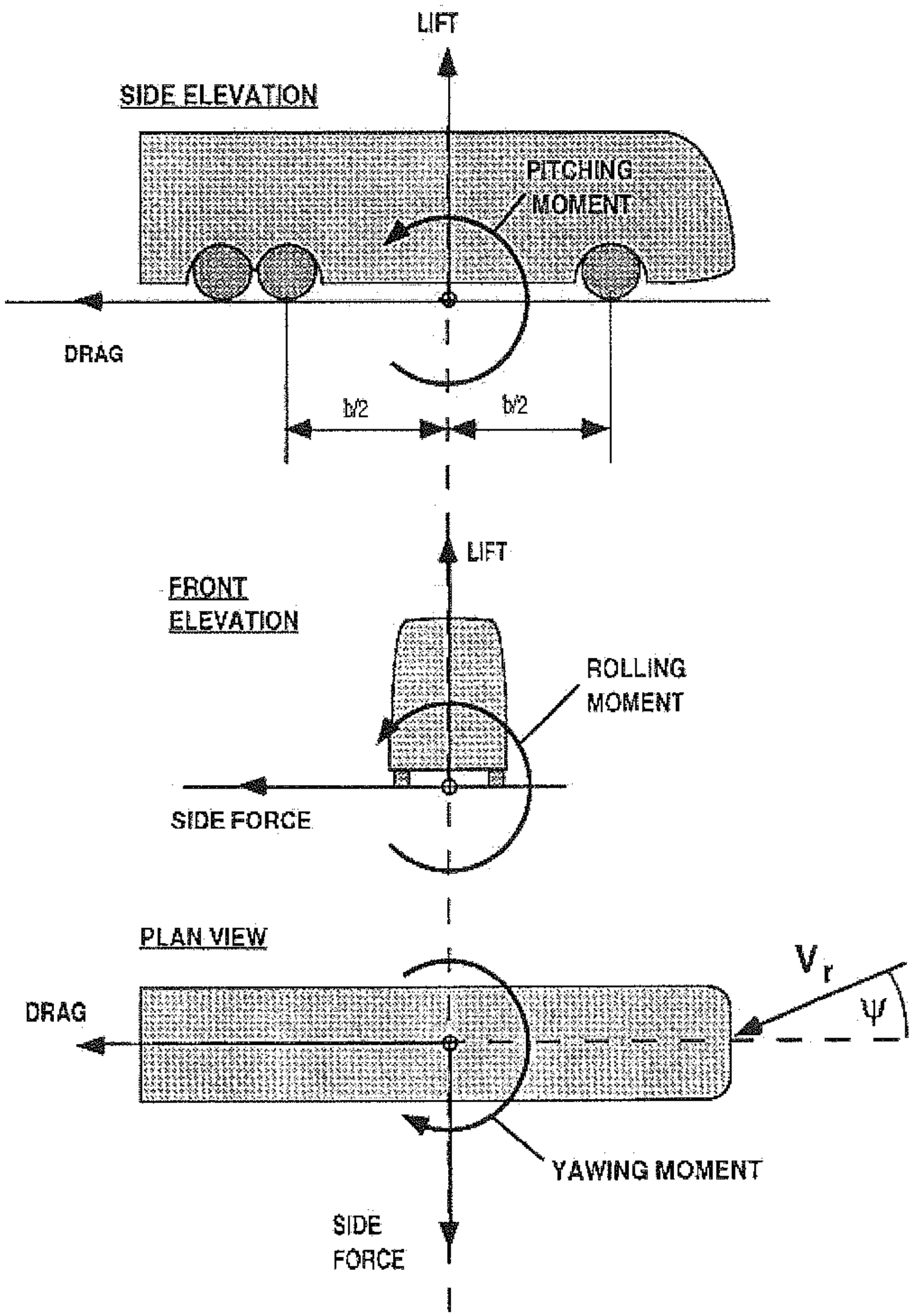

FIG. 6: MEASUREMENT CO-ORDINATE SYSTEM

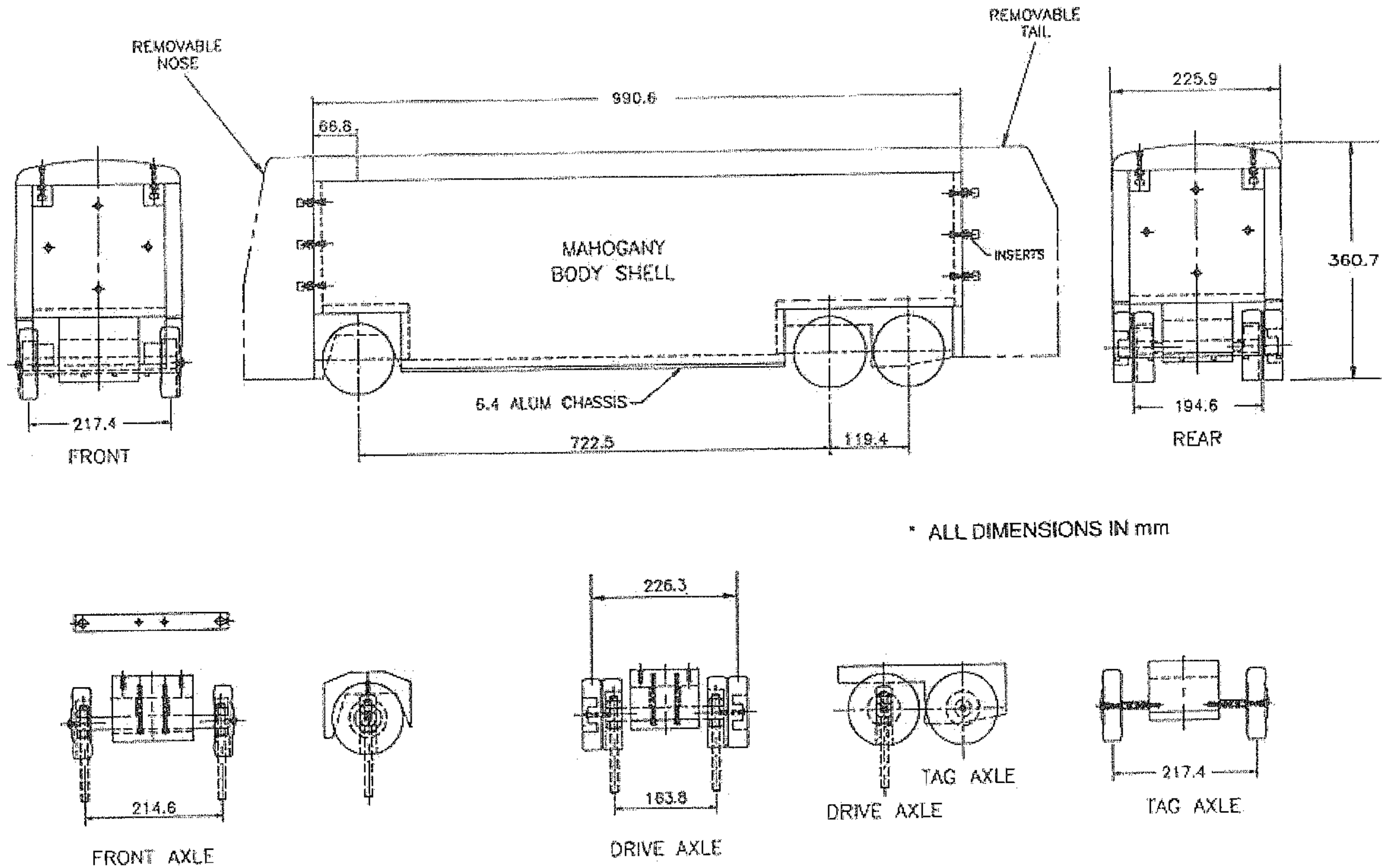

FIG. 7a: CHASSIS DETAILS

002308

002308

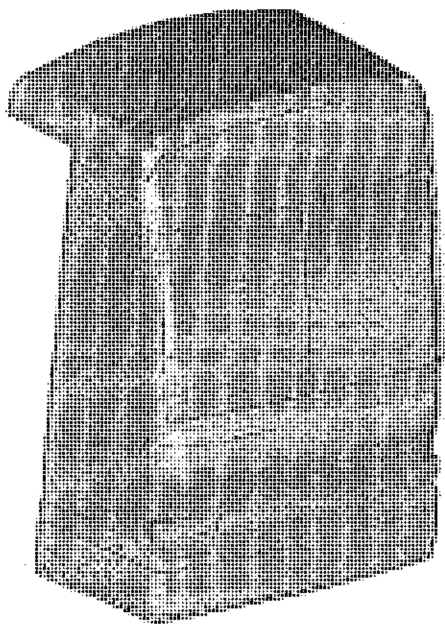

Standard MCI CJ3

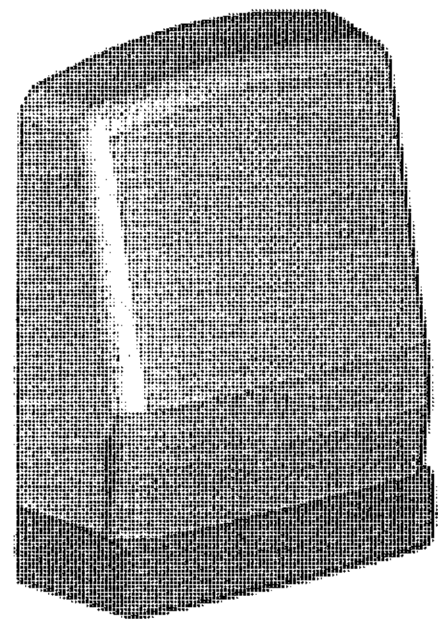

Smooth MCI CJ3

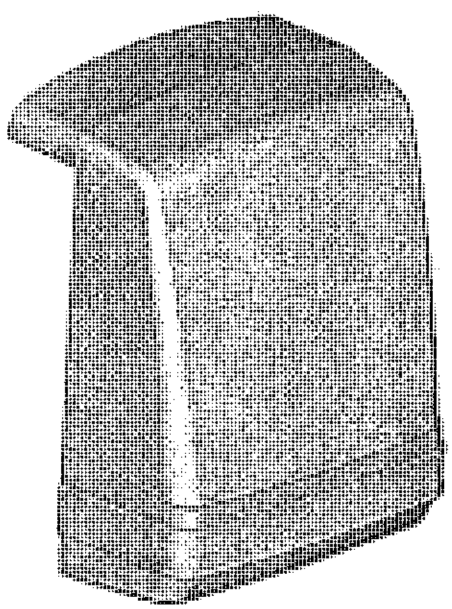

MCI Proposal 2

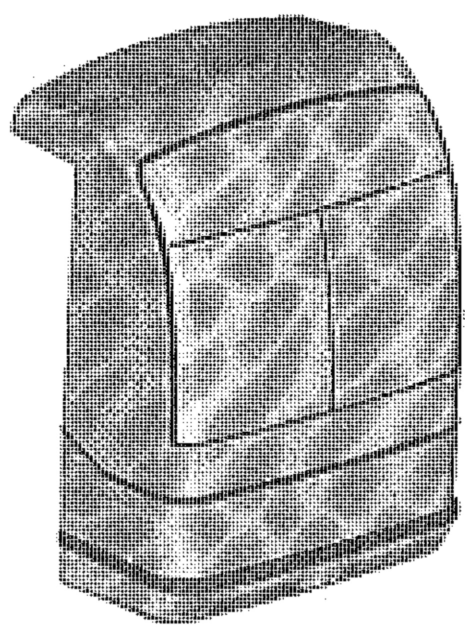

MCI Proposal 1

FIG. 7b: MCI FRONT-END CONFIGURATIONS

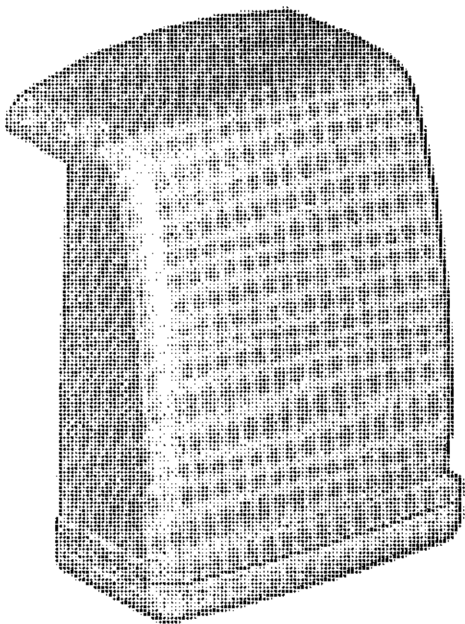

Prevost H3-40

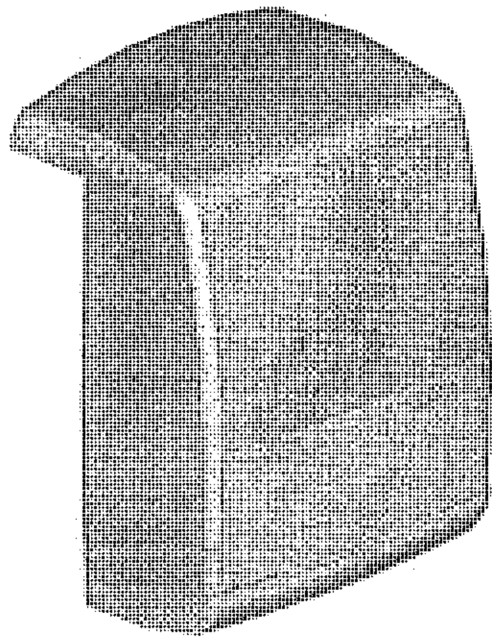

Mercedes 0404

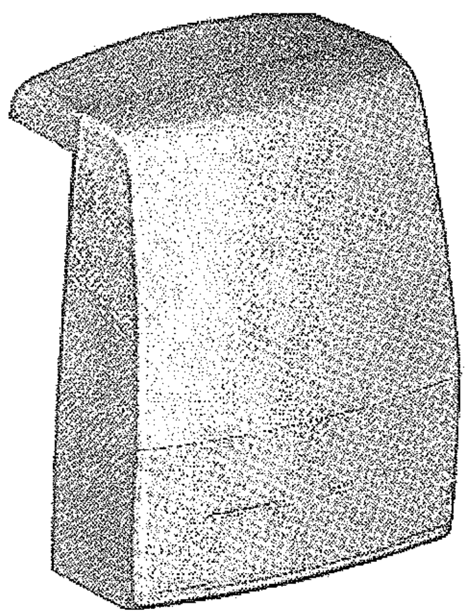

Setra S315

FIG. 7c: COMPETITORS' CONFIGURATIONS

002309

002309

002309

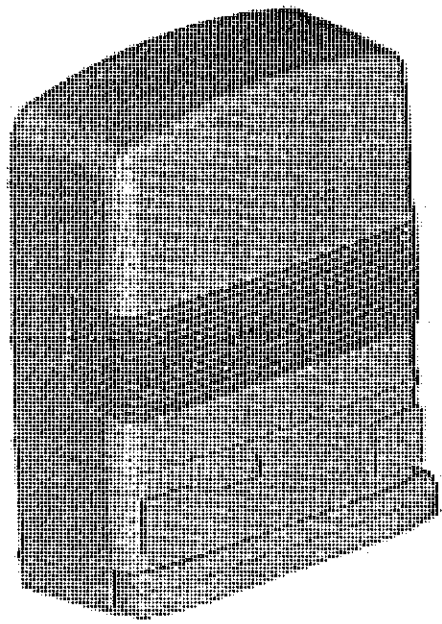

Standard MCI CJ3

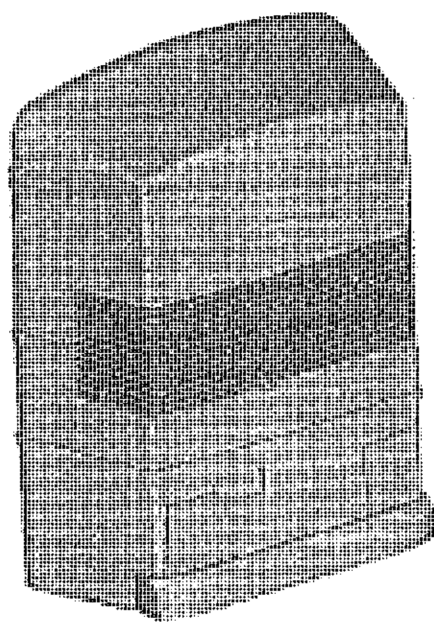

15° Beveled

FIG. 7d: REAR-END CONFIGURATIONS

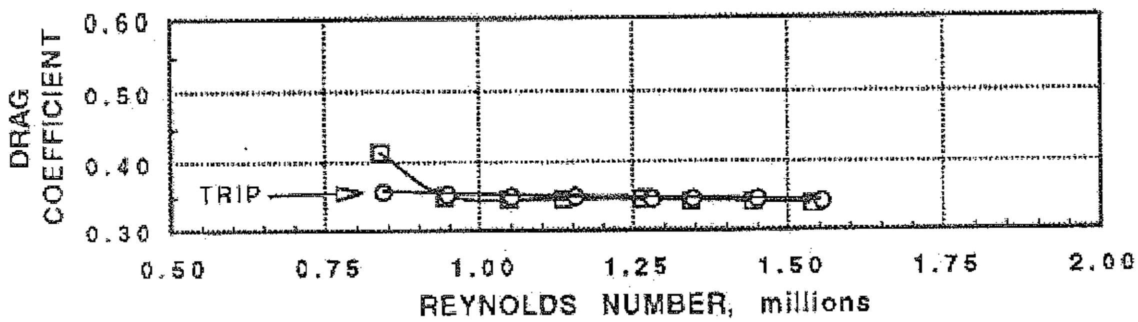

FIG. 8a: REYNOLDS NUMBER AND FLOW TRIP EFFECTS - PROPOSAL 1 FRONT

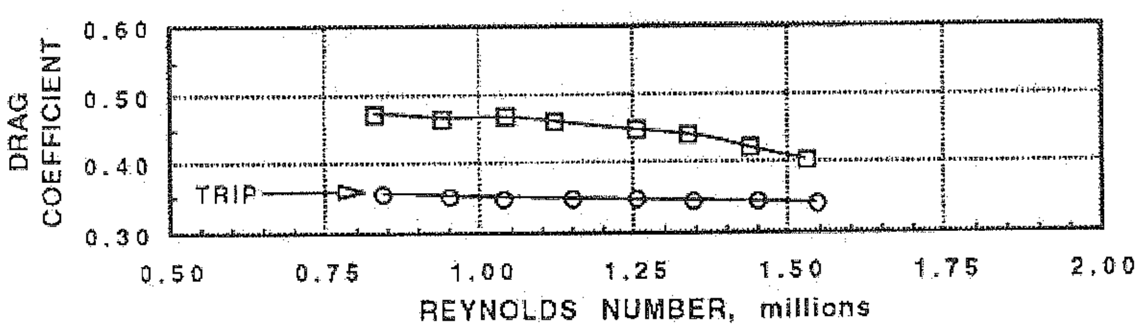

FIG. 8b: REYNOLDS NUMBER AND FLOW TRIP EFFECTS - PROPOSAL 2 FRONT

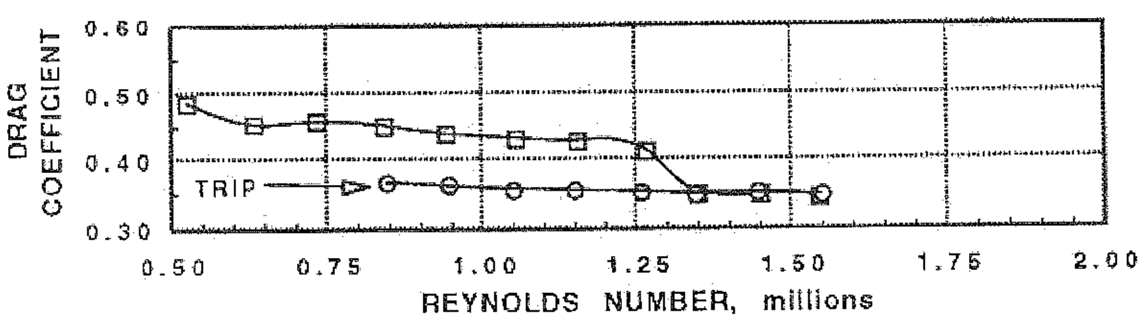

FIG. 8c: REYNOLDS NUMBER AND FLOW TRIP EFFECTS - SMOOTH C3 FRONT

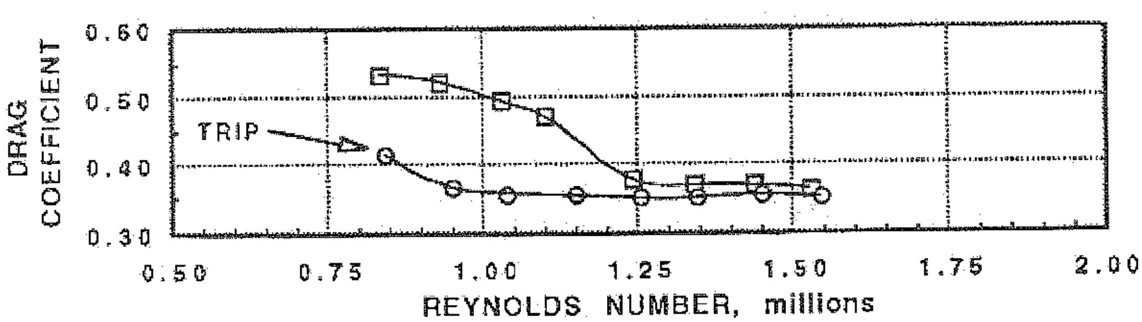

FIG. 8d: REYNOLDS NUMBER AND FLOW TRIP EFFECTS - PREVOST FRONT

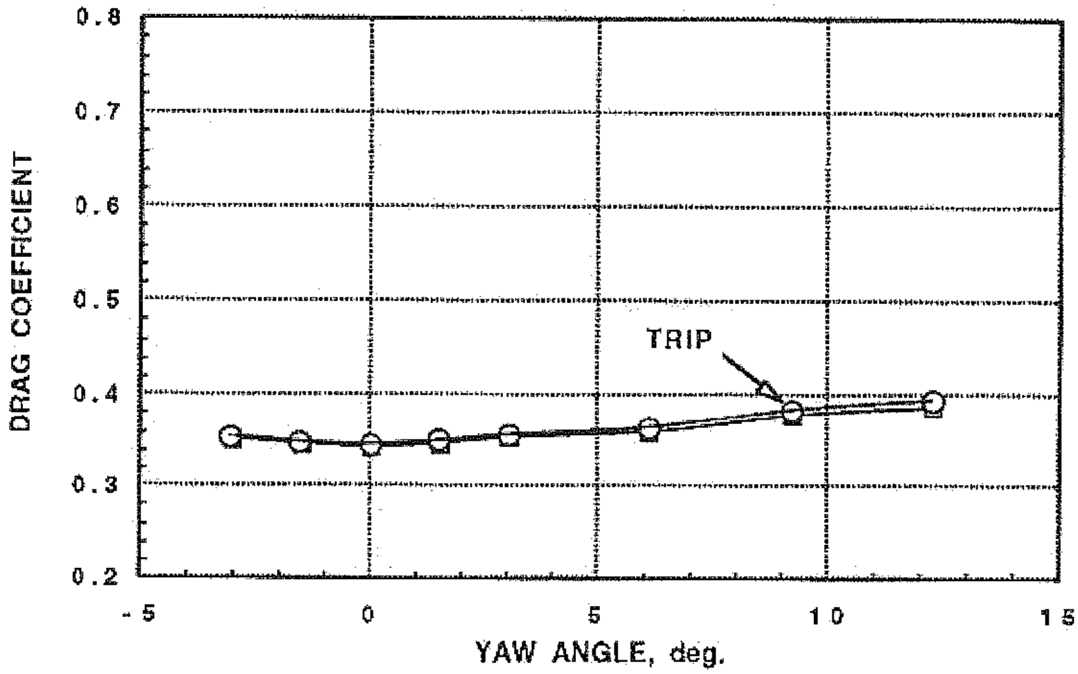

FIG. 9a: EFFECT OF FLOW TRIP - PROPOSAL 1 FRONT

002312

002312

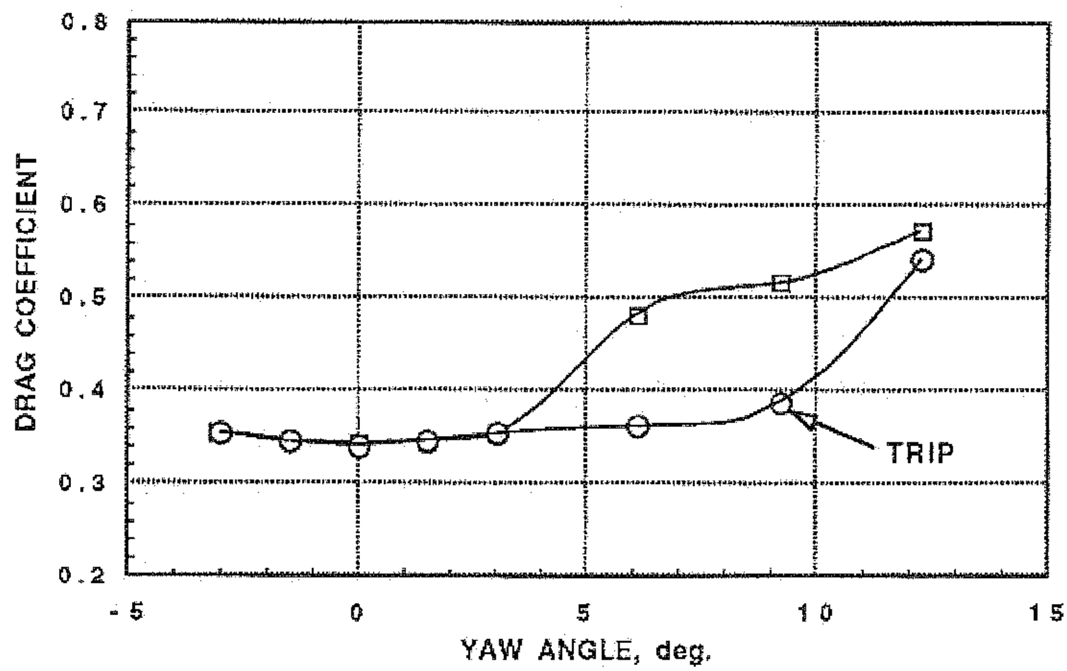

FIG. 9b: EFFECT OF FLOW TRIP - PROPOSAL 2 FRONT

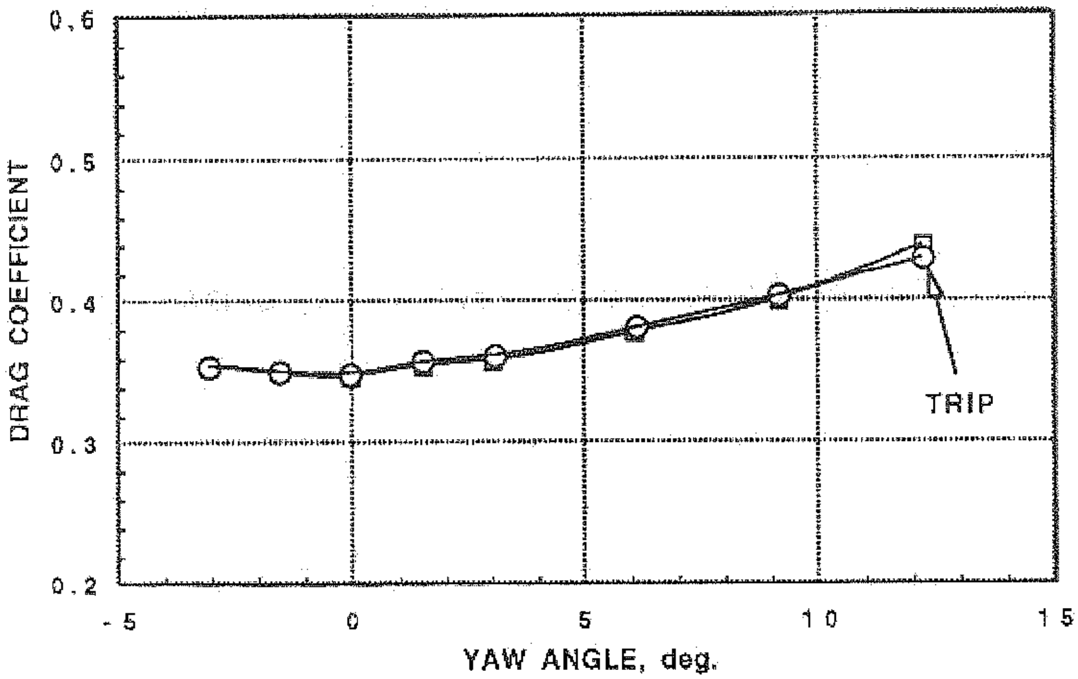

FIG. 9c: EFFECT OF FLOW TRIP - SMOOTH CJ3 FRONT

002313

002313

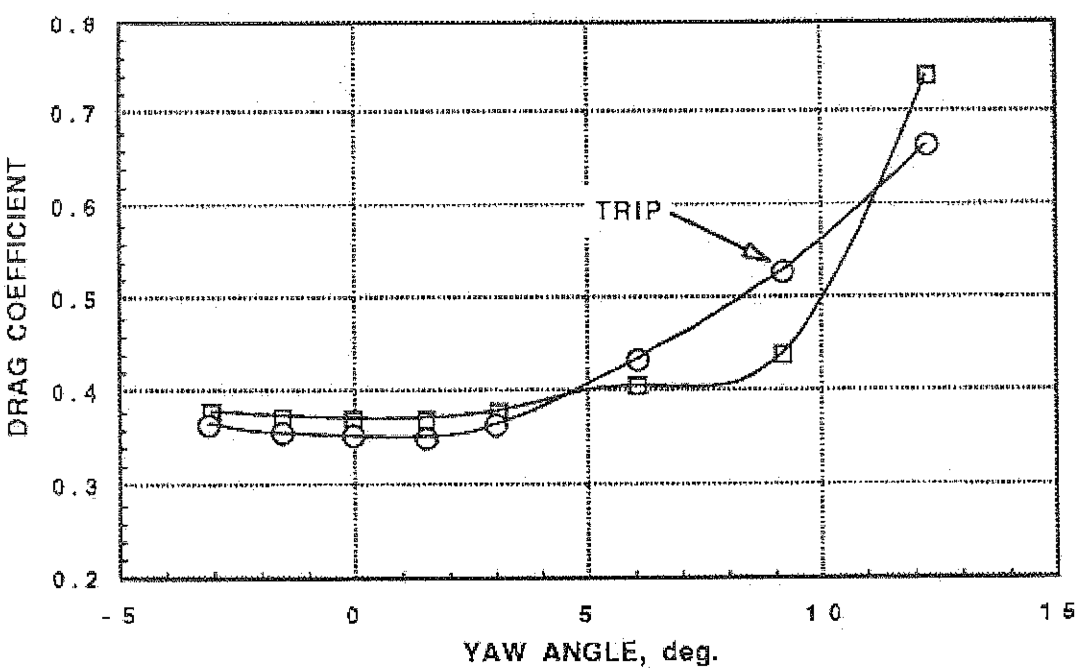

FIG. 9d: EFFECT OF FLOW TRIP - PREVOST FRONT

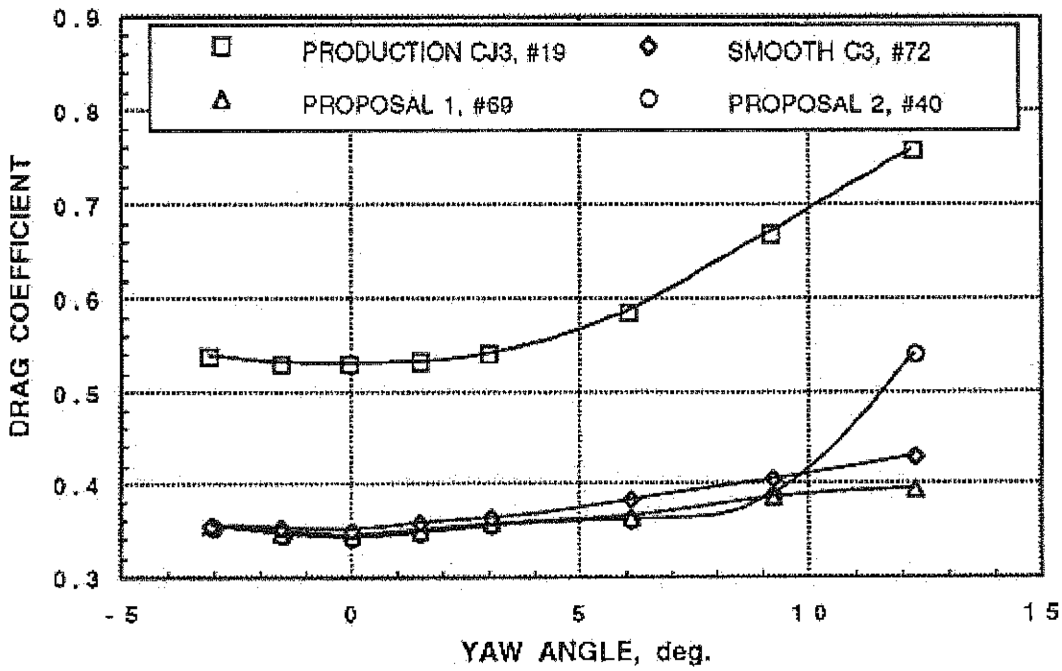

FIG. 10: COMPARISON OF FRONT END SHAPES - PRODUCTION CJ3 AND ALTERNATE PROPOSALS

002314

002314

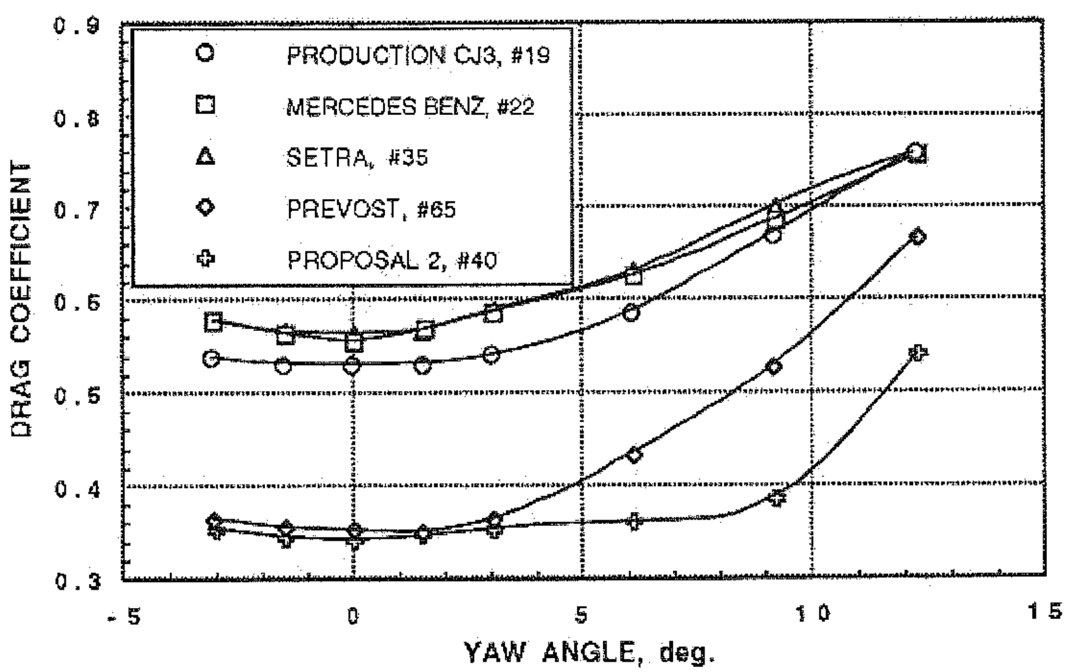

FIG. 11: COMPARISON OF FRONT END SHAPES - PRODUCTION CJ3, PROPOSAL 2, AND COMPETITORS

002314

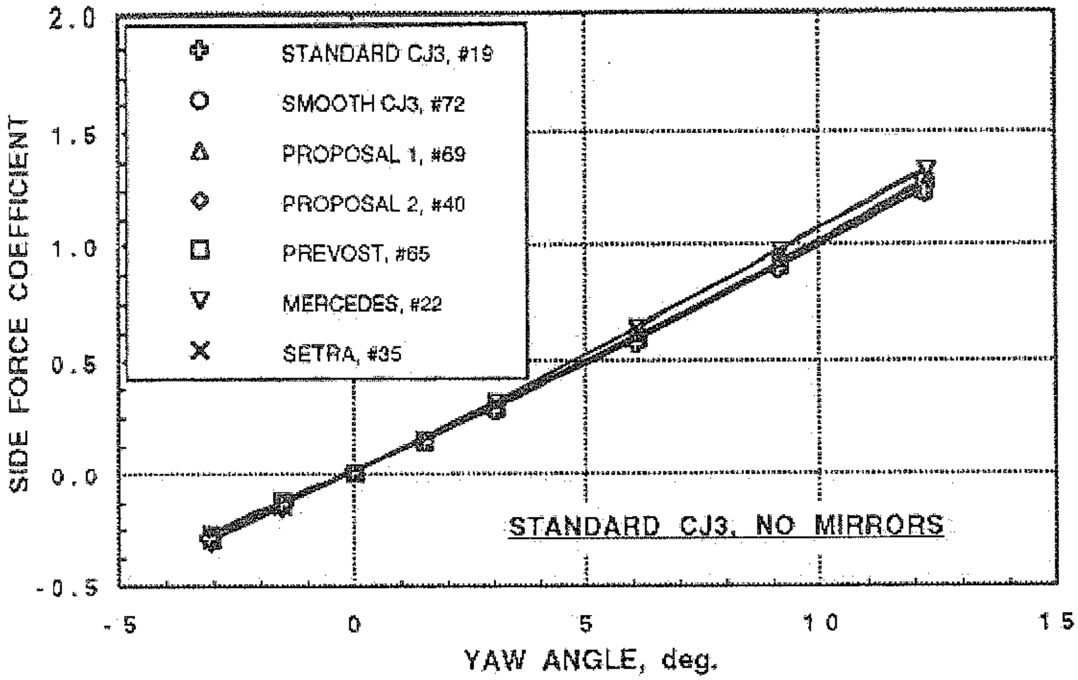

FIG. 12a: COMPARISON OF SIDE FORCE FOR THE VARIOUS FRONTS

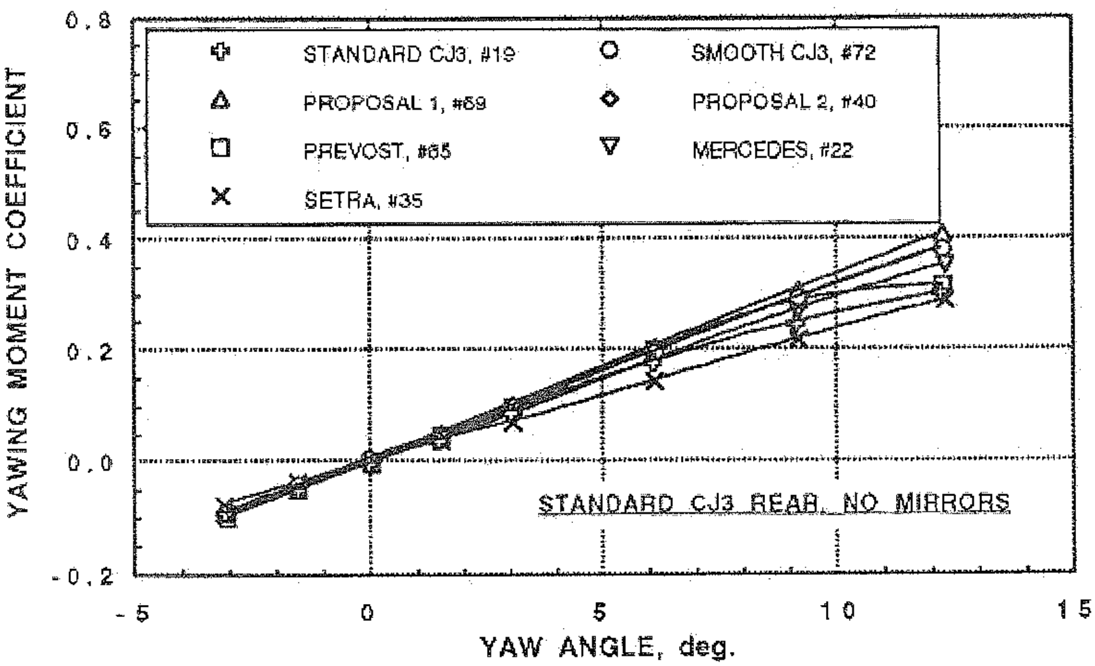

FIG. 12b: COMPARISON OF YAWING MOMENT FOR THE VARIOUS FRONTS

002315

002315

002315

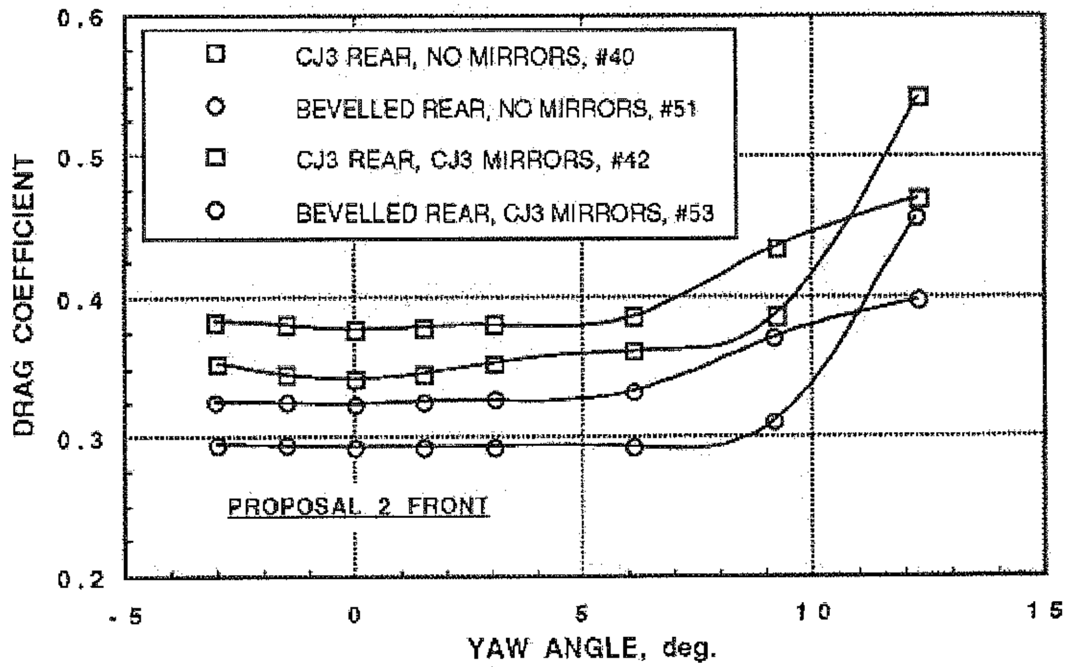

FIG. 13: COMPARISON OF BEVELLED AND STANDARD REAR ENDS WITH AND WITHOUT MIRRORS

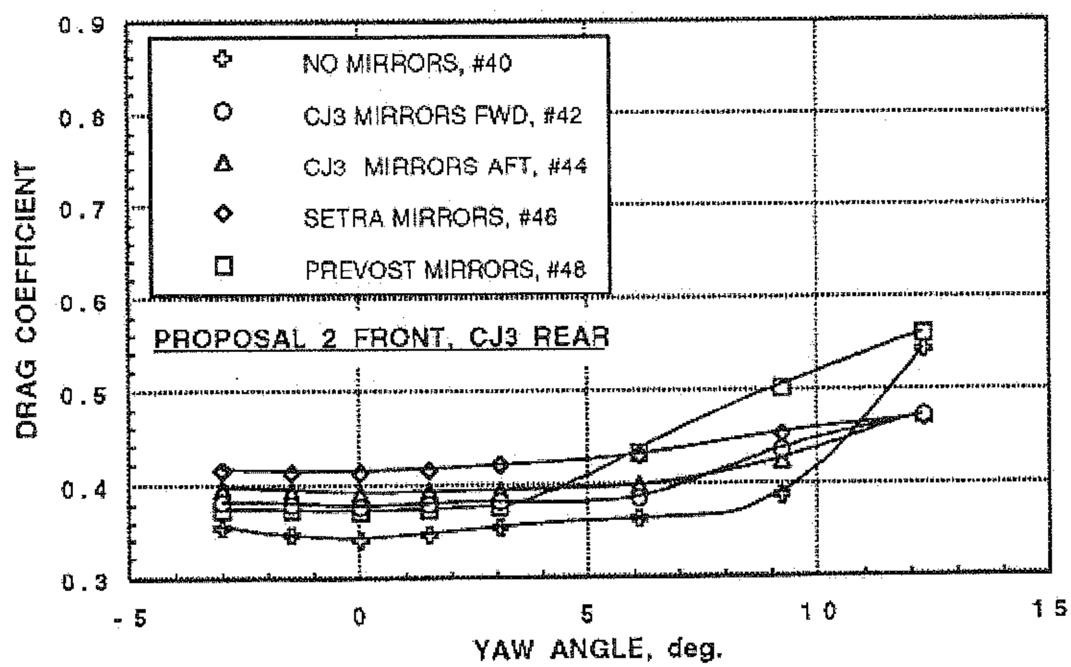

FIG. 14: EFFECT OF MIRROR TYPE AND LOCATION

002316

002316

MCI - 039892

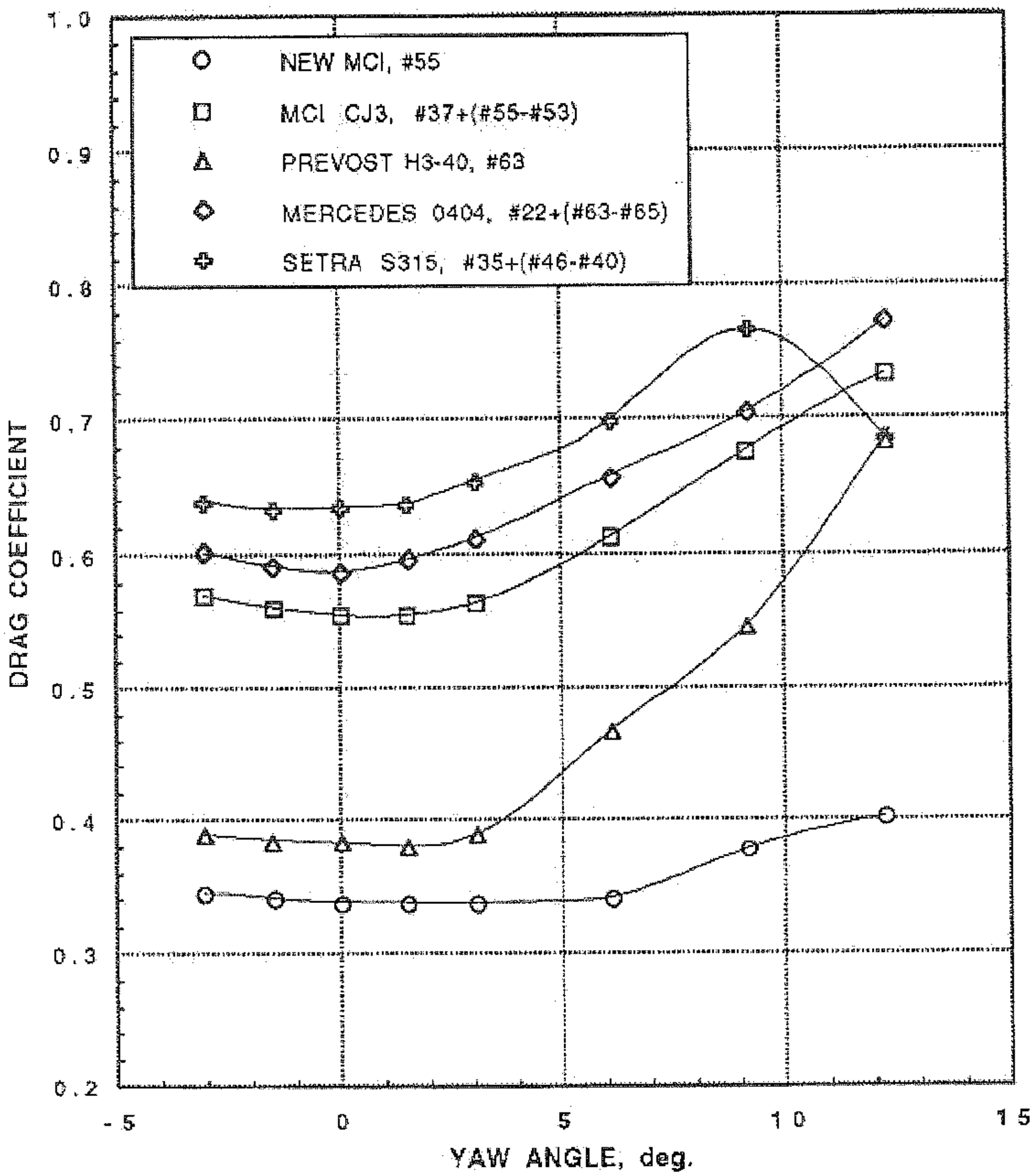

FIG. 15: DRAG COMPARISON OF MAIN CONFIGURATIONS WITH MIRRORS

002317

002317

002317

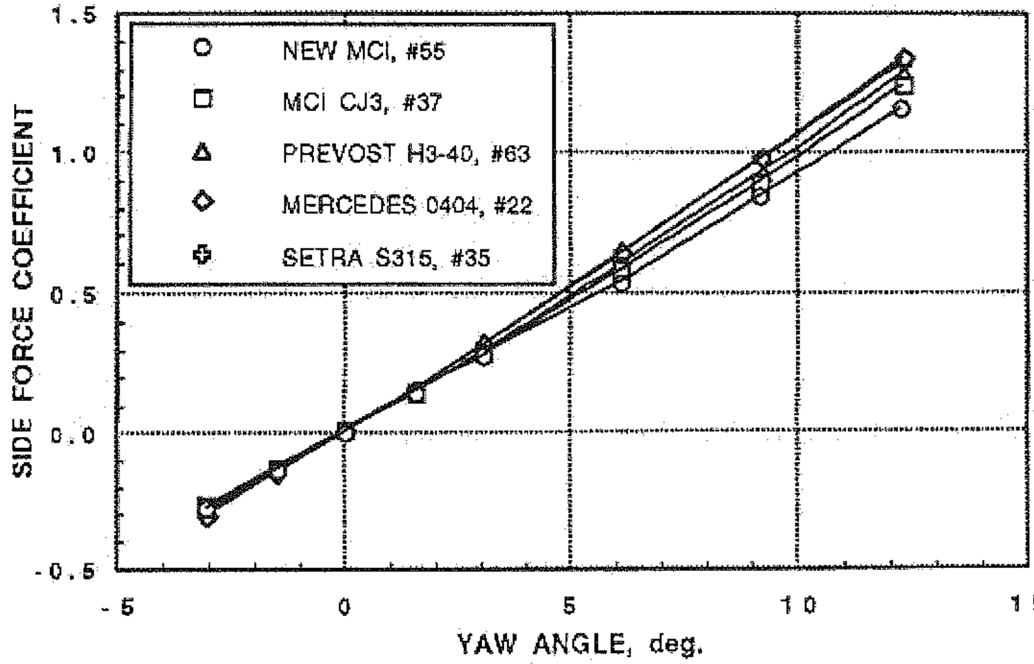

FIG. 16a: SIDE FORCE COMPARISON OF MAIN CONFIGURATIONS WITH MIRRORS

002318

002318

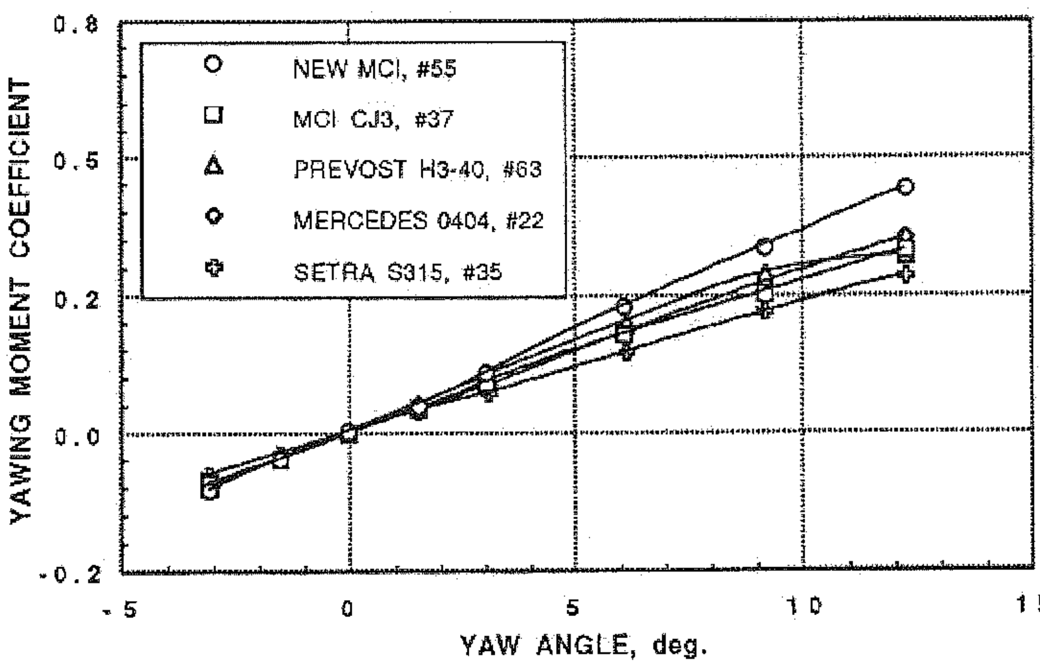

FIG. 16b: YAWING MOMENT COMPARISON OF MAIN CONFIGURATIONS WITH MIRRORS

002319

002319

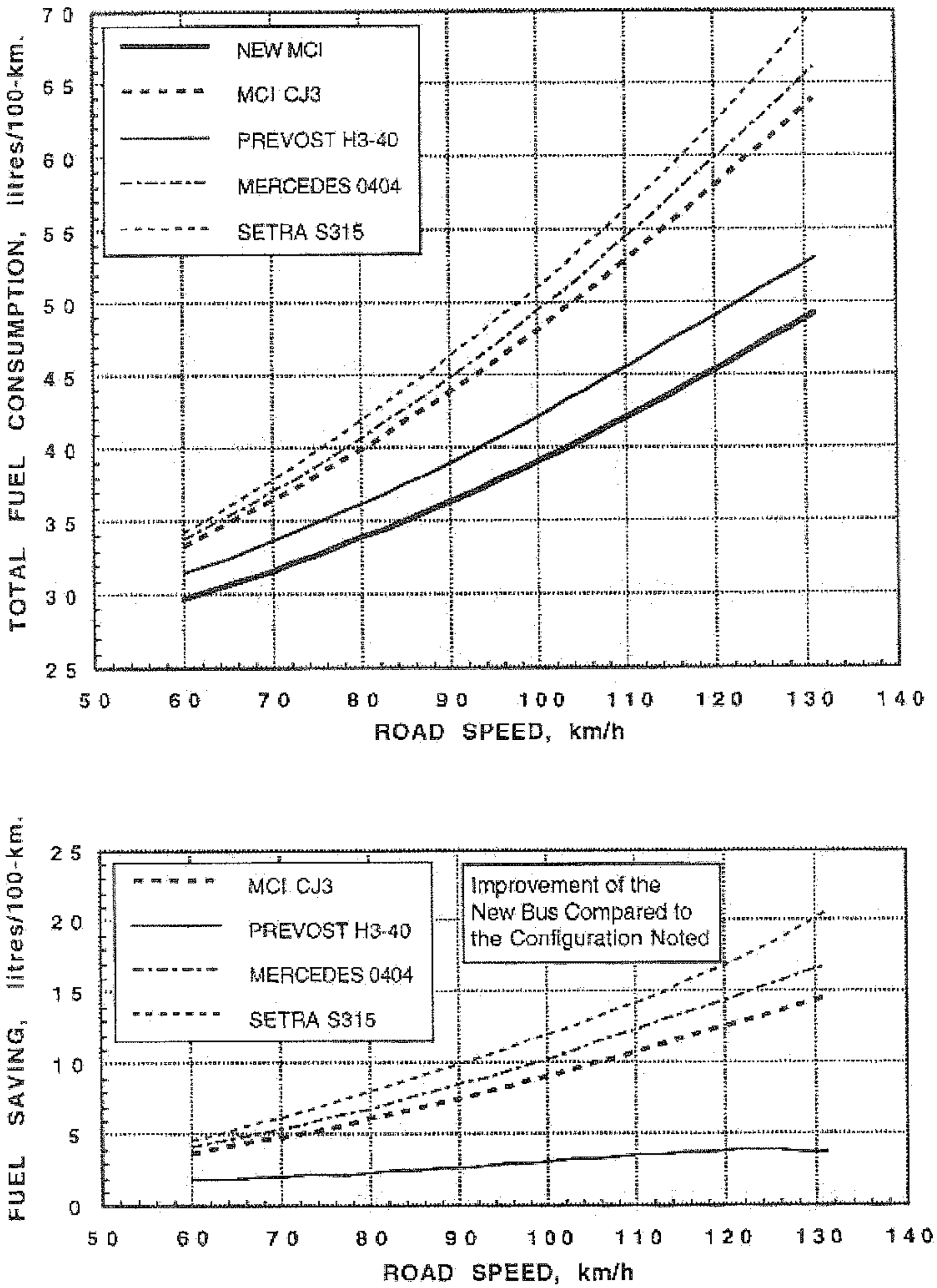

FIG. 17: SUMMARY OF THE PREDICTED FUEL CONSUMPTIONS OF THE MAIN CONFIGURATIONS AND THE SAVINGS PROVIDED BY THE NEW BUS

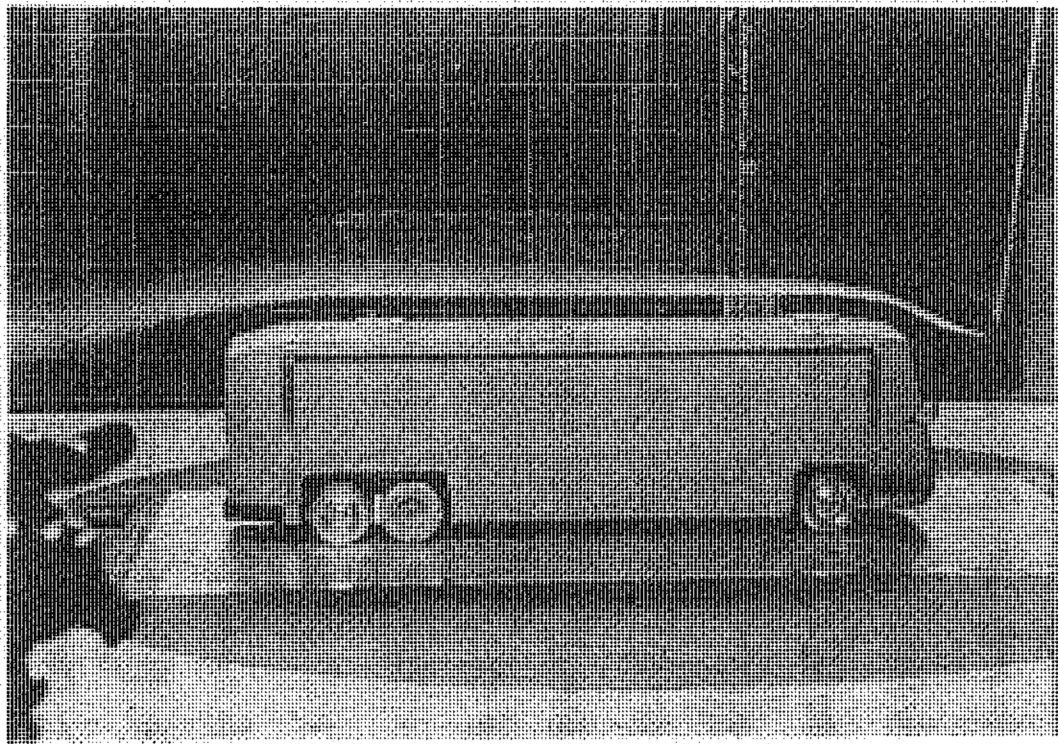

FIG. 18a: OVERALL FLOW FIELD

002320 002320

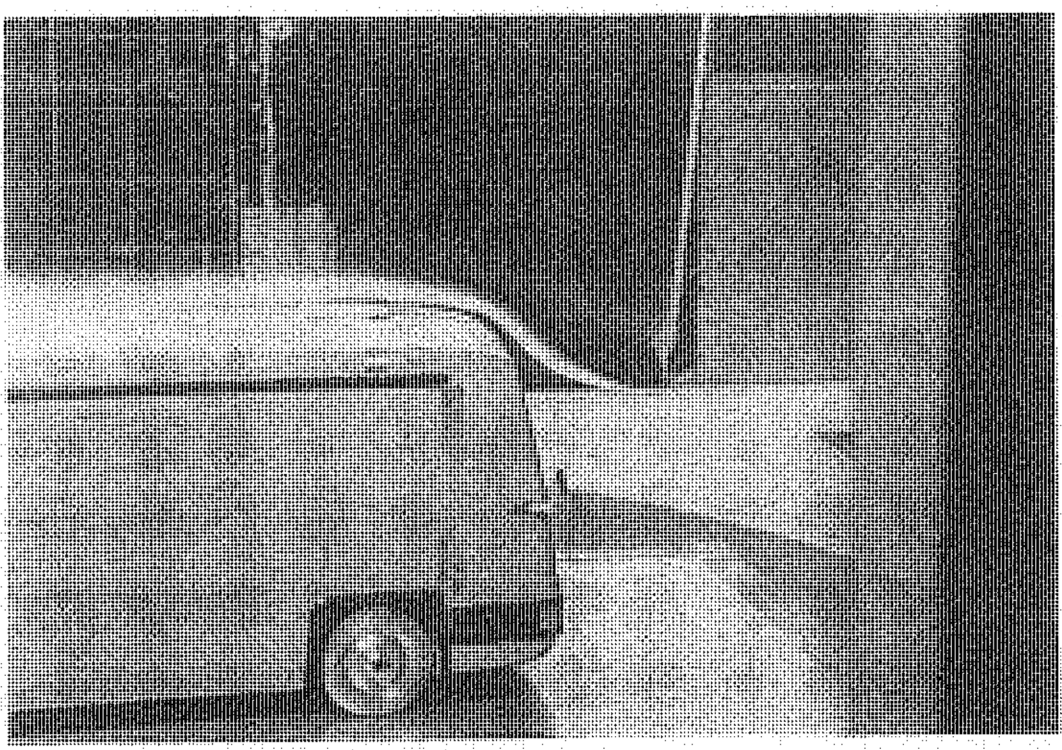

FIG. 18b: LEADING EDGE FLOW

002320

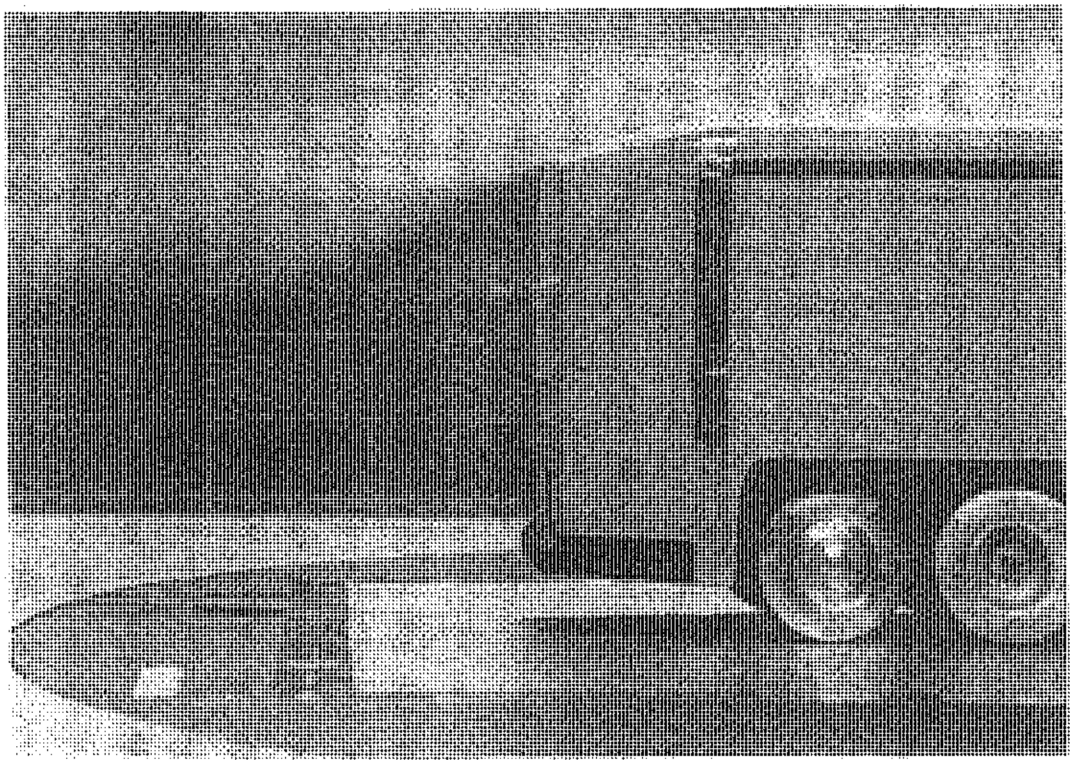

FIG. 18c: ATTACHED REAR BEVEL FLOW

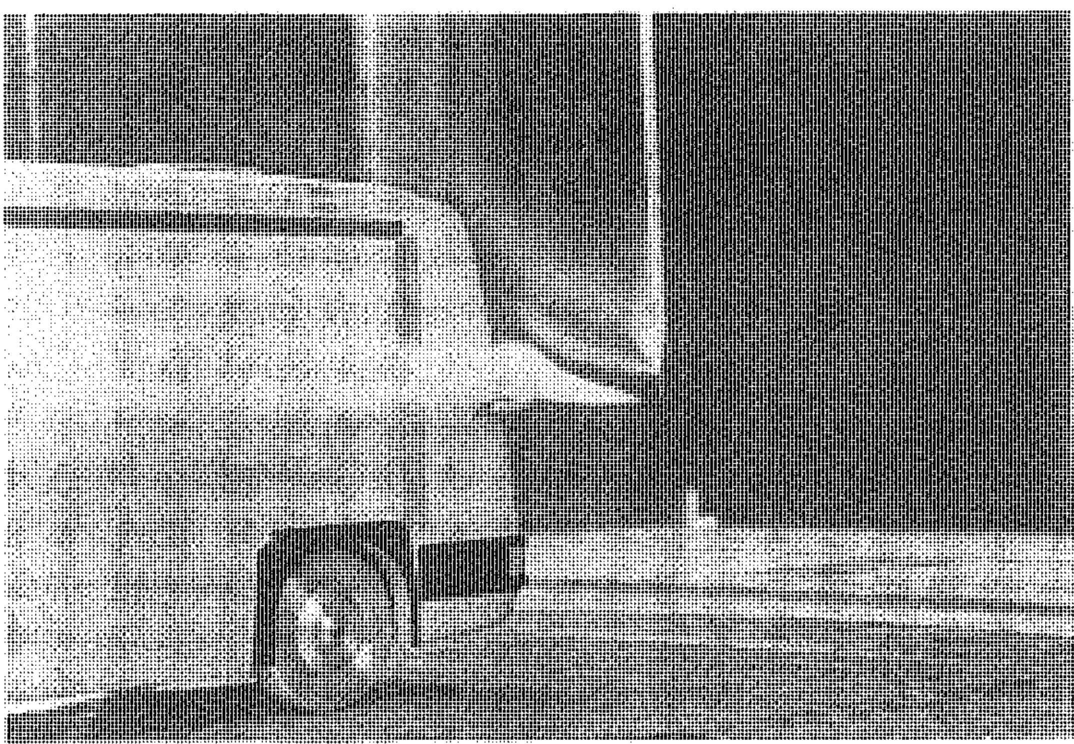

FIG. 18d: MIRROR WAKE

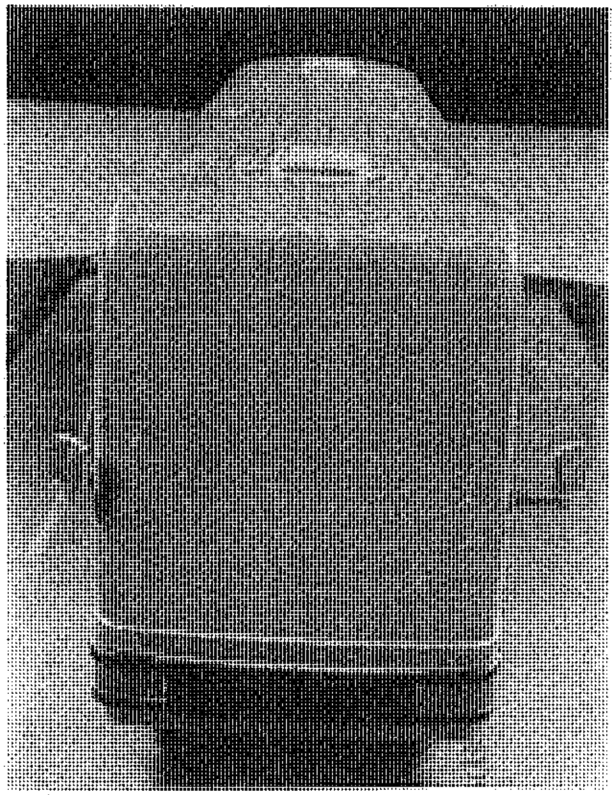

FIG. 19a: FRONT-FACE FLOW SHOWING STAGNATION POINT AT LOWER CENTRE

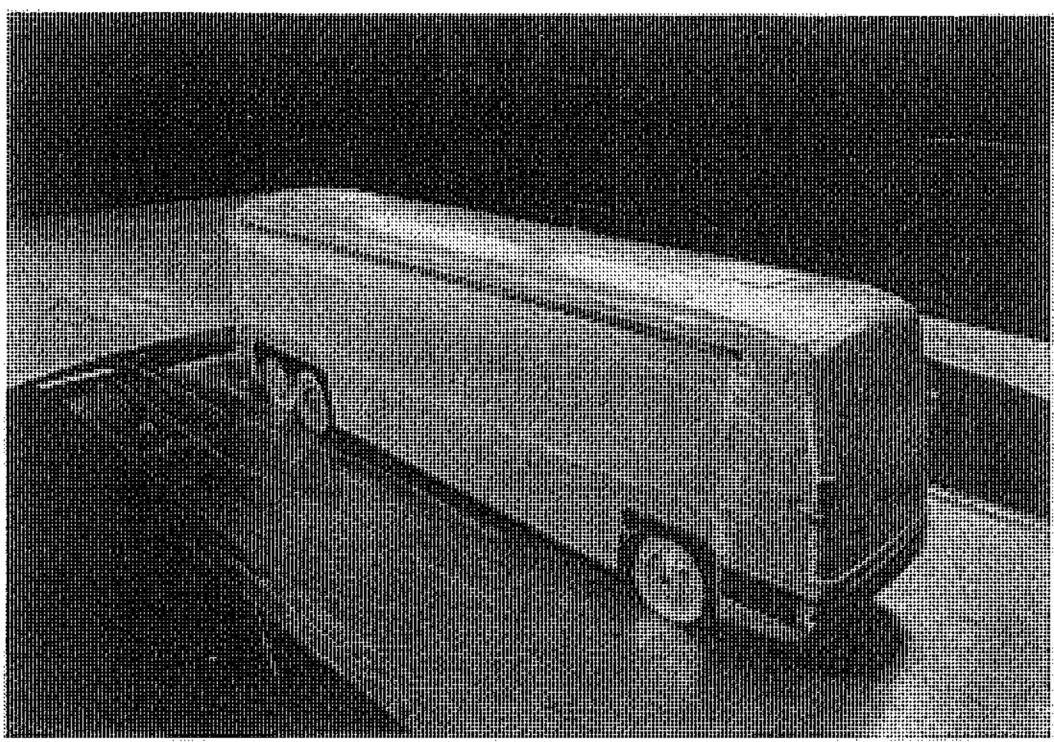

FIG. 19b: MIRROR-INDUCED FLOW

FIG. 19c: CLOSE-UP OF MIRROR-INDUCED FLOW

002323

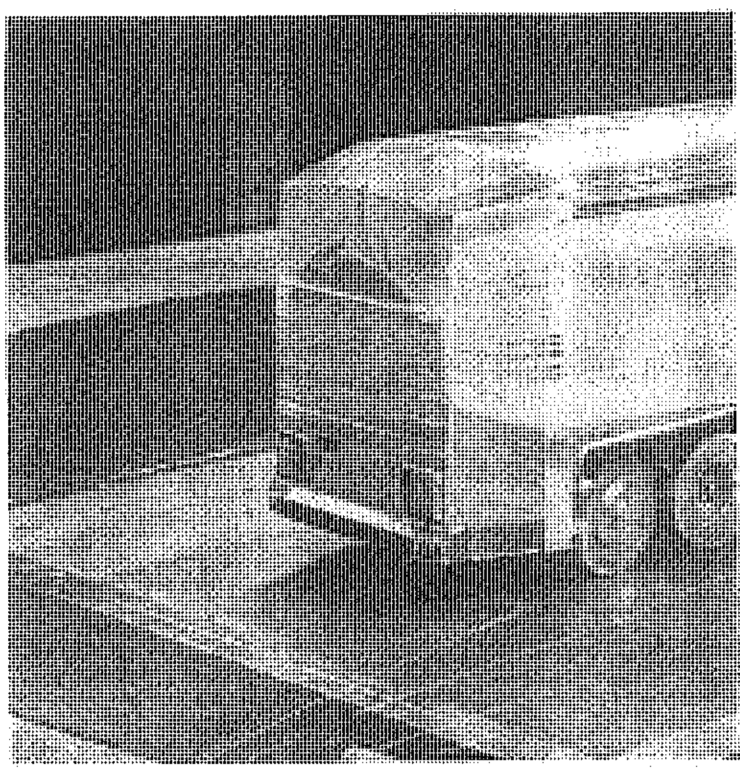

FIG. 19d: BASE FLOW

002323

APPENDIX 1: RUN LOG

RUN	TYPE	FRONT	REAR	TRIP	HATCH	RAIL	MIRROR	MISC	$\bar{C}_D$(88)	PHOTO
13	YAW	SMOOTH CJ3	STANDARD CJ3	NO	NONE	NONE	NONE	NONE	0.443	P1
14	Re									
16	YAW				STD	STD			0.443	P2
18	Re	STANDARD CJ3								P3
19	YAW								0.674	
21	Re	MERCEDES								P4
22	YAW								0.708	
25	Re	PROPOSAL 1								P5
26	YAW								0.435	
28	Re	PROPOSAL 2								P6
29	YAW								0.435	
31	Re	PREVOST								P7
32	YAW								0.472	
34	Re	SETRA								P8
35	YAW								0.717	
37	YAW	STANDARD CJ3					CJ3 FWD		0.689	P9
39	Re	PROPOSAL 2		YES			NONE			P10
40	YAW								0.434	
42							CJ3 FWD		0.479	P11
44							CJ3 AFT		0.498	P12

wrong appendix

002324
002324
002324

RUN	TYPE	FRONT	REAR	TRIP	HATCH	RAIL	MIRROR	MISC	$\bar{C}_D(88)$	PHOTO
46	YAW	PROPOSAL 2	STANDARD CJ3	YES	STD	STD	SETRA		0.524	P13
48							PREVOST		0.472	P14
50	Re		BEVELLED				NONE			P15
51	YAW								0.370	
53							CJ3 FWD		0.411	P11
55							CJ3, RIGHT FWD, LEFT AFT		0.428	P16
57								SKIRTS	0.421	P17
58								AIR DAM	0.467	P18
59								TIRE FAIRING	0.436	P19
60								VORTEX GEN.	0.434	P20
61						MOD		NONE	0.429	P21
63	YAW	PREVOST	STANDARD CJ3	YES	STD	STD	PREVOST		0.488	P22
65		PREVOST					NONE		0.449	P23
66	Re									
68		PROPOSAL 1								P24
69	YAW								0.439	
72		SMOOTH CJ3							0.444	P25

MCI - 039901

APPENDIX 2: PHOTOGRAPHIC LOG

P1	MCI Smooth CJ3 Front and Standard CJ3 Rear
P2	MCI Standard Hatch and Drip Rail
P3	MCI Standard CJ3 Front
P4	Mercedes 0404 Front
P5	MCI Proposal 1 Front
P6	MCI Proposal 2 Front
P7	Prevost H3-40 Front
P8	Setra S315 Front
P9	Standard CJ3 Front with Standard CJ3 Mirrors
P10	MCI Proposal 2 Front with Flow Trip
P11	Proposal 2 Front with Standard CJ3 Mirrors Forward
P12	Proposal 2 Front with Standard CJ3 Mirrors Aft
P13	Proposal 2 Front with Setra Mirrors
P14	Proposal 2 Front with Prevost Mirrors
P15	Rear End with 15° Bevels on Top and Sides
P16	Proposal 2 Front with Standard CJ3 Mirrors Forward and Aft
P17	Proposal 2 Front and Wheel Skirts
P18	Proposal 2 Front with Air Dam
P19	Proposal 2 Front with Tire Fairings
P20	Vortex Generators Immediately Upstream of Bevelled Rear
P21	Modified Drip Rail
P22	Prevost H3=40 Front with Prevost Mirrors
P23	Prevost H3=40 Front with Flow Trip
P24	Proposal 1 Front with Flow Trip
P25	Smooth CJ3 Front with Flow Trip

002326
002326

002326

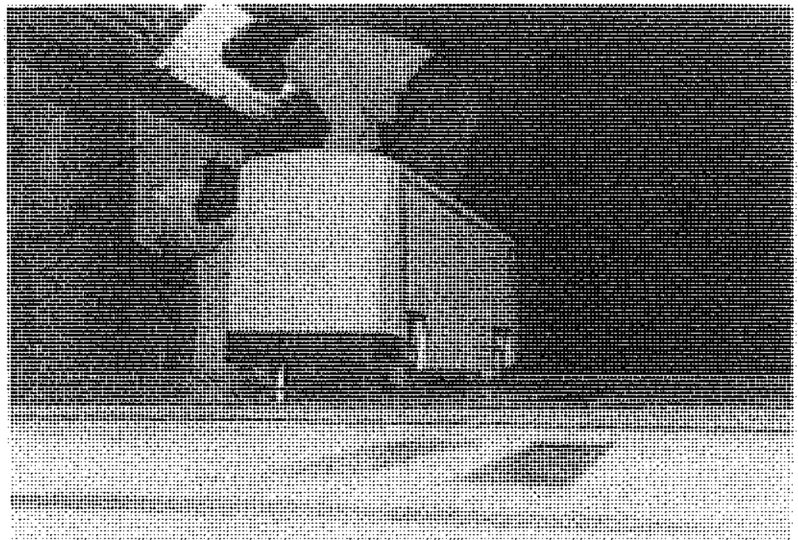

P1a: MCI SMOOTH CJ3 FRONT

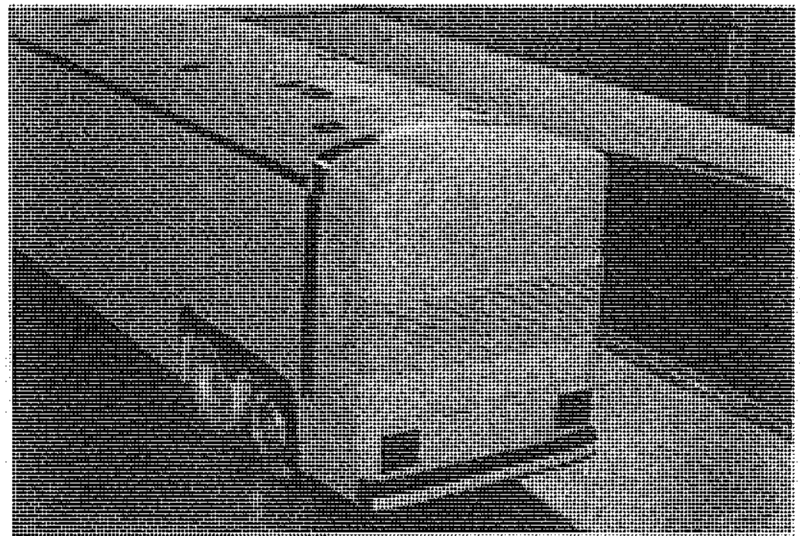

P1b: MCI STANDARD CJ3 REAR

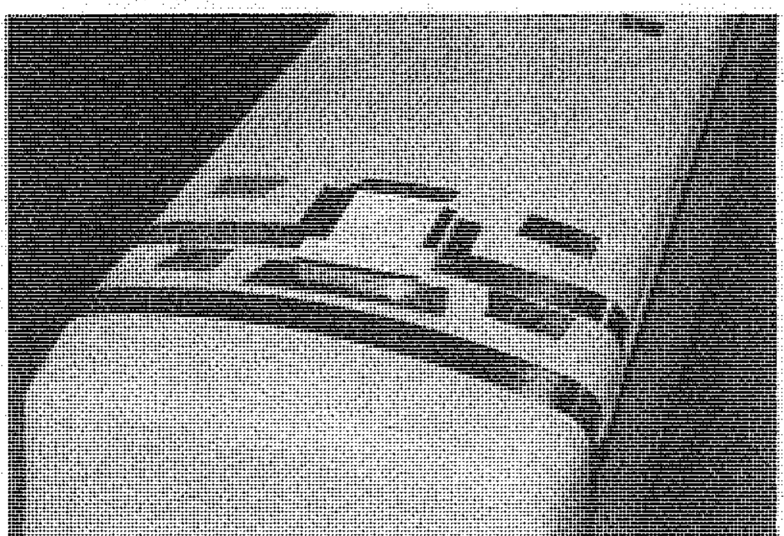

P2: MCI STANDARD HATCH & DRIP RAIL

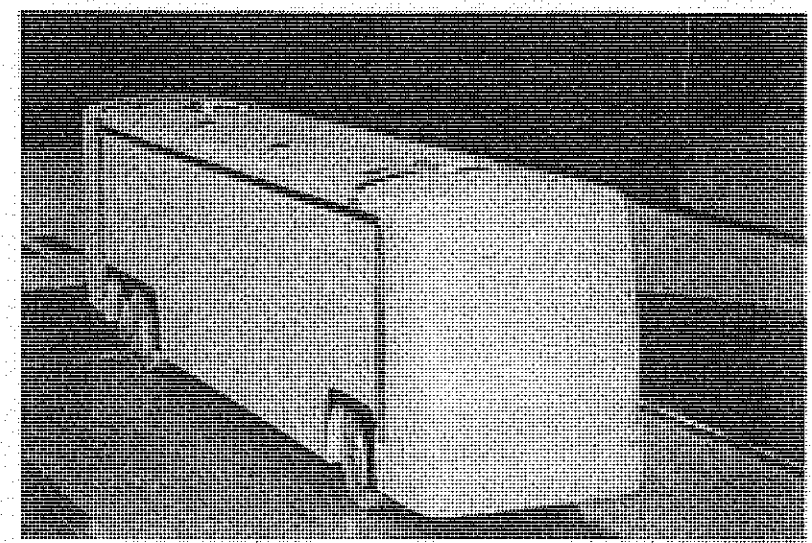

P3: MCI STANDARD CJ3 FRONT

MCI - 039903

002327
002327

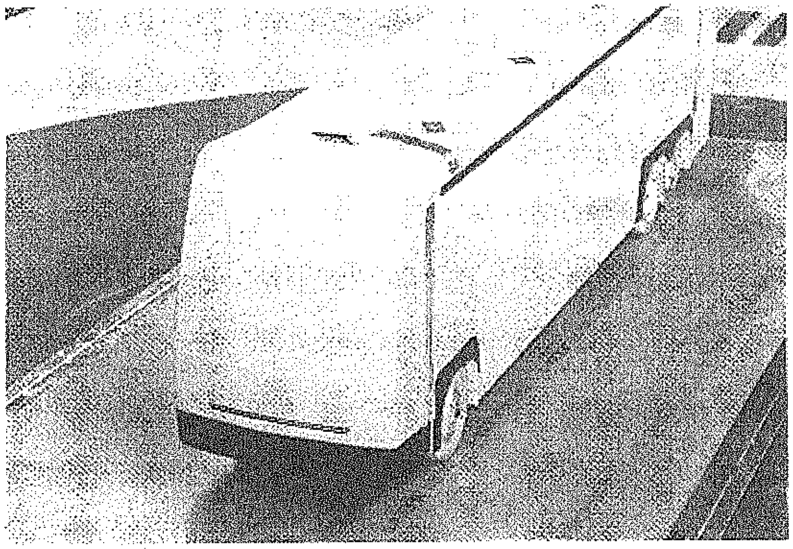

P4: MERCEDES 0404 FRONT

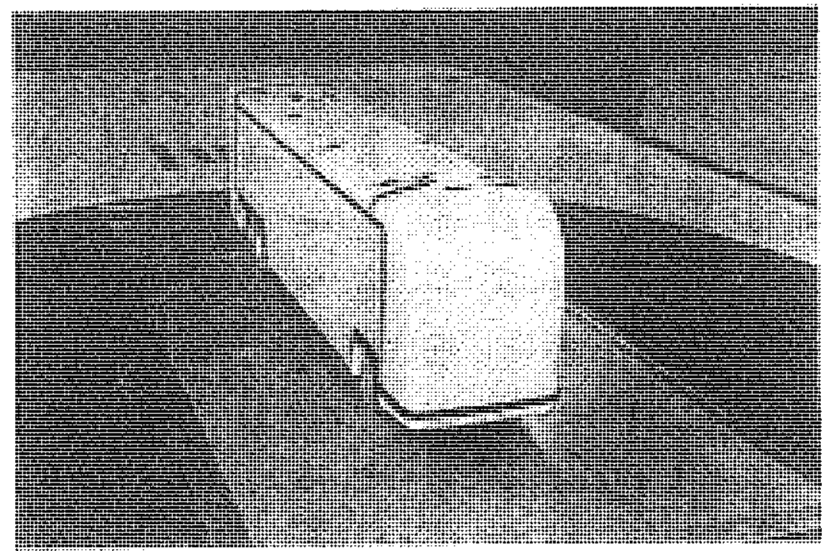

P5: MCI PROPOSAL 1 FRONT

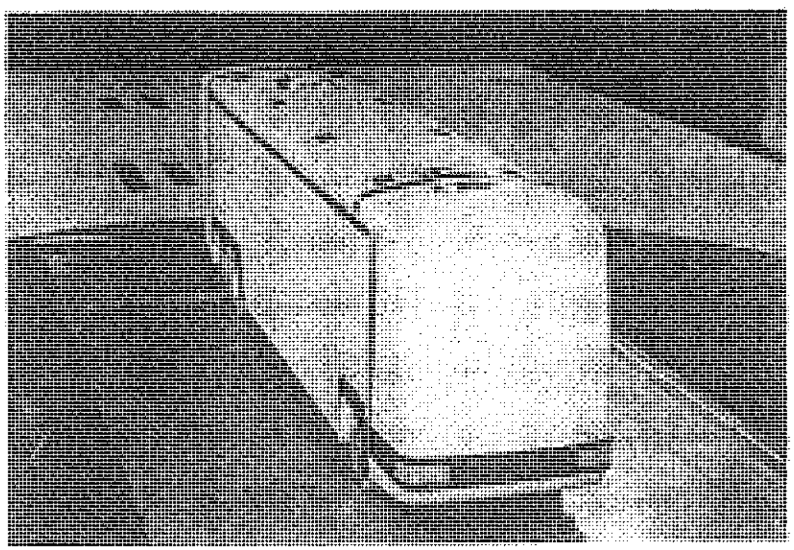

P6: MCI PROPOSAL 2 FRONT

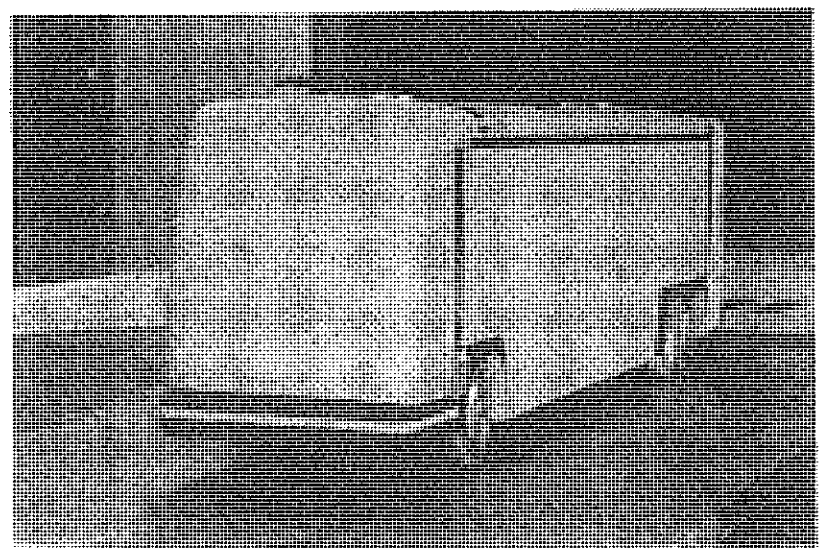

P7: PREVOST H3-40 FRONT

MCI - 039904

002328
002328
002328

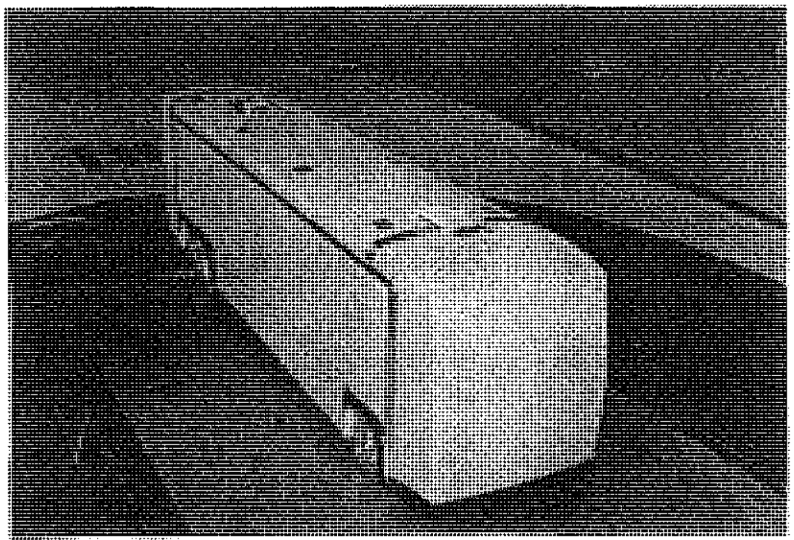

P8: SETRA S315 FRONT

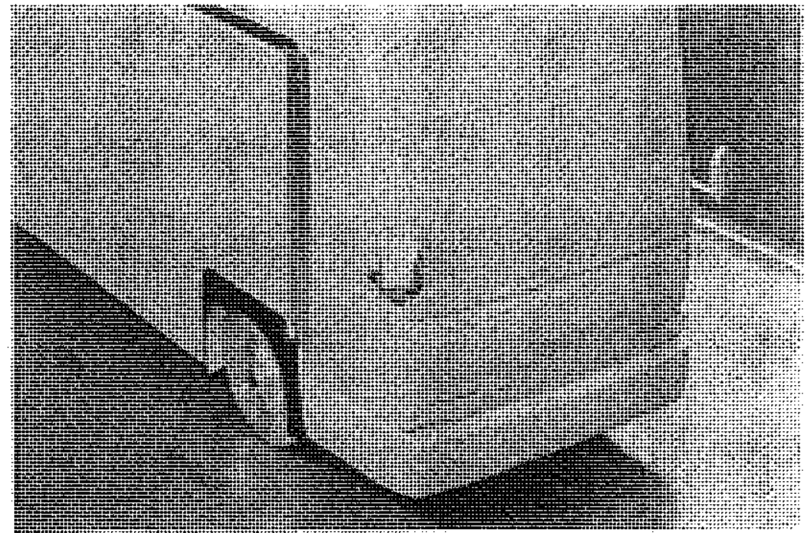

P9a: MCI STANDARD CJ3 FRONT WITH
STANDARD CJ3 MIRRORS FORWARD

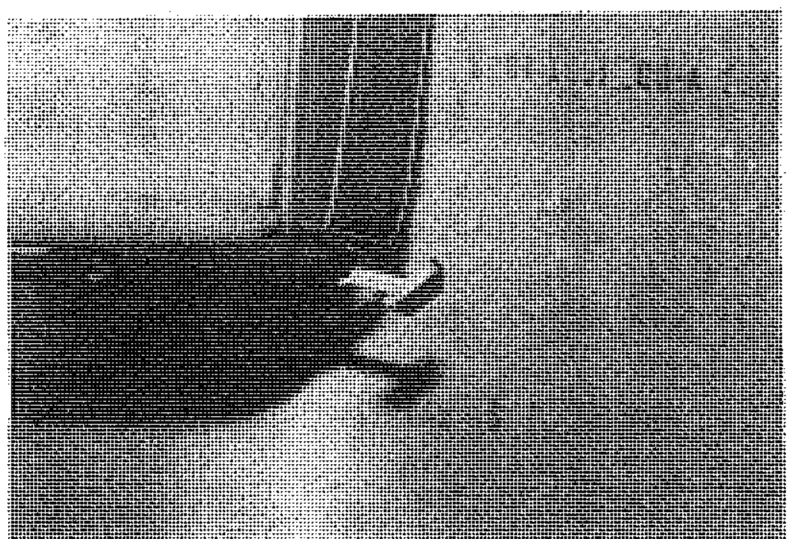

P9b: MCI STANDARD CJ3 FRONT WITH
STANDARD CJ3 MIRRORS FORWARD

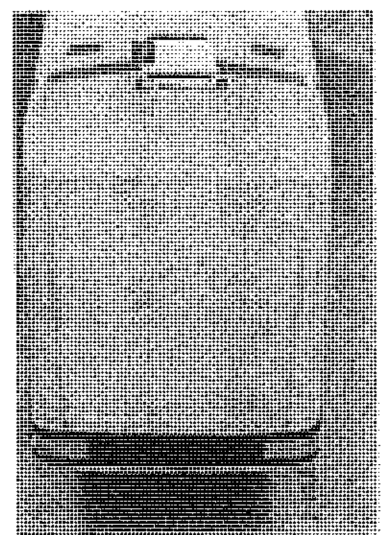

P10: MCI PROPOSAL 2 FRONT WITH TRIP

MCI - 039905

002329
002329
002329

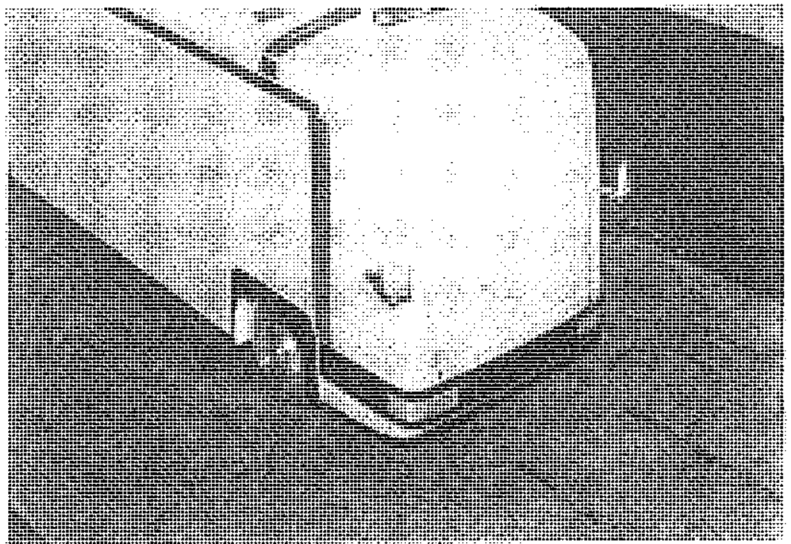

P11a: MCI PROPOSAL 2 FRONT WITH STANDARD CJ3 MIRRORS FORWARD

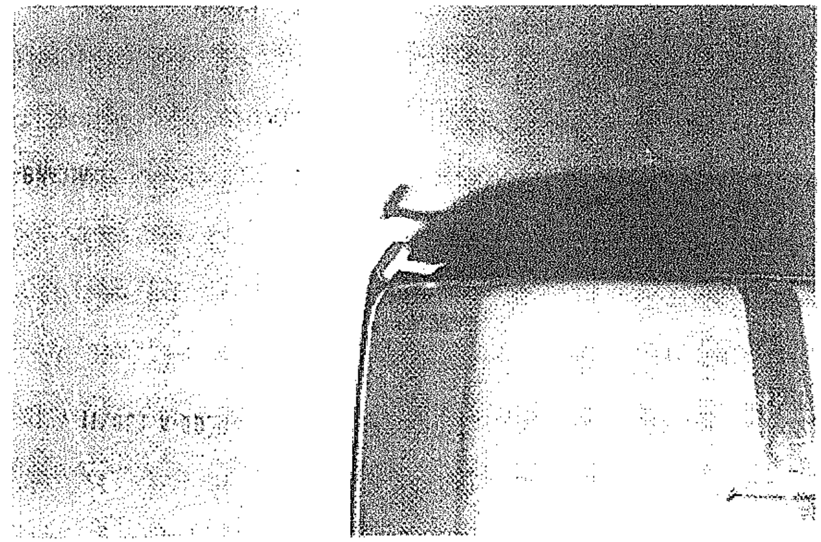

P11b: MCI PROPOSAL 2 FRONT WITH STANDARD CJ3 MIRROR FORWARD

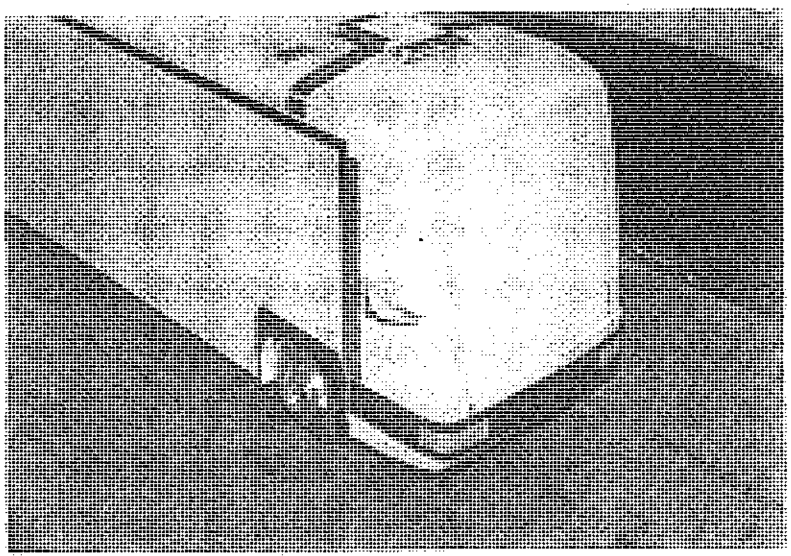

P12a: MCI PROPOSAL 2 FRONT WITH STANDARD CJ3 MIRRORS AFT

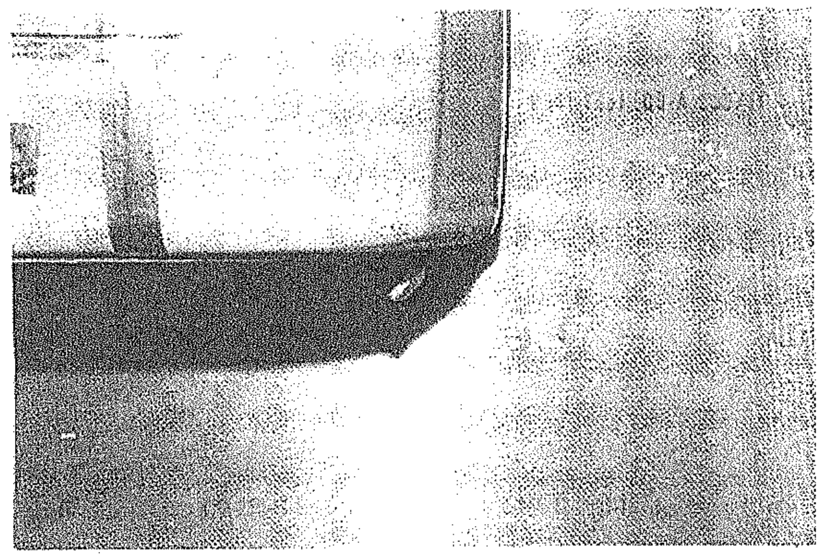

P12b: MCI PROPOSAL 2 FRONT WITH STANDARD CJ3 MIRROR AFT

002330
002330
002330

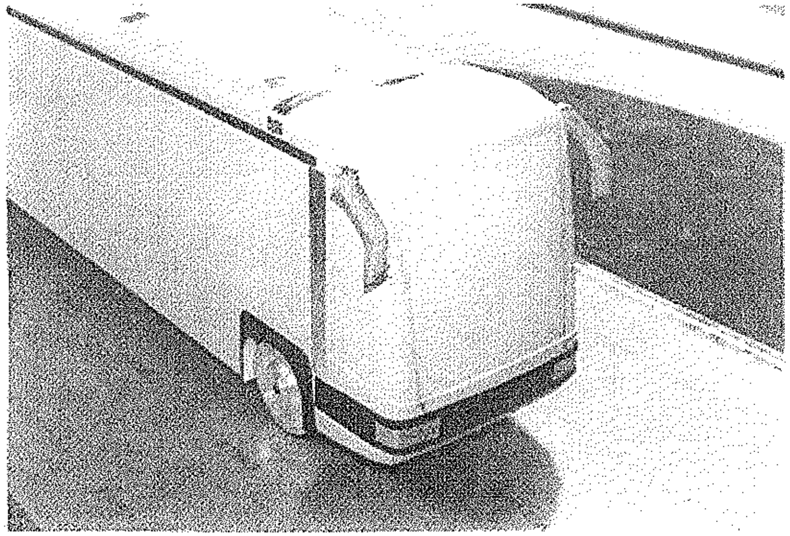

P13a: MCI PROPOSAL 2 FRONT WITH SETRA MIRRORS

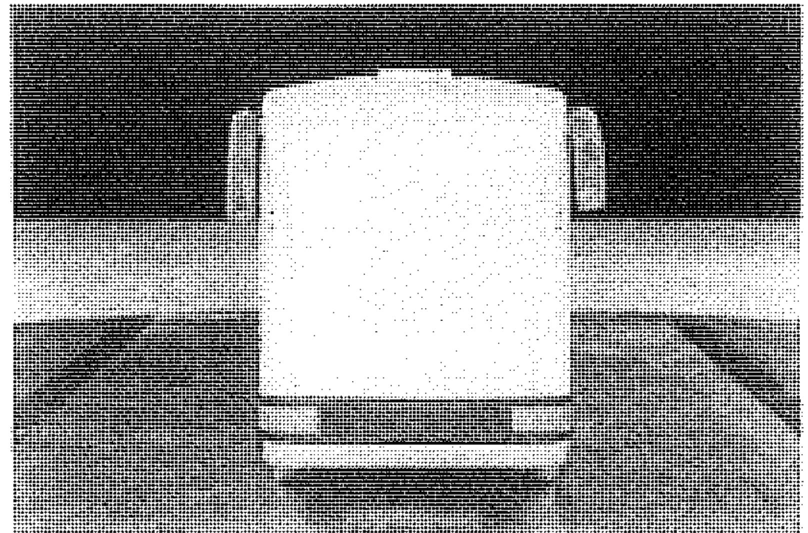

P13b: MCI PROPOSAL 2 FRONT WITH SETRA MIRRORS

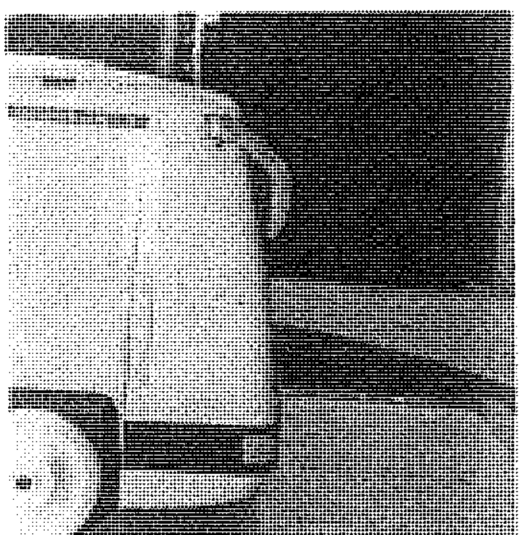

P13c: MCI PROPOSAL 2 FRONT WITH SETRA MIRRORS

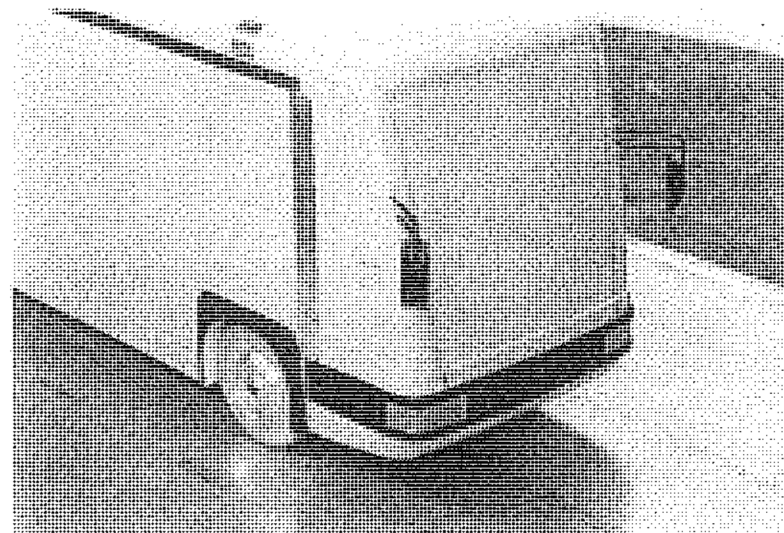

P14a: MCI PROPOSAL 2 FRONT WITH PREVOST MIRRORS

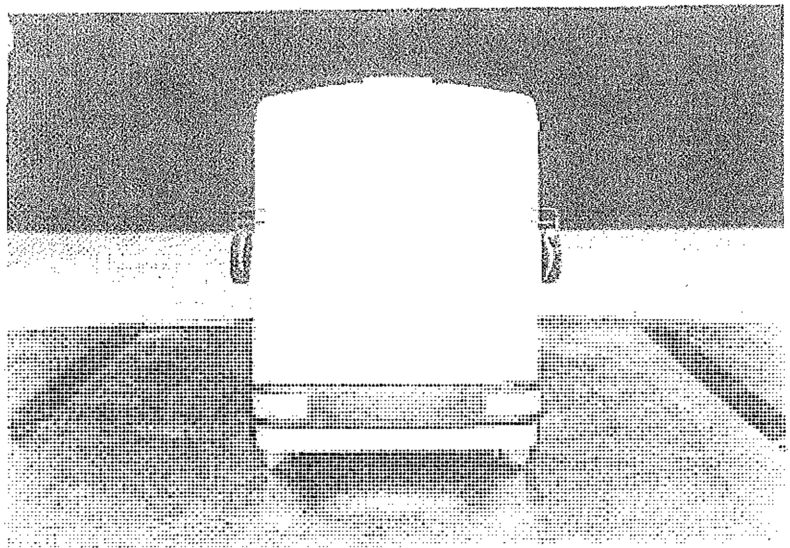

P14b: MCI PROPOSAL 2 FRONT WITH PREVOST MIRROR

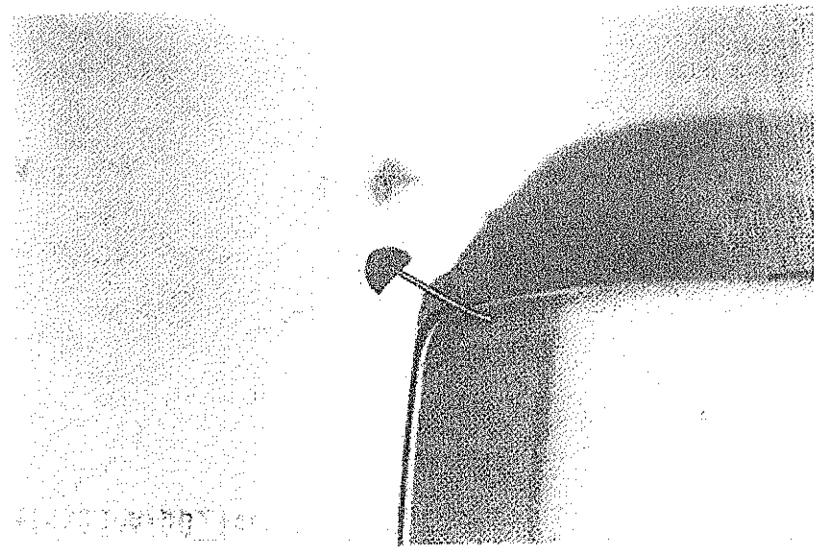

P14c: MCI PROPOSAL 2 FRONT WITH PREVOST MIRROR

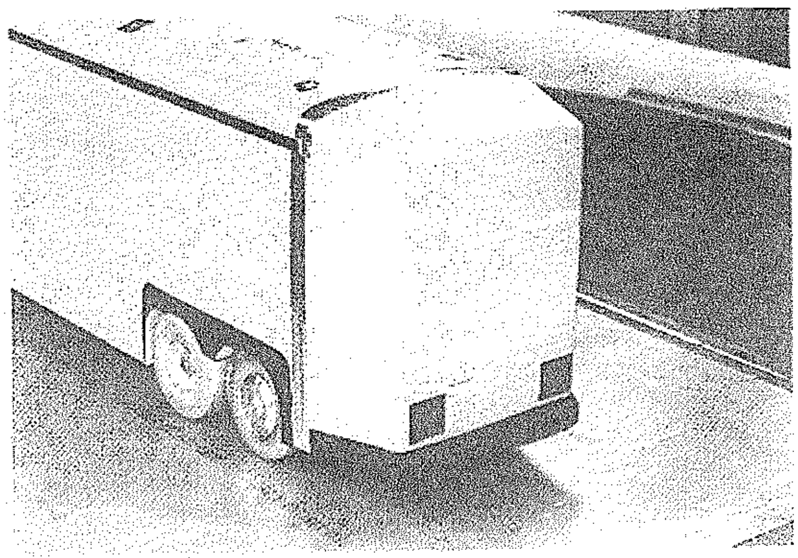

P15a: REAR END WITH 15° BEVELS ON TOP AND SIDE EDGES

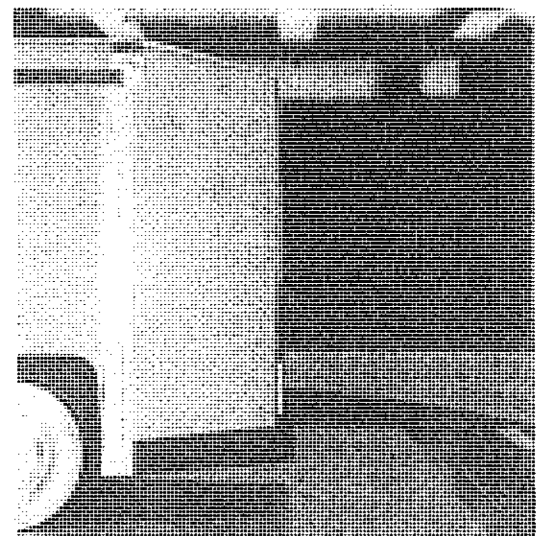

P15b: REAR END WITH 15° BEVEL ON TOP EDGE

MCI - 039908

002332
002332

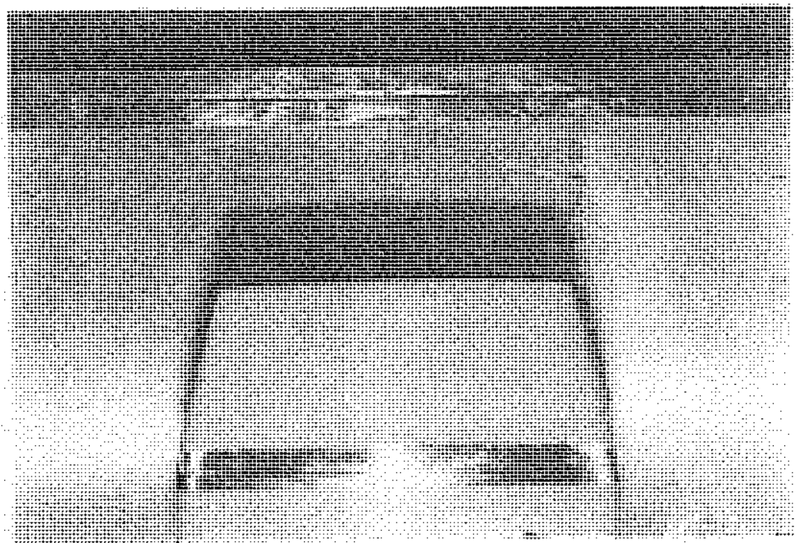

P15c: REAR END WITH 15° BEVELS
ON SIDE EDGES

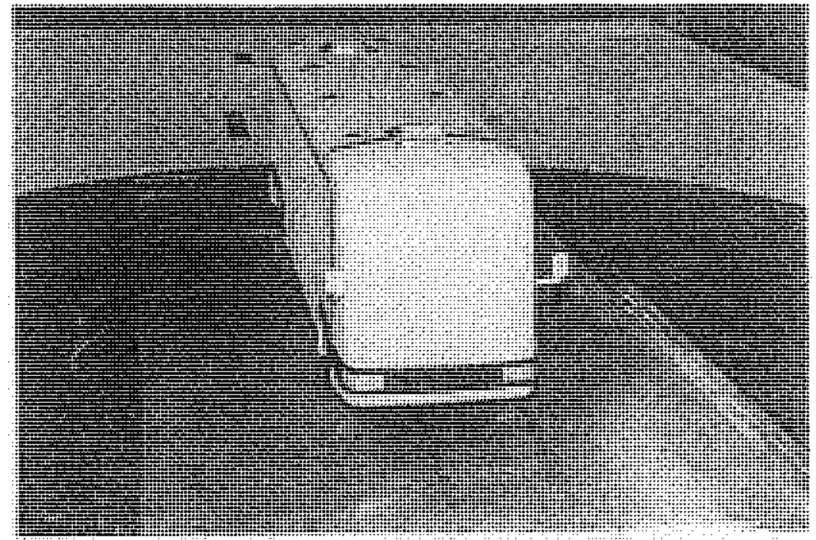

P16a: MCI PROPOSAL 2 FRONT WITH STANDARD
CJ3 MIRRORS FORWARD AND AFT

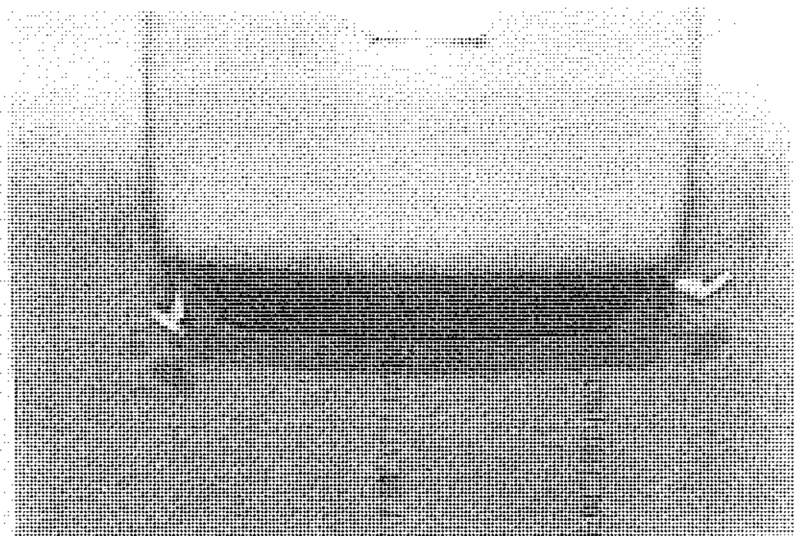

P16b: MCI PROPOSAL 2 FRONT WITH STANDARD
CJ3 MIRRORS FORWARD AND AFT

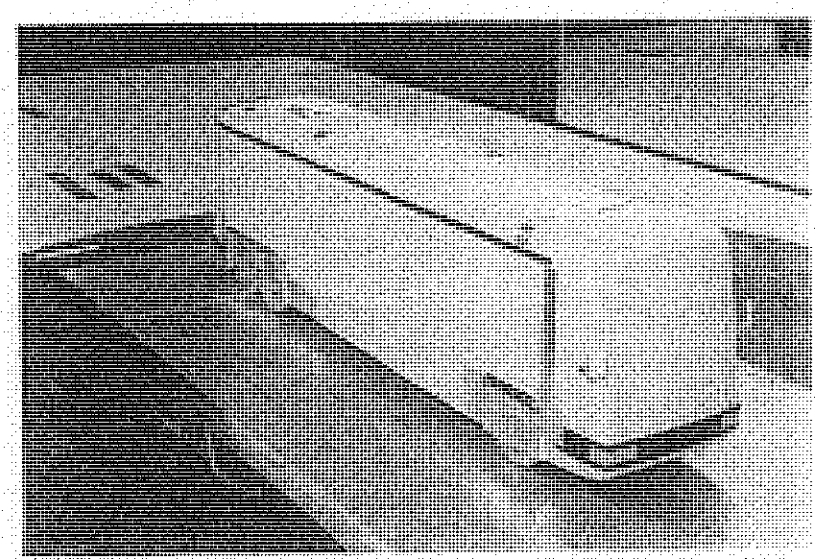

P17: MCI PROPOSAL 2 FRONT AND
WHEEL SKIRTS

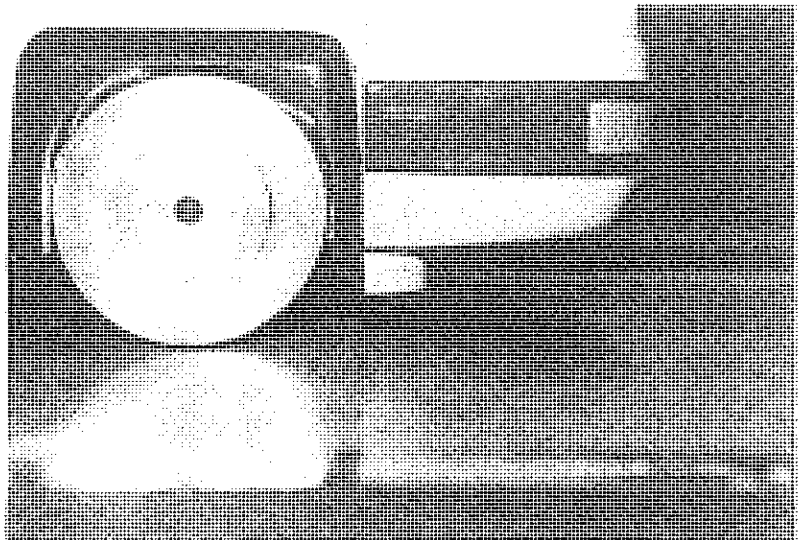

P18a: MCI PROPOSAL 2 FRONT WITH AIR DAM

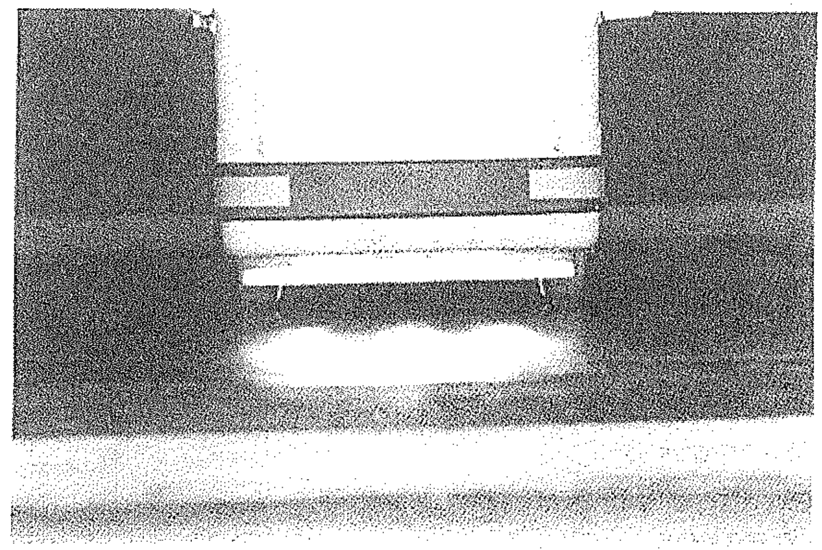

P18b: MCI PROPOSAL 2 FRONT WITH AIR DAM

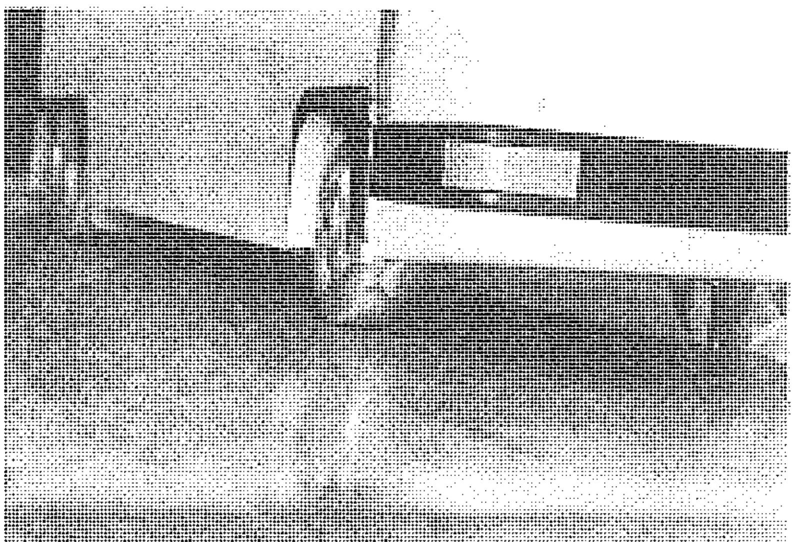

P19a: MCI PROPOSAL 2 FRONT WITH FRONT-TIRE FAIRING

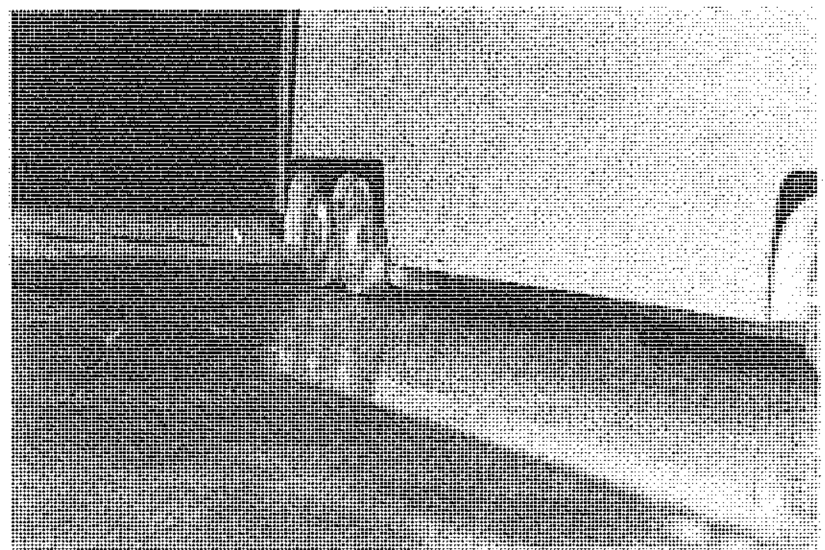

P19b: MCI PROPOSAL 2 FRONT WITH REAR-TIRE FAIRING

002334

002334

002334

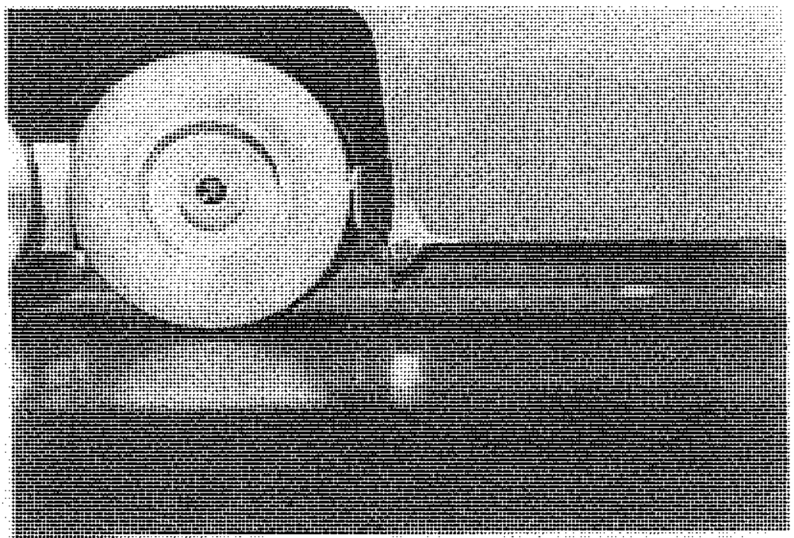

P19a: REAR-TIRE FAIRING

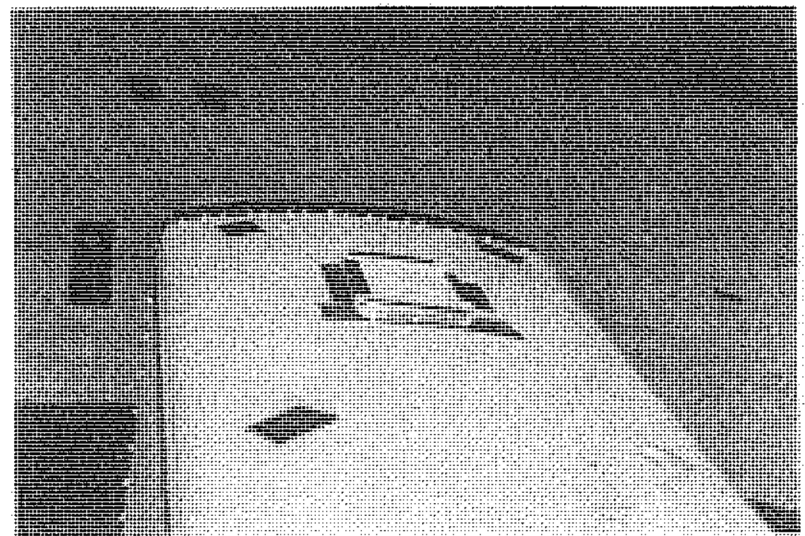

P20: VORTEX GENERATORS IMMEDIATELY UPSTREAM OF BEVELLED REAR

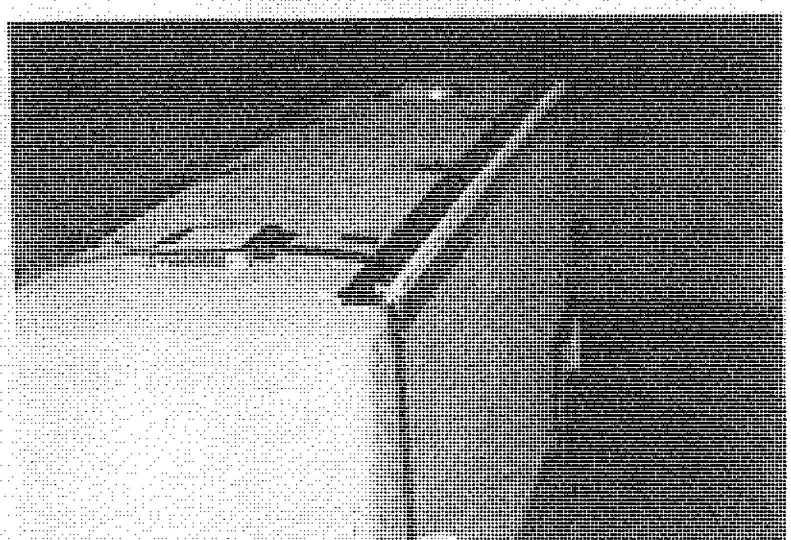

P21: MODIFIED DRIP RAIL

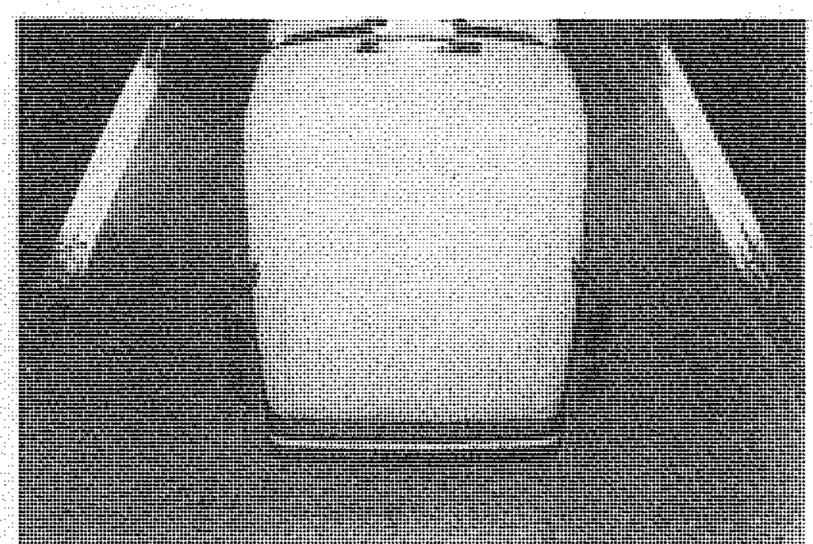

P22a: PREVOST H3-40 FRONT WITH PREVOST MIRRORS

002335
002335
002335

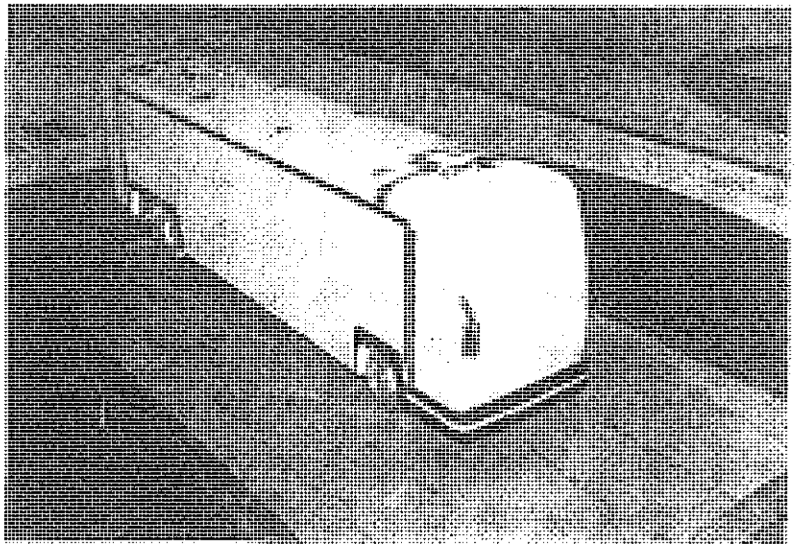

P22b: PREVOST H3-40 FRONT WITH PREVOST MIRRORS

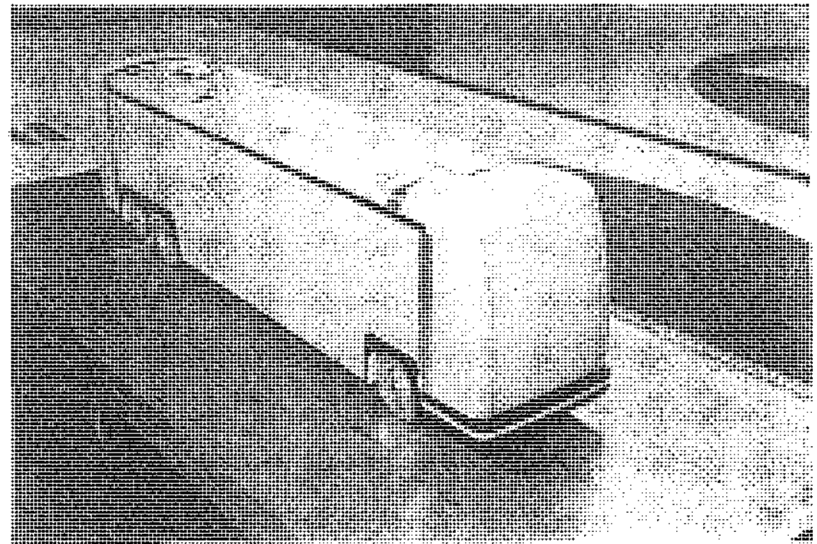

P23: PREVOST H3-40 FRONT WITH TRIP

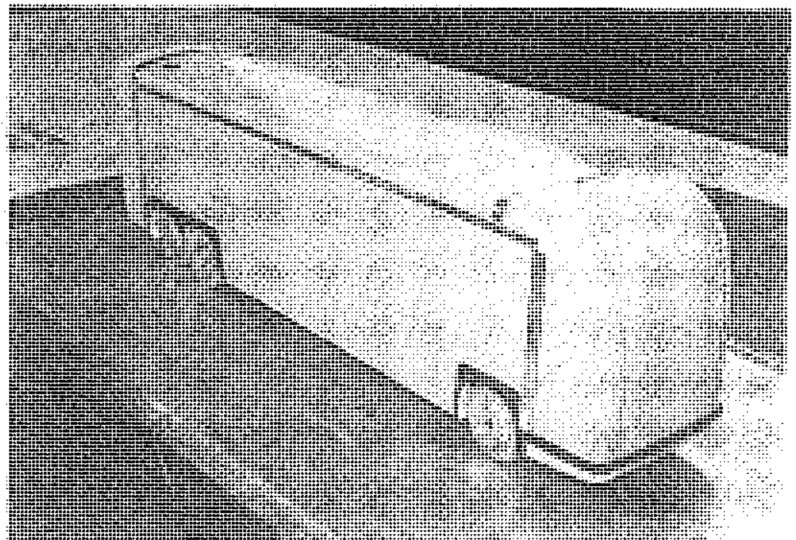

P24: MCI PROPOSAL 1 FRONT WITH TRIP

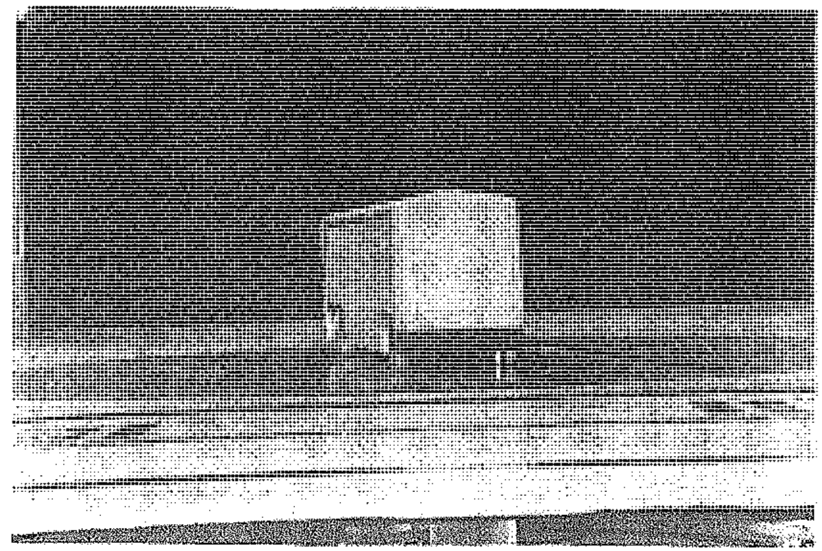

P25: MCI SMOOTH CJ3 FRONT WITH TRIP

MCI - 039912

002336
002336
002336

APPENDIX 3: DATA TABULATION

The following notation is used in the tabulations;

Rept/Tare/Run	=	Test number/Run no. for wind-off balance zero readings/Run no.
QC	=	reference dynamic pressure corrected for wall effects
Re	=	Reynolds number
PT	=	point number
VEL	=	test wind speed based on QC
CL	=	lift coefficient
CD	=	drag coefficient
CY	=	side force coefficient
CM	=	pitching moment coefficient
CN	=	yawing moment coefficient
CR	=	rolling moment coefficient

002337

002337

BUS TEST

Rept/Tare/Run 0607/012/013

C3 SMOOTH FRONT, C3 STANDARD REAR

ATM PRESS= 101.2 KPA TEMP= 24.08 C Density= 1.186 Kg/m3
Ref length=0.7225 m Ref Area= 0.08358 m2 QC= 3.90 Kpa
Re= 1.3566 Million

PT	VEL (m/s)	YAW (deg)	CL	CD	CY	CM	CN	CR
01	81.1	-2.95	-0.0156	0.3527	-0.2570	0.0421	-0.0924	-0.0597
02	81.3	-1.44	-0.0396	0.3473	-0.1139	0.0487	-0.0456	-0.0286
03	81.0	0.08	-0.0506	0.3481	0.0213	0.0509	0.0027	0.0044
04	81.3	1.60	-0.0447	0.3507	0.1578	0.0447	0.0507	0.0316
05	81.2	3.15	-0.0094	0.3561	0.3030	0.0316	0.0990	0.0654
06	81.1	6.21	0.0914	0.3801	0.6043	0.0273	0.1947	0.1333
07	80.4	9.27	0.2249	0.4037	0.9187	0.0316	0.2921	0.2055
08	79.8	12.35	0.4223	0.4496	1.2581	0.0256	0.3876	0.2834

Bus speed(mi/h)	Wind Averaged CD
35.00	0.410
45.00	0.387
55.00	0.376
65.00	0.369
75.00	0.365

BUS TEST

Rept/Tare/Run 0607/012/014

C3 SMOOTH FRONT, C3 STANDARD REAR

ATM PRESS= 101.2 KPA TEMP= 22.34 C Density= 1.193 Kg/m3
Ref length=0.7225 m Ref Area= 0.08358 m2 QC= 0.58 Kpa
Re= 0.5250 Million

PT	VEL (m/s)	YAW (deg)	CL	CD	CY	CM	CN	CR
01	31.1	-0.03	-0.0877	0.4856	-0.0131	0.1040	-0.0123	-0.0107
02	37.2	-0.03	-0.0836	0.4526	0.0009	0.0941	-0.0036	-0.0024
03	43.2	-0.03	-0.0793	0.4579	0.0027	0.0986	-0.0022	-0.0026
04	49.7	-0.03	-0.0758	0.4517	0.0055	0.0959	-0.0021	-0.0015
05	55.7	-0.03	-0.0703	0.4387	0.0086	0.0857	-0.0014	0.0001
06	62.5	-0.03	-0.0648	0.4331	0.0106	0.0877	-0.0013	0.0008
07	68.6	-0.03	-0.0616	0.4264	0.0115	0.0874	-0.0013	0.0007
08	75.6	-0.03	-0.0552	0.4143	0.0104	0.0862	-0.0015	0.0013
09	80.8	-0.03	-0.0539	0.3477	0.0092	0.0536	-0.0011	0.0013
10	87.2	-0.03	-0.0482	0.3489	0.0051	0.0543	-0.0013	0.0001
11	93.6	-0.03	-0.0419	0.3455	0.0031	0.0543	-0.0022	-0.0002

Bus speed(mi/h)	Wind Averaged CD
35.00	0.000
45.00	0.000
55.00	0.000
65.00	0.000
75.00	0.000

BUS TEST

Rept/Tare/Run 0607/015/016

C3 SMOOTH FRONT, C3 STANDARD REAR

ATM PRESS= 101.1 KPA TEMP= 24.40 C Density= 1.183 Kg/m3
Ref length=0.7225 m Ref Area= 0.08358 m2 QC= 4.22 Kpa
Re= 1.4083 Million

PT	VEL (m/s)	YAW (deg)	CL	CD	CY	CM	CN	CR
01	84.5	-3.07	-0.0069	0.3554	-0.2713	0.0415	-0.0951	-0.0645
02	84.4	-1.57	-0.0338	0.3500	-0.1293	0.0501	-0.0480	-0.0339
03	84.7	-0.05	-0.0460	0.3490	0.0089	0.0512	0.0000	-0.0013
04	84.4	1.48	-0.0450	0.3554	0.1502	0.0488	0.0454	0.0305
05	84.5	3.02	-0.0079	0.3588	0.2939	0.0345	0.0957	0.0647
06	84.2	6.07	0.0886	0.3781	0.5925	0.0268	0.1919	0.1345
07	83.4	9.14	0.2223	0.4012	0.9041	0.0272	0.2891	0.2049
08	83.1	12.21	0.4166	0.4401	1.2432	0.0210	0.3841	0.2833

Bus speed(mi/h)	Wind Averaged CD
35.00	0.409
45.00	0.387
55.00	0.377
65.00	0.371
75.00	0.367

BUS TEST

Rept/Tare/Run 0607/017/018

PRODUCTION C3 FRONT, C3 STANDARD REAR

ATM PRESS= 101.1 KPA TEMP= 21.88 C Density= 1.193 Kg/m3
Ref length=0.7225 m Ref Area= 0.08358 m2 QC= 1.46 Kpa
Re= 0.8386 Million

PT	VEL (m/s)	YAW (deg)	CL	CD	CY	CM	CN	CR
01	49.5	-0.01	-0.1150	0.5431	0.0136	0.0883	-0.0033	-0.0045
02	55.7	-0.01	-0.1106	0.5449	0.0142	0.0841	-0.0027	-0.0034
03	61.9	-0.01	-0.1044	0.5389	0.0143	0.0817	-0.0029	-0.0024
04	67.8	-0.01	-0.0988	0.5363	0.0152	0.0842	-0.0036	-0.0022
05	74.7	-0.01	-0.0947	0.5364	0.0133	0.0860	-0.0038	-0.0016
06	80.8	-0.01	-0.0885	0.5362	0.0121	0.0852	-0.0043	-0.0015
07	86.5	-0.01	-0.0839	0.5334	0.0094	0.0845	-0.0048	-0.0024
08	92.6	-0.01	-0.0782	0.5295	0.0052	0.0868	-0.0038	-0.0033

Bus speed(mi/h)	Wind Averaged CD
35.00	0.000
45.00	0.000
55.00	0.000
65.00	0.000
75.00	0.000

BUS TEST — Rept/Tare/Run 0607/017/019

PRODUCTION C3 FRONT, C3 STANDARD REAR

ATM PRESS= 101.1 KPA TEMP= 27.09 C Density= 1.173 Kg/m3
Ref length=0.7225 m Ref Area= 0.08358 m2 QC= 4.18 Kpa
Re= 1.2047 Million

PT	VEL (m/s)	YAW (deg)	CL	CD	CY	CM	CN	CR
01	84.4	-3.10	-0.0440	0.5390	-0.2758	0.0719	-0.0727	-0.0699
02	84.4	-1.58	-0.0767	0.5306	-0.1331	0.0828	-0.0496	-0.0396
03	84.2	-0.03	-0.0847	0.5304	0.0046	0.0834	-0.0040	-0.0044
04	84.4	1.47	-0.0625	0.5315	0.1442	0.0777	0.0392	0.0276
05	84.0	3.01	-0.0156	0.5410	0.2864	0.0797	0.0902	0.0641
06	83.6	6.06	0.0780	0.5864	0.5818	0.0855	0.1771	0.1308
07	82.9	9.13	0.2239	0.6696	0.8752	0.0953	0.2478	0.2116
08	81.8	12.20	0.4615	0.7581	1.2435	0.0870	0.3019	0.2963

Bus speed(mi/h)	Wind Averaged CD
35.00	0.662
45.00	0.612
55.00	0.584
65.00	0.567
75.00	0.558

BUS TEST — Rept/Tare/Run 0607/020/021

MERCEDES BENZ FRONT, C3 STANDARD REAR

ATM PRESS= 101.5 KPA TEMP= 21.69 C Density= 1.199 Kg/m3
Ref length=0.7225 m Ref Area= 0.08358 m2 QC= 1.47 Kpa
Re= 0.8434 Million

PT	VEL (m/s)	YAW (deg)	CL	CD	CY	CM	CN	CR
01	49.6	-0.02	-0.0500	0.3897	0.0141	0.1467	-0.0005	-0.0035
02	55.0	-0.02	-0.0478	0.5959	0.0139	0.1506	-0.0001	-0.0019
03	61.7	-0.02	-0.0429	0.5862	0.0153	0.1531	0.0006	-0.0018
04	68.0	-0.02	-0.0408	0.5896	0.0158	0.1563	0.0015	-0.0012
05	73.6	-0.02	-0.0369	0.5825	0.0160	0.1508	0.0019	-0.0013
06	80.3	-0.02	-0.0359	0.5773	0.0078	0.1481	-0.0003	-0.0031
07	86.8	-0.02	-0.0316	0.5691	0.0034	0.1448	-0.0022	-0.0051
08	73.0	-0.02	-0.0259	0.5668	-0.0003	0.1461	-0.0030	-0.0057

Bus speed(mi/h)	Wind Averaged CD
35.00	0.000
45.00	0.000
55.00	0.000
65.00	0.000
75.00	0.000

BUS TEST — Rept/Tare/Run 0607/020/022

MERCEDES BENZ FRONT, C3 STANDARD REAR

ATM PRESS= 101.5 KPA TEMP= 26.74 C Density= 1.178 Kg/m3
Ref length=0.7225 m Ref Area= 0.08358 m2 QC= 4.16 Kpa
Re= 1.3870 Million

PT	VEL (m/s)	YAW (deg)	CL	CD	CY	CM	CN	CR
01	84.0	-3.05	0.0139	0.5782	-0.3075	0.1355	-0.0928	-0.0054
02	84.0	-1.53	-0.0172	0.5647	-0.1513	0.1429	-0.0491	-0.0478
03	84.2	-0.01	-0.0250	0.5568	0.0050	0.1437	-0.0009	-0.0059
04	83.9	1.52	-0.0045	0.5684	0.1568	0.1504	0.0391	0.0345
05	84.2	3.06	0.0473	0.5973	0.3170	0.1489	0.0843	0.0788
06	83.6	6.11	0.2084	0.6252	0.6405	0.1554	0.1912	0.1605
07	82.7	9.19	0.4203	0.6862	0.9775	0.1707	0.2707	0.2455
08	81.8	12.26	0.6789	0.7542	1.3390	0.1692	0.3520	0.3370

Bus speed(mi/h)	Wind Averaged CD
35.00	0.685
45.00	0.643
55.00	0.620
65.00	0.606
75.00	0.598

BUS TEST — Rept/Tare/Run 0607/024/025

PROPOSAL #1 FRONT, C3 STANDARD REAR

ATM PRESS= 101.5 KPA TEMP= 23.98 C Density= 1.189 Kg/m3
Ref length=0.7225 m Ref Area= 0.08358 m2 QC= 1.47 Kpa
Re= 0.8355 Million

PT	VEL (m/s)	YAW (deg)	CL	CD	CY	CM	CN	CR
01	49.8	-0.02	-0.0671	0.4153	0.0131	0.0939	0.0056	-0.0068
02	56.1	-0.02	-0.0651	0.3512	0.0156	0.0766	0.0033	-0.0036
03	62.5	-0.02	-0.0637	0.3450	0.0146	0.0729	0.0039	-0.0031
04	67.9	-0.02	-0.0616	0.3450	0.0137	0.0700	0.0035	-0.0029
05	76.0	-0.02	-0.0553	0.3447	0.0113	0.0704	0.0029	-0.0024
06	81.2	-0.02	-0.0496	0.3420	0.0081	0.0702	0.0026	-0.0030
07	87.7	-0.02	-0.0443	0.3442	0.0085	0.0732	0.0023	-0.0027
08	94.1	-0.02	-0.0361	0.3404	0.0022	0.0734	0.0002	-0.0036

Bus speed(mi/h)	Wind Averaged CD
35.00	0.000
45.00	0.000
55.00	0.000
65.00	0.000
75.00	0.000

MCI - 039915

002339
002339

BUS TEST

Rept/Tare/Run 0607/024/026

PROPOSAL #1 FRONT, C3 STANDARD REAR

ATM PRESS= 101.5 KPA
Ref length=0.7225 m

TEMP= 29.00 C
Ref Area= 0.08358 m2
Re= 1.3860 Million

Density= 1.170 Kg/m3
QC= 4.24 Kpa

PT	VEL (m/s)	YAW (deg)	CL	CD	CY	CM	CN	CR
01	85.1	-3.04	0.0012	0.3506	-0.2794	0.0593	-0.0932	-0.0675
02	85.1	-1.53	-0.0400	0.3461	-0.1322	0.0725	-0.0484	-0.0367
03	84.9	-0.01	-0.0449	0.3419	0.0072	0.0715	0.0019	-0.0027
04	84.9	1.52	-0.0378	0.3461	0.1544	0.0718	0.0512	0.0277
05	85.0	3.05	0.0107	0.3534	0.3021	0.0650	0.1027	0.0651
06	84.7	6.11	0.1092	0.3592	0.6005	0.0490	0.2064	0.1367
07	84.0	9.19	0.2299	0.3778	0.9144	0.0447	0.3090	0.2111
08	83.6	12.26	0.4026	0.3872	1.2580	0.0316	0.4102	0.2897

Bus speed(mi/h)	Wind Averaged CD
35.00	0.383
45.00	0.371
55.00	0.363
65.00	0.358
75.00	0.356

BUS TEST

Rept/Tare/Run 0607/027/028

PROPOSAL #2 FRONT, C3 STANDARD REAR

ATM PRESS= 101.2 KPA
Ref length=0.7225 m

TEMP= 24.43 C
Ref Area= 0.08358 m2
Re= 0.8275 Million

Density= 1.184 Kg/m3
QC= 1.46 Kpa

PT	VEL (m/s)	YAW (deg)	CL	CD	CY	CM	CN	CR
01	49.6	-0.02	-0.0482	0.4733	0.0146	0.1207	-0.0006	-0.0051
02	55.9	-0.02	-0.0469	0.4655	0.0145	0.1169	-0.0012	-0.0046
03	62.4	-0.02	-0.0431	0.4685	0.0162	0.1193	-0.0011	-0.0033
04	67.2	-0.02	-0.0417	0.4618	0.0153	0.1140	-0.0007	-0.0025
05	75.9	-0.02	-0.0325	0.4492	0.0126	0.1133	0.0006	-0.0017
06	81.2	-0.02	-0.0258	0.4430	0.0133	0.1134	0.0002	-0.0016
07	87.8	-0.02	-0.0189	0.4235	0.0075	0.1111	-0.0014	-0.0027
08	93.9	-0.02	-0.0128	0.4046	0.0098	0.1083	0.0018	-0.0019

Bus speed(mi/h)	Wind Averaged CD
35.00	0.000
45.00	0.000
55.00	0.000
65.00	0.000
75.00	0.000

BUS TEST

Rept/Tare/Run 0607/027/029

PROPOSAL #2 FRONT, C3 STANDARD REAR

ATM PRESS= 101.5 KPA
Ref length=0.7225 m

TEMP= 29.48 C
Ref Area= 0.08358 m2
Re= 1.3799 Million

Density= 1.168 Kg/m3
QC= 4.22 Kpa

PT	VEL (m/s)	YAW (deg)	CL	CD	CY	CM	CN	CR
01	84.9	-3.05	0.0190	0.3543	-0.2836	0.0761	-0.0950	-0.0670
02	84.9	-1.53	-0.0187	0.3467	-0.1346	0.0856	-0.0495	-0.0373
03	84.8	-0.02	-0.0210	0.3423	0.0061	0.0845	-0.0023	-0.0037
04	84.9	1.51	-0.0131	0.3471	0.1533	0.0870	0.0443	0.0291
05	85.1	3.05	0.0287	0.3532	0.3057	0.0784	0.0949	0.0669
06	84.3	6.11	0.1274	0.4833	0.6148	0.0912	0.2065	0.1477
07	84.0	9.18	0.2724	0.5168	0.9300	0.0929	0.2983	0.2212
08	83.1	12.26	0.4498	0.5750	1.2851	0.0818	0.3901	0.3057

Bus speed(mi/h)	Wind Averaged CD
35.00	0.476
45.00	0.458
55.00	0.436
65.00	0.416
75.00	0.396

BUS TEST

Rept/Tare/Run 0607/030/031

PREVOST FRONT, C3 STANDARD REAR

ATM PRESS= 101.5 KPA
Ref length=0.7225 m

TEMP= 25.33 C
Ref Area= 0.08358 m2
Re= 0.8308 Million

Density= 1.184 Kg/m3
QC= 1.47 Kpa

PT	VEL (m/s)	YAW (deg)	CL	CD	CY	CM	CN	CR
01	49.9	-0.01	-0.1222	0.5340	0.0190	0.0700	0.0019	-0.0021
02	55.7	-0.01	-0.1166	0.5234	0.0166	0.0627	0.0005	-0.0022
03	62.0	-0.01	-0.1793	0.4941	0.0144	0.0591	-0.0045	-0.0028
04	66.5	-0.01	-0.1073	0.4721	0.0105	0.0524	-0.0080	-0.0033
05	75.2	-0.01	-0.0918	0.3770	0.0222	0.0314	0.0061	0.0025
06	81.5	0.00	-0.0853	0.3706	0.0236	0.0307	0.0056	0.0028
07	88.0	-0.01	-0.0802	0.3709	0.0214	0.0298	0.0047	0.0025
08	94.2	-1.96	-0.0732	0.3646	0.0032	0.0784	0.0025	-0.0008

Bus speed(mi/h)	Wind Averaged CD
35.00	0.000
45.00	0.000
55.00	0.000
65.00	0.000
75.00	0.000

MCI - 039916

002340

002340

BUS TEST — Rept/Tare/Run 0607/030/032

PREVOST FRONT, C3 STANDARD REAR

ATM PRESS= 101.5 KPA TEMP= 27.90 C Density= 1.166 Kg/m3
Ref length=0.7225 m Ref Area= 0.08358 m2 QC= 4.22 Kpa
Re= 1.3776 Million

PT	VEL (m/s)	YAW (deg)	CL	CD	CY	CM	CN	CR
01	85.0	-3.04	-0.0495	0.3802	-0.2639	0.0169	-0.0893	-0.0648
02	84.9	-1.52	-0.0741	0.3745	-0.1214	0.0284	-0.0433	-0.0335
03	84.9	-0.01	-0.0813	0.3716	0.0213	0.0313	0.0051	0.0016
04	84.9	1.51	-0.0670	0.3721	0.1534	0.0258	0.0522	0.0317
05	84.8	3.06	-0.0387	0.3797	0.2925	0.0192	0.1028	0.0657
06	84.3	6.11	0.0495	0.4001	0.5964	0.0108	0.2016	0.1382
07	84.0	9.18	0.1726	0.4598	0.9091	0.0163	0.2795	0.2115
08	82.3	12.26	0.4902	0.7371	1.3176	0.0613	0.3114	0.3289

Bus speed(mi/h)	Wind Averaged CD
35.00	0.501
45.00	0.417
55.00	0.404
65.00	0.396
75.00	0.390

BUS TEST — Rept/Tare/Run 0607/033/034

SETRA FRONT, C3 STANDARD REAR

ATM PRESS= 101.5 KPA TEMP= 25.46 C Density= 1.184 Kg/m3
Ref length=0.7225 m Ref Area= 0.08358 m2 QC= 1.40 Kpa
Re= 0.8310 Million

PT	VEL (m/s)	YAW (deg)	CL	CD	CY	CM	CN	CR
01	50.0	-0.01	-0.0678	0.5713	0.0105	0.1202	0.0010	-0.0069
02	55.7	-0.01	-0.0701	0.5765	0.0141	0.1191	0.0022	-0.0045
03	62.2	-0.01	-0.0678	0.5686	0.0152	0.1157	0.0030	-0.0029
04	65.5	-0.01	-0.0665	0.5677	0.0151	0.1148	0.0031	-0.0025
05	74.3	-0.01	-0.0583	0.5660	0.0144	0.1190	0.0031	-0.0018
06	80.5	-0.01	-0.0520	0.5673	0.0159	0.1198	0.0031	-0.0016
07	87.5	-0.01	-0.0441	0.5630	0.0104	0.1177	0.0018	-0.0022
08	92.8	-0.01	-0.0386	0.5636	0.0057	0.1207	0.0007	-0.0029

Bus speed(mi/h)	Wind Averaged CD
35.00	0.000
45.00	0.000
55.00	0.000
65.00	0.000
75.00	0.000

BUS TEST — Rept/Tare/Run 0607/033/035

SETRA FRONT, C3 STANDARD REAR

ATM PRESS= 101.5 KPA TEMP= 29.99 C Density= 1.166 Kg/m3
Ref length=0.7225 m Ref Area= 0.08358 m2 QC= 4.00 Kpa
Re= 1.3402 Million

PT	VEL (m/s)	YAW (deg)	CL	CD	CY	CM	CN	CR
01	82.8	-3.08	0.0082	0.5768	-0.2916	0.1087	-0.0753	-0.0742
02	84.0	-1.54	-0.0378	0.5460	-0.1378	0.1171	-0.0378	-0.0397
03	84.6	-0.01	-0.0465	0.5638	0.0081	0.1168	0.0016	-0.0027
04	84.7	1.51	-0.0282	0.5680	0.1605	0.1209	0.0393	0.0344
05	84.4	3.05	0.0199	0.5885	0.3158	0.1116	0.0720	0.0764
06	84.0	6.11	0.1563	0.6301	0.6383	0.1066	0.1448	0.1588
07	83.3	9.19	0.3611	0.7010	0.9757	0.1128	0.2177	0.2463
08	83.3	12.26	0.5973	0.7586	1.3237	0.1091	0.2870	0.3323

Bus speed(mi/h)	Wind Averaged CD
35.00	0.692
45.00	0.651
55.00	0.625
65.00	0.610
75.00	0.601

BUS TEST — Rept/Tare/Run 0607/036/037

PRODUCTION C3 FRONT WITH MIRRORS, C3 STANDARD REAR

ATM PRESS= 101.5 KPA TEMP= 27.76 C Density= 1.174 Kg/m3
Ref length=0.7225 m Ref Area= 0.08358 m2 QC= 4.18 Kpa
Re= 1.3837 Million

PT	VEL (m/s)	YAW (deg)	CL	CD	CY	CM	CN	CR
01	84.4	-3.07	-0.0512	0.5507	-0.2719	0.0731	-0.0910	-0.0682
02	84.1	-1.54	-0.0830	0.5451	-0.1341	0.0810	-0.0498	-0.0386
03	83.9	-0.02	-0.0893	0.5491	0.0078	0.0839	-0.0028	-0.0025
04	83.8	1.51	-0.0676	0.5441	0.1494	0.0774	0.0421	0.0304
05	84.0	3.05	-0.0230	0.5528	0.2874	0.0825	0.0912	0.0650
06	83.8	6.10	0.0768	0.6036	0.5833	0.0731	0.1777	0.1368
07	82.6	9.17	0.2010	0.6492	0.8920	0.0978	0.2538	0.2107
08	82.2	12.24	0.3932	0.7279	1.2387	0.0890	0.3313	0.2927

Bus speed(mi/h)	Wind Averaged CD
35.00	0.661
45.00	0.621
55.00	0.596
65.00	0.581
75.00	0.571

002341
002341

BUS TEST

Rept/Tare/Run 0607/030/039

PROP 2 FRONT WITH GRIT, C3 STANDARD REAR

ATM PRESS= 101.4 KPA TEMP= 23.51 C Density= 1.190 Kg/m3
Ref length=0.7223 m Ref Area= 0.08358 m2 QC= 1.49 Kpa
Re= 0.8399 Million

PT	VEL (m/s)	YAW (deg)	CL	CD	CY	CM	CN	CR
01	50.0	-0.22	-0.0441	0.3566	-0.0054	0.0878	-0.0044	-0.0088
02	56.5	-0.22	-0.0410	0.3529	-0.0049	0.0871	-0.0047	-0.0084
03	61.8	-0.22	-0.0411	0.3474	-0.0047	0.0840	-0.0045	-0.0073
04	68.6	-0.22	-0.0370	0.3472	-0.0048	0.0833	-0.0045	-0.0068
05	75.2	-0.22	-0.0334	0.3469	-0.0066	0.0826	-0.0050	-0.0068
06	81.0	-0.22	-0.0293	0.3428	-0.0087	0.0815	-0.0055	-0.0070
07	87.7	-0.22	-0.0216	0.3443	-0.0097	0.0852	-0.0058	-0.0070
08	94.2	-0.22	-0.0156	0.3414	-0.0144	0.0864	-0.0076	-0.0084

Bus speed(mi/h)	Wind Averaged CD
35.00	0.000
45.00	0.000
55.00	0.000
65.00	0.000
75.00	0.000

BUS TEST

Rept/Tare/Run 0607/030/040

PROP 2 FRONT WITH GRIT, C3 STANDARD REAR

ATM PRESS= 101.3 KPA TEMP= 27.81 C Density= 1.173 Kg/m3
Ref length=0.7225 m Ref Area= 0.08358 m2 QC= 4.20 Kpa
Re= 1.3862 Million

PT	VEL (m/s)	YAW (deg)	CL	CD	CY	CM	CN	CR
01	84.6	-3.04	0.0194	0.3534	-0.2822	0.0759	-0.0929	-0.0676
02	84.5	-1.53	-0.0190	0.3446	-0.1323	0.0861	-0.0470	-0.0378
03	84.6	-0.01	-0.0217	0.3414	0.0094	0.0864	0.0009	-0.0026
04	84.7	1.51	-0.0126	0.3460	0.1555	0.0904	0.0476	0.0290
05	84.6	3.05	0.0299	0.3537	0.3035	0.0810	0.0971	0.0653
06	84.6	6.11	0.1333	0.3615	0.5994	0.0675	0.1968	0.1362
07	84.0	9.19	0.2601	0.3866	0.9108	0.0620	0.2913	0.2097
08	82.2	12.26	0.4698	0.5420	1.2751	0.0854	0.3817	0.3044

Bus speed(mi/h)	Wind Averaged CD
35.00	0.422
45.00	0.374
55.00	0.365
65.00	0.359
75.00	0.357

BUS TEST

Rept/Tare/Run 0607/041/042

PROP 2 FRONT WITH GRIT AND C3 MIRRORS FWD, C3 STANDARD REAR

ATM PRESS= 101.3 KPA TEMP= 27.55 C Density= 1.173 Kg/m3
Ref length=0.7225 m Ref Area= 0.08358 m2 QC= 4.21 Kpa
Re= 1.3885 Million

PT	VEL (m/s)	YAW (deg)	CL	CD	CY	CM	CN	CR
01	84.7	-3.08	0.0202	0.3816	-0.2855	0.0850	-0.0948	-0.0691
02	84.6	-1.54	-0.0249	0.3798	-0.1373	0.0943	-0.0468	-0.0386
03	84.5	-0.02	-0.0288	0.3769	0.0047	0.0927	-0.0001	-0.0052
04	84.3	1.51	-0.0197	0.3795	0.1531	0.0952	0.0452	0.0282
05	84.6	3.05	0.0280	0.3806	0.3049	0.0839	0.0958	0.0665
06	84.5	6.11	0.1346	0.3853	0.6005	0.0660	0.1940	0.1361
07	83.3	9.18	0.2585	0.4341	0.9210	0.0690	0.2945	0.2159
08	82.3	12.26	0.4430	0.4698	1.2680	0.0656	0.3889	0.2966

Bus speed(mi/h)	Wind Averaged CD
35.00	0.434
45.00	0.409
55.00	0.394
65.00	0.387
75.00	0.385

BUS TEST

Rept/Tare/Run 0607/043/044

PROP 2 FRONT WITH GRIT AND C3 MIRRORS AFT, C3 STANDARD REAR

ATM PRESS= 101.3 KPA TEMP= 27.25 C Density= 1.174 Kg/m3
Ref length=0.7225 m Ref Area= 0.08358 m2 QC= 4.23 Kpa
Re= 1.3937 Million

PT	VEL (m/s)	YAW (deg)	CL	CD	CY	CM	CN	CR
01	84.8	-3.08	0.0075	0.3948	-0.2840	0.0830	-0.0923	-0.0683
02	84.5	-1.54	-0.0337	0.3929	-0.1367	0.0915	-0.0468	-0.0387
03	84.4	-0.02	-0.0372	0.3914	0.0107	0.0933	-0.0005	-0.0022
04	84.5	1.51	-0.0283	0.3935	0.1615	0.0928	0.0443	0.0321
05	84.6	3.05	0.0201	0.3938	0.3093	0.0826	0.0944	0.0671
06	84.4	6.11	0.1249	0.3974	0.6058	0.0649	0.1910	0.1392
07	84.1	9.18	0.2517	0.4242	0.9127	0.0618	0.2843	0.2128
08	83.7	12.25	0.4347	0.4717	1.2507	0.0606	0.3808	0.2925

Bus speed(mi/h)	Wind Averaged CD
35.00	0.438
45.00	0.415
55.00	0.405
65.00	0.400
75.00	0.398

MCI - 039918

BUS TEST Rept/Tare/Run 0607/045/046

PROP 2 FRONT WITH GRIT AND CEYRA MIRRORS, C3 STANDARD REAR

ATM PRESS= 101.3 KPA TEMP= 27.48 C Density= 1.173 Kg/m3
Ref length=0.7225 m Ref Area= 0.08358 m2 QC= 4.25 Kpa
Re= 1.3787 Million

PT	VEL (m/s)	YAW (deg)	CL	CD	CY	CM	CN	CR
01	85.1	-3.07	0.0244	0.4154	-0.2889	0.1024	-0.0919	-0.0704
02	84.9	-1.54	-0.0102	0.4124	-0.1322	0.1111	-0.0427	-0.0371
03	84.6	-0.02	-0.0117	0.4122	0.0129	0.1126	0.0059	-0.0021
04	84.6	1.51	-0.0042	0.4154	0.1635	0.1129	0.0540	0.0334
05	84.7	3.05	0.0354	0.4196	0.3164	0.1032	0.1053	0.0721
06	84.4	6.11	0.1215	0.4276	0.6169	0.0874	0.2095	0.1442
07	83.8	9.18	0.2316	0.4521	0.9288	0.0762	0.3123	0.2189
08	83.8	12.26	0.3927	0.4680	1.2653	0.0621	0.4127	0.2963

Bus speed(mi/h)	Wind Averaged CD
35.00	0.457
45.00	0.443
55.00	0.434
65.00	0.428
75.00	0.425

BUS TEST Rept/Tare/Run 0607/047/048

PROP 2 FRONT WITH GRIT AND PREVOST MIRRORS, C3 STANDARD REAR

ATM PRESS= 101.3 KPA TEMP= 27.00 C Density= 1.174 Kg/m3
Ref length=0.7225 m Ref Area= 0.08358 m2 QC= 4.26 Kpa
Re= 1.3983 Million

PT	VEL (m/s)	YAW (deg)	CL	CD	CY	CM	CN	CR
01	85.2	-3.07	0.0227	0.3745	-0.2845	0.0851	-0.0953	-0.0691
02	84.0	-1.54	-0.0240	0.3727	-0.1366	0.0953	-0.0476	-0.0393
03	84.7	-0.01	-0.0279	0.3712	0.0127	0.0959	0.0018	-0.0037
04	84.2	1.51	-0.0176	0.3732	0.1576	0.0969	0.0473	0.0292
05	84.7	3.05	0.0316	0.3763	0.3021	0.0853	0.0991	0.0655
06	84.1	6.11	0.1290	0.4330	0.6189	0.0837	0.2080	0.1467
07	83.7	9.18	0.2610	0.5022	0.9359	0.0913	0.2991	0.2259
08	82.8	12.26	0.4550	0.5598	1.2803	0.0893	0.3867	0.3070

Bus speed(mi/h)	Wind Averaged CD
35.00	0.484
45.00	0.446
55.00	0.422
65.00	0.406
75.00	0.397

BUS TEST Rept/Tare/Run 0607/049/050

PROP 2 FRONT WITH GRIT, REAR 15

ATM PRESS= 101.3 KPA TEMP= 26.02 C Density= 1.179 Kg/m3
Ref length=0.7225 m Ref Area= 0.08358 m2 QC= 1.60 Kpa
Re= 0.8607 Million

PT	VEL (m/s)	YAW (deg)	CL	CD	CY	CM	CN	CR
01	52.0	-0.02	0.1551	0.2964	0.0061	-0.0479	0.0068	-0.0043
02	56.4	-0.02	0.1520	0.2989	0.0038	-0.0437	0.0067	-0.0051
03	62.4	-0.02	0.1509	0.2963	0.0042	-0.0456	0.0069	-0.0045
04	67.6	-0.02	0.1502	0.2928	0.0044	-0.0499	0.0070	-0.0039
05	75.6	-0.02	0.1519	0.2919	0.0017	-0.0480	0.0074	-0.0043
06	83.5	-0.02	0.1530	0.2914	0.0003	-0.0455	0.0072	-0.0047
07	88.4	-0.02	0.1561	0.2899	-0.0030	-0.0456	0.0064	-0.0060
08	94.4	-0.02	0.1590	0.2912	-0.0100	-0.0454	0.0056	-0.0070

Bus speed(mi/h)	Wind Averaged CD
35.00	0.000
45.00	0.000
55.00	0.000
65.00	0.000
75.00	0.000

BUS TEST Rept/Tare/Run 0607/049/051

PROP 2 FRONT WITH GRIT, REAR 15

ATM PRESS= 101.3 KPA TEMP= 29.99 C Density= 1.163 Kg/m3
Ref length=0.7225 m Ref Area= 0.08358 m2 QC= 4.28 Kpa
Re= 1.3862 Million

PT	VEL (m/s)	YAW (deg)	CL	CD	CY	CM	CN	CR
01	85.8	-3.04	0.1866	0.2933	-0.2779	-0.0554	-0.0963	-0.0649
02	85.0	-1.54	0.1594	0.2920	-0.1469	-0.0508	-0.0400	-0.0397
03	85.1	-0.02	0.1539	0.2908	-0.0021	-0.0447	0.0056	-0.0055
04	85.4	1.51	0.1655	0.2921	0.1489	-0.0475	0.0534	0.0247
05	85.7	3.05	0.1963	0.2924	0.2812	-0.0541	0.1123	0.0600
06	85.7	6.11	0.3040	0.2924	0.5512	-0.0641	0.2268	0.1248
07	84.6	9.17	0.4325	0.3098	0.8363	-0.0693	0.3342	0.1652
08	83.4	12.23	0.6314	0.4573	1.1499	-0.0478	0.4488	0.2711

Bus speed(mi/h)	Wind Averaged CD
35.00	0.347
45.00	0.305
55.00	0.299
65.00	0.296
75.00	0.295

BUS TEST

Rept/Tare/Run 0607/052/053

PROP 2 FRONT WITH GRIT AND C3 MIRRORS FWD, REAR 15

ATM PRESS= 101.2 KPA
Ref length=0.7225 m

TEMP= 28.12 C
Ref Area= 0.08358 m2
Re= 1.3863 Million

Density= 1.170 Kg/m3
QC= 4.22 Kpa

PT	VEL (m/s)	YAW (deg)	CL	CD	CY	CM	CN	CR
01	84.9	-3.08	0.1822	0.3251	-0.2794	-0.0465	-0.0967	-0.0652
02	84.6	-1.54	0.1554	0.3246	-0.1493	-0.0436	-0.0414	-0.0403
03	84.9	-0.02	0.1515	0.3233	-0.0006	-0.0397	0.0070	-0.0043
04	85.0	1.51	0.1648	0.3259	0.1531	-0.0410	0.0537	0.0299
05	85.2	3.05	0.1967	0.3262	0.2813	-0.0472	0.1134	0.0611
06	85.1	6.10	0.3026	0.3326	0.5410	-0.0534	0.2339	0.1216
07	84.5	9.17	0.4270	0.3706	0.8427	-0.0580	0.3427	0.1979
08	83.5	12.24	0.6053	0.3969	1.1543	-0.0583	0.4479	0.2688

Bus speed(mi/h)	Wind Averaged CD
35.00	0.371
45.00	0.351
55.00	0.339
65.00	0.333
75.00	0.331

BUS TEST

Rept/Tare/Run 0607/054/055

PROP 2 FRONT WITH GRIT AND C3 MIRRORS (RIGHT FWD,LEFT AFT), REAR 15

ATM PRESS= 101.2 KPA
Ref length=0.7225 m

TEMP= 25.62 C
Ref Area= 0.08358 m2
Re= 1.4037 Million

Density= 1.179 Kg/m3
QC= 4.23 Kpa

PT	VEL (m/s)	YAW (deg)	CL	CD	CY	CM	CN	CR
01	84.7	-3.07	0.1849	0.3443	-0.2749	-0.0398	-0.1044	-0.0653
02	84.7	-1.54	0.1566	0.3410	-0.1419	-0.0380	-0.0476	-0.0380
03	84.5	-0.02	0.1520	0.3366	0.0022	-0.0356	0.0020	-0.0030
04	84.6	1.51	0.1625	0.3371	0.1508	-0.0364	0.0498	0.0294
05	84.9	3.05	0.1966	0.3375	0.2799	-0.0443	0.1086	0.0598
06	84.5	6.10	0.2993	0.3412	0.5390	-0.0479	0.2283	0.1189
07	83.9	9.17	0.4232	0.3769	0.8394	-0.0531	0.3362	0.1914
08	83.5	12.23	0.6091	0.4023	1.1532	-0.0540	0.4418	0.2660

Bus speed(mi/h)	Wind Averaged CD
35.00	0.379
45.00	0.360
55.00	0.349
65.00	0.343
75.00	0.341

BUS TEST

Rept/Tare/Run 0607/056/057

PROP 2 FRONT, GRIT, C3 MIRRORS (RIGHT FWD,LEFT AFT),WHEEL FAIRINGS, REAR 15

ATM PRESS= 101.2 KPA
Ref length=0.7225 m

TEMP= 25.63 C
Ref Area= 0.08358 m2
Re= 1.4041 Million

Density= 1.180 Kg/m3
QC= 4.23 Kpa

PT	VEL (m/s)	YAW (deg)	CL	CD	CY	CM	CN	CR
01	84.7	-3.09	0.2065	0.3267	-0.2725	-0.0414	-0.1087	-0.0652
02	84.1	-1.54	0.1849	0.3341	-0.1402	-0.0449	-0.0456	-0.0410
03	84.2	-0.01	0.1761	0.3315	0.0258	-0.0420	-0.0034	-0.0019
04	85.1	1.52	0.1921	0.3291	0.1858	-0.0431	0.0394	0.0348
05	85.0	3.05	0.2097	0.3162	0.2960	-0.0427	0.1059	0.0615
06	84.9	6.10	0.2861	0.3202	0.5555	-0.0342	0.2320	0.1209
07	84.0	9.17	0.4514	0.3504	0.8473	-0.0384	0.3523	0.1897
08	83.8	12.23	0.6489	0.3810	1.1702	-0.0504	0.4593	0.2681

Bus speed(mi/h)	Wind Averaged CD
35.00	0.357
45.00	0.339
55.00	0.330
65.00	0.325
75.00	0.324

BUS TEST

Rept/Tare/Run 0607/056/058

PROP 2 FRONT, GRIT, C3 MIRRORS (RIGHT FWD,LEFT AFT),VERTICAL AIR DAM, REAR 15

ATM PRESS= 101.2 KPA
Ref length=0.7225 m

TEMP= 25.64 C
Ref Area= 0.08358 m2
Re= 1.3943 Million

Density= 1.180 Kg/m3
QC= 4.18 Kpa

PT	VEL (m/s)	YAW (deg)	CL	CD	CY	CM	CN	CR
01	84.1	-3.07	0.0969	0.3644	-0.2404	-0.0339	-0.1070	-0.0616
02	84.2	-1.53	0.0887	0.3615	-0.1127	-0.0359	-0.0566	-0.0325
03	84.1	-0.02	0.1026	0.3678	0.0053	-0.0375	-0.0011	-0.0017
04	84.2	1.51	0.1140	0.3665	0.1251	-0.0342	0.0509	0.0241
05	84.3	3.04	0.1343	0.3691	0.2552	-0.0385	0.1073	0.0570
06	84.3	6.07	0.2109	0.3934	0.5215	-0.0524	0.2192	0.1180
07	83.4	9.16	0.3118	0.4340	0.8146	-0.0617	0.3261	0.1841
08	82.0	12.22	0.4418	0.4598	1.1431	-0.0708	0.4165	0.2607

Bus speed(mi/h)	Wind Averaged CD
35.00	0.430
45.00	0.406
55.00	0.393
65.00	0.384
75.00	0.380

002344

002344

002344

BUS TEST

Rept/Tare/Run 0607/056/059

PROP 2 FRONT, GRIT, C3 MIRRORS (RIGHT FWD,LEFT AFT),FWD TIRE FAIRINGS, REAR 15

ATM PRESS= 101.3 KPA TEMP= 26.42 C Density= 1.177 Kg/m3
Ref length=0.7225 m Ref Area= 0.08358 m2 QC= 4.32 Kpa
Re= 1.4128 Million

PT	VEL (m/s)	YAW (deg)	CL	CD	CY	CM	CN	CR
01	85.6	-3.08	0.1667	0.3495	-0.2912	-0.0329	-0.0758	-0.0705
02	85.3	-1.55	0.1947	0.3589	-0.1736	-0.0364	-0.0351	-0.0460
03	85.2	-0.02	0.1316	0.3426	0.0075	-0.0319	-0.0008	-0.0022
04	85.3	1.52	0.1604	0.3544	0.1901	-0.0342	0.0329	0.0387
05	85.6	3.05	0.1864	0.3476	0.3115	-0.0357	0.0940	0.0692
06	85.4	6.10	0.2770	0.3388	0.5449	-0.0307	0.2261	0.1212
07	84.7	9.17	0.4325	0.3777	0.8365	-0.0302	0.3414	0.1921
08	83.6	12.23	0.6302	0.4100	1.1473	-0.0492	0.4456	0.2665

Bus speed(mi/h)	Wind Averaged CD
35.00	0.384
45.00	0.364
55.00	0.353
65.00	0.348
75.00	0.349

BUS TEST

Rupt/Tare/Run 0607/056/060

PROP 2 FRONT, GRIT, C3 MIRRORS (RIGHT FWD,LEFT AFT),REAR VORTEX GEN, REAR 15

ATM PRESS= 101.2 KPA TEMP= 26.22 C Density= 1.177 Kg/m3
Ref length=0.7225 m Ref Area= 0.08358 m2 QC= 4.31 Kpa
Re= 1.4134 Million

PT	VEL (m/s)	YAW (deg)	CL	CD	CY	CM	CN	CR
01	85.6	-3.05	0.1711	0.3514	-0.2743	-0.0469	-0.1035	-0.0647
02	85.2	-1.54	0.1486	0.3507	-0.1524	-0.0400	-0.0440	-0.0399
03	85.1	-0.02	0.1405	0.3414	-0.0001	-0.0387	0.0034	-0.0031
04	85.1	1.51	0.1507	0.3407	0.1457	-0.0389	0.0515	0.0282
05	85.5	3.05	0.1855	0.3435	0.2791	-0.0447	0.1086	0.0599
06	85.5	6.10	0.2725	0.3457	0.5358	-0.0519	0.2305	0.1174
07	84.8	9.17	0.3501	0.3810	0.8358	-0.0554	0.3391	0.1914
08	83.5	12.23	0.6001	0.4058	1.1495	-0.0568	0.4451	0.2650

Bus speed(mi/h)	Wind Averaged CD
35.00	0.384
45.00	0.365
55.00	0.354
65.00	0.348
75.00	0.346

BUS TEST

Rept/Tare/Run 0607/056/061

PROP 2 FRONT, GRIT, C3 MIRRORS(RIGHT FWD,LEFT AFT),MOD DRIP RAILS, REAR 15

ATM PRESS= 101.2 KPA TEMP= 26.31 C Density= 1.177 Kg/m3
Ref length=0.7225 m Ref Area= 0.08358 m2 QC= 4.32 Kpa
Re= 1.4143 Million

PT	VEL (m/s)	YAW (deg)	CL	CD	CY	CM	CN	CR
01	85.7	-3.09	0.1747	0.3492	-0.2936	-0.0462	-0.1020	-0.0718
02	85.2	-1.55	0.1450	0.3440	-0.1547	-0.0431	-0.0477	-0.0410
03	85.1	-0.02	0.1363	0.3370	-0.0010	-0.0397	0.0017	-0.0038
04	85.1	1.51	0.1461	0.3376	0.1925	-0.0399	0.0506	0.0311
05	85.3	3.05	0.1823	0.3411	0.2993	-0.0472	0.1077	0.0655
06	85.4	6.11	0.2843	0.3430	0.6038	-0.0551	0.2236	0.1434
07	84.4	9.19	0.3930	0.3767	0.9670	-0.0640	0.3321	0.2454
08	83.1	12.27	0.5530	0.3902	1.3627	-0.0734	0.4419	0.3549

Bus speed(mi/h)	Wind Averaged CD
35.00	0.377
45.00	0.361
55.00	0.351
65.00	0.345
75.00	0.344

BUS TEST

Rept/Tare/Run 0607/062/063

PREVOST FRONT, GRIT, PREVOST MIRRORS,STD DRIP RAILS, STD REAR

ATM PRESS= 101.2 KPA TEMP= 26.52 C Density= 1.176 Kg/m3
Ref length=0.7225 m Ref Area= 0.08358 m2 QC= 4.29 Kpa
Re= 1.4079 Million

PT	VEL (m/s)	YAW (deg)	CL	CD	CY	CM	CN	CR
01	85.4	-3.09	-0.0520	0.3860	-0.2750	0.0193	-0.1006	-0.0690
02	85.3	-1.55	-0.0793	0.3830	-0.1305	0.0289	-0.0501	-0.0338
03	85.3	-0.02	-0.0904	0.3837	0.0135	0.0314	0.0012	-0.0036
04	85.2	1.51	-0.0694	0.3793	0.1521	0.0272	0.0510	0.0274
05	83.1	3.05	-0.0410	0.3885	0.2927	0.0158	0.1023	0.0608
06	84.8	6.11	0.0459	0.4666	0.6021	0.0323	0.2005	0.1409
07	83.4	9.18	0.1694	0.5467	0.9279	0.0427	0.2894	0.2208
08	81.4	12.24	0.4077	0.6836	1.2856	0.0376	0.3228	0.3103

Bus speed(mi/h)	Wind Averaged CD
35.00	0.507
45.00	0.476
55.00	0.447
65.00	0.428
75.00	0.415

MCI - 039921

002345
002345

BUS TEST Rept/Tare/Run 0607/064/065

PREVOST FRONT, GRIT, STD DRIP RAILS, STD REAR

ATM PRESS= 101.2 KPA TEMP= 23.26 C Density= 1.189 Kg/m3
Ref length=0.7225 m Ref Area= 0.08358 m2 QC= 4.27 Kpa
Re= 1.4247 Million

PT	VEL (m/s)	YAW (deg)	CL	CD	CY	CM	CN	CR
01	84.8	-3.07	-0.0533	0.3641	-0.2675	0.0151	-0.0986	-0.0656
02	84.7	-1.53	-0.0778	0.3556	-0.1237	0.0180	-0.0515	-0.0350
03	84.5	-0.02	-0.0869	0.3529	0.0124	0.0201	-0.0014	-0.0024
04	84.6	1.51	-0.0677	0.3510	0.1522	0.0161	0.0500	0.0284
05	84.7	3.05	-0.0414	0.3643	0.2967	0.0100	0.1004	0.0653
06	84.2	6.11	0.0415	0.4366	0.6006	0.0211	0.2003	0.1397
07	82.8	9.18	0.1751	0.5290	0.9231	0.0367	0.2869	0.2183
08	80.8	12.24	0.4110	0.6654	1.2860	0.0260	0.3163	0.3084

Bus speed(mi/h)	Wind Averaged CD
35.00	0.513
45.00	0.450
55.00	0.418
65.00	0.399
75.00	0.386

BUS TEST Rept/Tare/Run 0607/064/066

PREVOST FRONT, GRIT, STD DRIP RAILS, STD REAR

ATM PRESS= 101.2 KPA TEMP= 24.05 C Density= 1.185 Kg/m3
Ref length=0.7225 m Ref Area= 0.08358 m2 QC= 1.46 Kpa
Re= 0.8312 Million

PT	VEL (m/s)	YAW (deg)	CL	CD	CY	CM	CN	CR
01	49.7	-0.03	-0.1197	0.4146	0.0109	0.0357	-0.0087	-0.0055
02	56.5	-0.03	-0.1045	0.3656	0.0214	0.0260	-0.0010	-0.0006
03	63.0	-0.03	-0.1003	0.3573	0.0224	0.0197	-0.0008	-0.0007
04	68.1	-0.03	-0.0966	0.3550	0.0226	0.0205	-0.0001	0.0001
05	76.6	-0.03	-0.0912	0.3502	0.0167	0.0213	-0.0003	-0.0015
06	82.7	-0.03	-0.0879	0.3505	0.0126	0.0200	-0.0014	-0.0020
07	88.6	-0.03	-0.0841	0.3544	0.0122	0.0221	-0.0017	-0.0026
08	94.3	-0.03	-0.0780	0.3517	0.0089	0.0219	-0.0026	-0.0019

Bus speed(mi/h)	Wind Averaged CD
35.00	0.000
45.00	0.000
55.00	0.000
65.00	0.000
75.00	0.000

BUS TEST Rept/Tare/Run 0607/067/068

PROP #1 FRONT, GRIT, STD DRIP RAILS, C3 STD REAR

ATM PRESS= 101.5 KPA TEMP= 22.26 C Density= 1.196 Kg/m3
Ref length=0.7225 m Ref Area= 0.08358 m2 QC= 1.48 Kpa
Re= 0.8420 Million

PT	VEL (m/s)	YAW (deg)	CL	CD	CY	CM	CN	CR
01	49.7	-0.02	-0.0712	0.3573	0.0153	0.0802	0.0035	-0.0063
02	55.9	-0.02	-0.0714	0.3541	0.0164	0.0759	0.0039	-0.0037
03	63.2	-0.02	-0.0683	0.3485	0.0179	0.0720	0.0048	-0.0030
04	68.5	-0.02	-0.0640	0.3490	0.0176	0.0701	0.0053	-0.0030
05	76.6	-0.02	-0.0587	0.3473	0.0139	0.0694	0.0046	-0.0025
06	80.8	-0.02	-0.0549	0.3451	0.0139	0.0693	0.0045	-0.0027
07	87.5	-0.02	-0.0503	0.3467	0.0098	0.0724	0.0033	-0.0032
08	94.4	-0.02	-0.0451	0.3439	0.0073	0.0730	0.0024	-0.0037

Bus speed(mi/h)	Wind Averaged CD
35.00	0.000
45.00	0.000
55.00	0.000
65.00	0.000
75.00	0.000

BUS TEST Rept/Tare/Run 0607/067/069

PROP #1 FRONT, GRIT, STD DRIP RAILS, C3 STD REAR

ATM PRESS= 101.5 KPA TEMP= 27.37 C Density= 1.176 Kg/m3
Ref length=0.7225 m Ref Area= 0.08358 m2 QC= 4.24 Kpa
Re= 1.3966 Million

PT	VEL (m/s)	YAW (deg)	CL	CD	CY	CM	CN	CR
01	84.9	-3.08	-0.0125	0.3541	-0.2810	0.0618	-0.0932	-0.0694
02	84.9	-1.55	-0.0462	0.3478	-0.1316	0.0699	-0.0464	-0.0379
03	84.9	-0.02	-0.0508	0.3451	0.0106	0.0707	0.0039	-0.0039
04	84.7	1.51	-0.0446	0.3496	0.1541	0.0718	0.0527	0.0278
05	84.7	3.05	0.0020	0.3963	0.3039	0.0640	0.1039	0.0607
06	84.6	6.11	0.1017	0.3645	0.5955	0.0510	0.2066	0.1350
07	83.8	9.18	0.2274	0.3844	0.9115	0.0502	0.3079	0.2103
08	82.5	12.25	0.4086	0.3942	1.2508	0.0376	0.4074	0.3893

Bus speed(mi/h)	Wind Averaged CD
35.00	0.389
45.00	0.376
55.00	0.367
65.00	0.362
75.00	0.360

MCI - 039922

002346

002346

BUS TEST — Rept/Tare/Run 0607/070/071

C3 SMOOTH FRONT, GRIT, STD DRIP RAILS, C3 STD REAR

ATM PRESS= 101.5 KPA
Ref length=0.7225 m

TEMP= 23.07 C
Ref Area= 0.08358 m2
Re= 0.8446 Million

Density= 1.193 Kg/m3
QC= 1.50 Kpa

PT	VEL (m/s)	YAW (deg)	CL	CD	CY	CM	CN	CR
01	50.1	-0.03	-0.0729	0.3692	0.0176	0.0477	0.0061	-0.0049
02	55.9	-0.02	-0.0739	0.3617	0.0102	0.0424	0.0059	-0.0031
03	62.3	-0.02	-0.0727	0.3548	0.0207	0.0414	0.0070	-0.0022
04	68.3	-0.02	-0.0707	0.3555	0.0197	0.0420	0.0066	-0.0022
05	75.2	-0.02	-0.0670	0.3536	0.0160	0.0456	0.0054	-0.0026
06	80.7	-0.02	-0.0645	0.3492	0.0144	0.0464	0.0055	-0.0034
07	87.5	-0.02	-0.0613	0.3500	0.0058	0.0407	0.0039	-0.0043
08	94.3	-0.02	-0.0555	0.3474	0.0058	0.0491	0.0043	-0.0041

Bus speed(mi/h)	Wind Averaged CD
35.00	0.000
45.00	0.000
55.00	0.000
65.00	0.000
75.00	0.000

BUS TEST — Rept/Tare/Run 0607/070/072

C3 SMOOTH FRONT, GRIT, STD DRIP RAILS, C3 STD REAR

ATM PRESS= 101.5 KPA
Ref length=0.7225 m

TEMP= 28.09 C
Ref Area= 0.08358 m2
Re= 1.3901 Million

Density= 1.173 Kg/m3
QC= 4.23 Kpa

PT	VEL (m/s)	YAW (deg)	CL	CD	CY	CM	CN	CR
01	84.9	-3.07	-0.0260	0.3543	-0.2675	0.0380	-0.0886	-0.0668
02	84.9	-1.55	-0.0510	0.3500	-0.1266	0.0451	-0.0422	-0.0305
03	84.7	-0.03	-0.0613	0.3491	0.0097	0.0482	0.0052	-0.0044
04	85.0	1.50	-0.0584	0.3576	0.1469	0.0477	0.0496	0.0265
05	85.3	3.05	-0.0232	0.3623	0.2918	0.0320	0.0997	0.0626
06	84.5	6.11	0.0724	0.3817	0.5931	0.0251	0.1961	0.1339
07	84.2	9.18	0.2040	0.4040	0.9082	0.0311	0.2935	0.2064
08	83.5	12.24	0.3092	0.4278	1.2358	0.0254	0.3823	0.2848

Bus speed(mi/h)	Wind Averaged CD
35.00	0.408
45.00	0.390
55.00	0.380
65.00	0.374
75.00	0.370

002347
002347

APPENDIX 4: DATA PLOTS

The following plots are presented in the order performed. Each yaw run is summarized by plots of drag coefficient, side force coefficient, and yawing moment coefficient, all versus yaw angle. The run designations are coded in the set of 7 numbers at the top of each plot and they are interpreted as a first group of four digits for the test number followed by three digits for the run number. Thus:

060702 = Test 607, Run 26

002348

002348

002348

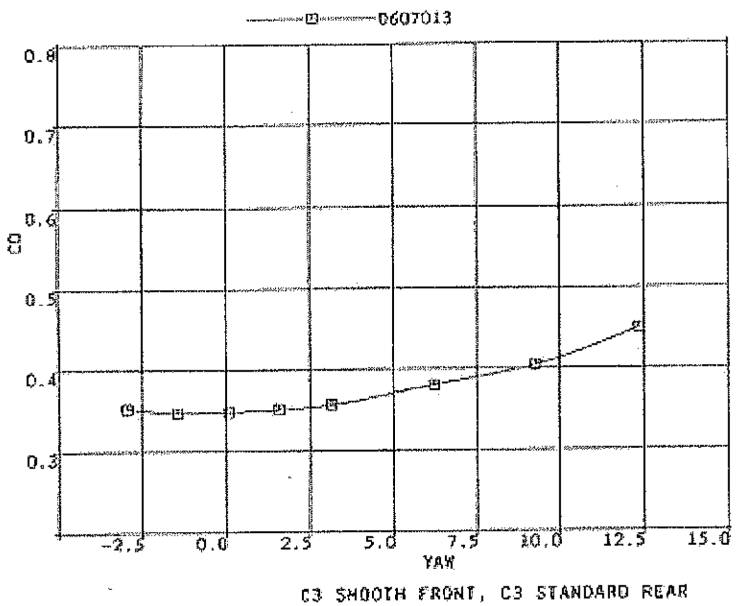

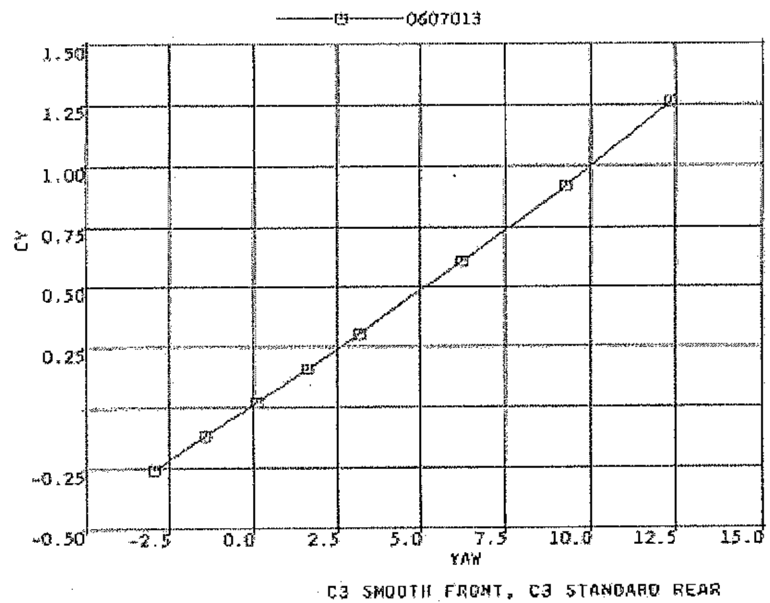

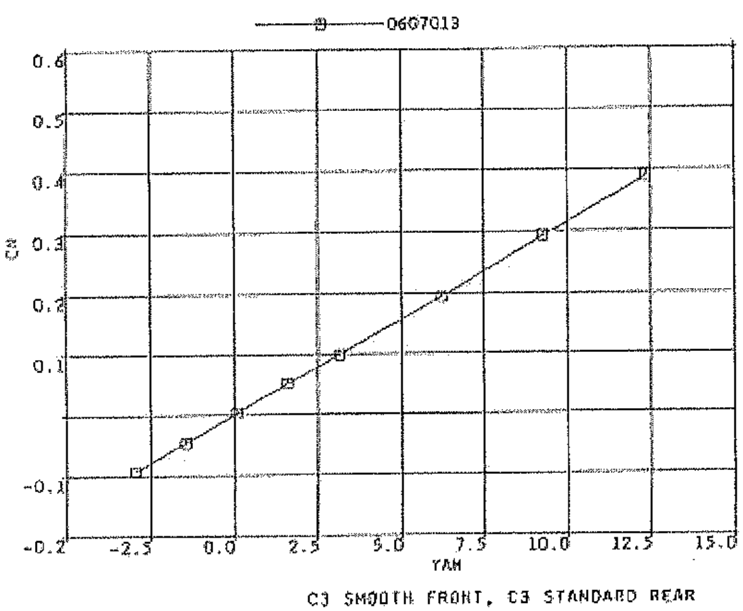

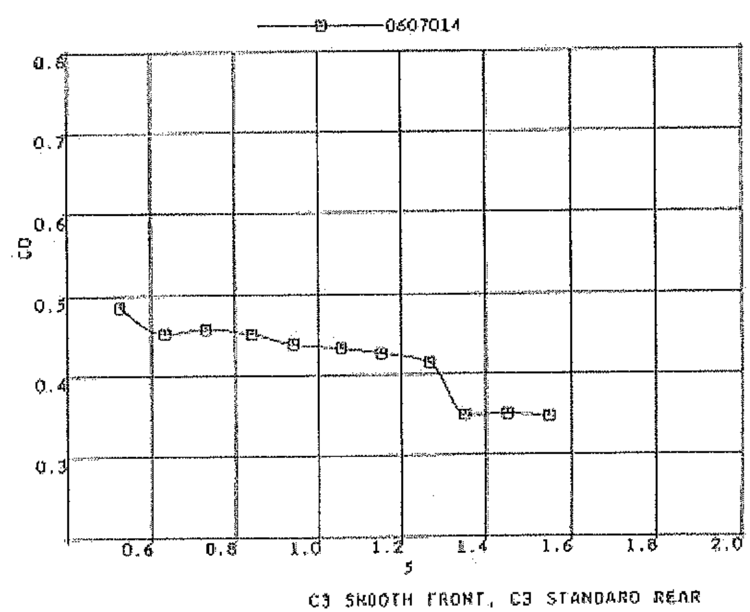

MCI - 039925

002349
002349

002350

002350

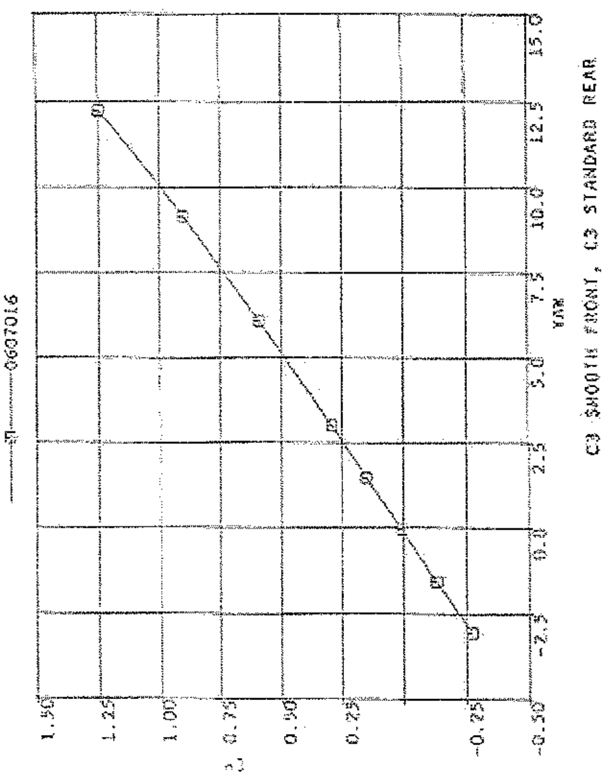

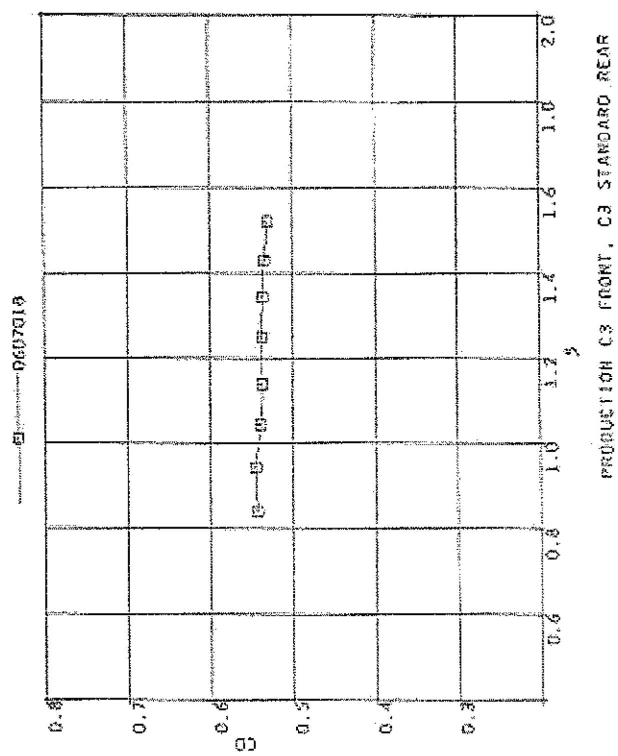

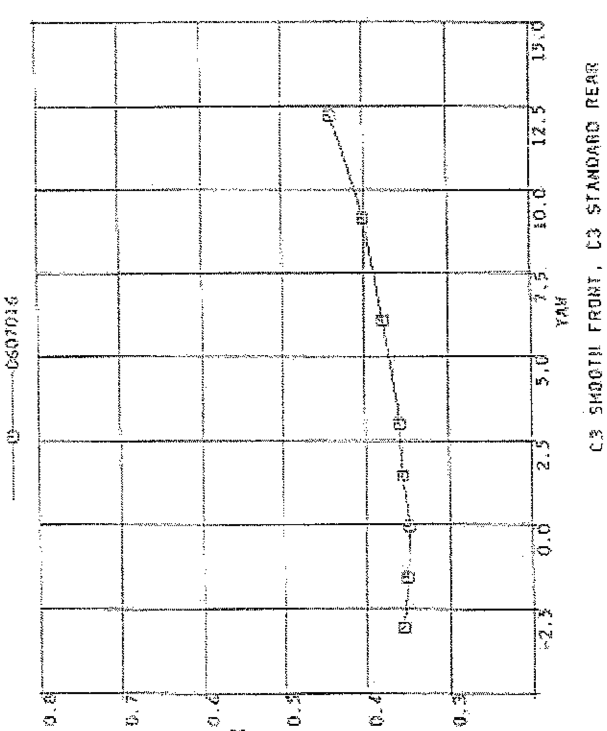

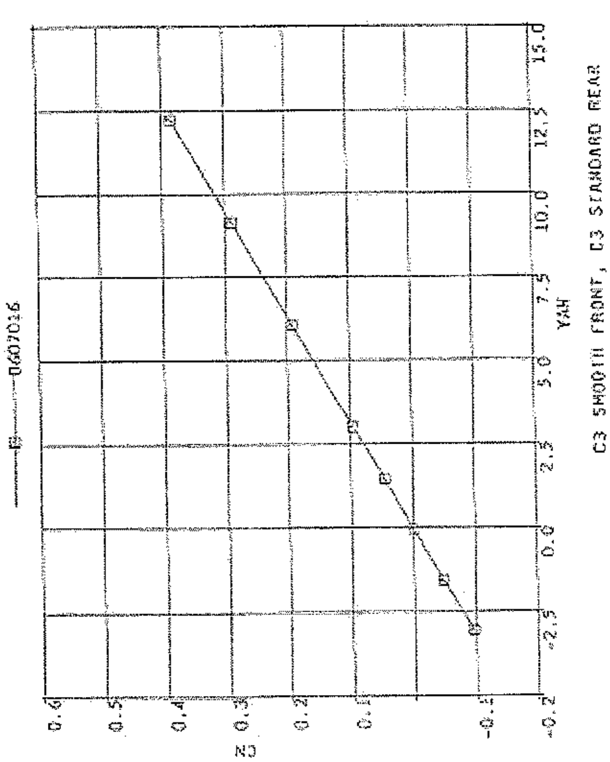

002350

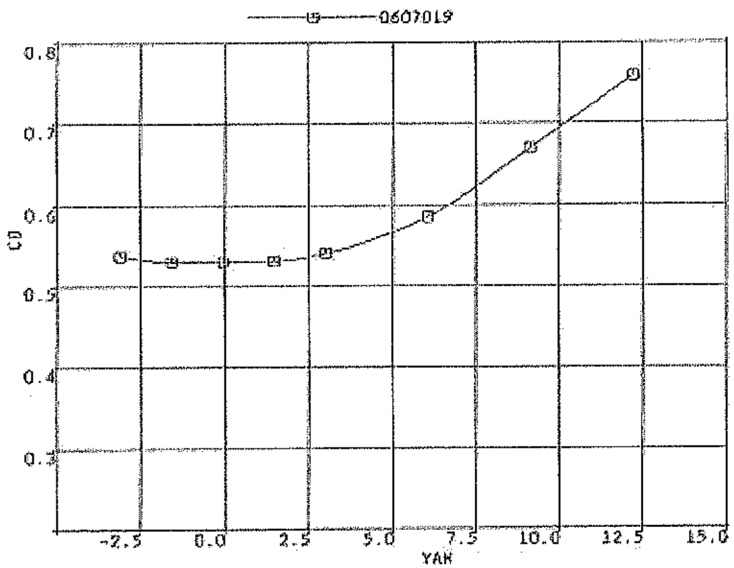

PRODUCTION C3 FRONT, C3 STANDARD REAR

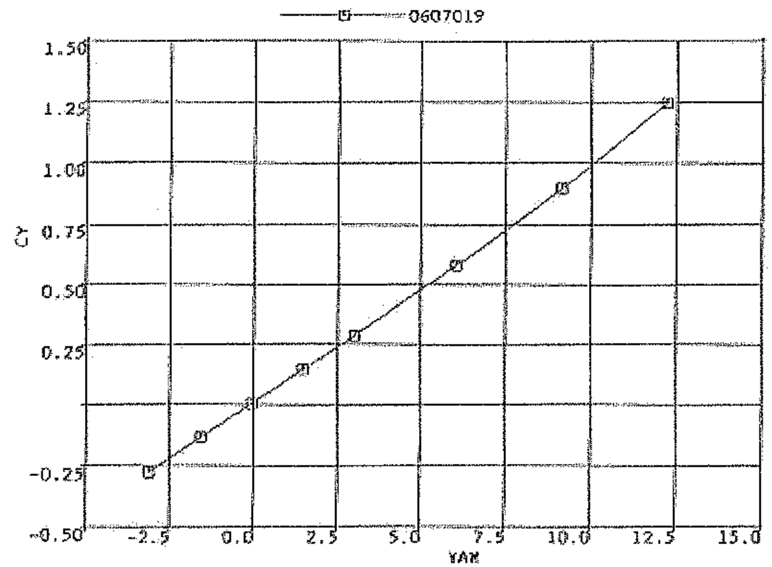

PRODUCTION C3 FRONT, C3 STANDARD REAR

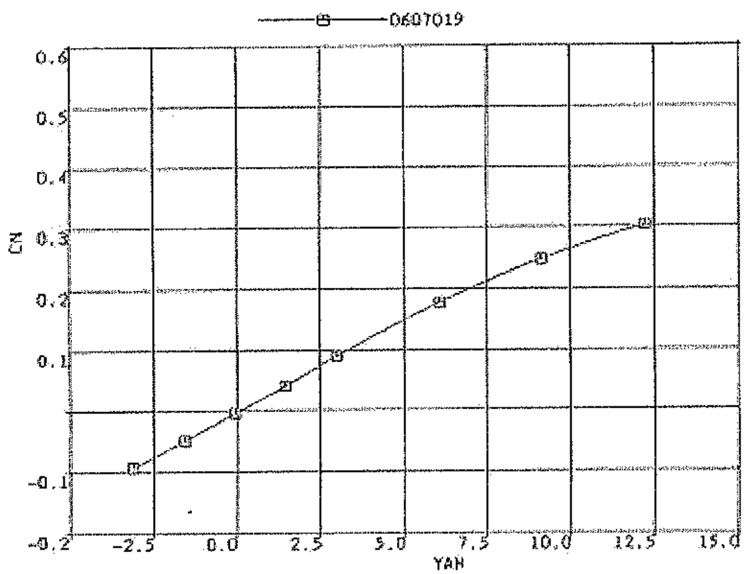

PRODUCTION C3 FRONT, C3 STANDARD REAR

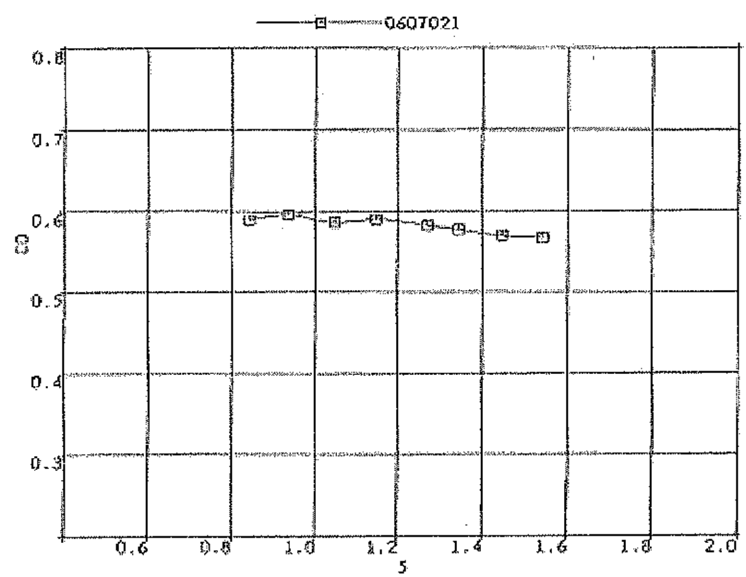

MERCEDES BENZ FRONT, C3 STANDARD REAR

MCI - 039927

002351
002351
002351

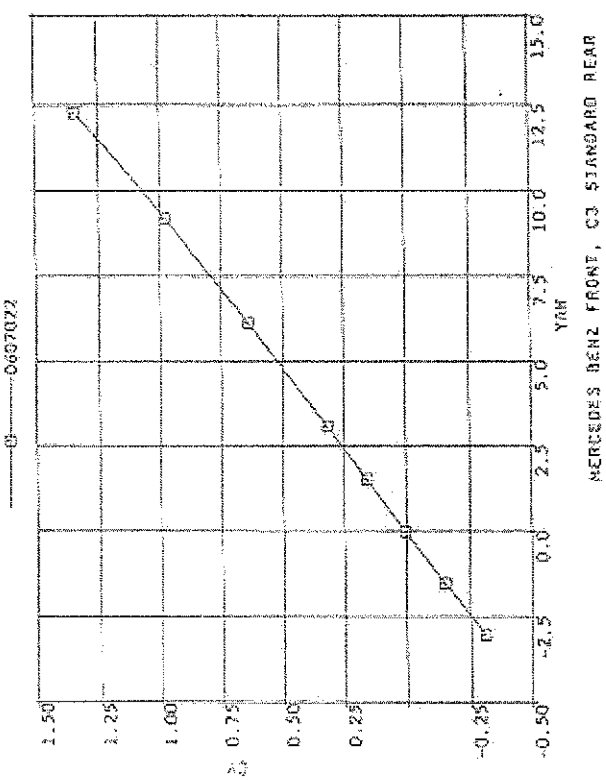

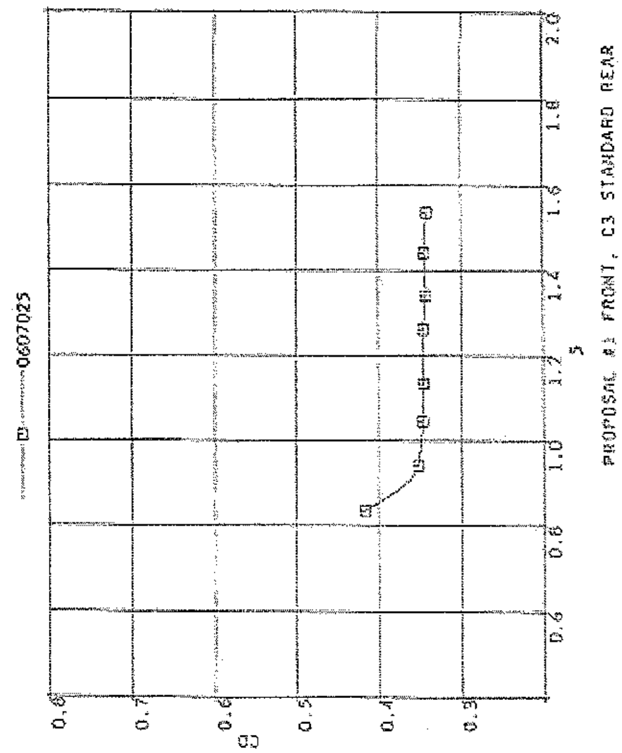

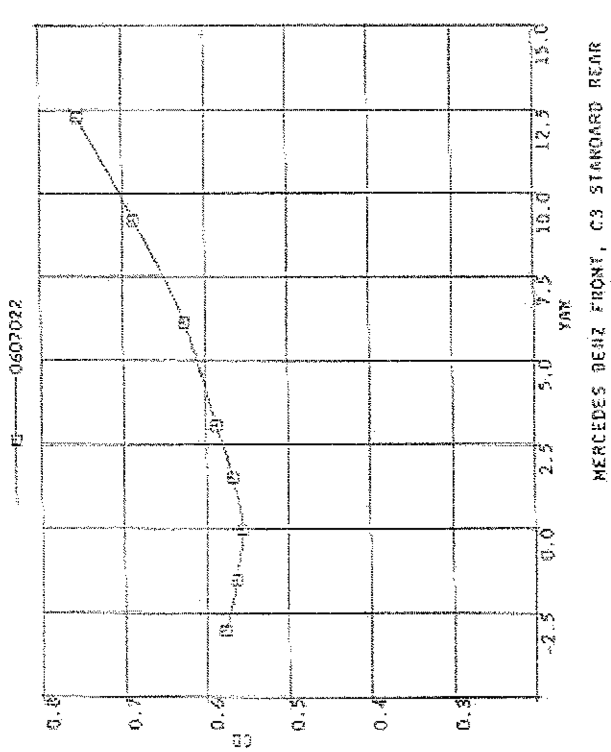

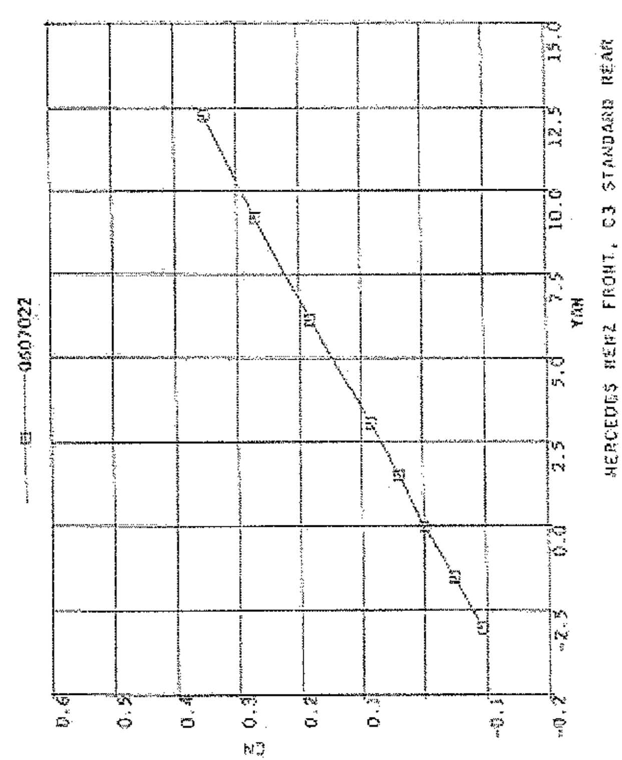

002352

002352

002352

002353

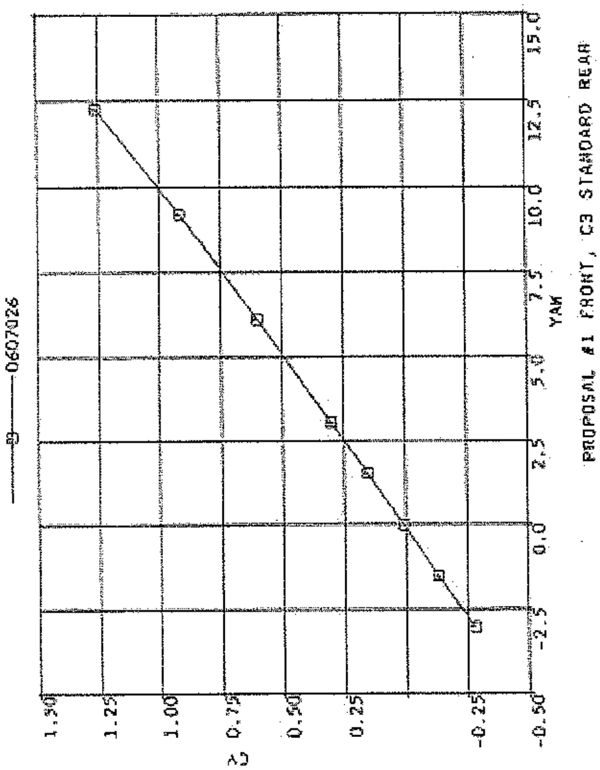

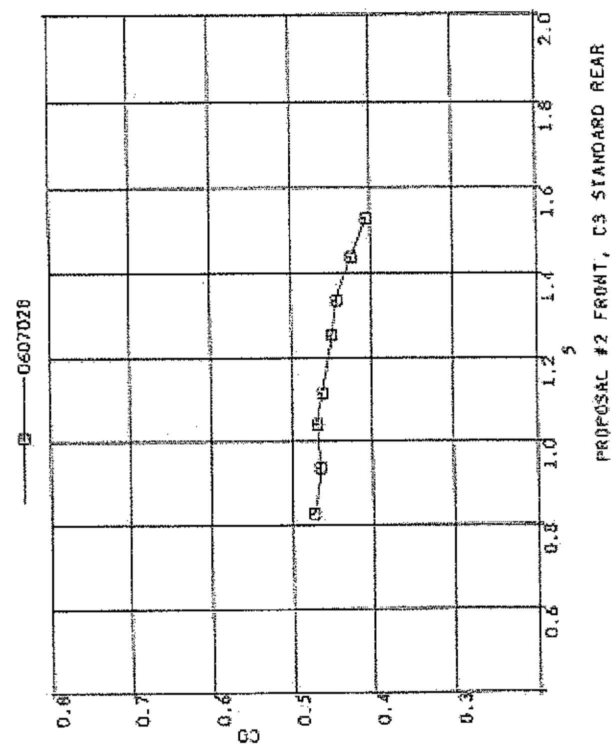

002353

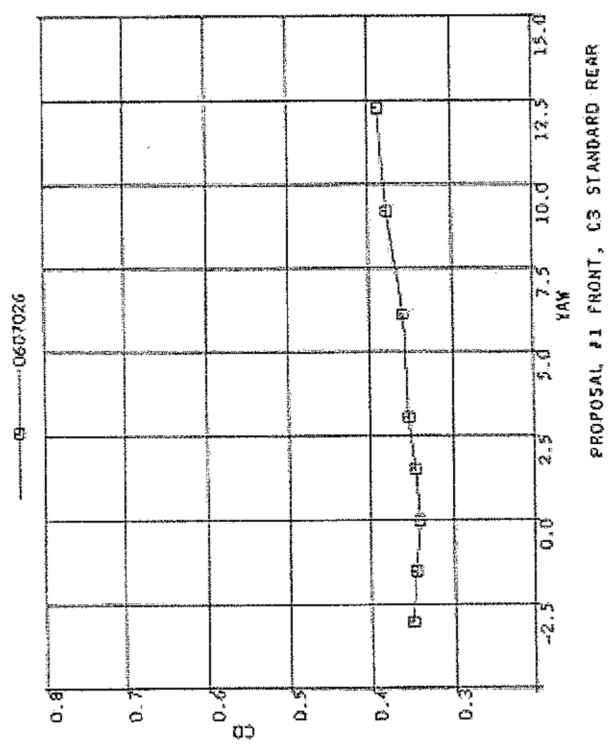

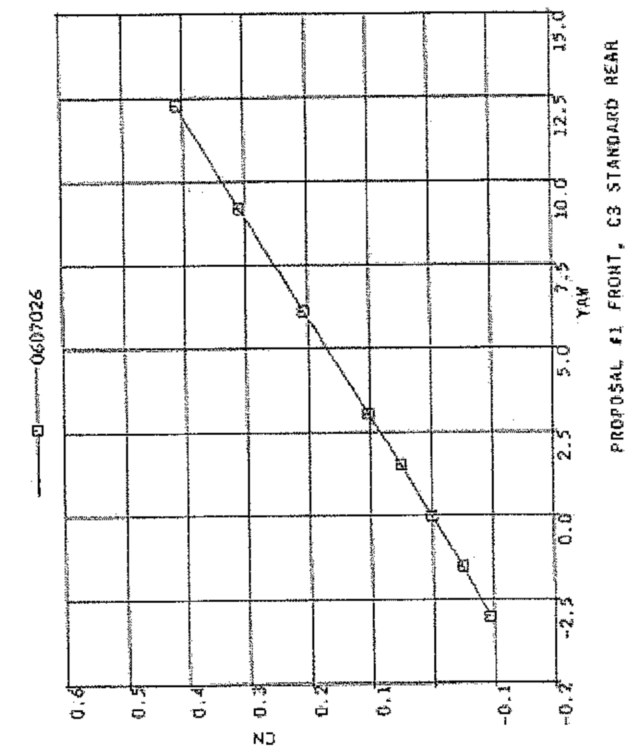

002353

002354

002354

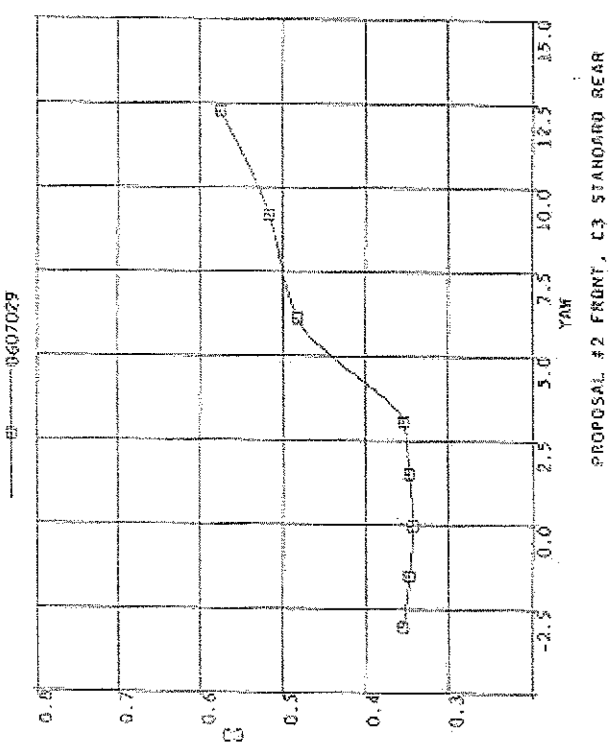

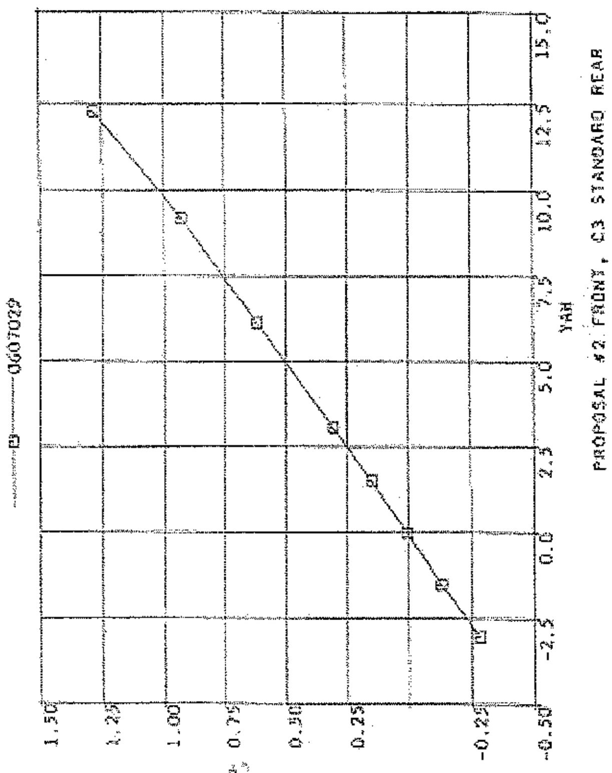

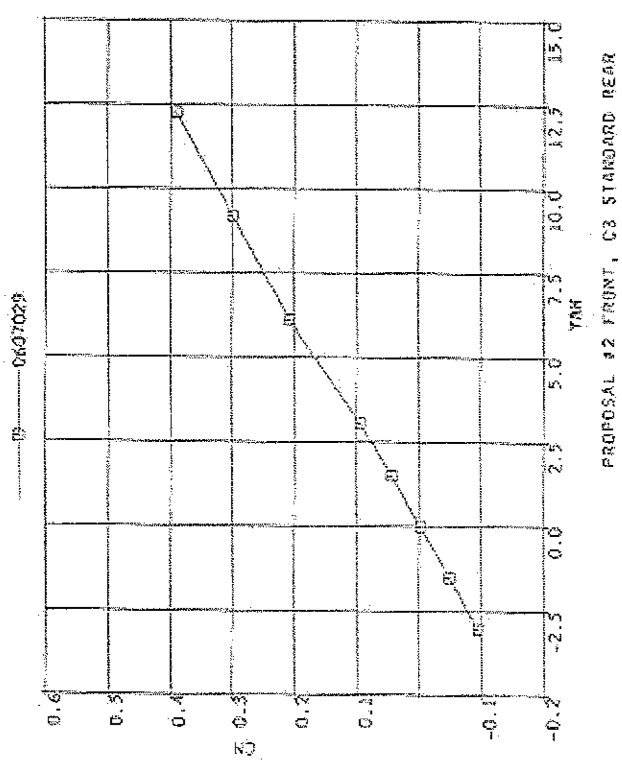

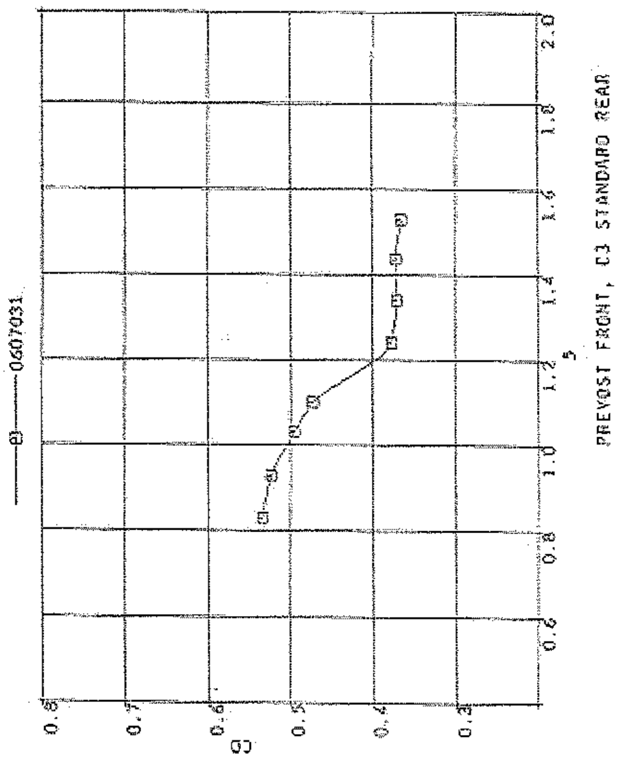

002354

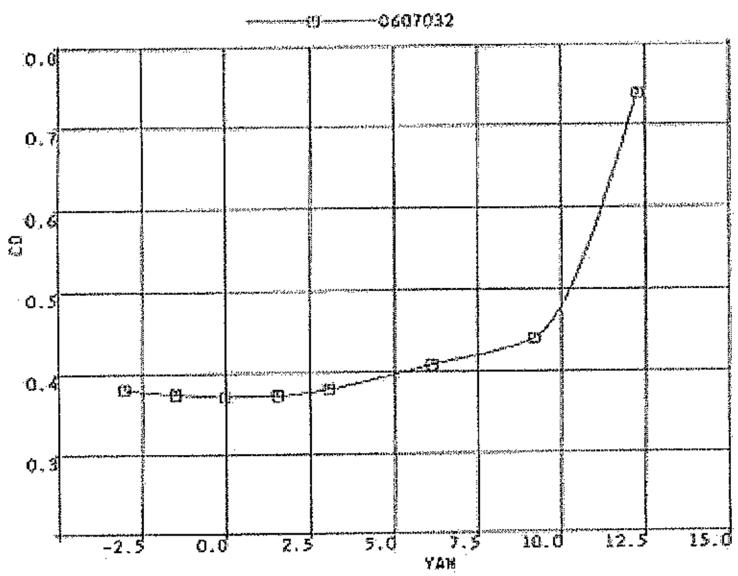

PREVOST FRONT, C3 STANDARD REAR

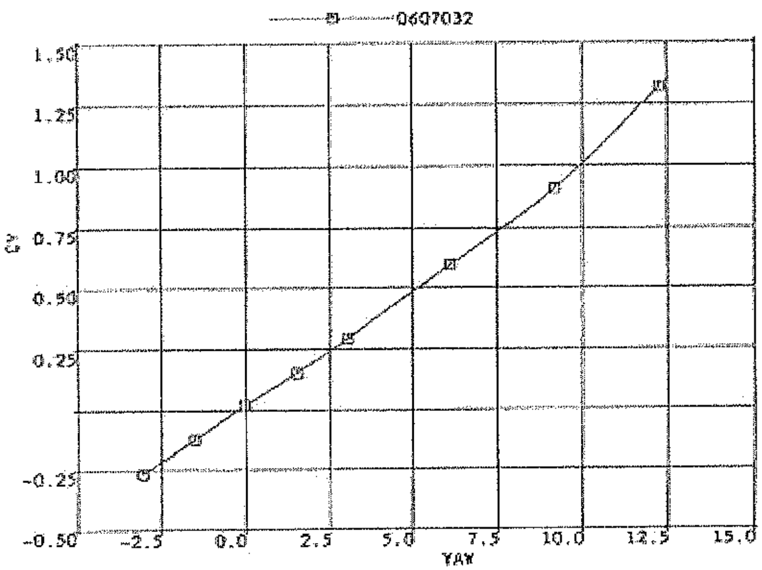

PREVOST FRONT, C3 STANDARD REAR

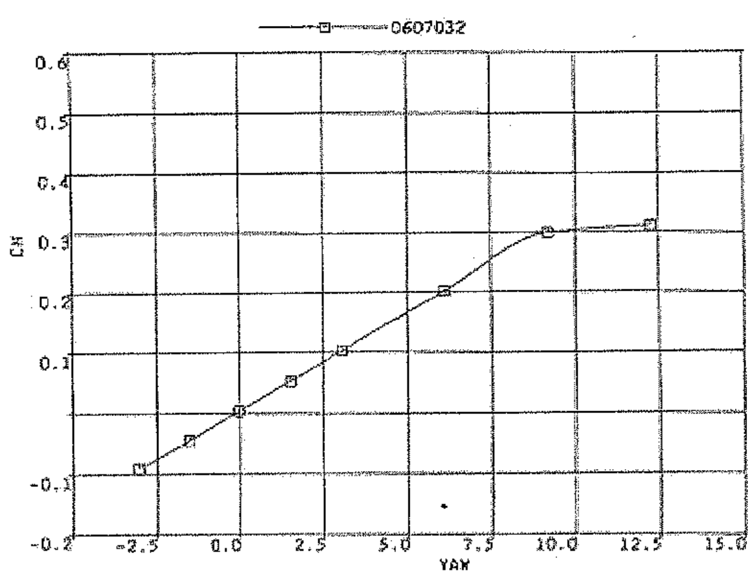

PREVOST FRONT, C3 STANDARD REAR

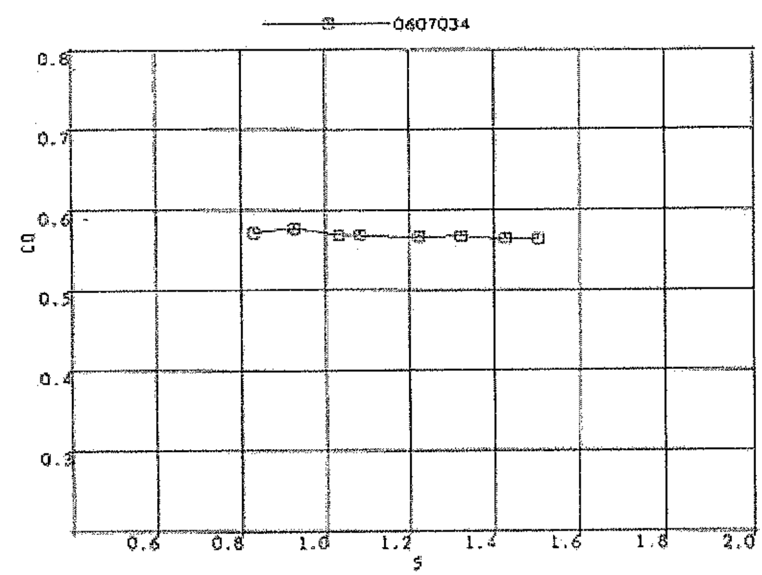

SETRA FRONT, C3 STANDARD REAR

002355
002355

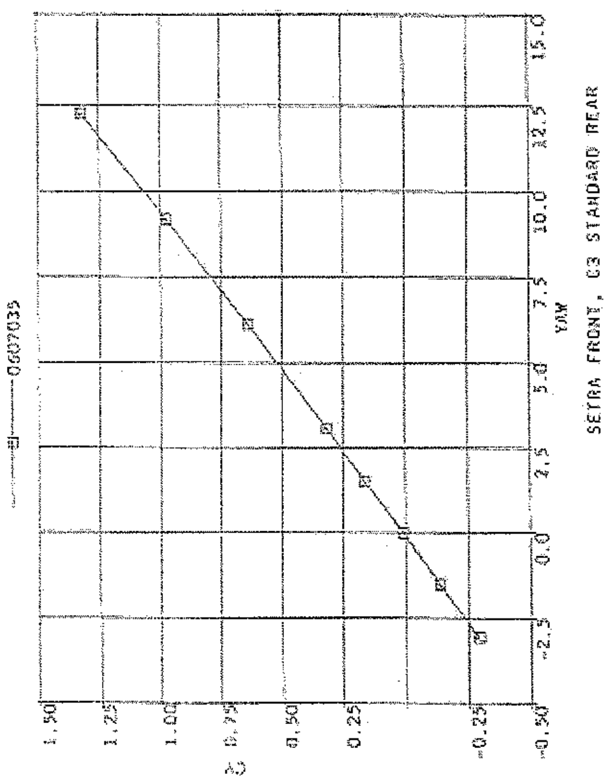

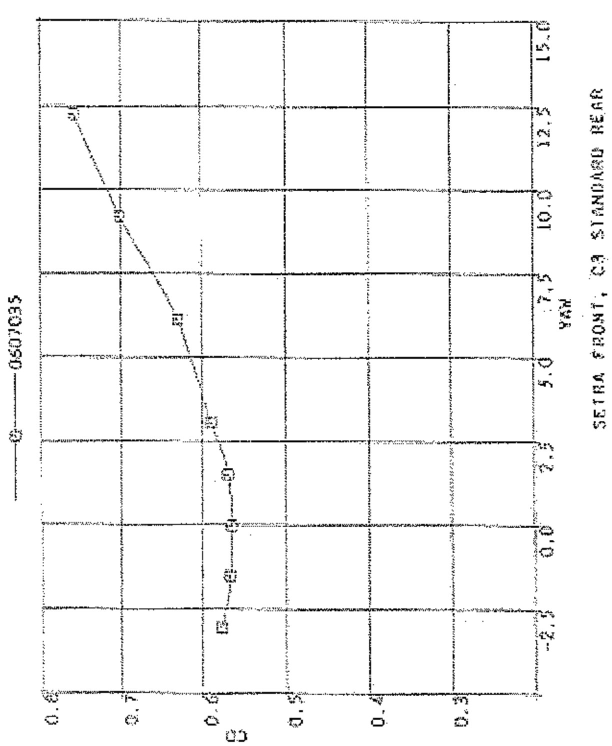

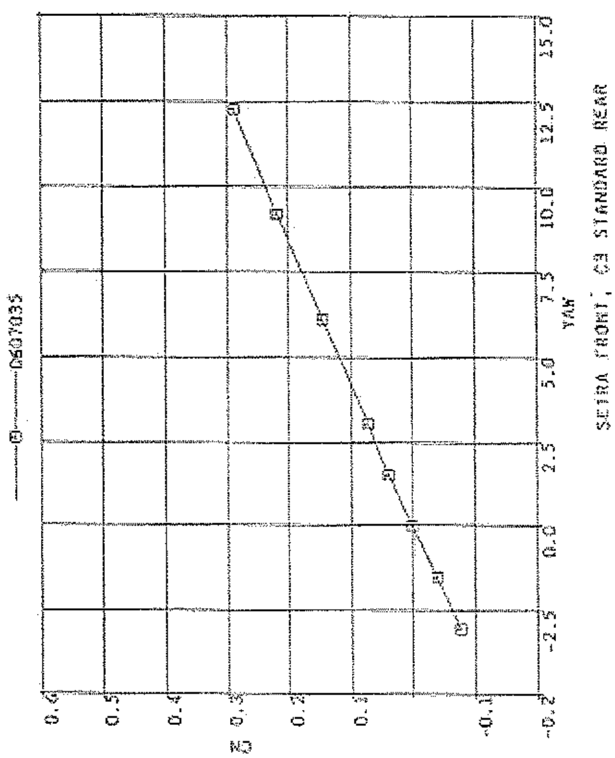

002356

002356

MCI - 039932

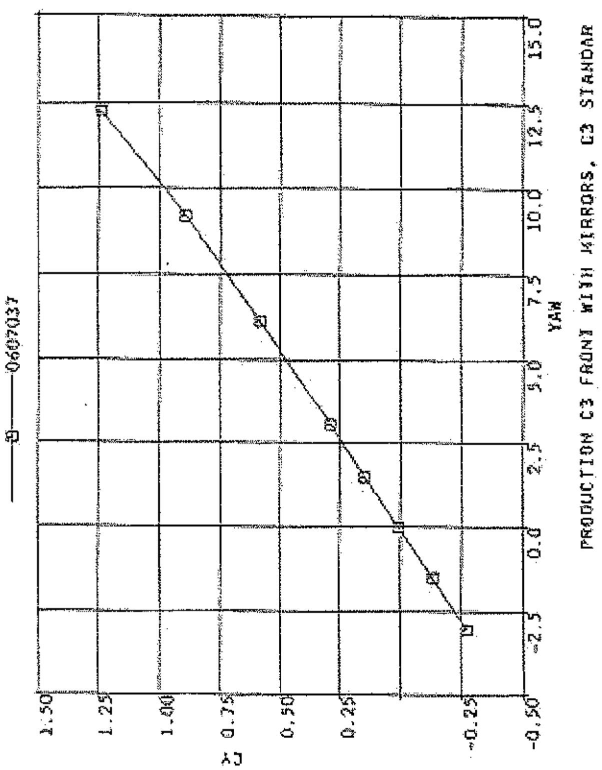

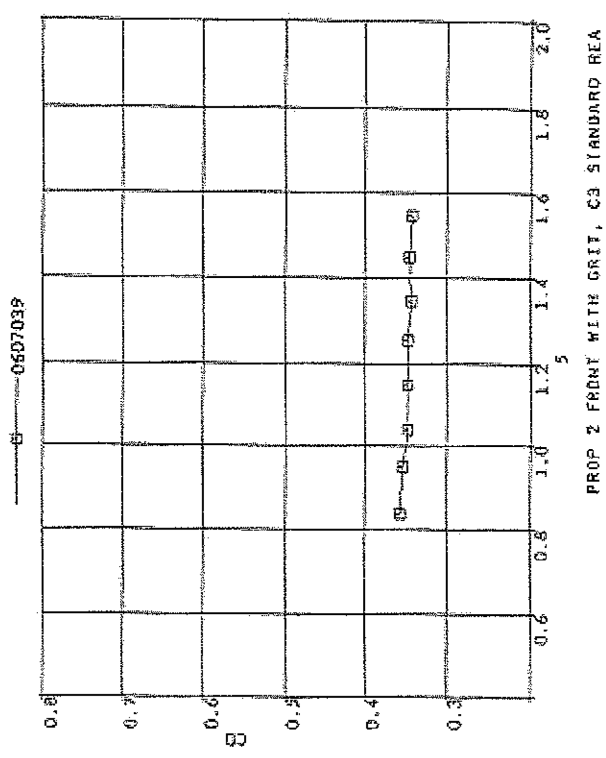

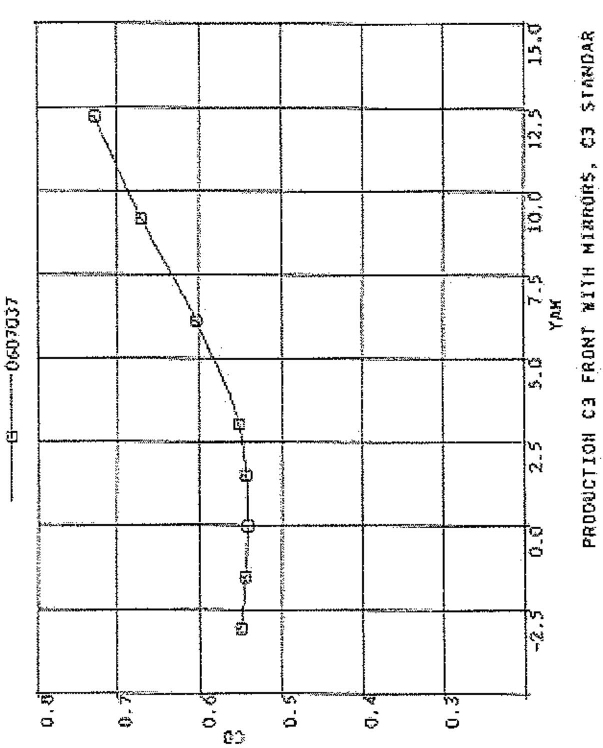

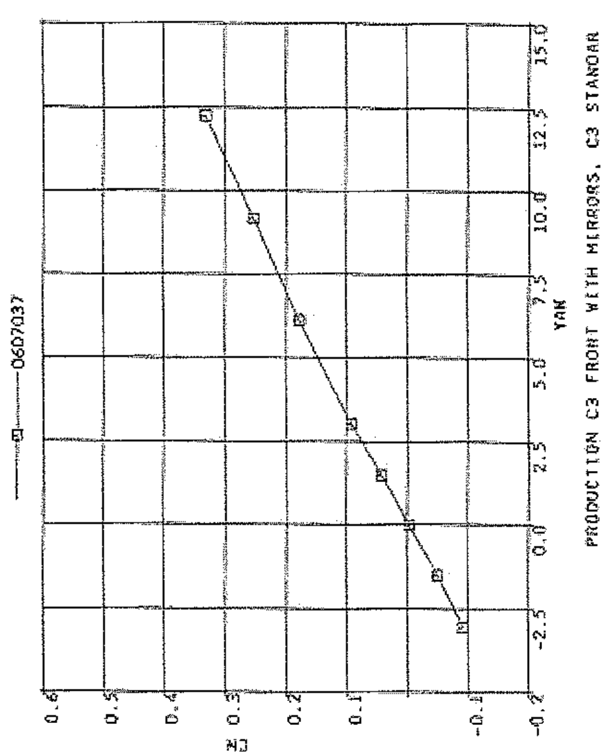

002357

002357

MCI - 039933

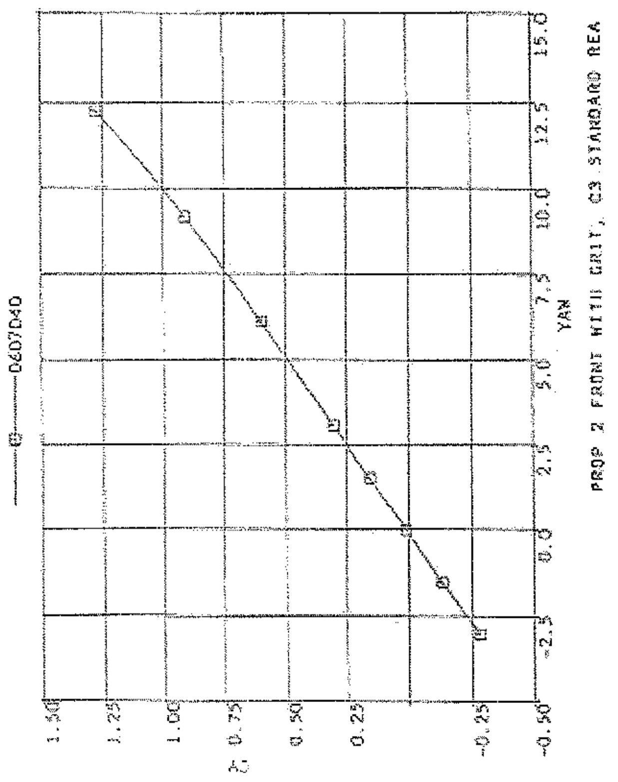

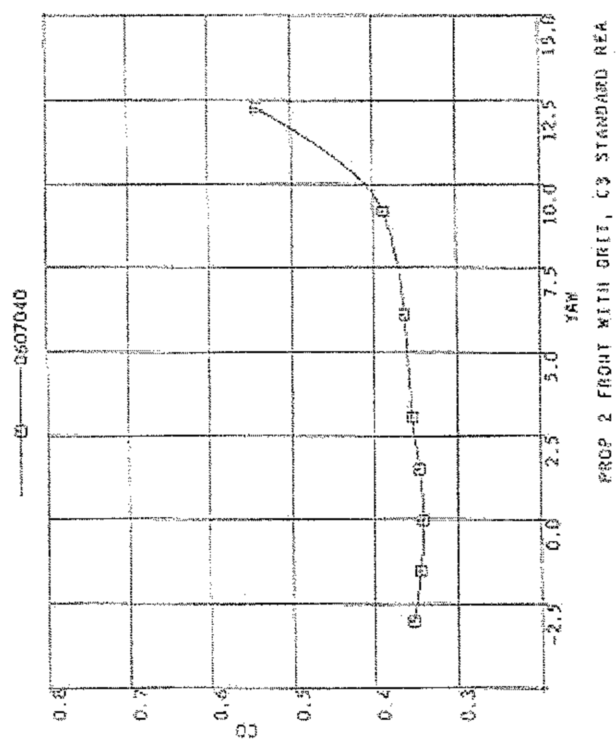

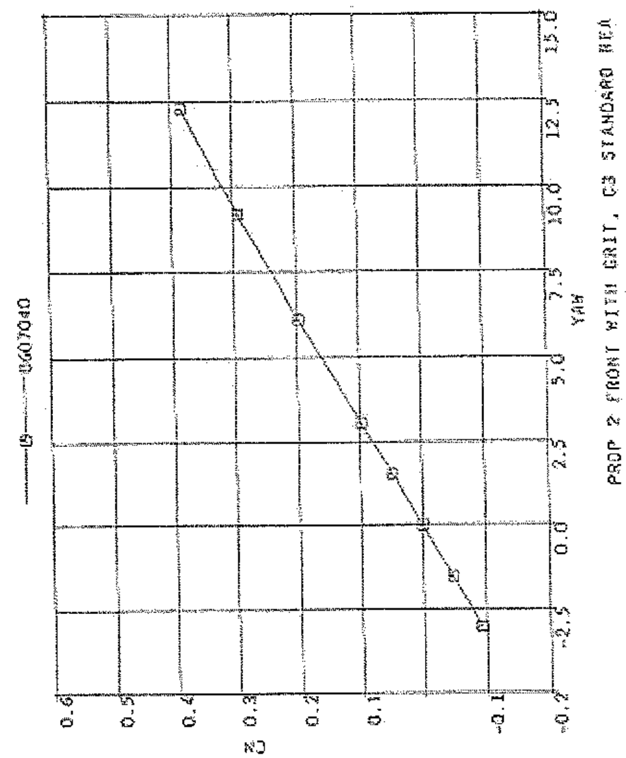

002358

002358

MCI - 039934

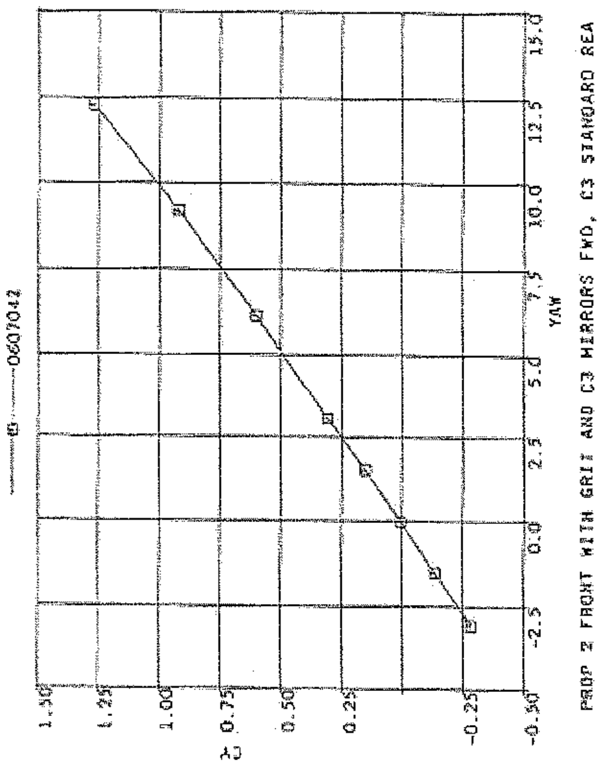

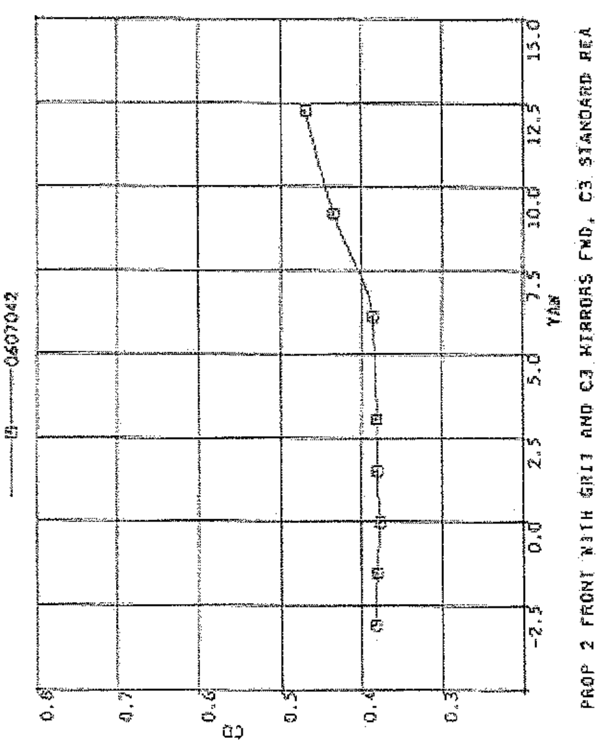

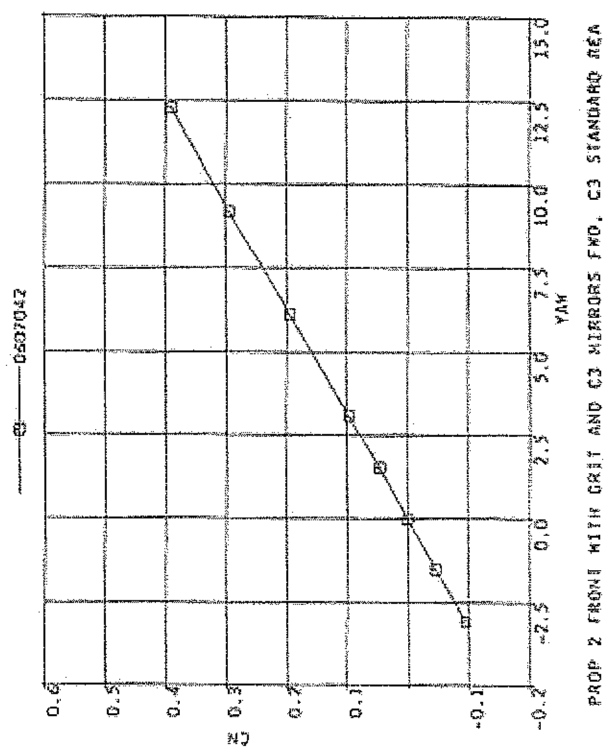

002359

002359

002359

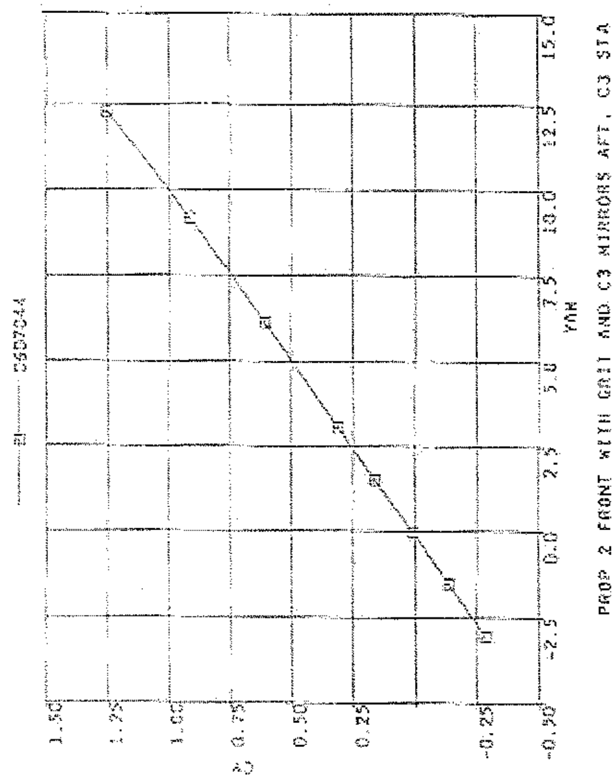

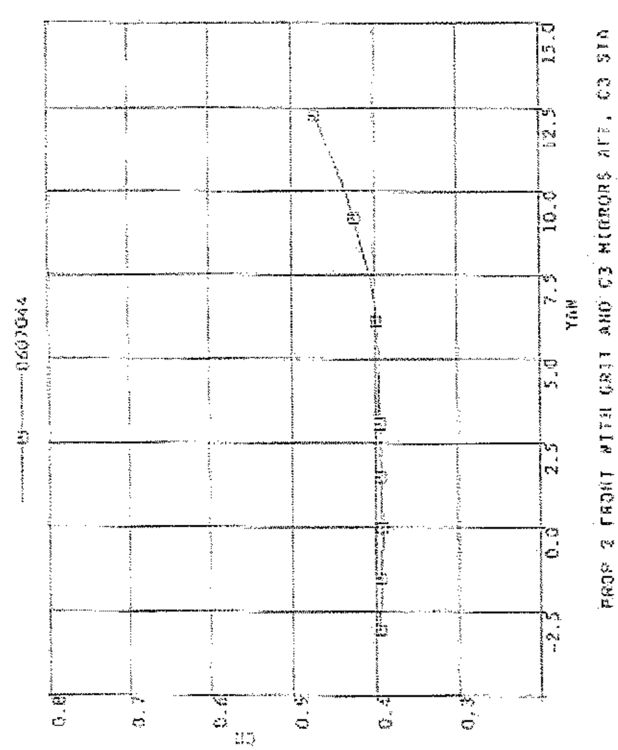

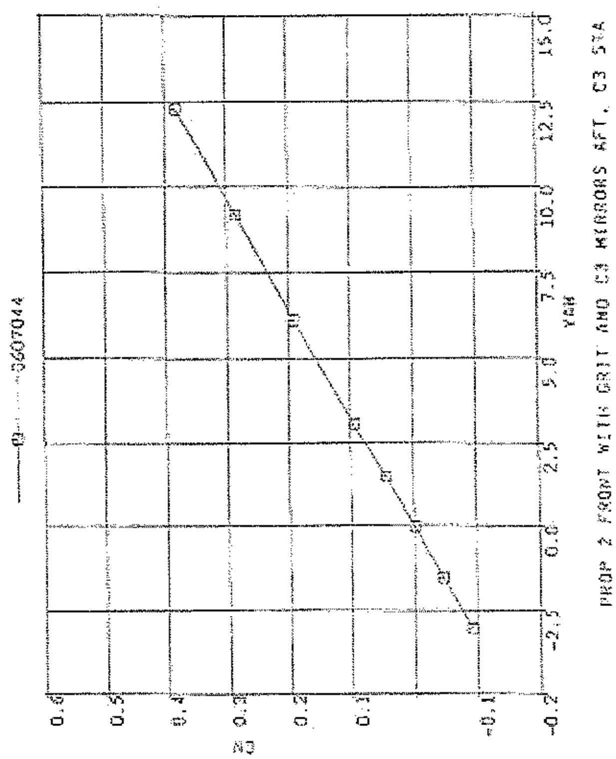

002360

002360

002360

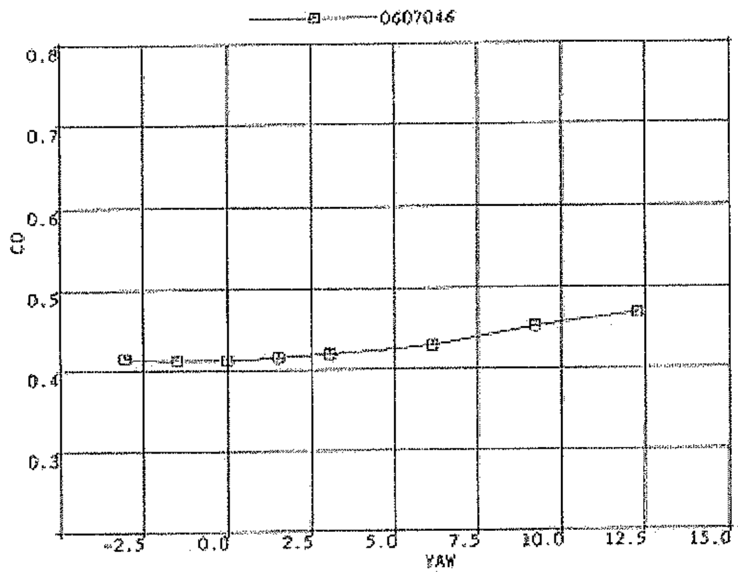

PROP 2 FRONT WITH GRIT AND CETRA MIRRORS, C3 STA

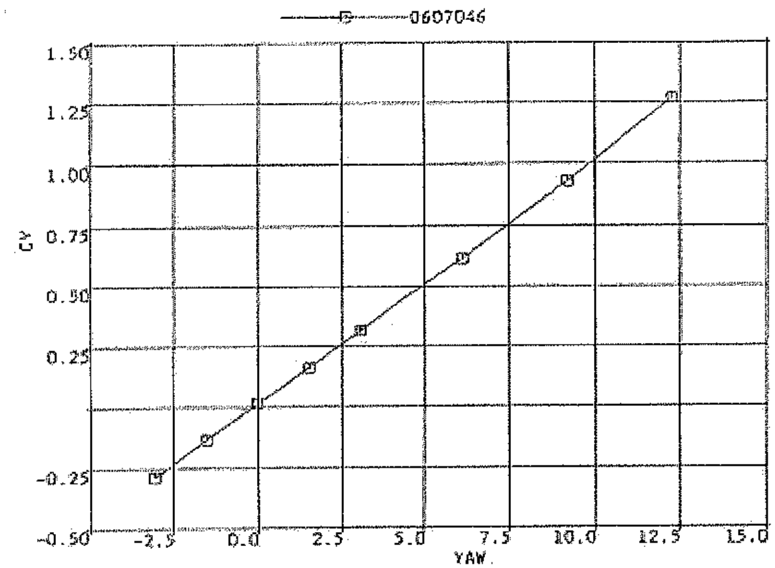

PROP 2 FRONT WITH GRIT AND CETRA MIRRORS, C3 STA

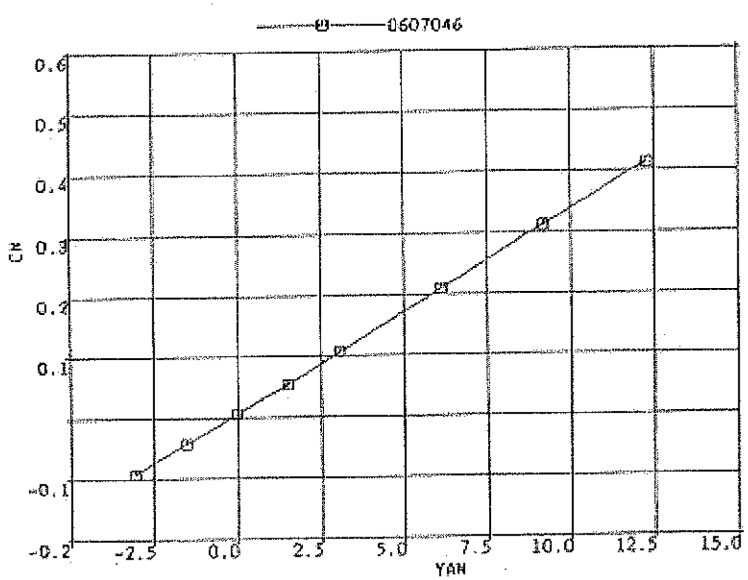

PROP 2 FRONT WITH GRIT AND CETRA MIRRORS, C3 STA

MCI - 039937

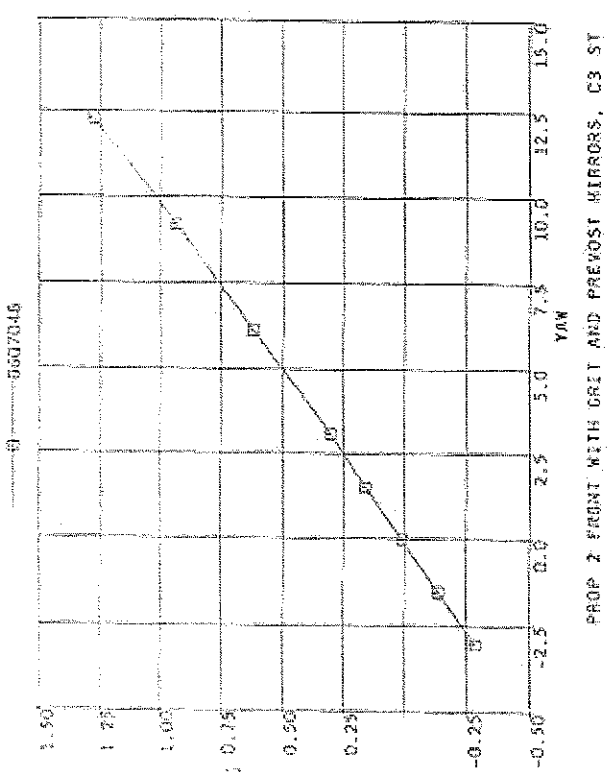

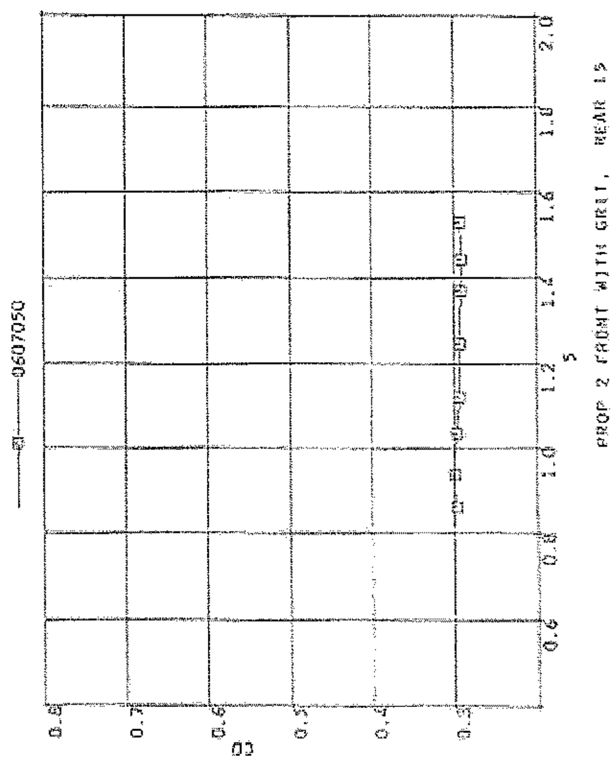

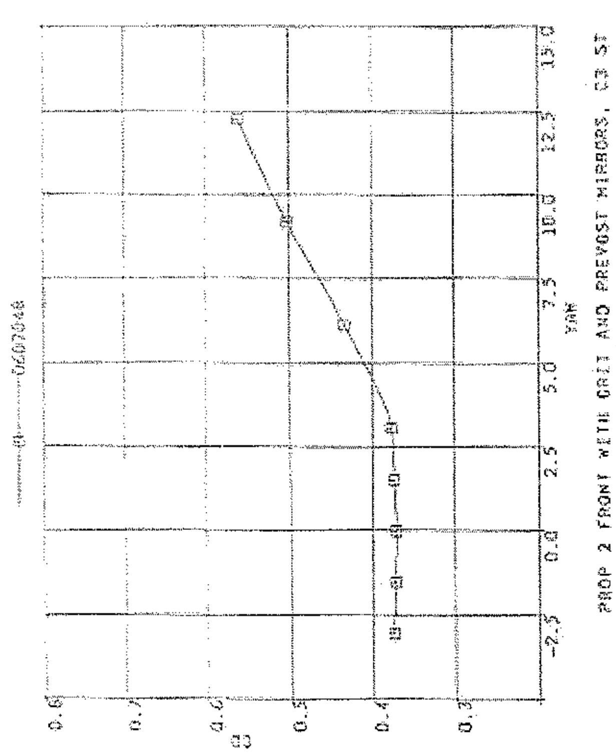

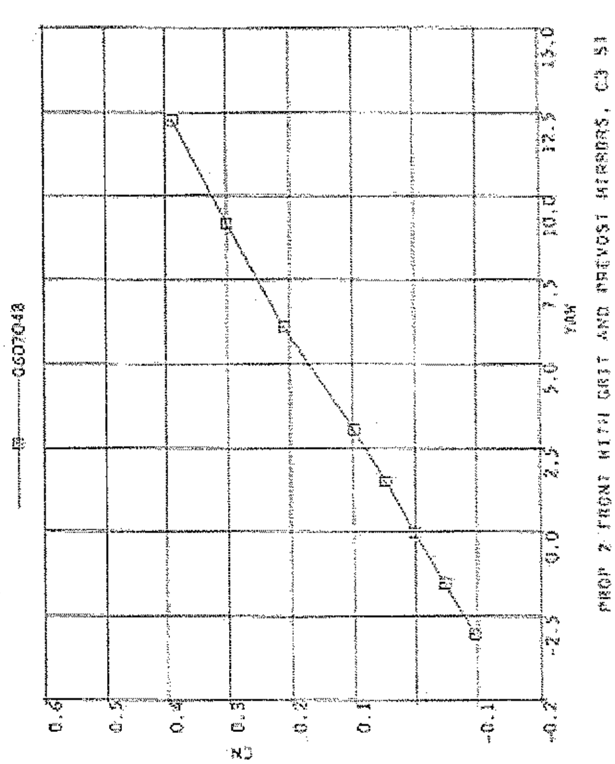

002362

002362

002362

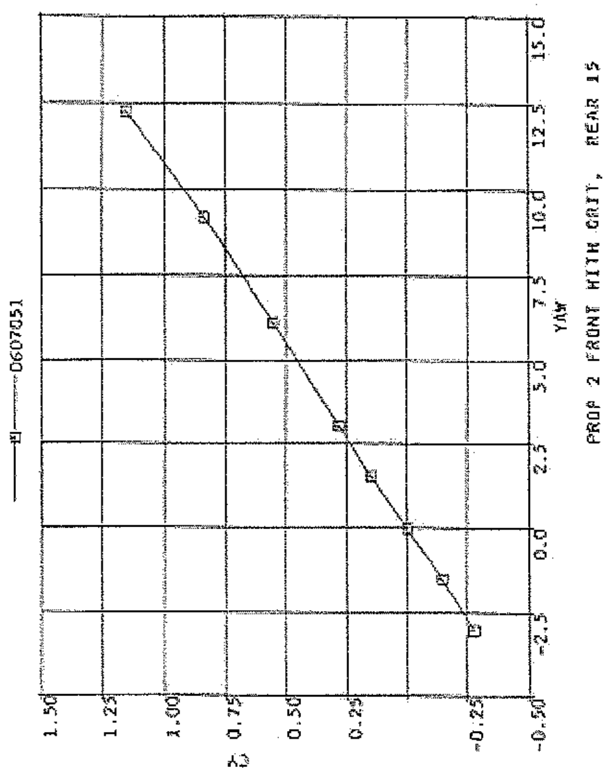

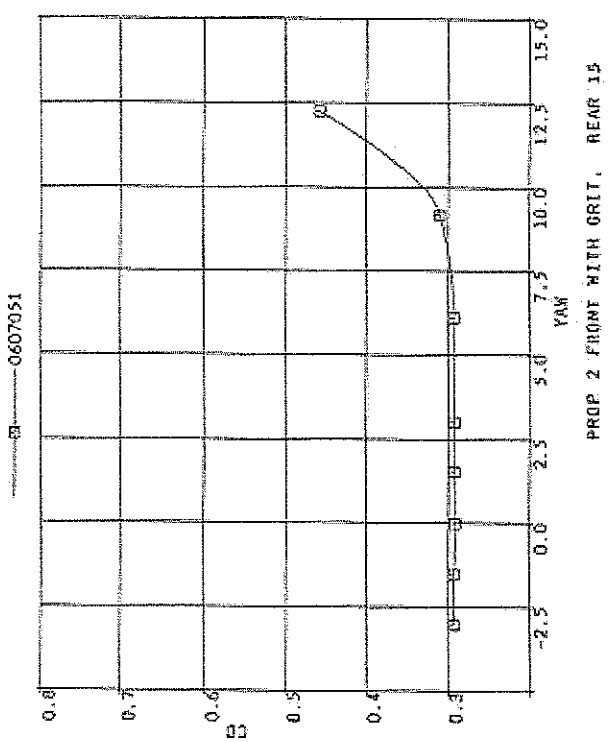

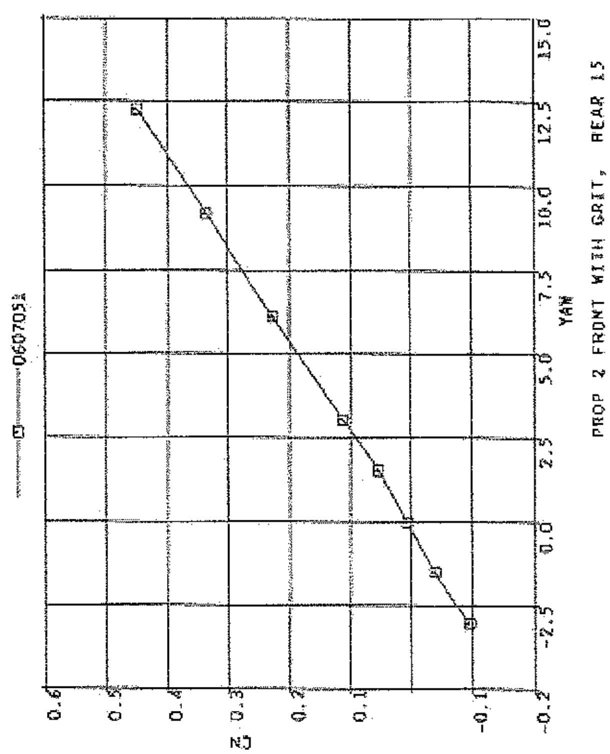

002363

002363

002363

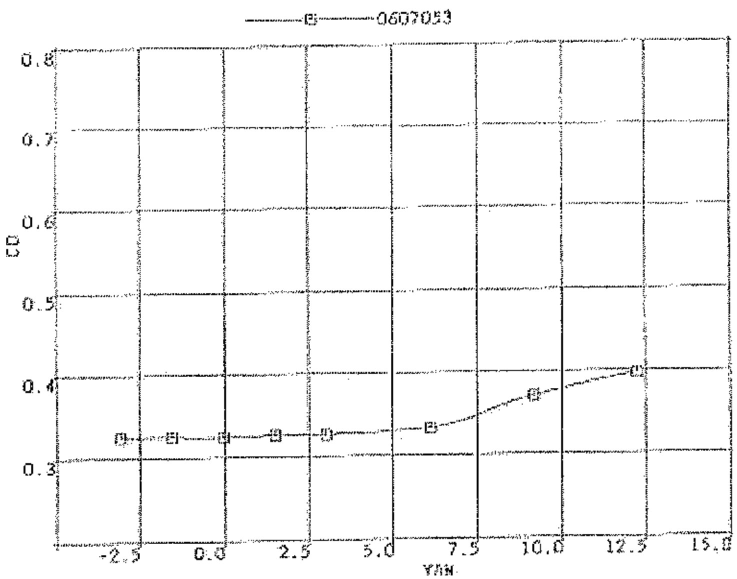

PROP 2 FRONT WITH GRIT AND C3 MIRRORS FWD, R

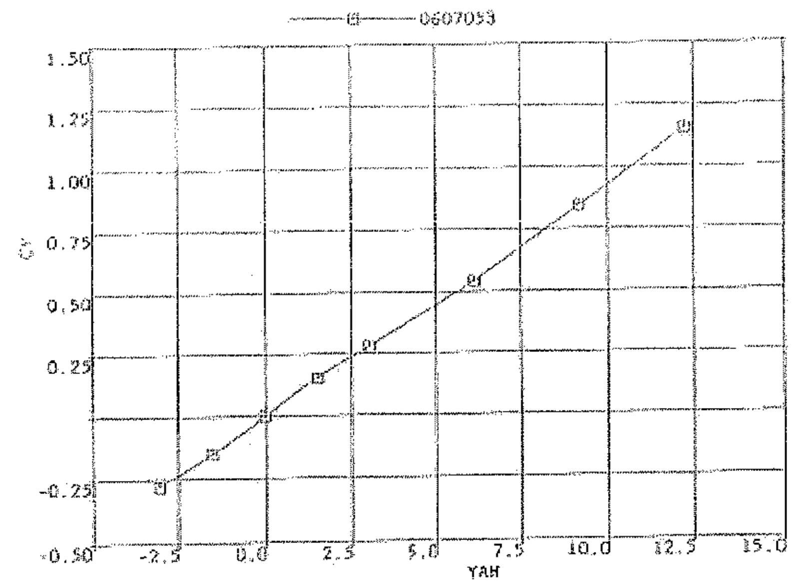

PROP 2 FRONT WITH GRIT AND C3 MIRRORS FWD, R

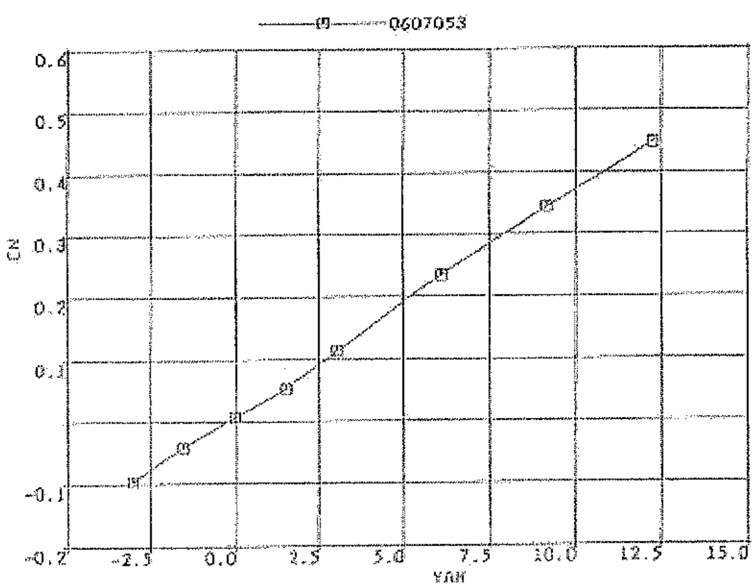

PROP 2 FRONT WITH GRIT AND C3 MIRRORS FWD, R

MCI - 039940

002364
002364
002364

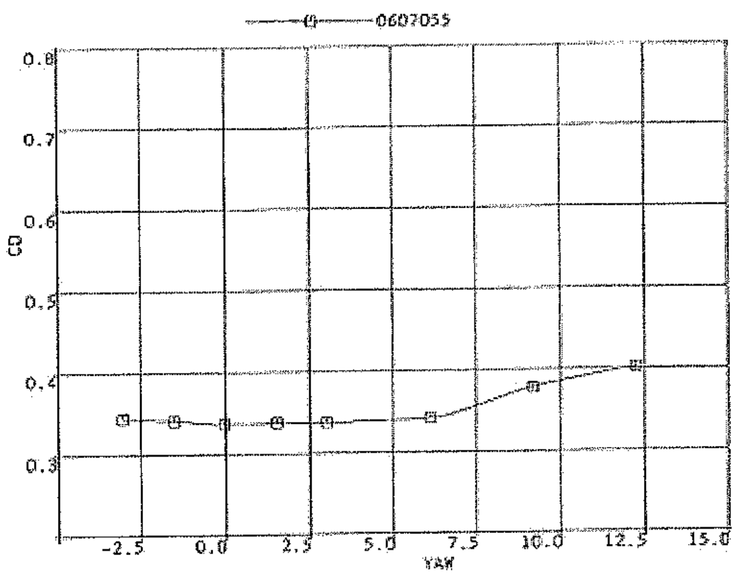

PROP 2 FRONT WITH GRIT AND C3 MIRRORS (RIGHT FWD,LEFT

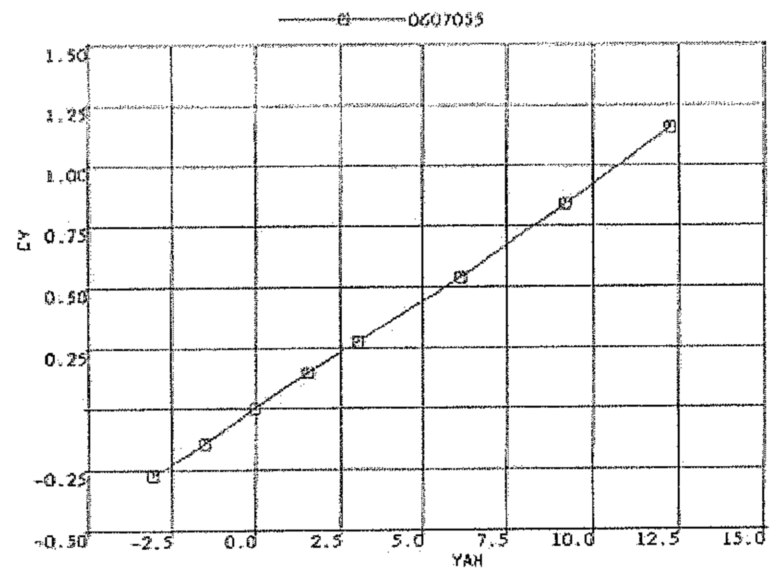

PROP 2 FRONT WITH GRIT AND C3 MIRRORS (RIGHT FWD,LEFT

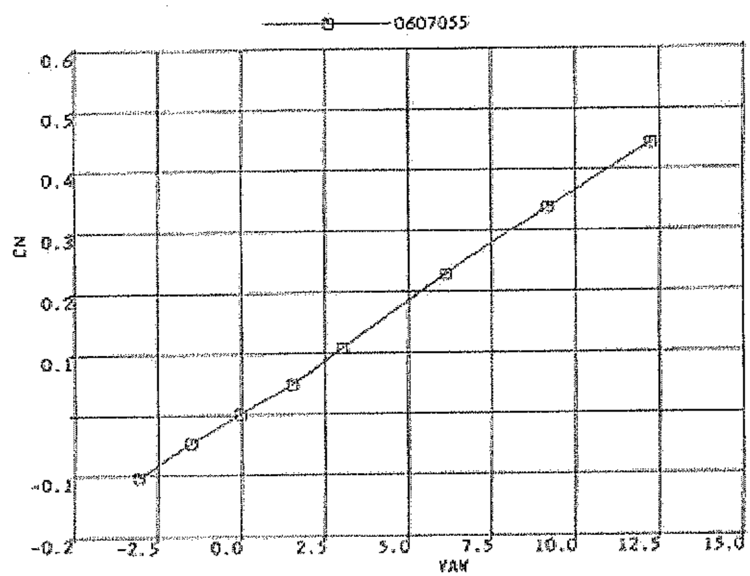

PROP 2 FRONT WITH GRIT AND C3 MIRRORS (RIGHT FWD,LEFT

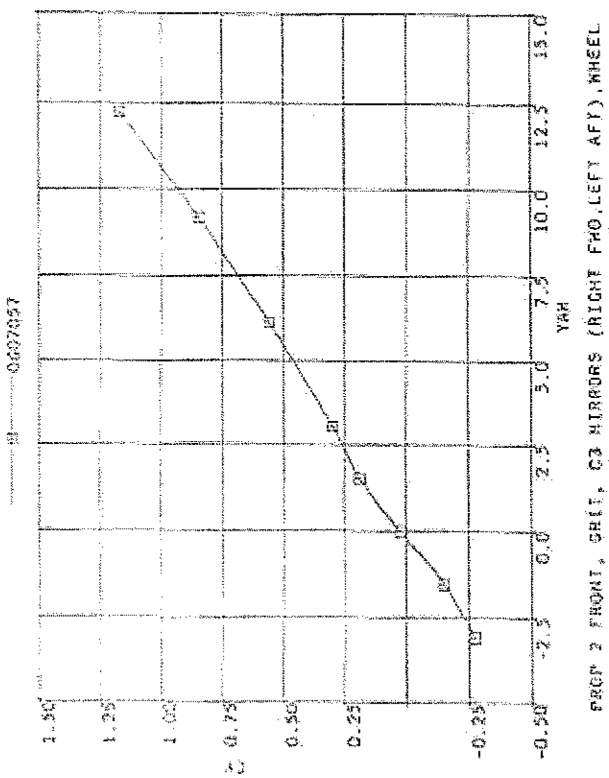

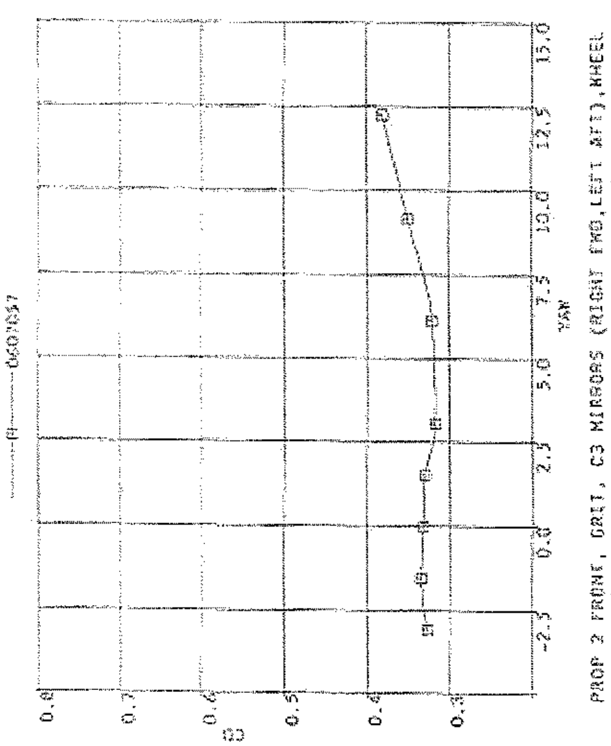

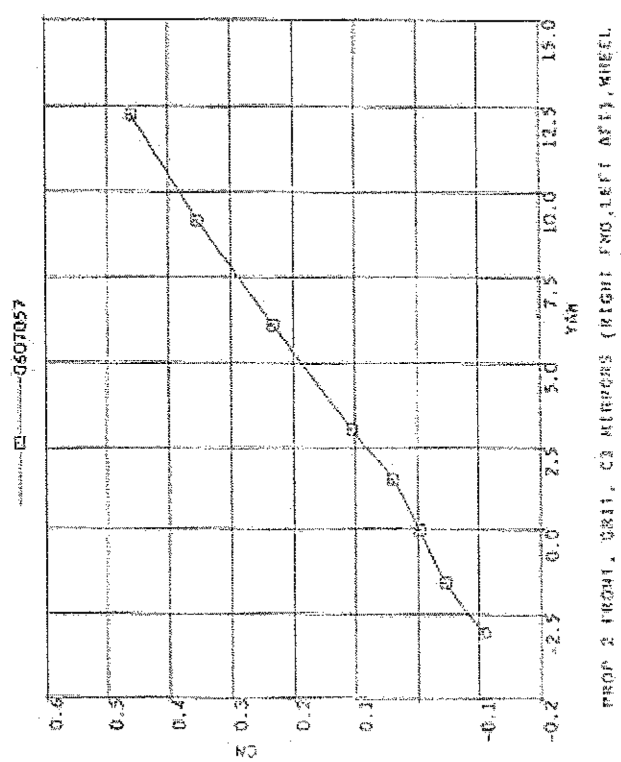

002366

002366

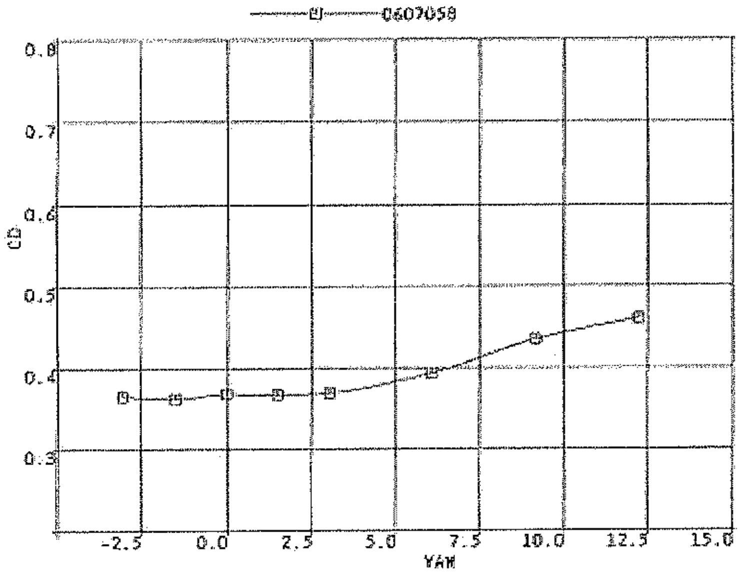

PROP 2 FRONT, GRIT, C3 MIRRORS (RIGHT FWD,LEFT AFT),VERTIC

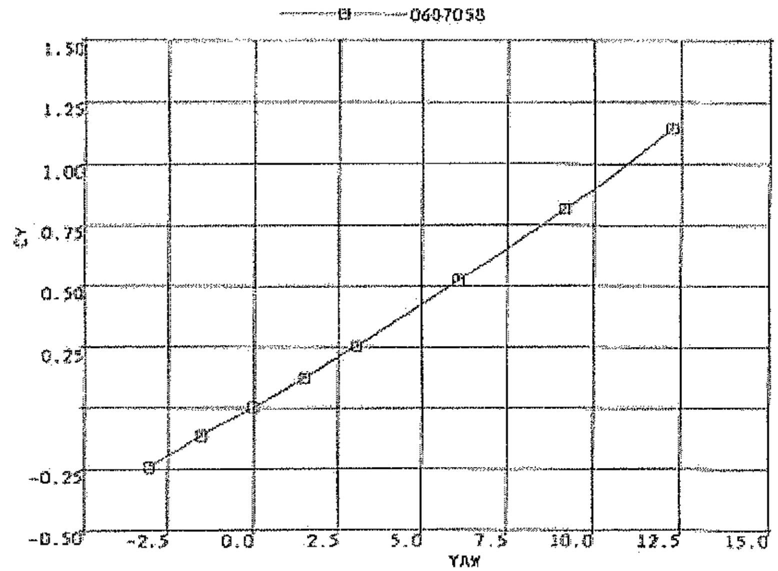

PROP 2 FRONT, GRIT, C3 MIRRORS (RIGHT FWD,LEFT AFT),VERTIC

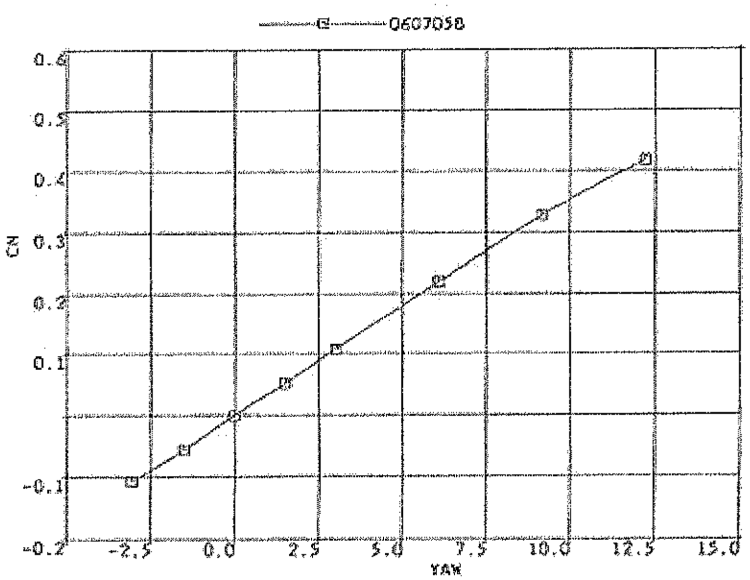

PROP 2 FRONT, GRIT, C3 MIRRORS (RIGHT FWD,LEFT AFT),VERTIC

002367
002367

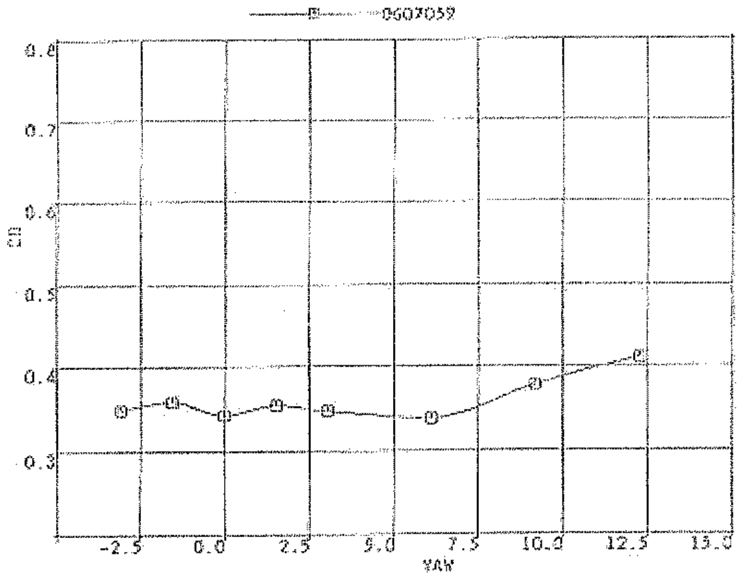

PROP 2 FRONT, GRIT, C3 MIRRORS (RIGHT FWD,LEFT AFT),FWD TI

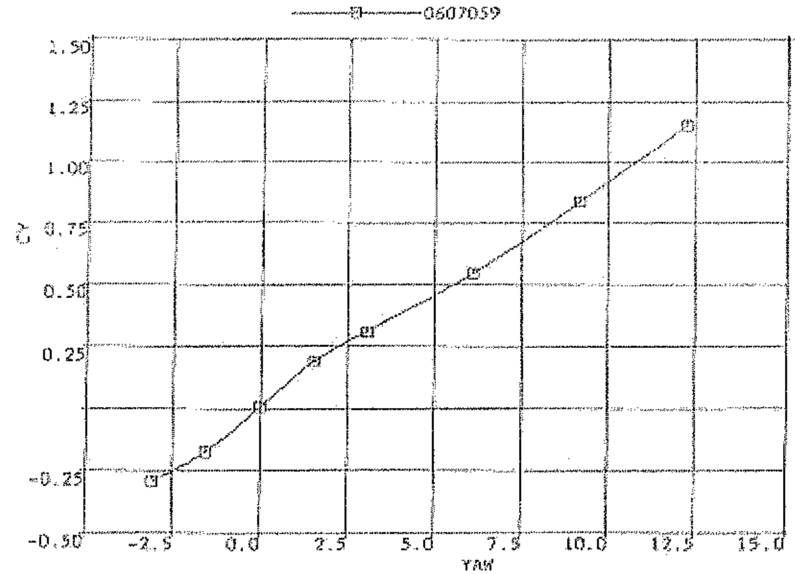

PROP 2 FRONT, GRIT, C3 MIRRORS (RIGHT FWD,LEFT AFT),FWD TI

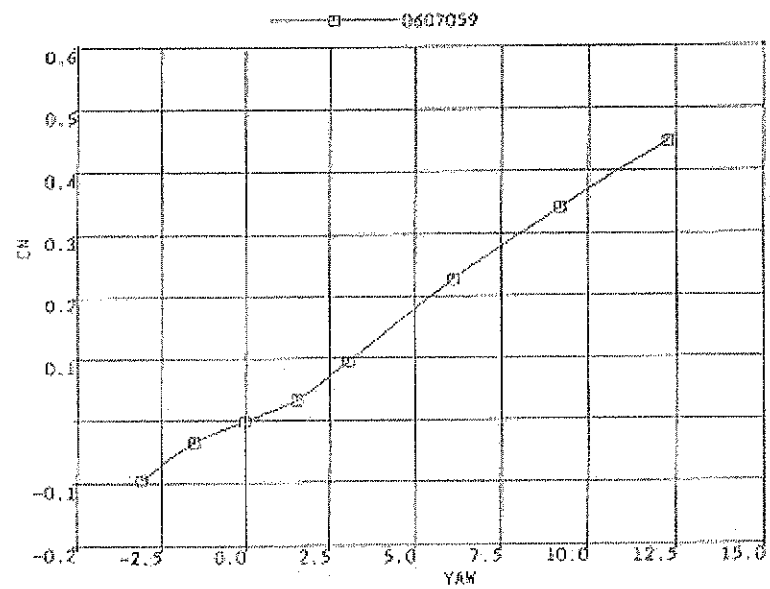

PROP 2 FRONT, GRIT, C3 MIRRORS (RIGHT FWD,LEFT AFT),FWD TI

002368

002368

002369

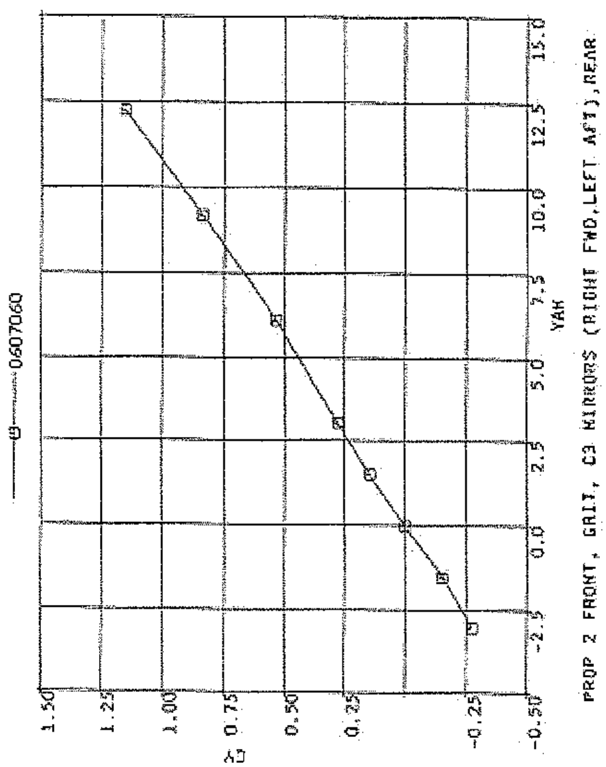

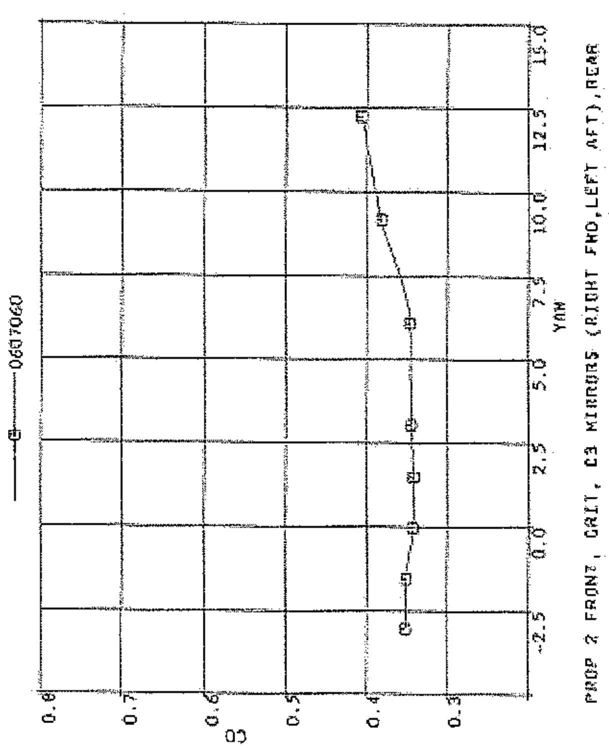

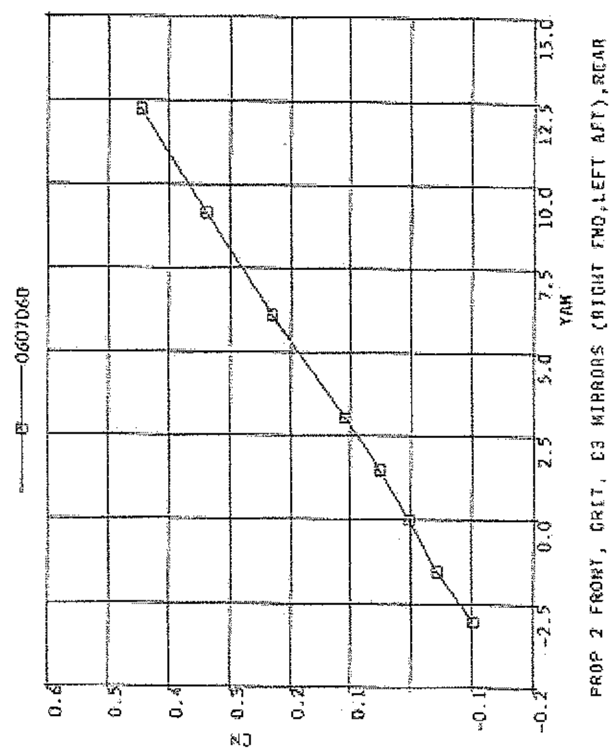

002369

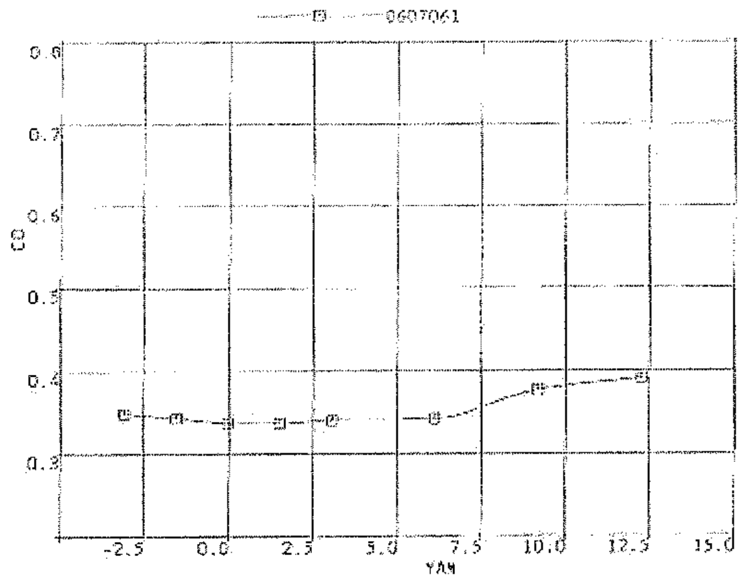

PROP 2 FRONT, GRIT, C3 MIRRORS(RIGHT FWD,LEFT AFT),MOD 0

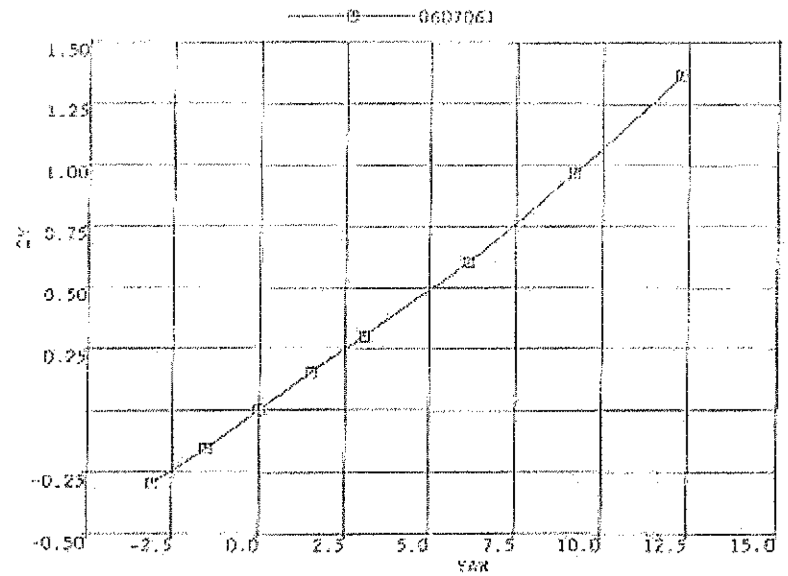

PROP 2 FRONT, GRIT, C3 MIRRORS(RIGHT FWD,LEFT AFT),MOD 0

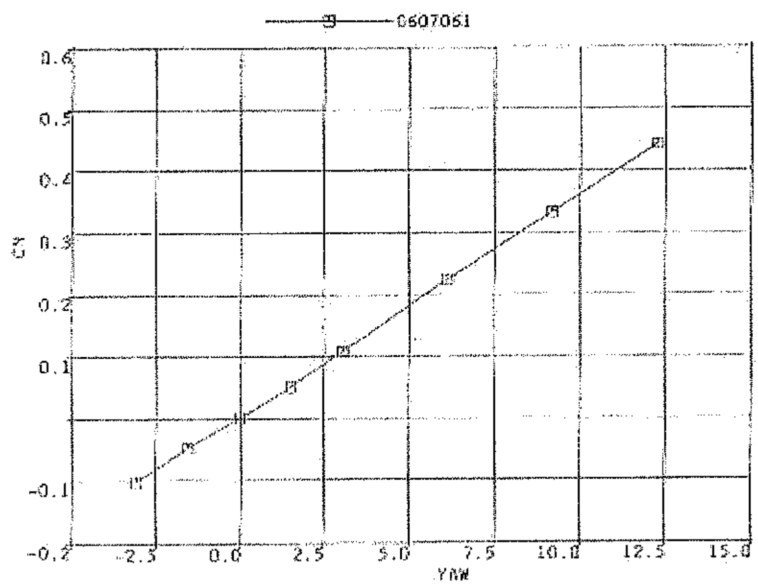

PROP 2 FRONT, GRIT, C3 MIRRORS(RIGHT FWD,LEFT AFT),MOD 0

MCI - 039946

002370

002370

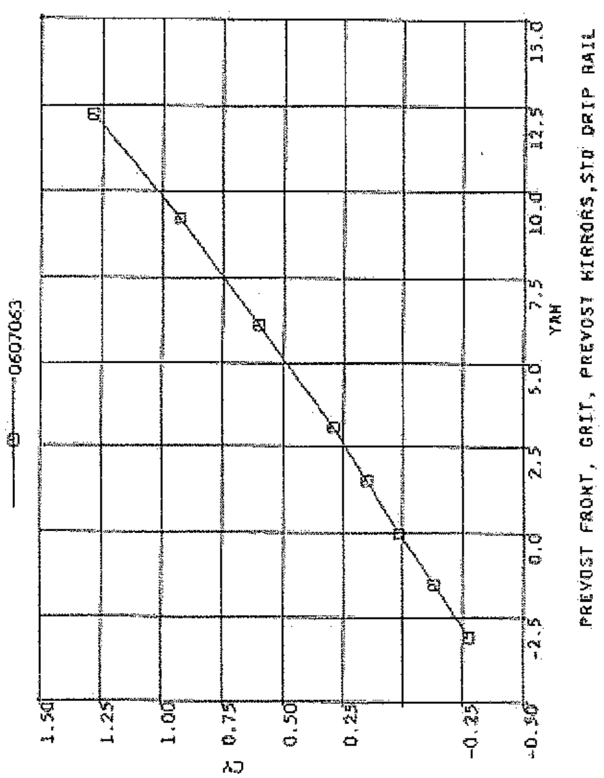

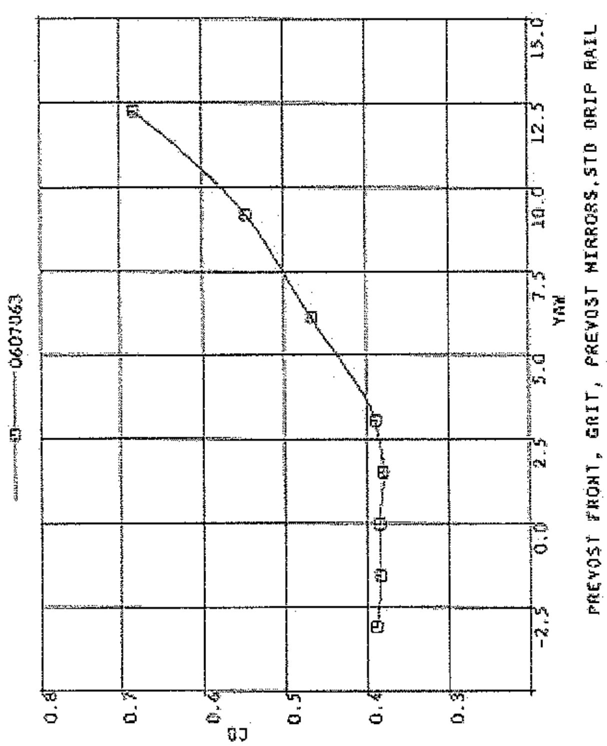

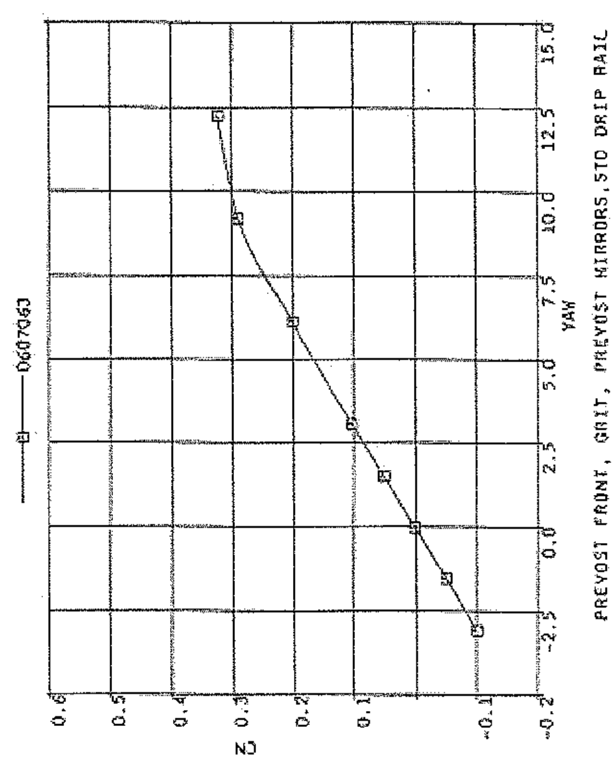

002371

002371

MCI - 039947

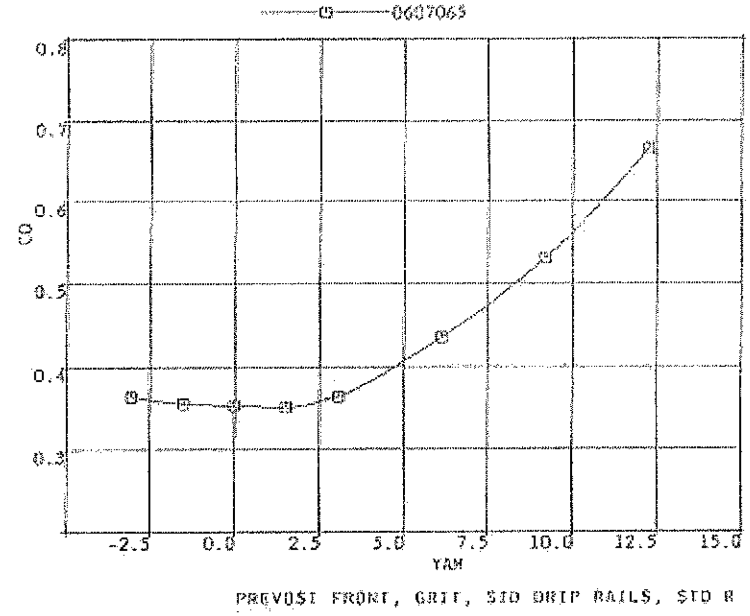
0607065
CD
YAW
PREVOST FRONT, GRIT, STD DRIP RAILS, STD R

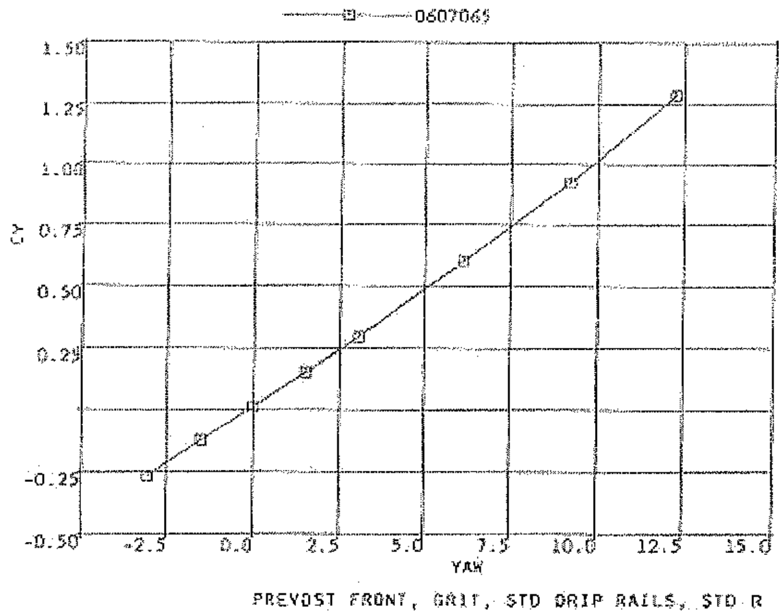
0607065
CY
YAW
PREVOST FRONT, GRIT, STD DRIP RAILS, STD R

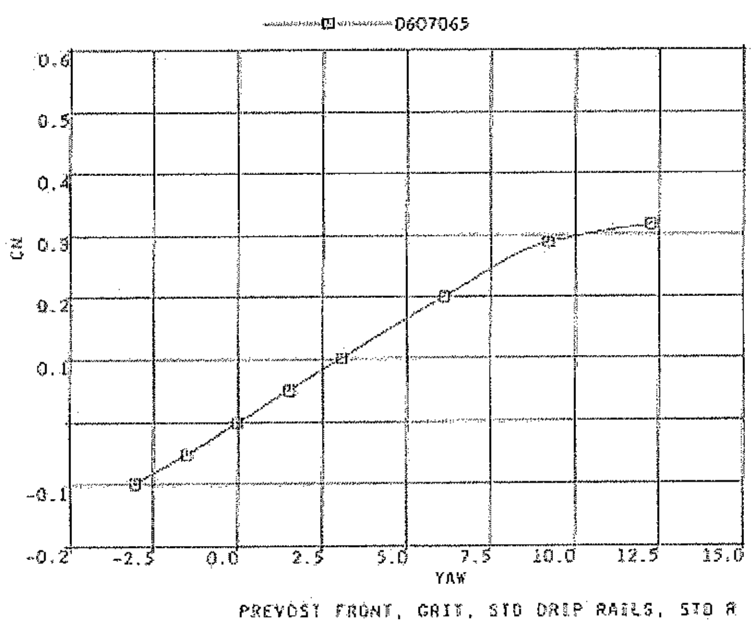
0607065
CN
YAW
PREVOST FRONT, GRIT, STD DRIP RAILS, STD R

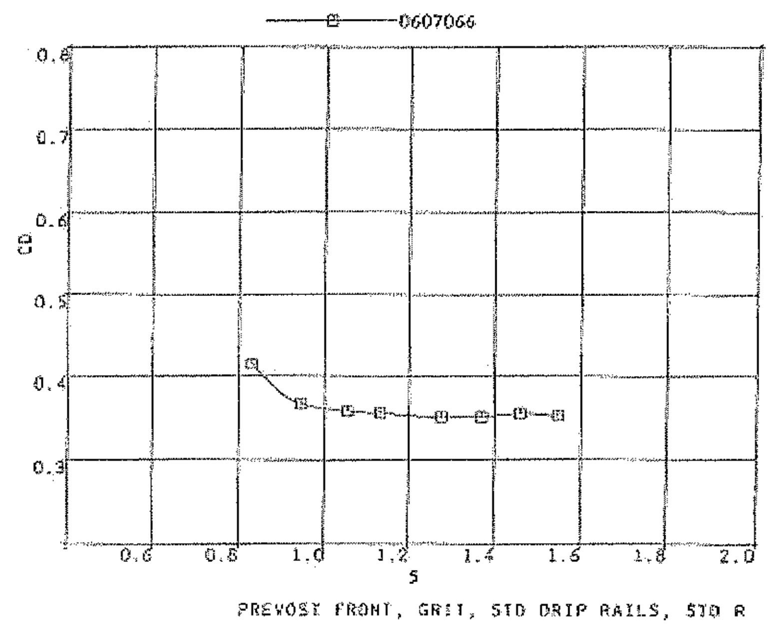
0607066
CD
S
PREVOST FRONT, GRIT, STD DRIP RAILS, STD R

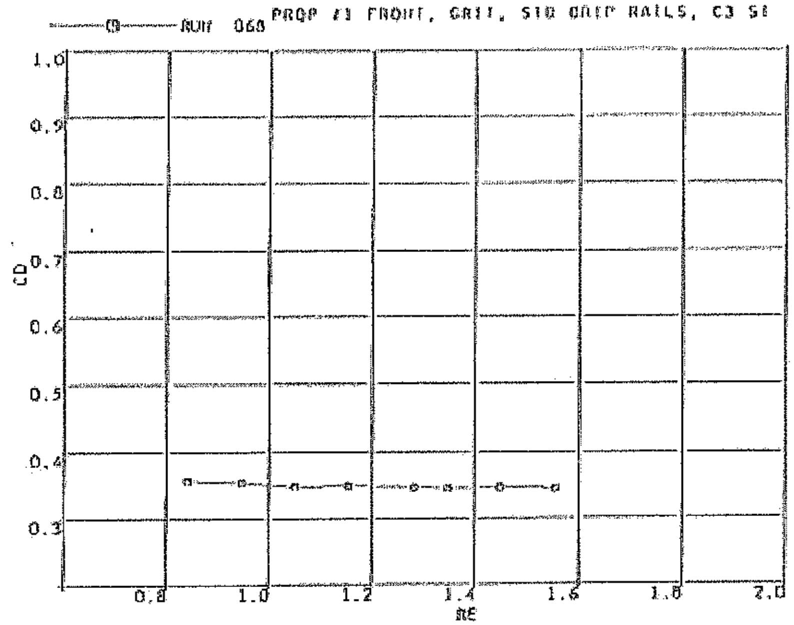

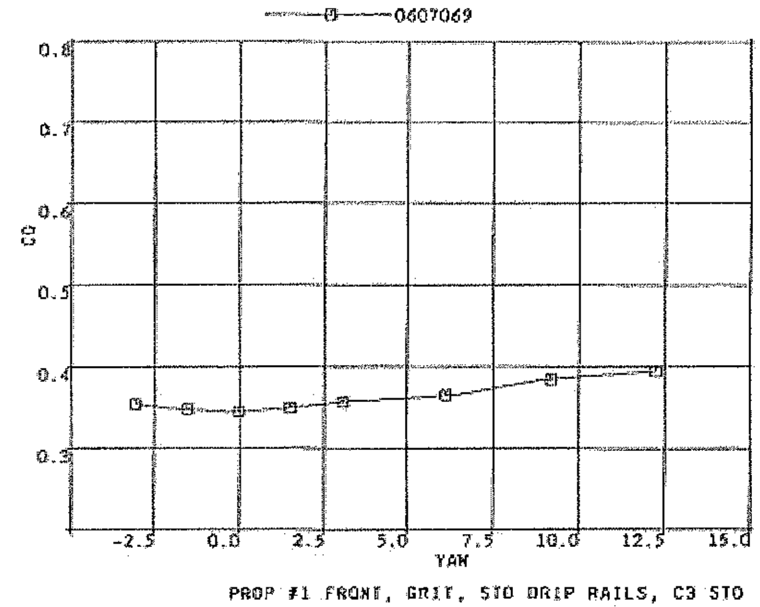

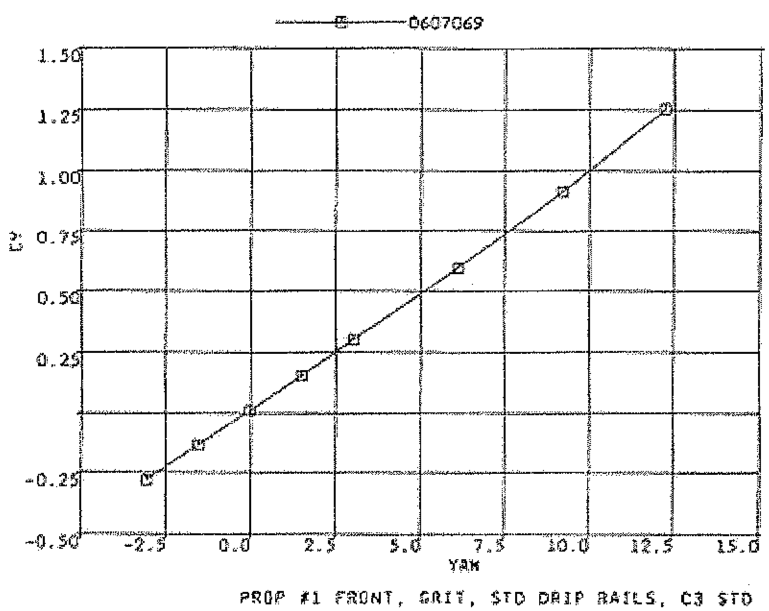

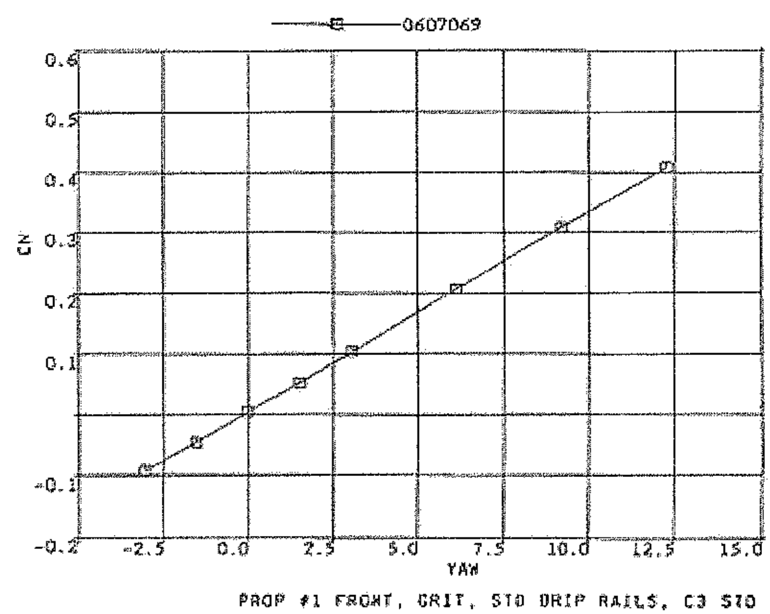

MCI - 039949

002373

002373

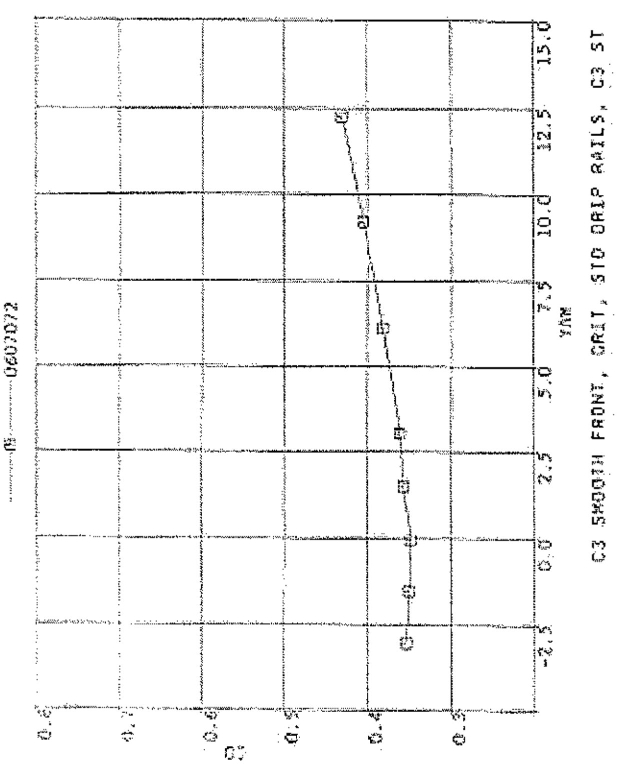

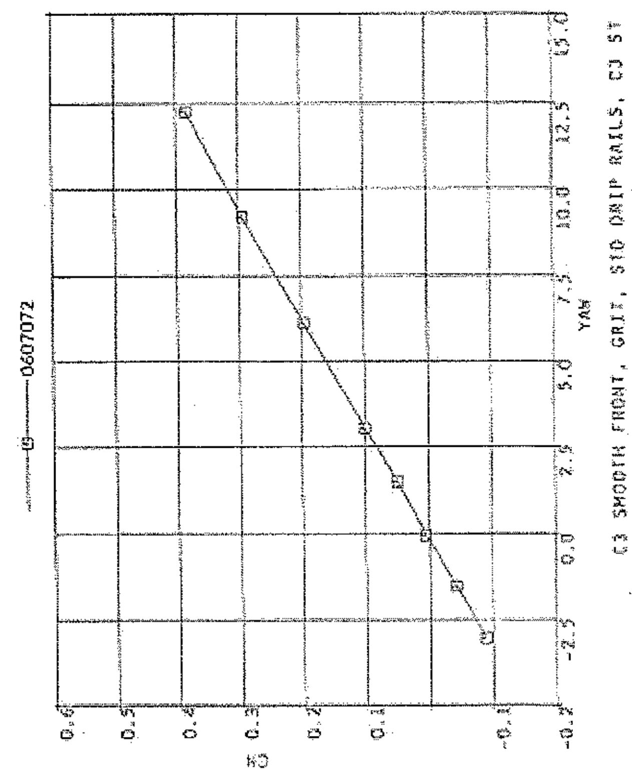

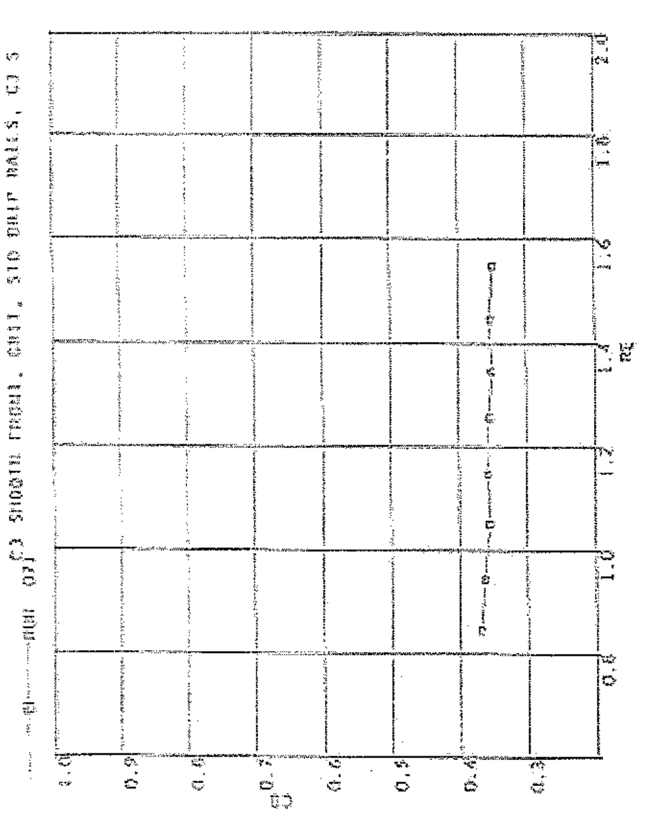

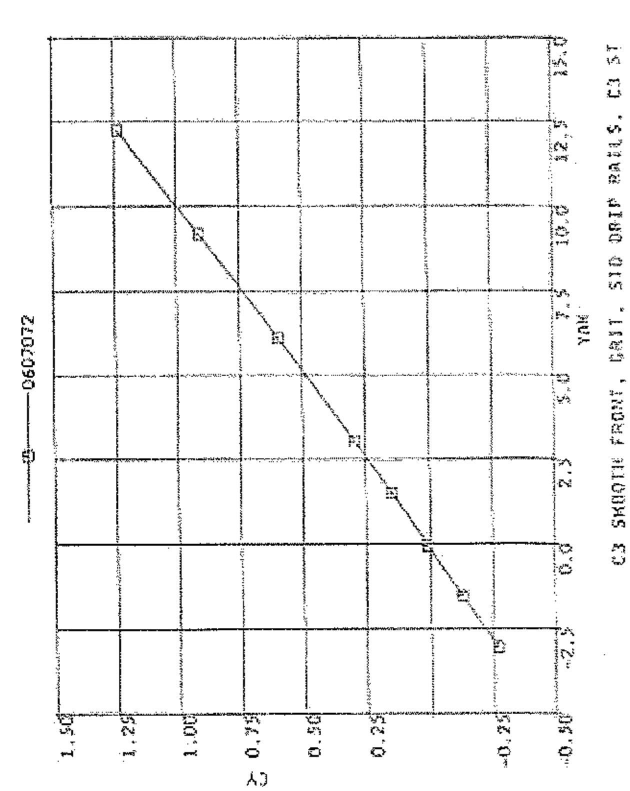

002374

002374

002375

002375

EXHIBIT 7

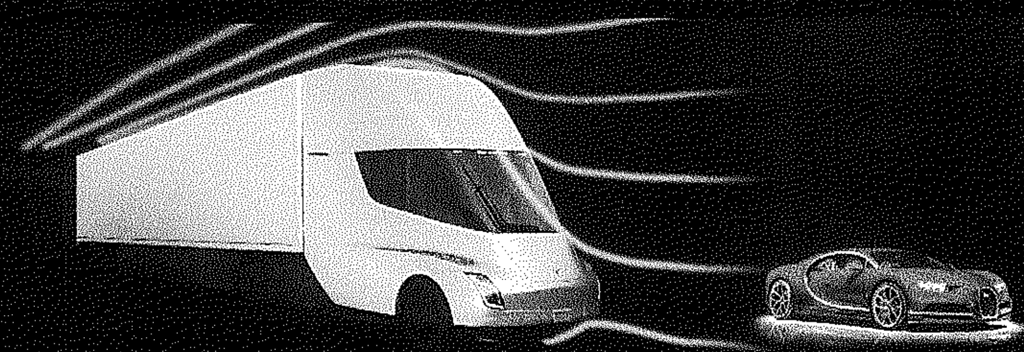

Cd	VEHICLE
0.36	Tesla Semi
0.65-0.70	Diesel Truck
0.38	Bugatti Chiron

002376
002376
002376

002377

002377

EXHIBIT 8

DISTRICT COURT

CLARK COUNTY, NEVADA

KEON KHIABANI and ARIA KHIABANI, minors by and through their natural mother, KATAYOUN BARIN; KATAYOUN BARIN, individually; KATAYOUN BARIN as Executrix of the Estate of Kayvan Khiabani M.D. (Decedent), and the Estate of Kayvan Khiabani, M.D.(Decedent),	)	CASE NO.: A-17-755977-C
Plaintiffs,	)	
vs.	)	
MOTOR COACH INDUSTRIES, INC. A Delaware corporation; MICHELANGELO LEASING INC. D/b/a RYAN'S EXPRESS, an Arizona corporation; EDWARD HUBBARD, a Nevada resident; BELL SPORTS, INC. D/b/a GIRO SPORT DESIGN, a California corporation; SEVENPLUS BICYCLES, INC. D/b/a Pro Cyclery, a Nevada corporation; DOES 1 through 20; and ROE CORPORATIONS 1 through 20.	)	
Defendants.	)	

VIDEOTAPED DEPOSITION OF BRAD LAMOTHE
LAS VEGAS, NEVADA
WEDNESDAY, OCTOBER 11, 2017

REPORTED BY: KAREN L. JONES, CCR NO. 694
JOB NO.: 422125

002378

002378

THE WITNESS: I'm not that familiar with the Setra, the full Setra line.

BY MR. KEMP:

Q. But you do understand in general that the more you round the corner like a bullet train, for example, the better aerodynamics you'll have? You do understand that?

A. Uh-huh.

Q. Yes?

A. And the higher the speed, the more of a factor that would be.

Q. Great. Whose job was it to make sure that the aerodynamics design of the J4500 was reasonably safe, in your term?

A. Well, I don't know that aerodynamics is a -- is a safety factor. The shape of the front of the coach, I'm not aware that that would be a safety factor.

Q. So as far as you know, when the J4500 was designed, no one looked at aerodynamics as a safety factor as far as you know?

MR. RUSSELL: Objection. Foundation.

THE WITNESS: Not to my knowledge.

BY MR. KEMP:

Q. Did you understand that a coach that had

002379

002379

Do you see that statement?

A. I see it.

Q. Did MCI make any effort in designing the J4500 to reduce the aerodynamic drag by modifying the shape of the front of the coach?

MR. RUSSELL: Objection. Foundation.

THE WITNESS: I have no knowledge of that.

BY MR. KEMP:

Q. So as far as you know, there was no effort made in that regard?

MR. RUSSELL: Same objection.

THE WITNESS: To my knowledge, no.

BY MR. KEMP:

Q. Now, flipping back to the front page, do you know whether or not A D R Systems made a formal proposal to MCI?

A. Not that I'm aware of.

Q. If someone made a formal proposal to attempt to reduce drag, how would that be processed? Where would it go? Who would get it? Who would evaluate it?

A. Well, it would depend how to came to the company. If it came -- if they approached our marketing group or if they approached our

Q. Why is lack of visibility on the right side not a hazard as opposed to a concern?

A. I don't believe there is lack of visibility on the right-hand side.

Q. You think that coaches have right -- have right-side visibility?

A. I believe they do.

Q. You think they do, okay.

I'll mark this as 2.

(Exhibit 2 marked.)

BY MR. KEMP:

Q. I've handed you for review an article marked as Exhibit 2 entitled, quote "Many buses have built-in blind spots that make driving them dangerous," unquote, by Brian Sherlock dated November 5th, 2015.

Do you see that the document?

A. I see it.

Q. In 2015, that's, what, 10, 12 years after the J4500 was designed?

A. About that, yes.

Q. And according to Mr. Sherlock -- let's go to page 2. He says, quote, "Essentially all transit buses in the United States are built as cheaply as possible with mirrors and pillars that

J4500 design project -- design process?

MR. RUSSELL: Objection. Foundation. You can answer.

THE WITNESS: Oh, okay. Well, I'm aware that we polled a wide variety of drivers as we were developing that coach.

BY MR. KEMP:

Q. Polled?

A. Polled. We had a wide variety in size and experience that sat in the driver's seat and that drove the coach under controlled circumstances to evaluate and give feedback.

Q. Well, we'll get to a little bit of that feedback here in a minute.

My question was what design actions, if any, were taken to eliminate or modify right-side blind spots?

A. None that I was directly involved with, so I don't know.

Q. Do you know if anything was done?

MR. RUSSELL: Objection. Foundation.

THE WITNESS: I don't know.

BY MR. KEMP:

Q. Now, if you go to the next page of the article, page 3, Mr. Hanley, president of the Bus

002382
002382

a clean sheet of paper that was basically designed on a computer screen. It was done in CAD.

Q. **So you think there was some sort of computer simulation done with regards to the E series to determine line-of-sight and visibility obstructions?**

A. I would think there probably was.

Q. **Thinking they were probably -- thinking that there probably was and telling me that there was are two different things. Do you recognize that?**

A. Right, but I can't say. I can't say I've seen it.

Q. **And why do you think it probably was done?**

A. Because that was part of the kind of things that we did.

Q. **Would you agree with me that to do a competent job of design engineering on the E series you would have to do the line-of-sight and visibility obstructions of some sort?**

A. I would say that would be best practice.

Q. **Why is that?**

A. It's just commonly accepted best practice.

Q. I think I asked this question, but I want to make sure. As we sit here today, do you know whether or not the air displacement from the front of a J4500 is greater than or less than the air displacement that you would get from a Setra 500 going at the same speed?

A. Well, I have no familiarity with the Setra 500, so I really couldn't comment on that.

Q. So the answer's, no, you don't know the answer to that question?

A. Can you repeat the question.

Q. Do you know whether or not the side force or air displacement generated by a J4500 is greater or less than that generated by a Setra 500 assuming that both vehicles are going 25 miles per hour?

A. I don't know.

MR. KEMP: Let me mark this as 3.

(Exhibit 3 marked.)

BY MR. KEMP:

Q. I'm going to hand you a document that's dated July 2012 with regards to the Setra. And specifically the document says on page four that they have done aerodynamic styling to lower fuel consumption. And it says that they have achieved a

002384

002384

drag coefficient of .33.

Do you see that statement?

A. I see that.

Q. Now, earlier you told me you thought the J4500 had a .3 or .4 drag coefficient as well; is that correct?

A. No. I said I speculated that it would be in some kind of a range of .3, .4.

Q. And in reality, it's more in the .8 range?

A. .8?

MR. RUSSELL: Objection. Foundation.

THE WITNESS: Not to my knowledge.

BY MR. KEMP:

Q. You still think it's .3 to .4?

A. I believe most tour coaches are in that range.

Q. All right. And next statement, "The designer -- the engineers designed the front of the Comfort Class 500 with larger radii for the roof slope.

Am I pronouncing that right?

A. Radii, I guess, yeah.

Q. How do you spell that? R-a-d-i-i, radii?

A. That's how they spelled it, yeah.
Q. Is that the way you're supposed to spell it?
A. To my knowledge, yeah.
Q. So in addition to making the right-hand corners more rounded, you can also make the -- the roof slope more rounded; is that correct, in theory?
A. In theory.
Q. Was any consideration given when you designed the 4500 to design it with a larger radii for the roof slope?
MR. RUSSELL: Objection. Foundation.
THE WITNESS: Not that I'm aware of.
BY MR. KEMP:
Q. Next statement, quote, "The A pillar was also redesigned enabling the flow loss on the front surface to be reduced significantly in placing the airflow in this area on the vehicle body," unquote.
Did I read that right?
A. That's what it says, yeah.
Q. Was any consideration given to doing that when you designed the J4500?
MR. RUSSELL: Objection. Foundation.
THE WITNESS: Not to my knowledge.
BY MR. KEMP:

002386

002386

Q. You could have made the J4500 -- designed and made the 4500 designed with a larger radii for the roof slope if you'd wanted to, right?

MR. RUSSELL: Objection.

THE WITNESS: I don't know if that's true or possible.

BY MR. KEMP:

Q. So you think Mercedes can make the Setra with a larger radii for the roof slope, but MCI cannot make a J4500 with a larger radii for the roof slope?

MR. RUSSELL: Object.

THE WITNESS: No, I don't think that. I think they're selling a different coach into a different market. They don't sell this in North America as far as I know.

BY MR. KEMP:

Q. I'm asking you if theoretically you could have designed and made the 4500 with a larger radii for the roof slope if you wanted to?

MR. RUSSELL: Objection. Foundation.

THE WITNESS: I guess it would be possible.

BY MR. KEMP:

Q. I mean this is not advanced space

technology. This is just changing the shape of a roof, right? Right?

MR. RUSSELL: Objection. Incomplete hypothetical. Argumentative.

BY MR. KEMP:

Q. Is there any reason you can think of why the Japanese could make a bullet train that's aerodynamic efficient in 1964 and MCI couldn't make a J4500 with a larger radii for the roof slope in 2007?

MR. RUSSELL: Objection. Incomplete hypothetical. Argumentative.

THE WITNESS: Trains and tour coaches are not the same vehicles.

BY MR. KEMP:

Q. I'm just asking if there's any reason you can think of that it couldn't be manufactured that way?

MR. RUSSELL: Same objections.

BY MR. KEMP:

Q. You know like, for example, you needed some rare part like lithium and it's not available or something like that. Okay. Any practical reason you can think of that MCI couldn't have made a J4500 with a larger radii for the roof slope?

MR. RUSSELL: Same objections.

THE WITNESS: I don't know.

BY MR. KEMP:

Q. **You don't know of any?**

A. I just don't know.

Q. **Can you give me any practical reason as we sit here today why MCI couldn't make a J4500 with a larger radii for the roof slope?**

MR. RUSSELL: Same objections.

THE WITNESS: No.

BY MR. KEMP:

Q. **Now the next statement they say that they redesigned the A pillar. Do you see that statement?**

A. I see that.

Q. **Is there any reason the J 45 couldn't have been made with a redesigned A pillar such as they did to the Setra 500?**

MR. RUSSELL: Same objections.

THE WITNESS: I think we asked that one, didn't we, a couple questions ago.

BY MR. KEMP:

Q. **I want to know if there's any practical reason it couldn't have been done.**

A. I don't know.

002390

002390

EXHIBIT 9

DISTRICT COURT

COUNTY OF CLARK, NEVADA

KEON KHIABANI and ARIA KHIABANI, minors by and through their natural mother, KATAYOUN BARIN, KATAYOUN BARIN, individually, KATAYOUN BARIN as Executrix of the Estate of Kayvan Khiabani, M.D. (decedent), and the Estate of Kayvan Khiabani, M.D. (Decedent),

Plaintiffs,

vs.

Case No. A-17-755977-C

MOTOR COACH INDUSTRIES, INC., a Delaware corporation; MICHAELANGELO LEASING, INC., d/b/a RYAN'S EXPRESS, an Arizona corporation; EDWARD HUBBARD, a Nevada resident; BELL SPORTS, INC., d/b/a GIRO SPORT DESIGN, a California corporation; SEVENPLUS BICYCLES, INC., d/b/a Pro Cyclery, a Nevada corporation; DOES 1 through 20; And ROE CORPORATIONS 1 through 20.

Defendants.

****

ORAL DEPOSITION OF
PABLO FIERROS
October 8, 2017

****

Job No.: 420700

002391

002391

Q. Okay. Great. Did there come a time that you worked for Motor Coach Industries or an affiliate of Motor Coach Industries?
A. I worked for Universal Coach Parts.
Q. And what time period did you work for them?
A. I believe it was '97 to 2000.
Q. And what was your job in general?
A. I was vice president and general manager.
Q. Where was Universal Coach Parts located?
A. In Chicago.
Q. And when you say Chicago, would that be Des Plaines?
A. That's correct.
Q. And that's D-E-S, new word P-L-A-I-N-E-S.
Who was your immediate supervisor while you were the vice president and general manager of Universal Coach Parts?
A. Jim Bernacchi.
Q. And I believe that's spelled B-E-R-N-A-C-C-H-I. Is that --
A. I believe that's -- I believe that's correct.
Q. Okay. And what was your understanding of Mr. Bernacchi's position at that time?
A. I believe he was the CEO of Motor Coach Industries.

002392

002392

002392

Q. Was he also the president?
A. I don't remember.
Q. Okay. But you think he was the CEO from '97 to 2000 when you were at Universal Coach Parts. Is that correct?
A. I believe he was the CEO, yes. I don't remember if he was both president and CEO. That I don't remember.
Q. Okay. Did you report directly to Mr. Bernacchi?
A. Bernacchi. I did.
Q. Did you re- -- okay.
A. You asked me that. I said yes.
Q. And where were you located at physically in terms of an office building?
A. I don't remember the address, but it was in a separate building than -- than Jim Bernacchi.
Q. Okay. And was it near Mr. Bernacchi's building?
A. About -- about 10 blocks away.
Q. And how many employees did you have as the vice president and general manager of Universal Coach Parts?
A. I believe the number was close to 1,200.
Q. Were they located at the same place you were?

002393

002393

about it. I don't know exactly how or when, but I do.
Q. Do you know a man named Chris Ferrone, F-E-R-R-O-N-E?
A. My God, I -- the -- the name sounds somehow familiar.
Q. Okay. And do you know a man named Mark Barron B-A-R-R-O-N, also named Mark Bowen, B-O-W-E-N?
A. The first one sounds more familiar than the second one.
Q. Does the second one, Mr. Barron or Bowen, sound familiar in any way, shape or form?
A. No, no.
Q. No? Okay.
A. Are you having --
Q. Do you remember?
A. Are you having problems hearing me?
Q. I think we're talking over each other a little bit.
A. Okay. Okay.
Q. I'm not having a problem hearing you, but -- but I think we're talking over each other a little bit.
Okay. Back to the S-1 Gard, do you remember at some point in time someone came to you and offered you this product, referring to the S-1 Gard?
A. Formally offering, no, I don't remember. I

J4500 or not. Is that correct?

A. Agree. It is correct. I couldn't tell you.

Q. Okay. Fair.

And does this letter remind you that you provided S-1 GARDs to New Flyer customers -- customers that had New Flyer buses?

A. I do not.

Q. All right. Apart from the S-1 Gard, are you familiar with any other type of barrier safety device that manufacturers of buses either did or could put in front of the right rear tires to move people or objects out of the way?

A. There was a device, I believe it was British, I don't remember the -- the name, but it was in the front of the bus and it attempted to do something similar to this. If you -- if you remember some of the spoilers that were popular in the '70s and '80s in race cars that looked like they were sweeping the front, that's what that device looked like.

Q. Okay. And did you sell any of those?

A. No.

Q. Okay. But that was designed for the front tires as opposed to the rear tires. Is that correct?

A. That was designed for the front of the bus for the whole bus.

002395

002395

Q. Okay. And have you heard the term spats, S-P-A-T-S, before?

A. No, I have not.

Q. How about wheel guards, have you heard of wheel guards that are attached to the rear tires?

A. Yes.

Q. Okay. And what do you call those?

A. Did you say "splash" a while ago?

Q. I said "spats."

A. Oh, spats, no. Spats, no.

Q. Spats.

A. What do I call the devices that go behind the wheels? The -- the splash guards you said?

Q. Okay. All right. Have you heard of the device, a protective barrier that goes on the outside of the rear tires to prevent the tires from coming into contact with something on the outside of it?

A. No, I -- I don't.

Q. Okay. While you were at Universal Parts [sic], did MCI ever solicit your -- your input with regards to safety features?

A. No. I -- I don't --

Actually, let me take that back. It is possible that they would ask me a question like that on a bus that they didn't manufacture, but it most likely -- it would have been a question as in check with your team, because they knew I was not an engineer so I couldn't give them a -- a -- an opinion. So -- so if they would have asked my opinion on a safety device, I think they would ask me more to check with my team.

Q. Okay. Did you have safety engineers on your team?

A. I did.

Q. How many?

A. I believe the department had three, four people that did some engineering work. They verified specs on products that we -- that we sold.

Q. Okay. And do you know whether or not those safety engineers ever evaluated the S-1 Gard?

A. I don't remember doing any evaluation of S-1 Gard.

Q. Before you sold or resold the product, would -- would the standard procedure be to do some sort of evaluation?

A. Absolutely.

Q. Okay.

A. I --

Q. Now --

A. There are many products in the bus that have already been used for years before that, no, we probably

002397

002397

did not do a complete and thorough investigation of every single part.

Q. Do you know what a proximity sensor is?

A. Yes.

Q. And, for example, some cars have devices that alert you whether or not there's a car or bicycle either to your front or on the side of you. Right?

A. Yes.

Q. And -- and -- and do you have a car like that yourself?

A. No.

Q. Now with regards to proximity sensors, while you were at Universal Coach Parts, did you sell any proximity sensors?

A. I don't remember.

Q. Do you remember one way or the other whether or not any devices that you were involved with in any way, shape or form had proximity sensors on it?

A. Not specifically, no.

Q. And after leaving Universal Coach Parts in 2000, did you have any involvement with the bus industry?

A. I went to work for ENroute Communications, which was a startup company doing wireless communication between the base and the moving coach transit bus,

002398

002398

train, vehicle. So we build wireless communication systems. And one of the industries that we attempted to go to was the bus industry.

Q. Okay. And what time period were you with them?

A. Them became me. I was part of the company. After the initial startup, I became owner of the company -- part owner of the company.

We -- 2000 to 2005 approximately.

Q. And then where'd you go in 2005?

A. I went back -- I went to -- I started a -- a consulting company doing sales consulting and I worked in the retail automobile. And after that I came to El Paso with my present employer.

Q. And that would be Stewart & Stevenson?

A. Correct.

Q. And that's spelled S-T-E-W-A-R-T, ampersand, Stevenson, S-T-E-V-E-N-S-O-N. Correct?

A. Stevenson, correct.

Q. Okay. Now, when you were with ENroute from 2000 to 2005, did you try and sell any products to MCI?

A. No.

Q. You didn't try to sell the wireless device to MCI?

A. No.

Q. Did you try to sell it to Universal Coach

002399

002399

Q. (BY MR. KEMP) Okay. Just to make sure we got it right. As you understand it today, the majority of buses have driver seat belts. Right?

A. Yes.

Q. And you don't know one way or the other whether or not the majority have passenger seat belts?

A. I don't know.

Q. Correct?

A. I don't know.

Q. But do you know that passenger seat belts are used in more buses today than they were back in 1997 through 2000? Do you know that one way or the other?

MR. DACUS: Object to form and foundation.

A. I don't know.

Q. (BY MR. KEMP) Okay. Now, do you have an understanding one way or the other whether or not a bus such as the J4500 creates an air blast or air displacement at its right front when it's traveling?

A. I have no idea.

Q. Okay. And are you aware that there -- or, strike that.

Have you ever heard of a part called a spoiler that goes along the front right side or the left side of the bus to change the air flow?

A. Not specifically in buses, no.

way?

A. No, I don't remember it, no.

MR. DACUS: Thank you. I don't believe I have any further questions.

MR. KEMP: Are you done, Mr. Dacus?

MR. DACUS: I am.

FURTHER EXAMINATION

BY MR. KEMP:

Q. Sir. You said that you saw a flier similar to and then you held up a document. Was that Exhibit 3?

A. No, the one that I held up was Exhibit 5. I was looking for the other one and I can't find it.

Q. Could you find Exhibit 3 for a second, please.

A. I have it.

Q. So the flier you saw was either the same or similar to Exhibit 3. Is that correct?

A. I guess. I guess. I don't specifically remember. It -- it -- it's -- it's vague in my memory.

Q. Okay. But you saw some flier similar to Exhibit 3 that related to the S-1 Gard. Is that correct?

A. Yeah, I think somebody handed to me something like that, yes.

Q. Okay. And Mr. Dacus asked you if you'd seen any technical papers.

002401

002401

Q. Was that something that happened a lot when you went to these trade shows, people would mail you stuff afterwards?
A. Hundreds.
Q. Hundreds of times?
A. Correct.
Q. Because you're a customer, they're trying to get your business. Right?
A. I -- yeah.
Q. Okay. And Counsel asked you if you'd seen any technical paper on the S-1 Gard. As you sit here today, do you remember one way or the other whether you saw Exhibit 7 before at any time?
A. No, I don't remember.
Q. So this may and may not have been among the hundreds of things that you were mailed after trade shows. Is that correct?
A. That's correct.
Q. And with regards to this particular trade show at Indianapolis in November 1998, as we sit here today, do you remember whether or not you went to that?
A. I probably did. I went to most of the trade shows so the likelihood that I went to this one is very high.
Q. And is it also high because Indianapolis is

002403

002403

EXHIBIT 10

DISTRICT COURT

COUNTY OF CLARK, NEVADA

KEON KHIABANI AND ARIA KHIABANI, MINORS BY AND THROUGH THEIR NATURAL MOTHER, KATAYOUN BARIN, ET AL.,

Defendants.

vs.

MOTOR COACH INDUSTRIES, INC., A DELAWARE CORPORATION, ET AL.,

Defendants.

No. A-17-755997-C

VIDEOTAPED DEPOSITION OF DAVID DORR, a witness herein, noticed by Kemp, Jones & Coulthard, at 355 South Grand Avenue, Los Angeles, California, at 10:08 a.m., on Wednesday, September 13, 2017, before Jana Ruiz, CSR 12837.

Job No.: 416514

002404

002404

Now, have you taken any courses in aerodynamics?
A. No.
Q. Okay.
What is your understanding, if you have an understanding, as to whether or not when a 2007 vintage J4500 is traveling 35 to 40 miles an hour, what is your understanding as to whether or not it causes air blasts or air displacements from the bus?
A. I don't know.
Q. Okay.
You don't know one way or the other whether it would cause air blasts or air displacements?
A. No, I don't.
Q. And same question with regards to the -- in the back, it has rear tires; correct?
A. Yes.
Q. Double set of rear tires.
What is your understanding, if any, with regards to whether or not a suction effect will be created when a bus is moving 35, 40 miles an hour from those two rear tires?
A. I don't -- I don't know.
Q. You don't know one way or the other whether there is a suction or not a suction?
A. I don't know.

002405

002405

002405

Q. Okay.
So is -- okay.
Do you have a standard sales pitch that you give to customers about the J4500?
A. No.
There's not a standard.
Q. Okay.
Well, let me ask a little differently then.
Since you don't know whether or not a J4500 will cause air blasts from the front, I assume you've never discussed that point with a customer?
A. No.
Q. I'm correct, you've never discussed that point with a customer?
A. I've never discussed that, no.
Q. And you've never discussed whether or not the back tires have some sort of suction effect with the customer?
A. No.
Q. Is that correct?
A. That's correct.
Q. Okay.
Now, I'd like to ask you to look at Exhibit -- sorry, Darrell -- Exhibit 26 with me; okay?
(Whereupon the document referred to is marked by

002406

002406

Q. So they were all J4500s?
A. Yes.
Q. Okay.
And so do you remember what course of time?
You said you started meeting with him in 2002.
When did you -- when is the last time you met with Mr. Haggerty?
A. Oh, I don't remember.
Q. Has it been within the last couple years or --
A. No.
Q. So -- okay.
But you do recall dealing with him with regards to approximately 50 J4500s; right?
A. Yes.
Q. Okay.
Now, earlier I asked you if you had communicated with any customer about the subject of air blast potential, and you said no.
Remember that testimony?
A. Yes.
Q. Yes? Okay.
Would I be correct that you did not have any communications with Mr. Haggerty during any one of these 50 bus sales about the potential for air blasts, if any, from the J4500?

002407
002407

A. Yes, you're correct.

Q. And same question about the rear tires sucking in, you didn't have any communications with him about that subject either; correct?

A. Correct, no communications.

Q. Okay.

Do you recall any specific subjects you did talk to Mr. Haggerty about, other than price and delivery dates?

A. It was price, trade values for trade buses, mostly numbers.

Q. Okay.

Now, going back to Exhibit Number 2, if you take a look at page 9, paragraph 15, there is a warning there.

You see that?

A. Page 9? Oh, MCI9. Okay.

Q. And the warning says, "This vehicle may contain HCFC R-134A refrigerant, a substance which harms public health and the environment by destroying ozone in the upper atmosphere."

Did I read that right?

A. Yes.

Q. And that is the only warning I see in Exhibit 2.

Do you see any other warning?

A. No.

002409

002409

EXHIBIT 11

002409

DISTRICT COURT

COUNTY OF CLARK, NEVADA

KEON KHIABANI and ARIA KHIABANI, minors by and through their natural mother, KATAYOUN BARIN; KATAYOUN BARIN, individually; KATAYOUN BARIN as Executrix of the Estate of Kayvan Khiabani, M.D. (Decedent), and the Estate of Kayvan Khiabani, M.D. (Decedent),

Plaintiffs,

Case No. A-17-755977-C

vs.

MOTOR COACH INDUSTRIES, INC., a Delaware corporation; MICHELANGELO LEASING INC. d/b/a RYAN'S EXPRESS, an Arizona corporation; EDWARD HUBBARD, a Nevada resident; BELL SPORTS, INC. d/b/a GIRO SPORT DESIGN, a California corporation; SEVENPLUS BICYCLES, INC. d/b/a Pro Cyclery, a Nevada corporation; DOES 1 through 20; and ROE CORPORATIONS I through 20.

Defendants.

VIDEO DEPOSITION OF CHRISTOPHER GROEPLER

September 14, 2017
11:09 a.m.

20 E Thomas Road, Suite 2200
Phoenix, Arizona, 85012

Prepared by: Sandra Marruffo, R.P.R., AZ C.R. 50815
Job Number: 418116

002410
002410

A. Yes.

Q. Okay. All right. Now, do you have a general understanding one way or the other whether or not air blasts are created at the front sides of a J4500 when it's traveling 35 or 40 miles an hour?

A. No.

Q. Okay. And broadening the question out, do you know way or the other whether or not if a J4500 moves about 35 or 40 miles an hour that there's any sort of disturbance of the air in the front of the bus?

A. No.

Q. Okay. Assuming, for the sake of argument, that there is an air blast created when a J4500 moves, do you disagree that that could potentially create a hazardous situation for pedestrians and people on bicycles next to the bus?

MR. ROBERTS: Objection to form, foundation.

MR. FREEMAN: Are we still operating under the agreement objection by one is objection by all?

MR. KEMP: Yes, that's fine by me.

MR. FREEMAN: Okay.

Q. BY MR. KEMP: Go ahead, sir. You can answer the question.

A. No, I don't know.

002412

002412

EXHIBIT 12

DISTRICT COURT

CLARK COUNTY, NEVADA

KEON KHIABANI and ARIA KHIABANI, minors by and through their natural mother, KATAYOUN BARIN; KATAYOUN BARIN, individually; KATAYOUN BARIN as Executrix of the Estate of Kayvan Khiabani, M.D. (Decedent), and the Estate of Kayvan Khiabani, M.D. (Decedent),

Plaintiffs,

vs.

MOTOR COACH INDUSTRIES, INC., a Delaware corporation; MICHELANGELO LEASING, INC. d/b/a RYAN'S EXPRESS, an Arizona corporation; EDWARD HUBBARD, a Nevada resident; BELL SPORTS, INC. d/b/a GIRO SPORT DESIGN, a California corporation; SEVENPLUS BICYCLES, INC. d/b/a PRO CYCLERY, a Nevada corporation; DOES 1 through 20; and ROE CORPORATIONS 1 through 20,

Defendants.

Case No. A-17-755977-C
Dept. No. XIV

VIDEOTAPED DEPOSITION OF WILLIAM BARTLETT

LAS VEGAS, NEVADA

FRIDAY, SEPTEMBER 8, 2017

REPORTED BY: HOLLY LARSEN, CCR NO. 680, CA CSR 12170
JOB NO.: 416787

002413

002413

BY MR. KEMP:

Q. **So you agree with me, if they know it's a potential hazard, they should tell you because you're the operator of their equipment?**

A. It's up to them. I can't tell them what to do.

Q. **But, as we sit here today, you don't know one way or the other whether or not a bus will create air turbulence or air blast that's going 30, 35 miles an hour?**

MR. ROBERTS: Form and foundation.

THE WITNESS: I don't know. I've never tested it myself.

BY MR. KEMP:

Q. **And getting a little more specific here, are you familiar with an MCI J4500?**

A. Yes.

Q. **You're familiar with an MCI J4500?**

A. Yes.

Q. **And you don't know whether or not that, if you're traveling 30, 35, 40 miles an hour, will cause air turbulence or air blasts; correct?**

A. I don't know for sure. I mean, I assume it might because it's a large vehicle. But I've never been outside of an MCI passing me at 45 miles an

002414

002414

002415

002415

EXHIBIT 13

DISTRICT COURT

CLARK COUNTY, NEVADA

KEON KHIABANI and ARIA KHIABANI, minors by and through their natural mother, KATAYOUN BARIN; KATAYOUN BARIN, individually; KATAYOUN BARIN as Executrix of the Estate of Kayvan Khiabani M.D. (Decedent), and the Estate of Kayvan Khiabani, M.D.(Decedent),

Plaintiffs,

vs.

MOTOR COACH INDUSTRIES, INC. A Delaware corporation; MICHELANGELO LEASING INC. D/b/a RYAN'S EXPRESS, an Arizona corporation; EDWARD HUBBARD, a Nevada resident; BELL SPORTS, INC. D/b/a GIRO SPORT DESIGN, a California corporation; SEVENPLUS BICYCLES, INC. D/b/a Pro Cyclery, a Nevada corporation; DOES 1 through 20; and ROE CORPORATIONS 1 through 20.

Defendants.

CASE NO.: A-17-755977-C

002416
002416

VIDEOTAPED DEPOSITION OF EDWARD HUBBARD
LAS VEGAS, NEVADA
WEDNESDAY, SEPTEMBER 20, 2017

REPORTED BY: KAREN L. JONES, CCR NO. 694
JOB NO.: 417421

Q. All right.
Have you taken any courses in aerodynamics?
A. No.
Q. Do you have any special training of any sort in aerodynamics?
A. No.
Q. Do you understand in general that a large object will alter the surrounding airflow?
A. I have no knowledge of that.
Q. Do you have any sort of understanding that a bus, if it's moving at 30, 35 miles an hour, will cause air blasts or air disturbances at the front of the bus? Have you ever heard of that?
A. Yes.
Q. You have heard of that? Okay.
In what respect have you heard that?
A. I'm sorry. Can you say that again?
Q. You said you have heard of that?
A. Of what? Of the --
Q. Of the bus, a large bus, is moving -- strike that. Let's make it more specific for you.
If a J4500 is moving forward at 30, 35 miles an hour, is it your understanding that there are no air blasts, some air blasts, air blasts

002417

002417

on some occasions?

A. I don't -- I don't know, sir.

Q. Don't know one way or the other?

A. No, sir.

Q. Okay. And we've referred to a number of different types of buses that you said you drove. And I wrote down that you drove -- one was Serta; right?

MR. CHRISTIANSEN: Setra.

MR. KEMP: I started off wrong and I'm going to screw up the whole case.

BY MR. KEMP:

Q. You have driven a Setra before?

A. Yes.

Q. Is that a Setra 417?

A. I don't know the number. I just know it's a Setra.

Q. Okay. And you've also driven a Volvo?

A. Yes, sir.

Q. And what were the other -- the MCI we talked about. What were the other two?

A. Prevost.

Q. P-r-e-v-o-s-t?

A. Yes.

Q. And what else?

into account in how you drove your bus?

MR. STEPHAN: Objection to form.

THE WITNESS: I've answered it. I don't know, sir. I don't know what you want me to say, but ...

BY MR. KEMP:

Q. Is there a reason you wouldn't take that into account?

A. Take what into -- the wind? I don't know anything about the wind.

Q. Assuming for the sake of argument that someone had told you --

A. I couldn't -- I can't answer that question because I don't know anything about the wind and I don't know who's telling me. I don't know --

Q. Okay. Well, let me make it more specific then.

Assuming today you got a bulletin from the manufacturer of the bus that said, Our bus creates a 10-foot air blast on the front, would you take that into account when you were driving the bus tomorrow, the next day, on?

MR. STEPHAN: Objection to form.

Answer.

THE WITNESS: Yes, sir.

BY MR. KEMP:

Q. And the reason you would take it into account is because why?

A. Because the bus manufacturer's telling me that it -- or --

Q. That it's a potential safety hazard; is that right?

A. Yeah.

Q. That's the reason you would take it into account, right?

A. I'm sorry?

Q. Right? That's the reason you would take it into account?

A. Because if that was part of my training, yeah. If that's what they told me, right.

Q. All right. Now let me ask you a related question.

Has anyone ever indicated to you that the rear tires on a bus can create a negative air situation, where people are sucked into the bus?

MR. STEPHAN: Objection to form.

BY MR. KEMP:

Q. Has anybody ever said that to you?

A. No.

MR. STEPHAN: Sorry. I didn't mean to interrupt. I don't really want to keep interrupting.

MR. KEMP: No, you're just supposed to say "Form; foundation." That's all you've got to say.

MR. STEPHAN: That's all I'm doing.

MR. KEMP: Believe me, I do it myself.

MR. STEPHAN: Thank you, sir.

BY MR. KEMP:

Q. Okay. Let's just make sure we got this down.

So you didn't have any information from any source, including the manufacturer, that there was some sort of suction when you're driving a J4500 at 30, 35 miles an hour, that would pull objects or potentially pull objects or people into the rear wheels?

MR. STEPHAN: Form; foundation.

THE WITNESS: No.

BY MR. KEMP:

Q. And when I say "the manufacturer," I'm referring to MCI, the manufacturer of the J4500.

You didn't have that information?

A. No.

Q. And in -- any source, you didn't know that from any source, right?

A. No.

Q. Now, same question that I asked before. If MCI had sent you a directive saying, Hey, you know, the rearview [sic] wheels potentially create a suction that can pull people in, would you take that into consideration in the future when you were driving the bus?

MR. STEPHAN: Form; foundation.

THE WITNESS: Yes.

BY MR. KEMP:

Q. And for the same reason; that it was a safety hazard, potential safety hazard?

A. Part of my training.

Q. Part of your training to be aware of potential safety hazards?

A. Correct.

Q. So if you knew that there were either air blasts or suction in the rear tires, you would -- you would take that into account in how you drive the bus?

MR. STEPHAN: Form; foundation.

THE WITNESS: Yes.

BY MR. KEMP:

002422

002422

Foundation.

THE WITNESS: I -- I would -- if something's going to alert me that I'm about to hit something before I hit it, or someone before, of course I'm going to do something.

But I don't know that that would have changed that situation, because of the maneuver that the gentleman made by just coming in as -- it was like this (indicating).

BY MR. KEMP:

Q. Okay.

A. It was -- it was -- it was a very -- that's --

Q. But if there had been some sort of warning light going off for whatever reason, you would have -- you would have heeded that?

MR. TERRY: Objection; form.

THE WITNESS: Again, I don't -- I don't know that.

BY MR. KEMP:

Q. My Mercedes has a proximity sensor. If there's a car to my right or an object to my right, there's a big red light that goes off in the mirror. You know? And there's a lot of cars where, if you do that, there's an audible warning.

If something like that had happened and you'd become aware that he was in that spot, even if you didn't see him, would you have done something about it?

A. I would have did exactly what I just did.

MR. TERRY: Objection to form.

THE WITNESS: Which was take evasive action to move away from the bike.

BY MR. KEMP:

Q. So if you'd been given some sort of warning at the 50 or the hundred, you would have taken evasive action earlier?

MR. TERRY: Objection; form.

THE WITNESS: Yes.

BY MR. KEMP:

Q. And the same, if one of your passengers had said, Hey, you're getting close to a bicyclist, at the 50 or the 100, you would have taken evasive action earlier?

A. Of course.

MR. STEPHAN: Will, he doesn't have the microphone on. Can you make sure we're getting this?

MR. KEMP: Are you getting this?

have a viewpoint.

BY MR. CHRISTIANSEN:

Q. Okay. Well, both of those gentlemen testified that they see in front of the bus that bicycle the entire way until the collision, the entire way southbound on Pavilion Center. Did you know that?

MR. STEPHAN: Objection; foundation. Form.

THE WITNESS: No.

BY MR. CHRISTIANSEN:

Q. And you did not see the bicyclist after the 300-foot mark that you told for us, when you believe you passed him at the cutout to the municipal bus stop?

A. Correct.

Q. You don't see him for a full 300-plus feet, until he just appears in your lane, right? That's your testimony?

A. Yes.

Q. And both of those gentleman who were seated behind you testified that he's in front of you and they can see him the entire way southbound down Pavilion Center.

MR. STEPHAN: Objection; form.

002425

002425

002426

002426

EXHIBIT 14

DISTRICT COURT

CLARK COUNTY, NEVADA

KEON KHIABANI and ARIA KHIABANI, minors by and through their natural mother, KATAYOUN BARIN; KATAYOUN BARIN, individually; KATAYOUN BARIN as Executrix of the Estate of Kayvan Khiabani, M.D. (Decedent), and the Estate of Kayvan Khiabani, M.D. (Decedent),

Plaintiffs,

vs.

MOTOR COACH INDUSTRIES, INC., a Delaware corporation; MICHELANGELO LEASING, INC. d/b/a RYAN'S EXPRESS, an Arizona corporation; EDWARD HUBBARD, a Nevada resident; BELL SPORTS, INC. d/b/a GIRO SPORT DESIGN, a California corporation; SEVENPLUS BICYCLES, INC. d/b/a Pro Cyclery, a Nevada corporation; DOES 1 through 20; and ROE CORPORATIONS 1 through 20,

Defendants.

Case No. A-17-755977-C
Dept. No. XIV

VIDEOTAPED DEPOSITION OF ERIKA BRADLEY

LAS VEGAS, NEVADA

TUESDAY, AUGUST 15, 2017

REPORTED BY: HOLLY LARSEN, CCR NO. 680, CA CSR 12170
JOB NO.: 407961A

002427
002427

Q. As we sit here today, do you know what made the bicyclist swerve?

A. I don't know.

Q. Could it have been windblast from the front of the bus?

MR. NUNEZ: Form objection.

THE WITNESS: It's possible.

BY MR. KEMP:

Q. Okay. Is there anything else you can think of that would make the bicyclist swerve based on what you'd seen of him?

MR. ROBERTS: Objection. Foundation.

THE WITNESS: When we were standing on the side talking and waiting for people to arrive, I remember speaking with one of the security guards. He had mentioned that they have bicyclists that bike from Red Rock and sometimes they get dehydrated and dizzy and that that could have happened. That made sense to me. At that point -- other than that, I didn't know what would have caused that to happen.

BY MR. KEMP:

Q. So the two operating theories are either a windblast or perhaps the bicyclist was physically impaired?

A. Correct.

002428

002428

Q. Okay. Anything besides that?

A. Not that I could think of.

Q. Okay. And as we sit here today, which makes more sense to you now?

A. After discussing the wind drafts, that could make sense.

MR. ROBERTS: Objection. Foundation.

BY MR. KEMP:

Q. So as we sit here today, you think it's more likely than not that the bicyclist started wobbling because of windblast?

MR. FREEMAN: Objection. Foundation.

THE WITNESS: That could be a possibility.

BY MR. KEMP:

Q. Okay. It could be a possibility, but that's the most likely possibility as we sit here today; right?

MR. ROBERTS: Objection.

MR. FREEMAN: Objection.

THE WITNESS: I'm not a scientist. I can't make that judgment.

BY MR. KEMP:

Q. Okay. I'm just asking what you saw.

A. Right.

Q. Okay. All right. Now, with regards to how

002429

002429

Q. Did you notice anything about whether his helmet was crushed or not, bicycle helmet?
A. I did not pay attention to his helmet.
Q. Do you know whether or not he had a bicycle helmet on at the time of --
A. He did have a helmet on.
Q. So you think his torso was crushed by the bus; is that correct?
A. I don't recall specifically. I think it was either, yes, his torso -- I don't think it was his legs.
Q. Okay. And what about the head? Do you know whether or not the head was impacted by the bus?
A. That, I don't know for sure.
Q. Don't know one way or the other?
A. No, sir.
Q. Okay. Let me show you a video that depicts a safety device known as the S-1 Gard.
(Video played.)
MR. KEMP: Okay. Stop.
BY MR. KEMP:
Q. First of all, with the exception of the safety device pushing the rider out of harm's way, that was pretty much the way you think the bicycle

rider in this case fell into the bus?

A. Yes.

MR. ROBERTS: Objection. Leading.

BY MR. KEMP:

Q. Torso under the back two tires?

A. I believe so, yes.

Q. Okay. So that video would be substantially similar to what you think happened?

A. Yes.

Q. Okay. Now, with regards to -- let me show you an actual S-1 device.

Okay. What this does is it fits on to the -- excuse me. It fits on the other way -- to the front of the back rear tire here and then here's the curved part. You understand from the video and looking at this how it works mechanically?

A. Uh-huh.

Q. Okay. Based on the facts as you saw them, do you think a device such as this would have saved the doctor?

MR. ROBERTS: Objection. Foundation.

THE WITNESS: It's possible.

BY MR. KEMP:

Q. Okay. I know it's possible, but based on what you saw and what you remember, do you think

002431

002431

002432

002432

EXHIBIT 15

DISTRICT COURT
COUNTY OF CLARK, NEVADA

KEON KHIABANI and ARIA KHIABANI, minors by and through their natural mother, KATAYOUN BARIN; KATAYOUN BARIN, individually; KATAYOUN BARIN as Executrix of the Estate of Kayvan Khiabani, M.D. (Decedent), and the Estate of Kayvan Khiabani, M.D. (Decedent)

Plaintiffs,

vs.

MOTOR COACH INDUSTRIES, INC., a Delaware corporation; MICHELANGELO LEASING INC., d/b/a RYAN'S EXPRESS, an Arizona corporation; EDWARD HUBBARD, a Nevada resident; BELL SPORTS, INC. d/b/a GIRO SPORT DESIGN, a California corporation; SEVENPLUS BICYCLES, INC. d/b/a Pro Cyclery, a Nevada corporation; DOES 1 through 20; and ROE CORPORATIONS 1 through 20,

Defendants

Case No. A-17-755977-C

Dept. No. XIV

Job No.: 430151

****

ORAL DEPOSITION OF
ROBERT RUCOBA
November 10, 2017

****

002433
002433

Correct?

A. I would agree with that.

Q. Okay. So can we rule out weather as a cause of the bicycle wobble?

A. Sure.

Q. All right. So what I'm left with is plaintiff's theory of windblast and no -- no evidence for any other cause.

MR. BARGER: Form.

Q. (By Mr. Kemp) I know you don't agree with windblast. I'm not suggesting you do. But none of the other causes have -- potential causes, six, you have any evidence that supports them.

A. And, again, with regard to wobble, I don't know how many times I've had to say this, but it's -- there is no physical evidence that I can rely upon. It's purely based on testimony. That's all we have to go with. Now, if we're going to talk about the causes of the crash, those are the factors I outlined for you at the beginning of the deposition.

Q. We'll get to the causes of the crash. You know, I always like to start at the beginning, which is the wobble, and then move to the contact. Okay? We'll get to the contact, I promise.

Are you familiar with that system?

A. Yes. Her's, I believe, does give you some sort of an audible signal as well.

Q. Okay. Did that come with the car or did you order that as an option?

A. I ordered that as an option.

Q. And why did you think a blind-spot warning system in your wife's Kia would be a good option?

A. Well, my wife's not a very good driver. I thought this would be an assistance to helping her drive better.

Q. Do you drive the car yourself?

A. I do.

Q. Have you found it to assist you well -- as well?

A. It's helpful.

Q. And I assume you're a good driver.

A. I think I am.

Q. Okay. So even a good driver like you can be assisted by a blind-spot warning system. Correct?

A. Sure.

Q. Have you had any problems when you're driving the Kia, you personally, when things

002436

002436

EXHIBIT 16

Robert E. Breidenthal
5722 NE 56th Street
Seattle, Washington 98105-2004

Daytime telephone (206) 685-1098
Home telephone (206) 522-8718
Fax (206) 543-0217
E-mail breidenthal@gmail.com

October 24, 2017

Eric Pepperman, Esq.
Attorney
Kemp, Jones & Coulthard, LLP
Wells Fargo Tower, 17th Floor
Las Vegas, NV 89169

Dear Eric:

I have reviewed the additional materials you sent me concerning the case of Khiabani v. MCI, which include

i) Opinion letter of Dr. James R. Funk dated October 19, 2017

ii) Opinion letter report of Mr. Kevan J. Granat dated October 18, 2017

iii) "A wind tunnel investigation of the aerodynamic characteristics of buses for motor coach industries", K. R. Cooper. Motor Coach Industries Engineering Test Report 93-0026, Institute for Aerospace Research, LTR-AA-9, August 1993.

My opinions are based on these documents.

1) The aerodynamic force on a cyclist depends on the speed of the relative wind. Thus the aerodynamic force on a moving cyclist would be different from the measured force on a stationary cyclist dummy. The force measurements on a cyclist reported by Mr. Granat (Reference ii) appear to be limited to an ATD cyclist dummy that is stationary.

2) The effect of the aerodynamic force on the dynamics of the cyclist will depend on the total impulse of the force, which is the integral of the force over time. The time interval that the force acts on a cyclist, and hence this integral, will be greater for a cyclist moving along in the same direction as the bus than for a stationary dummy because the bus passes a stationary dummy more rapidly than it passes the moving cyclist. Thus the impulse depends on the relative speed of the bus and the cyclist. The duration of the aerodynamic force increases over that on a stationary dummy by about a factor of about 2.2 for the moving cyclist at 13.5 mph and the bus speed of 25 mph, with a relative speed of 11.5 mph. Mr. Granat's Report (Reference ii) does not mention any impulse measurements.

3) This report also does not indicate the frequency response of the load cell used to measure the force. If the frequency response of the load cell is inadequate, the measurement of the transient force will not be correct. Neglecting ambient wind, the lateral airflow on a stationary dummy both before and after bus

passage is zero. Consequently, the average lateral aerodynamic force is also essentially zero. A slow load cell will tend to smear out the oscillating transient force and yield a low peak force.

4) Even with a perfect load cell of infinite frequency response, the inertia of the stationary dummy will tend to reduce the output of the load cell under rapidly oscillating aerodynamic loads. Only if the mass of the test dummy apparatus was zero would the force applied to the load cell equal the true instantaneous aerodynamic force. According to page 5 of Mr. Granat's Report, the ATD cyclist combination weighs 214.5 lbs. For the reasons listed in paragraphs 1-4, the force experiment with the stationary dummy is not similar to what occurred in the accident.

5) According to page 7 of the opinion letter of Dr. Funk, the cyclist's speed was approximately 13 - 14 mph. Using a figure of 13.5 mph instead of the value of 8 mph assumed in the illustrative example in my opinion letter of October 4th, I estimate that the magnitude of the oscillating lateral force on the cyclist is again approximately 10 lbs. The other assumptions are unchanged (an ambient wind out of the west of 6 mph, a local flow speed of 40 mph with respect to the bus at the position of the cyclist near the right front corner of the bus and a 30 degree angle of that flow). This estimate is conservative in the sense that it does not account for the additional contribution from a lateral pressure gradient toward the bus associated with curved streamlines near the region of separated flow.

6) The aerodynamic testing of various bus geometries in the MCI wind tunnel report (Reference iii above) indicates that by modifying only the shape of the front of the bus, the drag coefficient was reduced from 0.558 ("Standard CJ3") to 0.357 ("Proposal 2") at the higher tunnel speed of 120 km/h, a reduction of about 36% (Table 6.1 on page 13). This decrease in drag coefficient corresponds to a reduction in the region of separated flow, so that the effective aerodynamic width of the bus is reduced. Another shape, "Proposal 1", performed nearly as well. It appears that MCI did not use the optimum combination Proposal 2 with the beveled aft end in the accident bus.

002438

Very truly yours,

Robert E. Breidenthal

Robert E. Breidenthal

002439

002439

EXHIBIT 17

Alexander W. LaRiviere
Bicycle Accident Investigations
11842 Diggles St. / P.O. Box 130
Fort Jones, CA 96032

December 08, 2017

Will Kemp, Esq.
Kemp, Jones & Coulthard,LLP
Wells Fargo Tower, 17th Floor
Las Vegas, Nevada 89169

AMENDED REBUTTAL REPORT

Re: Khiabani vs. MCI

Dear Mr. Kemp:

I am amending my Rebuttal Report dated 10-22-2017. The opinions contained within my Rebuttal report dated 10-22-2017 have not changed, new field work was performed in support of my previously expressed opinions. The fieldwork that I performed demonstrates how a 35 mph wind force was measured to generate approximately 5.0 pounds of force upon the forward left side of a front wheel tire assembly, and how when 5.0 pounds of force is laterally placed upon a front wheel tire assembly it produces approximately 10.0 pounds of force on the left side of the handlebar, when measured 4 inches from the center of the stem clamp on the left side of the handle bar, along the angle of the steering column, to the corresponding location on the seat post.

An exemplar Scott Racing road bicycle was loaded with a person weighing 192 pounds. The person was mounted upon the seat and was measured for weight distribution under the front and rear tires. A mounted calibrated load cell was used to measure the weight under each tire. The weight distribution was measured with the rider in three different seated riding positions; (a) no hands on the handlebars, (b) only the right hand on the handlebar, (c) both right and left hands on the handlebars. The weight under each of the front and rear tires was measured at each hand position.

Results: (a) Front wheel, no hands 65 lbs.
(b) Front wheel, right hand only 77 lbs.
(c) Front wheel, both hands 86 lbs.
(d) Rear wheel, no hands 121 lbs.
(e) Rear wheel, right hand only 137 lbs.
(f) Rear wheel, both hands 147 lbs.

The exemplar Scott Racing bicycle was then loaded with weights, the front wheel was placed upon a load cell and was measured at 65 pounds. The bicycle's front wheel tire assembly, with 65 pounds measured under the front tire, was then placed upon a smooth piece of used roadway asphalt, a

002440
002440
002440

calibrated push/pull scale was used to measure the pounds of force exerted by the 35mph wind speed. A modified van traveling at approximately 35 mph was used to create the 35mph wind speed. The bicycle was mounted within the van, perpendicular to the van, approximately in the middle of the van. The piece of asphalt was mounted to a platform which extended beyond the side of the van, the front wheel of the bicycle was extended out the open side of the van approximately 15 inches (the side door of the van had been removed). When the van was traveling at approximately 35mph, approximately 5 pounds of lateral force was measured on the side of the tire, at the rear portion of the front wheel tire assembly.

Handlebar Leverage Test: When the van was traveling at approximately 35mph, using a calibrated push/pull force gauge which was mounted between the left side of the handlebar (at two different locations) and the seat post, along the angle of the steering column, the force was measured at 10 pounds of force at 4 inches from the center of the stem and 5 pounds at 8 inches from the stem.

Additional Opinion: It is my opinion, that the Scott Racing bicycle that I used for my testing is substantially similar to the subject bicycle, and the results would be the same if the subject bicycle were used for same testing.

Attached to this report are 6 photos depicting the methodology I used.

002441

Respectfully submitted,

Alexander W. LaRiviere

002441

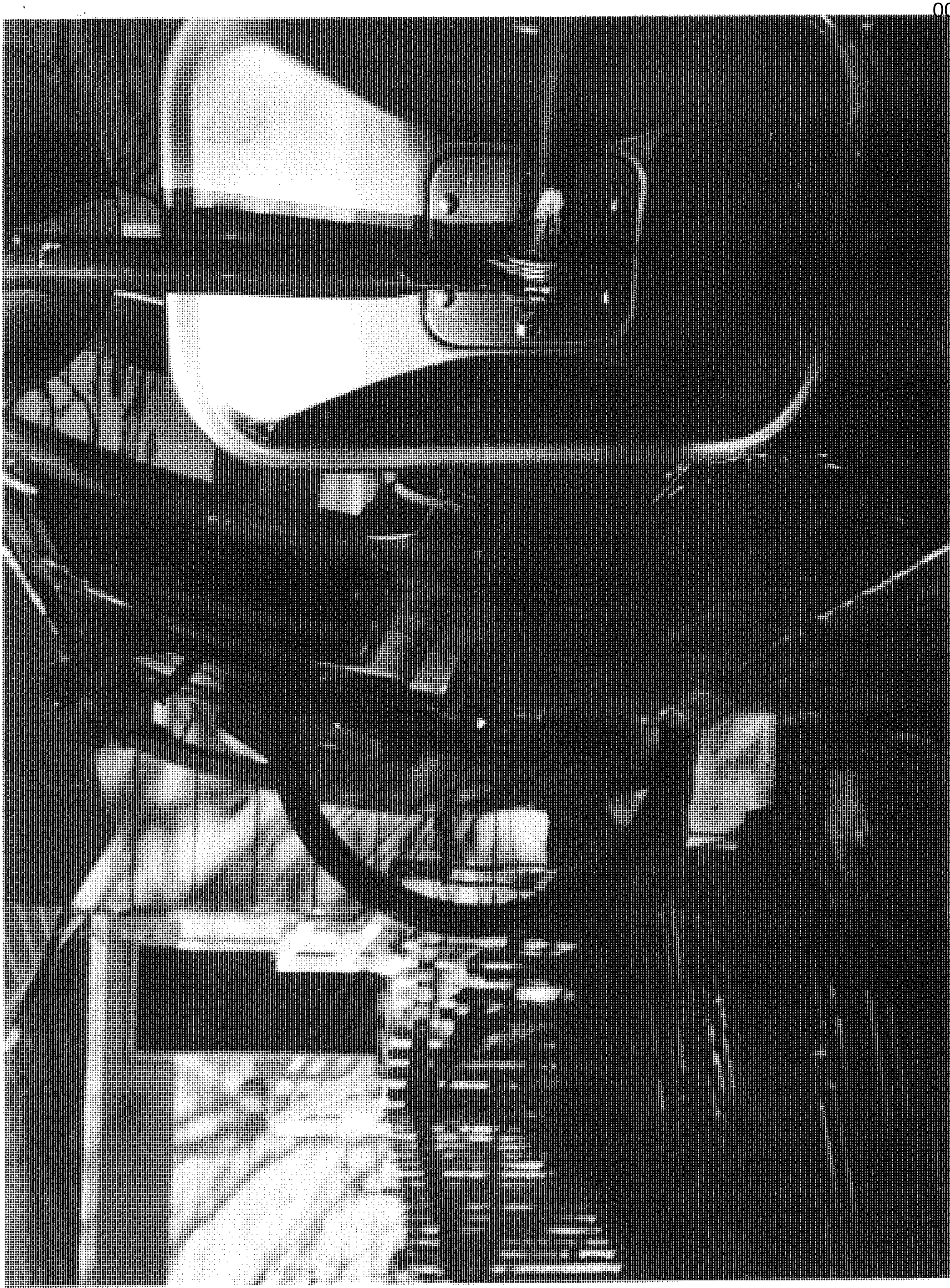

002442

002442

002443

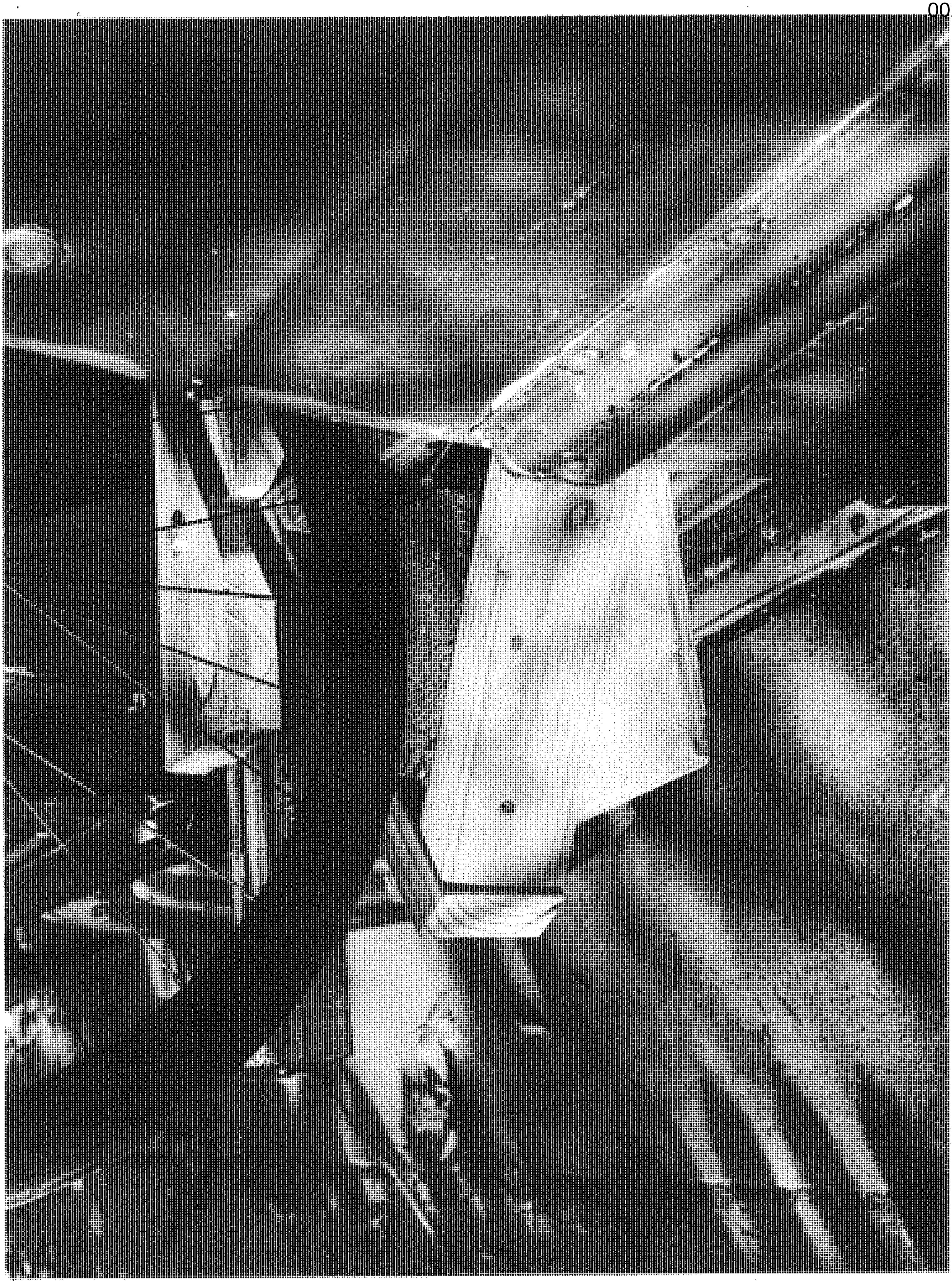

002443

002443

002443

002444

002444

002445

002445

002445

002446
002446

002446

002447

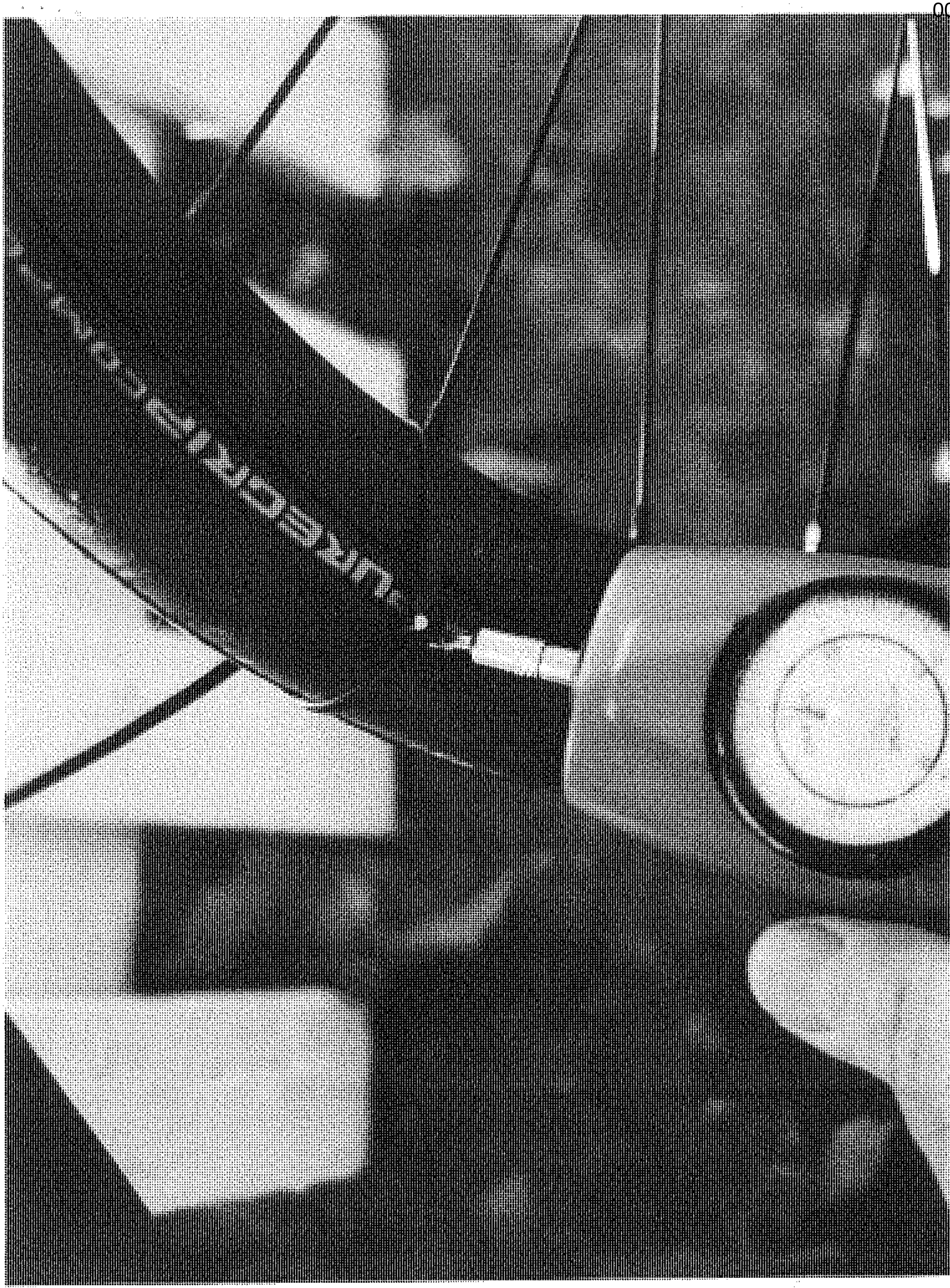

002447

002447

002447

002448

002448

EXHIBIT 18

002448

DISTRICT COURT

CLARK COUNTY, NEVADA

KEON KHIABANI and ARIA KHIABANI, minors by and Through their natural mother, KATAYOUN BARIN; KATAYOUN BARIN, individually; KATAYOUN BARIN as Executrix of the Estate of Kayvan Khiabani, M.D. (Decedent) and the Estate of Kayvan Khiabani, M.D. (Decedent),	)	
Plaintiffs,	)	
vs.	)	Case No. A-17-755977-C Dept. No. XIV
MOTOR COACH INDUSTRIES, INC., a Delaware corporation; MICHELANGELO LEASING, INC., d/b/a RYAN'S EXPRESS, an Arizona corporation; EDWARD HUBBARD, a Nevada resident; BELL SPORTS, INC. d/b/a GIRO SPORT DESIGN, A California corporation; SEVENPLUS BICYCLES, INC. d/b/a Pro Cyclery, a Nevada corporation; DOES 1 through 20; and ROE CORPORATIONS 1 through 20,	)	VIDEOTAPE AND ZOOM VIDEOCONFERENCE DEPOSITION OF MICHAEL CARHART, PH.D.
Defendants.	)	

Tuesday, December 12, 2017

10:05 a.m. to 12:56 p.m.

Pages 1 through 141, inclusive, Volume I

Job Number 434820

002449

002449

bus manufacturer should reduce the drag coefficient, if possible?

A. Well, I -- I think there's a -- there's probably a benefit with respect to fuel economy.

Q. So you --

A. Now -- now, that --

Q. -- think --

A. -- that might have to be balanced against whether it still looks like what it needs to look like in order to serve its function, if -- if it's geometrically consistent with what it needs to do. Things like that.

Q. So fuel economy and other reasons, you would agree that a manufacturer should reduce the drag coefficiency of their busses?

A. They -- they could, to improve fuel economy.

Q. And they should?

A. They could.

Q. Was there a reason they shouldn't improve fuel -- fuel economy?

A. Well, again, to maintain the other functions of the bus, coach, whatever it is.

Q. All right. Now, assuming for the sake of argument that you could have reduced the drag

coefficiency by a factor of 2, in other words, cut it in half, would you expect that the air displacement coming off the front of the bus would also be reduced?

A. Oh, I haven't done -- I haven't done the calculation, but half of a pound is still -- is still insignificant and trivial in the context of controlling a bicycle.

Q. And when you say it's insignificant and trivial, you don't know what one half of a pound will result in on the handlebar; is that right?

A. It's not exerted on the handlebar, sir.

Q. If you exert pressure on the tire, does it not transmit the pressure to the right handlebar?

A. I -- I guess you're arguing some hypothetical where the -- the load is only on the three o'clock position on the tire, and I'm just having trouble with that.

Q. So you think if there's air displacement coming off the bus, it hits all of the tire equally at all times?

A. Well, you -- you're arguing that it's somehow differentially affected, and I -- I don't -- I don't see that basis. And -- and you need --

Q. Dr. Kato --

A. -- cross-sectional area for the load to accumulate. And I --

Q. That's what Dr. -- that's what Dr. Kato's paper said that you agreed with a minute ago.

A. I -- I did not agree with your proposition. That this is a load exerted on a --

Q. But you're --

A. -- portion of the --

Q. You --

A. -- tire? You're -- you're -- you're just mixing up the words that he's got in his text.

He isn't talking about load being applied to a portion of the bicycle tire. He's talking about a load in the outward direction on the bicycle and rider, and he's talking about a load in the inward direction. We evaluated those, Mr. Granat measured those. He evaluated their magnitude. They are small.

Q. Let me know when you -- you're done and I'll ask my next question.

A. I'm through.

Q. Okay. So when you say it's insignificant and trivial, you can't tell -- tell me what you think would be significant and non-trivial in terms of an air blast.

A. I -- I -- you know, I didn't take it up to a destabilizing condition. We -- we evaluated loads that were four and a half times through the rocket engines what the disturbance is from the bus. Didn't -- didn't do anything. It was barely perceptible. I think what was percept --

Q. Four and a half times --

A. -- what was perceptible was the -- the noise of the rocket firing, but in terms of the load, I could barely perceive that.

Q. Okay. Four and a half times what?

A. Four and a half times the load levels measured when the bus passed the cyclist, the -- the ATD cyclist at 25 miles an hour.

Q. One of which was two and a half? Yes?

A. That was inside 2 feet.

Q. So you're saying that you used this rocket test to measure 4.5 times 2.5?

A. No. The majority of Mr. -- Mr. Granat's observations were below 1, and the one that you're focused on was on a very tight pass.

Q. Well, the witness testimony is that the bike was within 1 and 2 feet of the bus, right?

A. There's witness testimony all over the map. There's witness testimony that the bus moved into the bike lane.

MR. KEMP: All right. Why don't we take our first break.

THE VIDEOGRAPHER: Please stand by.

This will mark the end of video number one. The time is 11:24 a.m. We are off the record.

(Off record, in recess from 11:24 a.m. to 11:36 a.m.)

THE VIDEOGRAPHER: We are on the record. The time is 11:36 a.m.

This marks the beginning of video number two in the deposition of Michael Carhart, Ph.D.

Please begin when ready.

BY MR. KEMP:

Q. All right. Doctor, could we look back at Exhibit 2, please, your December 6th, 2017, report.

A. I'm ready.

Q. Okay. And I'm interested in page 2 where you say, quote, "The projections demonstrate a lack of compression of the EPS foam liner in the region on the left side of the helmet."

A. Right.

Q. What -- what does that mean?

A. Well, as I understood Dr. Stalnaker's testimony, he opined that the helmet was overrun, and

002455

002455

EXHIBIT 19

DISTRICT COURT

COUNTY OF CLARK, NEVADA

KEON KHIABANI and ARIA KHIABANI, minors by and through their natural mother; KATAYOUN BARIN; KATAYOUN BARIN, individually; KATAYOUN BARIN as Executrix of the Estate of Kayvan Khiabani, M.D. (Decedent), and the Estate of Kayvan Khiabani, M.D. (Decedent), Plaintiffs, vs. MOTOR COACH INDUSTRIES, INC., a Delaware corporation, et al. Defendants.	)	Case No. A-17-755977-C

DEPOSITION OF DAVID KRAUSS, PH.D., taken on behalf of Plaintiff, at 12777 West Jefferson Boulevard, Suite 300, Los Angeles, California, 9:17 a.m., Thursday, November 9, 2017, before LINDA D. WHITE, Certified Shorthand Reporter Number 12009 for the State of California, pursuant to Notice.

Job No.: 430147

REPORTED BY:
LINDA D. WHITE, CSR NUMBER 12009

002456

002456

BY MR. KEMP:

Q. And the reason I think you said to have proximity sensors is that in the case where there are blind spots, it might alert the driver to a potential hazard, right?

A. Well, there are a lot of reasons for proximity sensors, right? One is kind of the blind spot detector. Like I said, I've got the kind in my wife's car when we pull into the garage and as we approach that front wall, it beeps at us. That's very useful.

Backing up, you're getting close to a vehicle. It beeps at you. Those are all proximity sensors. And depending what the maneuver is and where they're located, they can be extraordinarily useful. For this particular application, they don't help.

Q. And this particular application we're talking about is not running over Dr. Khiabani?

A. Preventing this particular accident, yes.

Q. And in your report you indicate that this bus does have a blind spot of -- I think you said 52 inches. Is that what you said? It's on Page 5, underneath Figure 1.

A. It's about a 40-inch -- oh, wait. Bear with me. Hang on.

So that was at five feet out. You lose the visibility of the bicyclist completely for about 40 inches.

At three feet away you always have at least partial visibility of a cyclist.

Q. And by partial visibility, you're talking about the top of his head, a piece of the handlebar or something?

A. Yeah. It could be something small like that. That's how we define sightlines. And you need to bear in mind when you look at these. I agree with you. If we take a snapshot, which I've actually done in the report here, and show kind of what you're describing, you're absolutely right.

I mean, if you're riding along or you're next to somebody and that's all you have continuously, I agree. That's not that useful. But when you're doing a visibility study and quantifying sightlines, those count because it's dynamic.

So, for example, if you see the bike up ahead, you have that input that at some point, yes, part of it's going to disappear. Maybe all you need is a much smaller signal.

And that's really what we have is when

you're far back, you can see more of the bus. When you pass the bus more -- or sorry -- pass the bike more, you can see more of the bike through the mirrors. That's really what I'm getting at here is you have to quantify. You have to have a cutoff of when it disappears for that reason.

Q. So what you're saying is that -- is when the bike's five feet away from the bus, when the front axle of the bicycle was between 6 and 46 inches from the front of the bus, none of the bicycle was visible?

A. Correct. That's through windows and/or the mirrors.

Q. So that would be a 40-inch blind spot at the right corner, basically?

A. A blind spot is universal, right? It's not just the right corner. It's when the bus is five feet laterally separated from the bus to the right of the bus. When it's between, again, six inches and 46 inches from the front, you lose visibility of the bus for that period of time.

Q. You lose visibility of the bike?

A. Sorry. Of the bike. Excuse me.

Q. So given the fact you have this 40-inch blind spot, you think you should have proximity

002459

002459

sensors on the bus or that you should not have proximity sensors?

A. Well, again, a 40-inch gap here may sound material on the page, but let's just take passing a bike. Let's say, that we're passing at the same 13-mile per hour speed differential, 20 feet per second.

(Reporter requests clarification)

THE WITNESS: We're going to cover 40 inches and -- what is that -- about a quarter of a second.

BY MR. KEMP:

Q. Uh-huh.

A. So it's -- that's about a quarter of the time of a typical glance to a mirror. So you may look up and there may not be anything there, but it will appear before you even have time to look away from the mirror.

Q. Okay. You do understand that the bus was approaching an intersection at the time of impact?

A. I do.

Q. And usually when you approach intersections, you look left to the adjoining traffic, the traffic that is coming in to you?

A. Not when there's a traffic signal, not typically.

Q. So you just blow through the green and you don't look to see whether people have actually stopped? That's your practice?

MR. RUSSELL: Objection. Foundation; relevance; speculation.

THE WITNESS: Typically, the case is we put a lot of faith in our traffic signals. Yes.

BY MR. KEMP:

Q. So you don't think Mr. Hubbard should have looked to the left to see if the other people were obeying the red light traffic signal before he went through the intersection?

A. So to the extent it had just turned red, which I don't think we have any testimony on the timing of the phasing, no. I mean, he was going through. It was clear. Nobody was encroaching on his path. He was right about that. And people typically don't look left and right when they go through a green light.

Q. Well, actually, the training manual for the bus company says he should look left and right when he's going through a light. That's what they train these people to do.

A. Okay. That's fine. I'm not saying it's a bad practice. Saying typically when you study driver-looking behavior, you have a green and you're going straight, you continue on doing that.

Q. Okay. All right. So I think you said that you don't know one way or the other whether the J4500 has ever had proximity sensors or other blind spot detection capability, right?

A. Correct.

Q. Okay. Why don't we take a look at Exhibit 6. Yeah.

A. Okay.

Q. And this is a brochure for the current edition of the J4500, the 2017/2018 edition. And I would ask you to look specifically at Page 21 where it talks about specifications. You looking at 21?

A. Getting there. Okay.

Q. And Item Number 2 is the Bendix wingman advance system with adaptive cruise control and collision mitigation functionality. And then the second to the last item is the side-view cameras integrated into the mirror head. Do you see those two things?

A. I do.

Q. Okay. Prior to today, did you know that the current edition of the J4500 came equipped with a wingman system made by Bendix that has collision

002463

002463

EXHIBIT 20

DISTRICT COURT

CLARK COUNTY, NEVADA

KEON KHIABANI and ARIA KHIABANI, minors by and through their natural mother, KATAYOUN BARIN; KATAYOUN BARIN, individually; KATAYOUN BARIN as Executrix of the Estate of Kayvan Khiabani, M.D. (Decedent), and the Estate of Kayvan Khiabani, M.D. (Decedent),

Plaintiffs,

vs.

MOTOR COACH INDUSTRIES, INC., a Delaware corporation; MICHELANGELO LEASING, INC. d/b/a RYAN'S EXPRESS, an Arizona corporation; EDWARD HUBBARD, a Nevada resident; BELL SPORTS, INC. d/b/a GIRO SPORT DESIGN, a California corporation; SEVENPLUS BICYCLES, INC. d/b/a PRO CYCLERY, a Nevada corporation; DOES 1 through 20; and ROE CORPORATIONS 1 through 20,

Defendants.

Case No. A-17-755977-C
Dept. No. XIV

VIDEOTAPED DEPOSITION OF VIRGIL HOOGESTRAAT

LAS VEGAS, NEVADA

FRIDAY, OCTOBER 13, 2017

REPORTED BY: HOLLY LARSEN, CCR NO. 680, CA CSR 12170
JOB NO.: 425410

002464
002464

Q. And by "spray pattern," you're just basically looking at where that goes?

A. Correct.

Q. Okay. Does that really have anything to do with aerodynamics?

A. I didn't think so. But, I mean --

Q. Okay. All right. Now, Item Number 4 asked for the general parameters of the design or engineering for right-side visibility for the time period 1997 to 2016. Do you see that one?

A. Yes.

Q. Okay. What were the general parameters limited to the E series and the J series?

A. At that time, we did a computer model that we'd look and we'd locate the eye in the driver's seat. And from that eye, get the view that the driver would see. There was studies done in that regard. There's no records of those studies because they were studies.

Q. Okay. Are those called line of sight or visibility optimization studies or something like that?

A. Well, we called them line of sight. It would show you what you could see from the driver's seat. You would locate the driver's eye and you

002465

002465

would look out as far as what the -- particularly the windshield and the wiped area and the defrost area and those kind of things are clear.

Q. When you do the line-of-sight study, how do you account for the fact that drivers are different sizes and they put their seats in different adjustment --

A. There's SEE guides on the 5 percentile, the 50 percentile, to 90 percentile. You try to move the eye relative to those.

Q. So you think there was computer modeling done for the E series and the J series?

A. It was not done for the J series. I think it was done for the E series because that would be common practice.

Q. Okay. And so the computer modeling in general was done to try to see what the driver would see with regards to, in this case we're talking about right-side visibility?

A. In this particular case, what he would see looking through the windshield to the mirror and down to the right-side visibility.

Q. And you said you don't think the computer modeling exists as we sit here today?

A. I have found no records of it. But back

002466
002466

scenario where it's all glass.

Q. Let's go to a real J4500.

A. Let's go real world.

Q. Okay.

A. If that's all right. And, yeah, it will -- it is a blind spot. Although because the driver is quite a ways away from it, the angle is very narrow for the right-hand A pillar. But an A pillar in all vehicles creates somewhat of a blind spot.

Q. Okay. And what about -- between the window and the bottom of the side of the bus there's something called a sill we've heard it referred to? The sill divides the window on the right side from the bottom. What do you call that?

A. You can call it anything you want. It can be called a sill.

Q. Okay. So the solid structure, if it is solid, of the bus, under the window from the sill on down, that would also be a right-side obstruction?

A. No.

Q. Why not?

A. Because when the driver is driving the bus, his number one thing is to look out the windshield to see where he's going.

Q. Okay.

002467

002467

is this a computer model, or what is this?

A. Both.

Q. So computer models were done for the J series?

A. No. I said they were not.

Q. Were not. Yeah, that's what I thought you said.

A. Previously I said they were not.

Q. Okay. So the only computer model is the one for the E series that no records exist for?

A. I presume they were done because that's our standard practice.

Q. So when you said they were done, you think -- you don't know for an actual fact that they were done. You think they may have been done. Is that fair to say?

A. I cannot tell you that they were done because I have found no records of them because we don't keep records of study. I'm saying it's just their standard practice.

Q. When you say "their standard practice," you're referring to MCI's standard practice or bus manufacturers in general or what?

A. Bus manufacturers in general would look -- do look into that.

retrofit on the whole brake control system. Again, you still have the engine communication system issue.

Q. Do you know, as we sit here, whether or not the WABCO system could be retrofitted to the pre-2014 J series?

A. I mean, if you replaced the engine, replaced the whole brake control system, and replaced the instrument panel and replaced all that --

Q. Why would you have to replace the brake system?

A. The brake control system.

Q. Okay.

A. If you replaced all -- the whole electrical system, the brake control -- I mean, it's a bus. If you took everything out of it down to the frame and started over, you could probably do it.

Q. Okay. That would be expensive I assume?

MR. RUSSELL: Objection. Foundation.

THE WITNESS: It would far exceed the value of the bus.

BY MR. KEMP:

Q. Okay. Was there any consideration to using a proximity sensor that did not include brake

002469

002469

involvement prior to 2014?

A. Not that I'm aware of.

Q. And are you aware that there are retrofit kits on the market for proximity sensors that will purportedly give you some sort of warning of side collisions?

A. There's a lot of aftermarket kits for various things out there.

Q. Okay. And do you know whether there's an aftermarket kit for proximity sensors that would serve as some sort of warning of side detection?

A. I'm sure there is. There's a lot of kits for various things out there.

Q. Okay. And has MCI investigated those?

A. Well, today MCI has a 360-camera system that it offers. It also offers a camera in the mirror.

Q. Okay. Before we get to that, let's talk about the off-market kits that we were talking about. Did MCI investigate whether or not to use any of those?

A. Not that I was involved in.

Q. Okay. And, in theory, that type of off-market kit could be retrofitted to a J series bus and at least have a warning feature if not an

moved out of the way of the rear tires?

A. There was several scenes that they had put together and I don't recall that one, but it could have been there.

Q. Okay. Let me ask it a little differently. Do you recognize that there's a theoretical potential that pedestrians or bicyclists could potentially be run over by rear tires of a bus under some scenarios?

A. There may be a scenario where that could occur.

Q. Okay. And generally -- you understand generally that that could happen under some scenarios?

A. It's possible that that could happen.

Q. Okay. And basically bus manufacturers have always known that?

MR. RUSSELL: Objection. Foundation. Outside the scope.

THE WITNESS: Have always known what?

BY MR. KEMP:

Q. Well, let's put it differently. You knew back in, let's say, 2000 that this was a potential scenario?

A. There's a potential that a bus tire can

002471

002471

Q. Okay. Has there been any consideration made to making a more extensive fender for the J4500?

A. I don't know what that means.

Q. Have you seen buses that they have the wall just cover the entire -- or coaches, excuse me, cover the entire rear wheel section with surface material?

A. Coaches?

Q. Yeah.

A. I've seen transit buses.

Q. Okay. You've seen transit buses like that.

A. I have not seen coaches.

Q. Okay. And what do you call a transit bus when it does that?

A. I don't know.

Q. Have you heard the term "spat"?

A. You can call it that, I guess, if that's what they call it.

Q. Have you heard that term?

A. I've heard the term "spat."

Q. Okay. And what does that mean to you?

A. It's just the decorative closeout over the tires, tire area.

Q. And would I be correct that spats preclude

002472

002472

humans from coming into contact with the tires to a greater extent than the fender on a J4500 would?

MR. RUSSELL: Objection. Foundation.

THE WITNESS: I don't know that. I don't see why it would.

BY MR. KEMP:

Q. Okay. If you have a person next to a J4500, there's basically no barrier between the tires and the person; right?

A. Certainly the tires are exposed if that's what you mean.

Q. Yeah, the tires are exposed. And in the transit bus with spats, the tires are not exposed; right?

A. Yeah, part of the tire is not exposed.

Q. Okay. And by -- basically there's 3 or 4 inches of the tire exposed. That's it; right?

A. I don't know the exact dimension. I know part of the tires are exposed.

Q. Has there been any consideration given to making the fender of the J4500 larger or more encompassing so less of the tire's exposed?

A. In a motor coach, we can't do that.

Q. Why is that?

A. A motor coach has tremendous -- is used in

002474

002474

EXHIBIT 21

DISTRICT COURT

COUNTY OF CLARK, NEVADA

-o0o-

KEON KHIABANI and ARIA KHIABANI, minors by and through their natural mother KATAYOUN BARIN, et al.,	)	
Plaintiffs,	)	Case No. A-17-755977-C Department No. XIV
vs.	)	
MOTOR COACH INDUSTRIES, INC., a Delaware corporation; MICHELANGELO LEASING, INC., dba RYAN'S EXPRESS, an Arizona corporation, et al.,	)	
Defendants.	)	

VIDEOTAPED DEPOSITION OF
MARY WITHERELL
AUGUST 24, 2017
RENO, NEVADA

REPORTED BY: AMY JO TREVINO, CCR #825, CSR #5296

JOB NUMBER 411087

002475

002475

Q What kind of car do you have?
A A Toyota Highlander.
Q And if I told you that since 2000 there has been proximity sensors in Mercedes that can detect whether a car is in front of you at a certain range, would that surprise you?
MR. ROBERTS: Objection, foundation.
THE WITNESS: Not with a Mercedes. I know new cars have lane detection in front, but --
MR. KEMP:
Q And when you were at Ryan's Express, did anyone at Ryan's Express design buses?
A Not that I'm aware of.
Q Did they make buses?
A No, sir.
Q Was MCI one of the companies that provided buses to Ryan's Express?
A Yes, sir.
Q Are you familiar with an MCI, model of an MCI bus called a J-4500?
A Yes, sir.
Q And is it your understanding that MCI made that particular bus?
A Yes, sir.
Q Did you expect that MCI would design its buses in a reasonably safe manner?

002476

002476

A Yes.

MR. ROBERTS: Objection, form, foundation.

MR. KEMP:

Q Go ahead.

MR. ROBERTS: You can answer, that's just for the court later on to rule on.

THE WITNESS: I would assume, yes.

MR. KEMP:

Q And why so?

A Just because it's a mode of transportation, just like all the car companies and everything.

Q And have you seen buses with proximity sensors?

A I have not, no.

Q And if I told you Volvo was making buses with proximity sensors, would that refresh your recollection in any way?

A Well, we had a couple of Volvos, but I don't recall that they had proximity sensors on them.

Q Do you think a proximity sensor based on your experience with buses would be a good safety feature for a bus?

MR. FREEMAN: Objection, foundation.

THE WITNESS: My opinion, my personal opinion yeah, it would be a good idea.

MR. KEMP:

Q Why is that?

002477

002477

mini buses. But basically I think that was it.

Q So quite a few different brands you have driven?

A Yes, sir.

Q And are you familiar with the standard of quality in the motor coach industry?

A Yes, sir.

Q Did you ever feel that the MCI J-4500 that you used to drive was unsafe as compared to other manufacturers' motor coaches?

A No, sir.

Q Mr. Kemp talked to you about visibility. Did you ever feel that you couldn't see enough in order to drive safely and avoid pedestrians and bicyclists and other motor vehicles?

A The older MCI, I know the mirrors you had more blind spots than the newer MCIs. But every bus you still, you can't just sit there, you got to move your head.

Q Okay. And even though you had never heard rock and roll, we got a video here, and you know that you moved your head back and forth to make sure --

A Right, you can't just sit stationary. You got to move to look.

Q That you are looking around blind spots or obstructions?

A Right. And the right side is the worst side.

Q Do you remember about what year of manufacturer you

002478

002478

cities it would be a good idea to have all cars have seatbelts?

A Yeah.

Q Same for air bags?

A Yes.

Q Same for proximity sensors?

A I think the -- right now is it required? No. Personal opinion, should, you know, maybe they be on buses, yes, but I can't speak other than that personal opinion.

Q Okay. And the reason you have that personal opinion is, as you already said, the right side is the quote, worst spot for blind spots, right?

A Correct. Yes, sir.

MR. ROBERTS: Objection, foundation.

MR. KEMP:

Q And that's based on your years as a bus driver and a bus safety analyst, it's your opinion that the right side of the bus is the worst spot for blind spots, correct?

A Correct, and also just as a CDL driver.

Q And by worst spot, do you mean less visibility on the right side than any other area?

A You have more blind spots on the right side than you do on the left.

Q So if you are going to put -- if you were going to put a proximity sensor on one side or the other, it should be on the right side certainly in your opinion?

A In my opinion, yes, sir.

Q Now, we talked about the MCI J-4500, and I believe Mr. Roberts misspoke, or someone misspoke, saying it didn't come out until 2010 or something like that. It actually came out in the year 2000. Are you aware of that?

A I don't recall exactly but sounds reasonable.

Q But in your view the older MCI, whatever that means, had a problem because the mirror had more blind spots; is that correct?

MR. ROBERTS: Objection, form.

THE WITNESS: It was the blind spot based on where it was positioned you had spots to the front, more blind spots, yes.

MR. KEMP:

Q And that would be the older MCI; is that correct?

A Yes, sir.

Q And as we sit here today do you know whether or not the 2008 MCI was what you would consider an older MCI?

MR. ROBERTS: Objection, form and incomplete.

THE WITNESS: It was older than 2008.

MR. KEMP:

Q Are you aware of what's commonly called a European mirror that comes from the top down as opposed to from the side of the bus up?

A On the Setras, like the Setras look like --

002480

002480

A Just my personal opinion, sir, yes.

Q And so just to make sure this is real clear on the record, in your personal opinion the Setra, with the overhead mirrors has less right side blind spots than a J-4500; is that correct?

A In my personal opinion, yes, sir.

Q So if the only factor was right side visibility, you would prefer a Setra over a J-4500?

MR. ROBERTS: Objection to form.

THE WITNESS: Personally, yes, sir.

MR. KEMP:

Q And we alluded to one of the potential criticisms of the overhead mirror is that some drivers aren't familiar with it, and they might bump into things going in and out of the yard; is that fair to say?

A Yes, sir.

Q But if you are a good driver that's not a problem, right?

A Yes, sir, but sometimes, you know, space requirements getting that bus in, you know, with the posts and pillars and you just got to be on your game.

Q Okay. Well, you got to be on your game anyway, because you are a common carrier, right?

A Correct.

Q Okay, and speaking about common carrier, Ryan's was

should be doing.

Q And what did you mean when you say you are trying to get over?

A If you can maneuver over, because even if you got three feet, I mean if you can change the lane, that's the best, but you know.

MR. ROBERTS: Okay. Thank you, ma'am. Nothing further, Will.

EXAMINATION

BY MR. KEMP:

Q Okay, just briefly. You said that you didn't think the J-4500 blind spots were, in Mr. Roberts words, unreasonably unsafe, unquote. Okay, do you remember that testimony?

A Yes, sir.

Q But they can be improved upon, right?

A Yes, sir.

Q And is there any reason why you shouldn't be as safe as possible whether you think -- I'm not sure I know what you mean by unreasonable, but is there any reason in your mind why you shouldn't be as safe as possible?

A Well, you would hope everybody is as safe as possible.

Q Now, with regards to the right side blind spot of a J-4500, would I be correct that the closer you get to the

002482
002482

bicycle when you are overtaking it, the more of a problem the blind spot becomes?

A As you are overtaking there will be a spot where you are going to really have to adjust and look, yes.

Q So the closer you get, the more of a problem the blind spot potentially becomes on a J-4500; is that correct?

A Well, it's any bus, sir, it's not just the J-4500.

Q But the closer you get to that bicyclist, the more of a problem the blind spot becomes in terms of visibility, right?

A Well, you have got to pay more attention.

Q Because the -- it becomes a bigger problem in terms of visibility, correct?

A Correct.

Q And would I also be correct that when you are 400 feet behind a bicyclist or 350 or 250, it's hard to determine whether you will be two feet, three feet, four feet within that bicyclist when you go past him?

MR. ROBERTS: Objection to form.

THE WITNESS: It's hard to distinguish how close you are going to be?

MR. KEMP:

Q Right.

A Not if you are using, you know, the markers on the bus, you should know how far you are from.

Q Okay. So you think if you are 400 feet away from a

002484

002484

EXHIBIT 22

Press Releases

PRESS RELEASE

Model Overview: 2008 Volvo S80

Jun 04, 2007 | ID: 11653

Manufacturer's Suggested Retail Price

S80 3.2: $38,705

S80 T6 AWD: $42,045

S80 V8 AWD: $49,210

Destination: $745

002485

All new last year, the acclaimed Volvo S80 gains an exciting new dimension in performance for 2008 with the introduction of the turbocharged T6 AWD. This revolutionary new model fits perfectly between the normally aspirated S80 3.2 and the flagship S80 V8 AWD.

Based on the S80's compact 3.2-liter 235-horsepower inline-6 cylinder engine, the T6 version has a displacement of 3.0 liters, producing 281 horsepower and 295 lb.-ft. of torque. Maximum torque is on tap from just 1,500 rpm and remains available all the way up the rev range, resulting in remarkably quick acceleration and smooth drivability.

The somewhat smaller cylinder displacement of the T6, owing to slightly narrower cylinder bore and shorter stroke, is compensated by a single turbocharger with twin-scroll technology. This takes in exhaust gases in two stages with inflow divided into lots of three cylinders each. Thus, the T6 permits the use of a more compact and simplified turbo that provides extremely swift response with the lowest possible fuel consumption and exhaust emissions.

Like the S80 V8, the T6 is fitted with Volvo's All Wheel Drive with Instant Traction. Using an electronically controlled hydraulic clutch, the system distributes drive between the front and rear wheels to ensure the best possible road grip in all situations. All S80s feature a standard six-speed "Geartronic" transmission.

Volvo's first V8-powered sedan continues to put out 311 horsepower and 325 lb.-ft. of torque. Changes to the S80 V8 include more standard premium features with bright taillight trim, brushed aluminum lower door side moldings, Classic Wood inlay center console and soft leather seating surfaces. The world first Personal Car Communicator (PCC) is now standard on the S80 V8 and remains optional on other variants.

In nearly every area of occupant protection the S80 expands Volvo's leadership in both preventative and protective safety. Innovations include a side airbag with dual chamber construction for enhanced hip and chest protection. Clever structural design employs four different grades of steel for predictable crash energy absorption. The S80 also features the next generation of WHIPS rear impact protection and new approaches to pedestrian safety.

Adaptive cruise control, optional on all S80s, uses a radar sensor to measure the distance to vehicles ahead and automatically adjust vehicle speed. Collision warning with brake support works in concert with the system, alerting the driver and applying the brakes if needed. The Blind Spot Information System (BLIS) is another high-tech option. Cameras near the outside mirrors detect vehicles that might be in a blind spot and relay the information to the driver.

On the inside, the S80's cabin is fitted with a super-slim center console, premium leather seating surfaces and real wood inlays. A power driver's seat with memory, power font passenger seat and power sunroof is among the list of standard amenities. Also included is a high performance sound system with 6-disc CD changer, auxiliary input, MP3 capability, a 160-watt amplifier and eight speakers.

All models can be enhanced with the optional Dynaudio Package that adds a 650-watt amplifier, Dolby Pro-Logic II Surround Sound and 12 Dynaudio® speakers. Rear seat headphone jacks and audio controls are new this year. Sirius TM Satellite Radio is also included. Other options include the Volvo Navigation System with HDD, DVD map data and remote control and a dual screen rear seat entertainment system.

Keywords:
2008, S80 (2008-2016)

Descriptions and facts in this press material relate to Volvo Car Group's international car range. Described features might be optional. Vehicle specifications may vary from one country to another and may be altered without prior notification.

(/us/en-us/download/11653/doc/doc/)

002487

002487

EXHIBIT 23

Pedestrian Detection in Transit Bus Application: Sensing Technologies and Safety Solutions

Fanping Bu, Ching-Yao Chan, *Member, IEEE*
California PATH Program, University of California at Berkeley
1357 S. 46th Street, Richmond, CA 94804, USA

***Abstract*—Pedestrian safety is a primary traffic issue in urban environment. The use of modern sensing technologies to improve pedestrian safety has remained an active research topic for years. A variety of sensing technologies have been developed for pedestrian detection. The application of pedestrian detection on transit vehicle platforms is desirable and feasible in the near future. In this paper, potential sensing technologies are first reviewed for their advantages and limitations. Several sensors are then chosen for further experimental testing and evaluation. A reliable sensing system will require a combination of multiple sensors to deal with near-range in stationary conditions and longer-range detection in moving conditions. An approach of vehicle-infrastructure integrated solution is suggested for the pedestrian detection in transit bus application.**

***Index Terms*— Pedestrian detection, Vehicle infrastructure integration, Transit bus, Radar, Laser scanner**

002488

I. Introduction

Pedestrian safety is a primary traffic issue in urban environment. A glance of national crash statistics [1] shows that about 15 % (4,882 out of 42,116 in 2001) of fatalities result from pedestrian-type accidents. The California statistics compiled by Office of Traffic Safety (OTS) and California Highway Patrol (CHP) [2, 3] also reflect a significant numbers of pedestrian incidents with 689 out of 3,730 fatalities in the year of 2000 in all collisions being pedestrians. Even though the percentage of these accidents may not be the highest among all categories of accidents or collisions, these incidents represent a considerable hazard to the public since they often involve severe injuries or fatalities of pedestrians. It is therefore a great incentive to deploy modern sensing technologies to assist drivers in identifying the presence and movements of pedestrians.

The detection and prevention of pedestrian accidents is not trivial, to say the least. First of all, in urban traffic environment the patterns of vehicle and pedestrian movements are very complicated. On city streets, there are numerous locations where pedestrians may choose to cross in front of vehicle trajectories suddenly. Modern sensing technologies have not matured to the extent that can provide the solution for a reliable and an accurate means of identifying pedestrians in urban traffic environment with a cluttered background and a range of visibility under various weather and roadway conditions. A more pragmatic approach for the field deployment of pedestrian detection technology will be to target a specific application or scenario where an integrated system approach can play an important role.

Pedestrian detection for transit bus has the potential to be deployed in the field in the near future. First, transit buses encounter a large volume of pedestrian traffic in their routes, bus stops, and intersections. Second, accidents involving transit buses are compounded into transit operational and cost problems and impact on mobility and efficiency. Third, transit buses run on pre-known routes and are primary candidates to integrate infrastructure and vehicle-based solutions. Finally, transit buses are higher-priced vehicles and thus can be initial candidates for advanced technology solutions with minimum cost impact.

Even with the advancements of sensing technologies, the applicability of a single type of sensor for different operating conditions remains doubtful. In this paper, a technology review is provided first in Section II for the potentially applicable sensing technologies. Promising candidate sensors for transit bus application is further investigated through experimentation in Section III. A vehicle infrastructure integrated (VII) approach is suggested in Section IV and Section V provides a summary and conclusion for the paper.

002488

II. Sensor Technologies Review

Different sensing technologies such as piezoelectric sensor, ultrasonic sensor, microwave radar, laser scanner and computer vision can be used for pedestrian detection. The review in this section will examine different technologies used for pedestrian detection and analyze their advantages and limitations.

A. Piezoelectric Sensor

For the application of pedestrian detection, piezo-cables with piezoelectric material are usually fabricated into a "mat". When a person steps onto the mat, electrical signal is generated until the person leaves the mat. Piezoelectric detectors are used to detect the presence of waiting pedestrian at a controlled road crossing for PUFFIN (Pedestrian User-Friendly Intelligent Crossing) and PUSSYCATS (Pedestrian Urban Safety System and Comfort at Traffic Signals) [4].

Piezoelectric detector is a simple reliable sensor for pedestrian detection. It does not require complex signal processing. However, it does require physical contact between the pedestrian and the sensor mat. Therefore, piezoelectric detector is usually used for the intersection pedestrian crossing.

0-7803-8961-1/05/$20.00 ©2005 IEEE.

002488

B. Ultrasonic Sensor

Ultrasonic detectors emit ultrasonic wave. When vehicles or pedestrians pass by, the transmitted sound wave is reflected back to the receiver. Based on the reflected signal, objects can be detected for their presence along with their distance and speed. There are two basic types of ultrasonic sensors depending on the waveform of ultrasonic wave [5]. Pulse ultrasonic sensors measure the distance or presence of objects by sending a pulsed ultrasound wave and then measuring the flight time of reflected sound echo. Continuous wave ultrasonic sensors output continuous ultrasonic wave of certain frequency and use Doppler principle to detect moving object and its speed.

Ultrasonic detector can detect objects up to 30 feet. The limitations of ultrasonic sensors can be summarized as follows [6, 7]. First, in order to minimize lost bounced back ultrasound energy from target, the preferred installation configurations are either directly facing downward (i.e. nadir incidence angle) above targeting area or aiming from a horizontally mounted side viewing position (side fired). Second, clothing has some effects on pedestrian detection. Usually, clothes made of natural fiber are more absorbent to sound wave than clothes made of synthetic fiber. Therefore, pedestrian wearing synthetic fiber (e.g. nylon) is easily detected compared with pedestrian wearing natural fiber (e.g. cotton). Finally, weather conditions change like temperature, pressure, humidity and wind will affect the performance of ultrasonic sensors. This is because the speed of sound varies according to temperature and pressure of the medium.

C. Microwave Radar

Microwave radar works in a way very similar to ultrasonic sensors. In stead of sound wave, electromagnetic wave is transmitted from microwave radar antenna. Based on the analysis of bounced back signals, objects can be detected together with their distance and speed.

Microwave radars can be classified into different categories based on the transmitted electromagnetic wave form. Doppler radar transmits a continuous wave of constant frequency. Such electromagnetic wave, when reflected from a moving object, will have frequency shift. By analyzing the frequency shift, the speed of object can be calculated. Doppler radar alone can only detect moving object with relative speed larger than certain threshold. Another type of microwave radars transmit frequency-modulated or phase-modulated signal, for example a type of radar sensor is based on frequency modulated continuous wave (FMCW) technology [8]. The distance to target is determined by time delay of the return signal. Ultra wide band (UWB) radar is a new emerging technology which has great potentials in ITS application [9]. The basic concept is to transmit and receive an extremely short pulse of radio wave. The resultant waveforms are extremely broadband. The precision timing of pulses inherent to UWB radar, and the successful development of advanced timer technology has enabled UWB radar capable of detection, ranging and motion sensing of personnel and objects with centimeter precision.

Radar sensors can provide accurate object distance and speed without complex signal processing (compared with computer vision). Radar technology can operate in different environmental conditions (e.g. bad weather, poor visibility or harsh environmental impacts like ice, snow or dust coverage). If installed on the vehicle, it can be hidden behind un-shielding materials with no influence on vehicle's appearance and thus does not disturb vehicle design. To further differentiate detected objects, (e.g. pedestrians or other traffic participants) the power spectral density characteristics of reflected signal can be analyzed [10].

D. Laser Scanner

Another technology that has been evaluated for pedestrian and object detection is a Laser scanner, such as a high-resolution laser range finder [11]. The laser scanner emits infrared laser pulses and detects the reflected pulses. The measurement principle is based on the time-of-flight method. Scanning of the measurement beam is achieved by rotating prism and covers a viewing angle of up to 360 degree. The original data from laser scanner is much like vision image data in the horizontal scanning plane with accurate distance (centimeter level) and azimuth angle information (from 0.25 degree to 1 degree depending on scanning frequency). Therefore a procedure similar to image processing can be applied here. In [26], multiple laser scanners connected by LAN are used to track pedestrians in a given area. For the application on vehicles, vehicle model is setup to compensate vehicle motions [12]. In order to compensate vehicle pitch motion, multilayer laser scanner with more than 1 scanning plane is designed [5].

The excellent range accuracy and fine angular resolution make laser scanners suitable for applications in which a high resolution image of surrounding is required. However, since they are optical sensors, different weather conditions like fog or snow will limit their detection range. The signal processing is a little more complex for laser scanner compared with ultrasonic or microwave radar, therefore dedicated CPU may be needed.

E. Computer Vision

Vision based pedestrian detection is a natural choice based on the human's own experience. Although video camera can obtain very rich information about the surrounding environment compared with the radar or laser scanner, the image sequences can not be used for anything directly without further interpretation. Different algorithms are proposed to detect pedestrians in the image sequences acquired from video camera. Recent research shows two main trends. Motion based approaches take into account temporal information and tries to detect the periodic features of human gait in the movement of candidate patterns. On the other hand, the shape based approaches rely on shape feature to recognize pedestrians.

Motion based approaches uses rhythmic features or motion patterns unique to human being. Although motion based approaches provide an efficient way to reduce the number of false positive candidates, there are several limitations on motion based approaches. First, motions based schemes cannot detect stationary pedestrians obviously or pedestrians in unusual movement like jumping. Second, the pedestrian's feet or legs should be visible in order to extract rhythmic features or motion patterns. Third, the recognition procedure requires a sequence of images, which delays the identification until several frames later and increases the processing time.

Shape based methods allow the recognitions of both moving and stationary pedestrians. The primary difficulty associated with this approach is how to accommodate the wide range of variations in pedestrian appearances due to pose, various articulations of body parts, lighting, clothing and occlusion. The key issues here are: first, find a concise yet sufficient human shape feature representation. Second, maintain a balance between accuracy of detection and processing time. To achieve real-time processing, trade-off has to be made between accuracy of classification and processing time. Two step pedestrian approaches are used to relieve such computational burden in [14-18]. Usually a coarse segmentation step is carried out first to separate foreground and interesting region from background. Distance measurement from stereo vision can be used for segmentation step. The fine analysis of separated foreground objects is then followed to check for the presence of pedestrians.

Although shape based method is more general, the major drawbacks associated with shape method are, 1) high false positive rate due to variation of human shape and changing lighting conditions, 2) heavy computation burden when performing feature matching. Different approaches are proposed to resolve these drawbacks. In [19], the single frame shape match is combined with motion analysis to reduce false positive rate. A specialized system-on-a-chip hardware solution is used to increase processing speed in [20]. In [21], knowledge about certain cites and situations (e.g. traffic light, pedestrian crossing etc) are used as priori information to optimize the vision processing algorithm. Sensor fusion approach is suggested in [22] where multiple sensors are used (e.g. radar and laser scanner) together with computer vision to reduce false positive rate.

Compared with camera operating on visible spectrum, infra-red (IR) camera [23] is not that sensitive to the change of lighting condition. The advantage of passive infra-red sensor is the ability to detect pedestrian without illuminating the environment. Pedestrians are bright and sufficiently contrasted with respect to the background in IR images and can be recognized by their shape and aspect ratio. To reduce the cost for infra-red camera which is used mostly in military application before, low cost 16 by 16 array infra red detectors are used in groups to not only count the pedestrian number passing by, but also capture pedestrians' moving trajectories along certain corridor in [24]. Honda has developed an intelligent night vision system which will be available on the new Honda Legend [25]. Two far infra-red cameras are installed in the front bumper. The target distance is acquired by the stereo infra-red vision from two cameras. Pedestrians can be identified by the shape recognition and their movements are tracked through vector analysis. The system will provide the driver visual and audio cautions when it detects pedestrians in or approaching the vehicle's path.

III. Experimental Studies of Promising Sensing Technologies for Transit Bus Application

Computer vision with image processing is a very promising technology and there have been commercial developments for other roadway or vehicle based safety applications, such as sign or lane recognition. However, for pedestrian detection, there is limited availability of products that can be purchased for evaluation. Several different sensors are selected for further experimental test and review. The sensors include IBEO laser scanner (scanning LIDAR), Eaton VORAD EVT-300 radar (Doppler radar), IRIS people counter (infrared based sensor), MS SEDCO SmartWalk 1800 (microwave radar) and SENIX Ultra-100 (ultrasonic sensor). Detailed testing and results on IBEO laser scanner and Eaton VORAD EVT-300 radar will be presented. The rest is summarized in table 1.

A. IBEO Laser Scanner

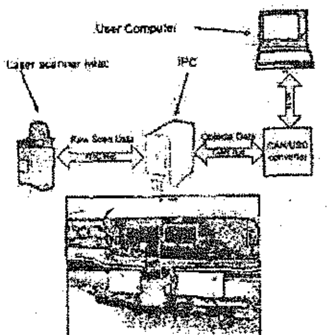

Fig. 1 Evaluation System Configuration and installation

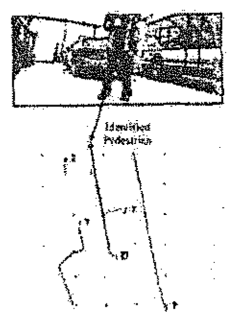

Fig. 2 Test Scenario with walking pedestrian

The tested system consists of a laser scanning head mounted on the front bumper of a Buick LeSabre, an industrial PC (IPC) and a user computer (Fig. 1). The raw scan data is sent to IPC via ARC net. Object detection and tracking algorithm is running on IPC. The results are a set of object data with each object's size, position and velocity. The object data is sent to the host computer via standard CAN bus. To facilitate user visualization, a CAN/USB converter is added so that user computer could receive object data through standard USB port.

A set of tests are conducted in the PATH vehicle tent under stationary conditions. Fig. 2 shows a pedestrian walking in front of the laser scanner. The laser scanner identifies the object as a pedestrian according to its size and velocity. Fig. 3 shows an interesting scenario. A cart is moving in front of the laser scanner. Since the scanning plane of laser scanner is cutting in the middle of the cart, the cart is actually recognized as two pedestrians by the laser scanner. Two poles close to each other are identified as a pedestrian due to its size and velocity. The Buick car behind the cart is also divided into two objects because of the cart's blocking.

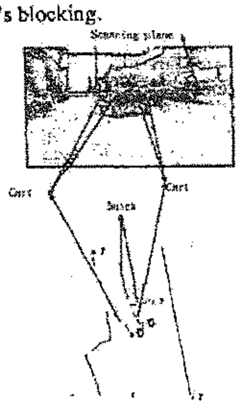

Fig. 3 Test Scenario with moving cart

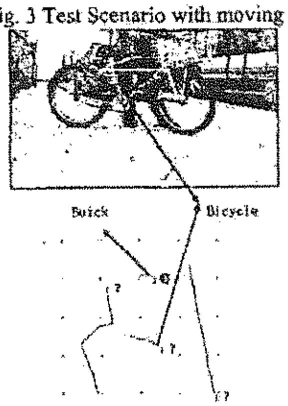

Fig. 4 Pedestrian with bicycle

Fig. 4 shows a pedestrian walking his bicycle in front of laser scanner. The bicycle blocks the pedestrian completely on the scanning plane. So the laser scanner only detects a bicycle sized object and could not detect the pedestrian behind. The bicycle also blocks part of the Buick. The remained part detected by the laser scanner is about the size of a pedestrian and it is recognized as a pedestrian.

The test results show that IBEO Laser scanner can provide object information with accurate distance (centimeter level) and azimuth angle (from 0.25 degree to 1 degree depending on scanning frequency). However since the laser scanner we tested can only provide object contours on one scanning plane, the information is quite limited for the pedestrian detection in the complex urban scenario and false detection or missing target will happen if decision is solely based on such limited information (see Fig. 3 and Fig. 4).

B. Eaton VORAD EVT-300 radar

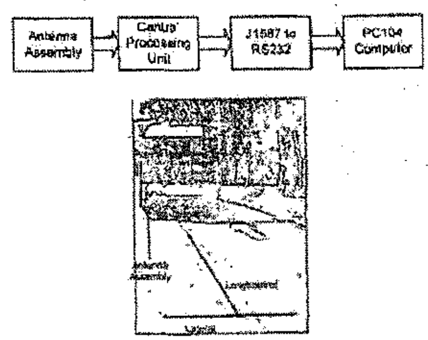

Fig. 5 Evaluation setup and configuration

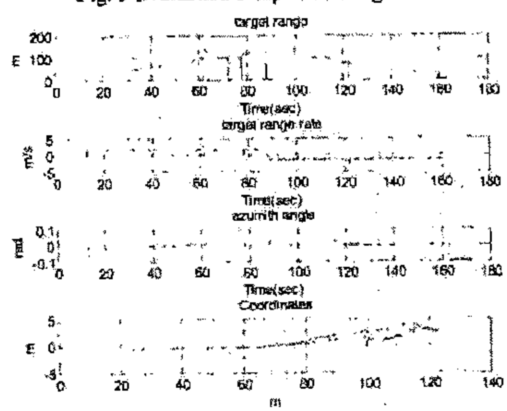

Fig. 6 Pedestrian walking in front of stationary bus longitudinally

Fig. 5 shows the system configuration of a testing system we installed on a New Flyer CNG 40 footer bus. The antenna assembly of Eaton VORAD VT-300 Doppler radar is installed behind the bumper. Central processing unit processes information from antenna assembly. Target information like target ID, distance, azimuth angle and target velocity is sent out through J1587 bus by central processing unit. A J1587 to RS232 converter is installed so that onboard PC104 computer can read and log such information through serial port.

To evaluation the sensor performance, a set of evaluation tests are performed on PATH test track for both stationary bus scenario and moving bus scenario. First we parked the bus on the test track. A pedestrian walks in front of the bus from the longitudinal direction and the lateral direction as shown in Fig. 5. Fig. 6 shows the target information acquired when the pedestrian walks longitudinally back and forth along the yellow double solid line in the Fig. 5. The Eaton VORAD radar can detect the target up to about 130m with slow speed (<0.5m/s).

When pedestrian changes his walking direction, the detected speed drops to zero for a few seconds. At that time, Eaton VORAD radar cannot detect still (relative to bus) target, so we will see the target lost for a few seconds but reacquired after pedestrian picks up his speed to the other direction. The scenario also shows that the minimum distance for Eaton VORAD radar is about 5m.

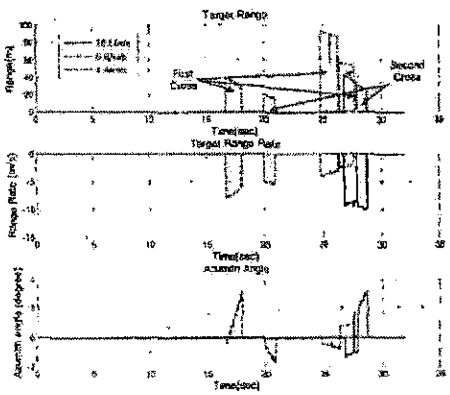

Fig. 7 Pedestrian walking in front of a moving bus laterally

Experiments are also conducted when the pedestrian crosses laterally in front of the bus at distances of 10, 15 and 20 meters. The Eaton VORAD radar can not detect the moving pedestrian in all three cases. This is due to the operating principle of Eaton VORAD radar. Eaton VORAD radar is a Doppler radar. The sensitivity of a Doppler radar is relative low to the target moving along the direction perpendicular to its radar wave propagating direction. Since the relative distance change between radar antenna and target is very small, it is difficult for the radar processor differentiate such small amount of frequency drifting from noises. Fig. 7 shows the target information acquired when the bus is moving about 10mph (4.44m/s), 15mph (6.67m/s) and 24mph (10.67m/s). A pedestrian crosses the test track from lateral direction twice in the same place at each speed. Both crosses are picked up by radar under different speeds. The target speed is about the same as the vehicle moving speed since pedestrian cross the track laterally. The azimuth angle changes its sign because pedestrian crosses the track back and forth.

The testing results show that:

1) Eaton VORAD radar has a relatively long distance detection range over 120 meters. The shortest detection distance from experimental data is about 5 meters.
2) Eaton VORAD radar can only detect target which is moving relative to the radar due to its Doppler principle
3) Any target maintains relative still to the radar can not be detected. Unless a relative motion can create certain amount relative distance change, the target with relative motion can not be detected either. For example, the test data shows the sensitivity of radar drops significantly to the target with relative motion along the direction perpendicular to radar wave propagating direction

C. Functional Performance Comparison of Evaluated sensors

Similar tests are conducted for IRIS people counter, MS SEDCO SmartWalk and SENIX Ultra-100. Among those sensors that have been evaluated, a list of characteristics, attributes, and performance specifications are given below for comparative studies.

TABLE I
Summary of sensor evaluating test

Product	Technology Category	Detection Range (m)	Accuracy	Target Tracking range (m)/ Field of view	Application for Transit Bus
IBEO laser scanner	Lidar	0 - 250	+- 5 cm	0 – 50/ 270 degrees	Long range; bus moving
EVT-300 radar	Doppler radar	3 - 140	5%/+- 1 m	3 – 140/ 12 degrees	Long range; bus moving
IRIS people counter	Infrared	2 - 5	On-off	N/A/ 60 degrees	Short range; bus stop
MS SEDCO SmartWalk 1800	Doppler radar	2 - 15	On-off	N/A/ 45-60 degrees	Short range; bus stop
SENIX Ultra-100	Ultrasonic	0.15 - 3	On-off	N/A	Short range; bus stop

IV. Vehicle-Infrastructure Integrated System Approach for Transit Bus Pedestrian Detection

Given the challenging operating environment of transit buses, it is apparent that a complete and reliable sensing system for pedestrian detection can benefit from the combined use of multiple sensors. For example, the requirements of pedestrian detection are different for situations when buses are stopped at bus tops or near intersections versus when the buses are moving at relatively higher speeds in cruising conditions. Furthermore, any one particular type of technology may have difficulties meeting all necessary requirements in various lighting conditions, or rainy and foggy and inclement weather conditions, not to mention that most sensor have limited field of view to monitor traffic in all directions. In addition, the clutter background and complex moving patterns of all objects on urban streets demand sophisticated processing of sensor inputs to avoid false detection and recognition.

In order to overcome the technical challenges of the aforementioned problem, a sensor-fusion and segmented approach is necessary. For example, ultrasonic sensor arrays and infrared detectors can be installed at selected locations around the bus to alert drivers of pedestrians near the bus. This can prevent inadvertent contacts or collisions with pedestrians when the bus is in transitions states from stopped positions. On the other hand, infrared camera, laser scanner, and radar can be used for long-range detection in situations when drivers are unable or unaware of pedestrians at a distance.

One other promising approach has recently emerged with the advancement of wireless communication technologies. For example, the US Federal Communications Commission recently announced the details of the licensing and roadside unit registration process for Dedicated Short Range Communications (DSRC) in the 5.9 GHz band. DSRC can be applied for many applications, a primary one of which is

002492

002492

002492

002493

roadway safety. In a potential transit solution, a vehicle-infrastructure solution can be constructed. For example, an evaluated microwave pedestrian detector (such as MS SEDCO SmartWalk) is ideal for monitoring pedestrian movements on crosswalks. In traffic conditions where drivers have obstructed views or limited visibility to pedestrian crossing areas, an infrastructure sensor can be used to detect objects and a wireless signal can be sent remotely to a receiver on the bus with a visual or audio alert given to the driver. This suggested approach is particular sensible because transit buses run on fixed routes and safety solutions can be selectively deployed at high-risk locations along the bus routes.

V. Conclusion

The work presented in this paper represents recent efforts taken by the research team to address pedestrian safety. With a survey of latest technology developments and available products, a number of sensors were selected for evaluation to assess their applicability for transit bus platforms. Through experimental exploration, the characteristics and limitations of individual sensors were investigated and compared.

For large-scale deployment, certainly cost considerations will play a big role in the selection of technologies or components. Either to be used for a specific function, or to be integrated within a complete solution, products need to be cost competitive for a broad-based utilization. Even though certain promising and sophisticated technologies may be cost prohibitive currently, they may become more affordable in the future as they find marketable applications and unit costs are reduced in mass production.

With the consideration of distinct operating environment of transit buses, the detection problem is handled with a two-prong approach: one aiming for short-range when buses are near bus-stop or intersections, and the other targeting longer-range detection when buses are cruising at higher speeds. A viable option to provide an integrated solution will be to combine infrastructure sensors, at strategic locations such as crosswalks or high risk areas, and wireless communication links to send detection signals to an on-board unit to alert drivers of potential threats.

Acknowledgment

This work was sponsored by the California PATH Program of the University of California, in cooperation with the State of California Business, Transportation and Housing Agency, Department of Transportation. The contents of this paper reflect the views of the authors, who are responsible for the facts and accuracy of the data presented herein. The contents do not necessarily reflect the official views or policies of the State of California.

The authors wish to thank our colleagues, David Marco, Thang Liao, David Nelson, Susan Dickey, Paul Kretz, and Bart Duncil, for their generous supports and contributions in the study.

References

[1] http://www.nhtsa.dot.gov
[2] http://www.chp.ca.gov
[3] http://www.nrs.ca.gov
[4] SRF Consulting Group, Inc. "Bicycle and Pedestrian Detection", *Mn DOT research report*, 2003
[5] "NIT Phase II: Evaluation of Non-Intrusive Technologies for Traffic Detection", *Mn DOT research report*, SRF No. 3683, 2002
[6] D. Beckwith and K. Hunter-Zaworski, "Passive Pedestrian Detection at Unsignalized Crossings", *77th Annual Transportation Research Board Meeting*, 1998 (Paper No. 980725).
[7] D. Noyce and R. Dharmaraju, "An Evaluation of Technologies for Automated Detection and Classification of Pedestrians and Bicyclists", *Massachusetts Highway Department report*, 2002
[8] P. Knoll, B. Schaefer, H. Guettler, M. Bunse and R. Kallenbach, "Predictive Safety System – Steps Towards Collision Mitigation", *SAE Technical Paper*, 2004-01-1111, 2004
[9] D. Scherrer and R. Burghert, "Short Range Devices, RFID, Bluetooth, Ultra Wideband Systems and Automotive Short Range Radars: Overview and Latest Development" *OFCOM report*, 2003
[10] D. Gavrila, M. Kunert and U. Lages, " A multi-sensor approach for the protection of vulnerable traffic participants- the PROTECTOR project", *IEEE Instrumentation and Measurement Technology Conference*, pp. 2044-2048, 2001
[11] A. Ewald, V Willhoeft, "Laser Scanners for Obstacle Detection in Automotive Applications", in *Proc. of the IEEE Intelligent Vehicles Symposium*, pp. 682-687, 2000
[12] K. C. Fuerstenberg and U. Lages, "Pedestrian Detection and Classification by Laserscanners", *Proc. of 9th EAEC International Congress*, June 2003
[13] K. C. Fuerstenberg, K. Dietmayer and V. Willhoeft, "Pedestrian Recognition in Urban Traffic using a Vehicle based Multilayer Laserscanner", in *Proc. of the IEEE Intelligent Vehicles Symposium*, pp. 31-35
[14] D. Gavrila and V. Philomin, "Real-Time Object detection for "SMART" Vehicles", in *Proc. of IEEE Intl. Conference on Computer Vision*, pp. 87-93, 1999
[15] L. Zhao, " Stereo- and Neural Network-Based Pedestrian Detection", *IEEE Transactions on Intelligent Transportation Systems*, Vol. 1, No. 3 pp.148-154, 2000
[16] U. Franke and S. Heinrich, "Fast Obstacle Detection for Urban Traffic Situations", *IEEE Transactions on Intelligent Transportation Systems*, Vol. 3, No. 3 pp. 173-181, 2002
[17] http://www.gavrila.net
[18] A. Broggi, M. Bertozzi, A. Fascioli and M. Sechi, "Shape-based Pedestrian Detection", in *Proc. of IEEE Intelligent Vehicle Symposium*, pp. 215-220, 2000
[19] A. Shashua, Y. Gdalyahu and G. Hayun, "Pedestrian Detection for Driving Assistance Systems: Single-frame Classification and System Level Performance" in *Proc. of IEEE Intelligent Vehicle Symposium*, 2004
[20] http://www.mobileye.com
[21] P. Lombardi and B. Zavidovique, "A Context-Dependent Vision System for Pedestrian Detection", *IEEE Intelligent Vehicle Symposium*, pp378-383, 2004
[22] D. M. Gavrila, "Sensor-based pedestrain protection", *IEEE Intelligent Systems*, vol. 6, no. 5, pp. 77-81, 2001
[23] F. Xu and K. Fujimura, " Pedestrian Detection and Tracking with Night Vision", in *Proc. of IEEE Intelligent Vehicle Symposium*, 2002
[24] J. Kerridge, A. Armitage, D. Binnie and L. Lei, "Monitoring the Movement of Pedestrians Using Low-cost Infrared Detectors: Initial Findings", *TRB Annual Meeting*, 2004
[25] http://world.honda.com/HDTV/IntelligentNightVision/200408/
[26] H. Zhao and R. Shibasaki, "A Novel System for Tracking Pedestrians using Multiple Single-row Laser Range Scanners", *IEEE Trans. On Systems, Man and Cybernetics*, Vol. 35 No. 2 pp283-291 2005

002493

002493

P02475

002493

002494

002494

EXHIBIT 24

PRODUCTS: OTHER

Eaton VORAD enhances collision warning system

Posted: Sep 2, 2005 9:22 AM | Last Updated: Aug 1, 2014 10:48 AM

Eaton VORAD
Eaton VORAD Technologies, a subsidiary of Eaton Corp., is partnering with Preco Electronics of Boise, Idaho, to offer a stand-alone side-object-detection system. This side sensor will be added to Eaton's current VORAD safety product line. It's a compact, cost-effective, radar-based object-detection system for trucks, buses, and RVs. The Eaton VORAD EVT-300 Collision Warning System uses in-cab display units with a series of warning lights and audible tones to warn the driver of the presence of objects and vehicles in its way, giving the driver time to take action to avoid a collision. Call 1-800-826-4357 or visit www.roadranger.com.

Related Links:
http://www.roadranger.com
http://www.roadranger.com
http://www.roadranger.com
http://www.roadranger.com

002496

002496

EXHIBIT 25

People




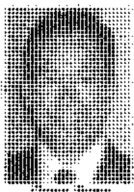

International Motor Coach Group has awarded the title of Alliance Partner of the Year to *Brenda Borwege*, vice president of marketing for **ABC Companies**.

The award recognizes an IMG alliance partner that "participates in industry leadership roles, promotes IMG within the industry, actively participates in IMG programs, and demonstrates vision and commitment to building relationships with IMG shareholders.

"Brenda exemplifies a true partner who is always willing to offer assistance and participates in all efforts to build our industry," said IMG Chairman *Jack Wigley*.

ABC Companies has appointed *Andrew Fung* its director of engineering services. Working in the company CustomerCare Division, and reporting to division vice president *Chuck Avery*, Fung will be responsible for the direction of the technical staff, including engineers, field technicians and the CustomerCare call center. He will provide customers with technical support for their ABC products while serving as the liaison between customers and the product manufacturers. He also will be responsible for new product development, including buses, parts and services. A graduate of the University of Manitoba with a degree in engineering, Fung has spent the past 12 years working in the motorcoach industry, most recently as director of fleet support engineering for **Motor Coach Industries**. He has relocated to the Orlando area from Louisville, Ky.

Prevost Car has appointed *Mark Armstrong* as branch manager of its parts and service center in Mira Loma, Calif. Armstrong will be responsible for overseeing day-to-day operations of the facility.

Armstrong is a former sales director for a high-end electronics manufacturer and holds an MBA in technology management and a bachelor's degree in electrical engineering.

"Mark's background in engineering, process standardization and ISO standards will be an asset to us as we move forward with our branch standardization program," said Prevost Service Network Manager *Randy Castillo*.

Gene Perro has joined the **P.A. Post Agency** of Mahwah, N.J., a leading motorcoach industry insurance agency and brokerage, as a sales executive.

Perro comes to P.A. Post Agency with more than 20 years of insurance experience, most recently as an executive with **KMA Insurance Agency** in Burnsville, Min. He has been focused on the passenger transportation industry for the past 15 years.

"Gene Perro's extensive experience and abilities in providing insurance programs for the transportation industry is a great asset to P.A. Post Agency, said *Brad Post*, president of the family owned agency.

E-mail Perro at *gperro@postfinancial.com*.

FirstGroup eyes October to complete Laidlaw deal

ABERDEEN, Scotland — The takeover of Laidlaw International and its subsidiary, Greyhound Lines, by First Group PLC is expected to be completed early next month.

Scotland-based FirstGroup announced it was close to clearing the final obstacle — U.S. antitrust approval — in the way of completing its acquisition of Laidlaw, which owns Greyhound.

FirstGroup's announcement was followed by a statement from Laidlaw saying that "substantial progress" had been made in discussions with the antitrust division of the U.S. Justice Department about the major share of the American school bus market the takeover would give FirstGroup.

Rachael Borthwick, FirstGroup's corporate communications director, said the company had reached agreement in principle with the Justice Department officials and with a group of state attorneys general which had expressed an interest in the deal.

The interest by the state attorneys stems from the extensive school bus services operated by both Laidlaw and FirstGroup.

In its announcement, FirstGroup said it expected to conclude an agreement with the antitrust division which would allow it to complete the deal by Oct. 7.

Coach America to retrofit lifts

RIVERSIDE, Calif. — Complete Coach Works has received a contract for the installation of wheelchair lifts in MCI coaches operated by Coach America's operation in Long Beach, Calif.

The contract includes providing Ricon wheelchair lifts and custom installation, including integration of the lifts into the bus system.

Three lifts are expected to be installed this year, with three more next year.

John Romero, maintenance manager of Coach America in Long Beach, said Complete Coach Works was chosen for the work because of its "vast experience with these types of modifications. Their emphasis on quality and customer satisfaction have served us well in the past, and we are happy to have Complete Coach Works as a key service provider and supplier."

DaimlerChrysler Fla. center gains seal

GREENSBORO, N.C. — DaimlerChrysler Commercial Buses North America says its Florida service and parts center has been awarded the Blue Seal of Excellence by the National Institute for Automotive Service.

The award is the highest level of certification by the institute.

"We are extremely proud that our parts and service center of Florida has been recognized…," said Patrick Scully, chief commercial officer for DaimlerChrysler Commercial Buses North America.

002498

002498

EXHIBIT 26

DISTRICT COURT

COUNTY OF CLARK, NEVADA

- -

CASE NO. A-17-755977-C
DEPT NO. XIV

KEON KHIABANI and ARIA KHIABANI, minors by and through their natural mother, KATAYOUN BARIN; KATAYOUN BARIN, individually; KATAYOUN BARIN, as Executrix of the Estate of Kayvan Khiabani, M.D. (Decedent) and the Estate of Kayvan Khiabani, M.D. (Decedent),

Plaintiffs,

vs.

MOTOR COACH INDUSTRIES, INC., a Delaware corporation; MICHELANGELO LEASING INC., d/b/a RYAN'S EXPRESS, an Arizona corporation; EDWARD HUBBARD, a Nevada resident; BELL SPORTS, INC. d/b/a GIRO SPORT DESIGN, a California corporation; SEVENPLUS BICYCLES, INC. d/b/a Pro Cyclery, a Nevada corporation; DOES 1 through 20; and ROE CORPORATIONS, 1 through 20,

Defendants.

- -

DEPOSITION OF BRAD ELLIS
Monday, August 28, 2017
Winnipeg, Manitoba, Canada
Job Number 413397

002499

002499

Q And is that your signature on it?
A Yes.
Q Can you read for the record what the letter says?
A Sure. It says:

"Ken: By the way of this letter, New Flyer Engineering maintains the position that the installation of the S-1 Gard in New Flyer facilities does not compromise the integrity of the chassis or suspension of the coach on which it is installed, nor is it expected to impact the functionality or integrity of other systems in the coach."

Signed by myself.
Q And at the time that you signed it, what does it indicate your job position was?
A I was working under engineering at that point. There was -- if I recall, there was a time where I got moved out of manufacturing when I got my engineering paper work, my professional engineering stamp. And there was a time in between when I ran -- I got to structural engineering manager eventually, but there was a transition time where I still worked with the manufacturing engineering personnel along

002500
002500